



**NOVEL TECHNIQUES FOR MICROENCAPSULATION OF  
PROBIOTIC BACTERIA**

**A Thesis Submitted for the Degree of  
Doctorate of Philosophy**

**By**

**Shwan Abdullah Hamad**

**BSc. Honours in  
Chemistry with Forensic Science and Toxicology**

**April, 2012**

“Concern for man and his fate must always form the chief interest of all technical endeavours. Never forget this in the midst of your diagrams and equations”

**Albert Einstein**

## **ACKNOWLEDGMENTS**

I would like to express my gratitude to my supervisor Dr Vesselin N. Paunov for all the help and guidance he provided for me throughout this research project. I also thank my industrial supervisor Dr Simeon D. Stoyanov from Unilever R&D Netherlands for useful comments and discussions.

Many thanks to colleagues and staff in Surfactants and Colloid Group at the University of Hull for their support and friendship.

I would also like to thank Mr Anthony Sinclair for his help with the SEM images, and Miss Lucy Besnard for her contribution in chapter 6 of this thesis.

I am very grateful to my family and friends for being very patient and supportive all the way.

I must thank Dr Amro Dyab for his guidance at the beginning of this research project. I also would like to thank Dr Mustafa Ozmen for his help with the preparation of magnetic nanoparticles.

Last but not least, my appreciation goes to EPSRC-UK and Unilever R&D Netherlands for providing funds for this PhD research project.

## **DEDICATIONS**

I dedicate this thesis to my parents, especially my wonderful mother, without her this was impossible.

I also dedicate this thesis to my son “Jino” and my beautiful daughter “Princess Lana”. They were the driving force behind my motivation and success.

## PUBLISHED ARTICLES AND PRESENTATIONS

Some of the contents of this thesis have been published as advanced articles in international journals and some have been presented in various events:

### Publications

- S. A. Hamad, A. F. K. Dyab, S. D. Stoyanov and V. N. Paunov. “Triggered release kinetics of living cells from composite microcapsules” *PCCP*, 2012, resubmitted after revision.
- S.A. Hamad, S. D. Stoyanov and V. N. Paunov, “Triggered Cell Release from Shellac-Cells Composite Microcapsules” *Soft Matter*, 2012, **8**, 5069-5077, DOI: 10.1039/C2SM07488E.
- S. A. Hamad, A. F. K. Dyab, S. D. Stoyanov and V. N. Paunov, “Encapsulation of living cells into sporopollenin microcapsules” *J. Mater. Chem.*, 2011, **21**, 18018-18023. DOI: 10.1039/C1JM13719K.

## **Conference presentations and activities**

- Chapters 3 and 4 of this thesis will be presented at Materials Research Society in Boston, Massachusetts, USA, 2012.
- Presented under the title of “Encapsulation of living cells in Sporopollenin microcapsules”, at 10<sup>th</sup> International Materials Chemistry Conference in Manchester, UK, 2011.
- Presented under the title of “Microencapsulation of probiotics” at 14<sup>th</sup> UK Polymer Colloids Forum in Cottingham village, Hull, UK, 2009.
- Presented under various titles at group seminars and departmental colloquia at the Department of Chemistry- University of Hull, UK, 2009-2012.
- Some of the contents of this thesis have been presented to a wider audience at Unilever-Vlaardingen, Netherlands on two occasions.

## **ABSTRACT**

Microencapsulation of living cells such as probiotic bacteria can be used for the protection of the cells from harsh conditions such as low pH and mechanical stress in the digestive system. In this thesis we demonstrate various novel strategies to microencapsulate living yeast cells as a model for probiotic bacteria. We prepared and used sporopollenin microcapsules to encapsulate yeast cells by compressing the sporopollenin particles into a pellet which was exposed to an aqueous suspension of yeast cells in the presence of a biocompatible surface active agent. We also demonstrate that the viability of the cells is preserved after the microencapsulation.

We fabricated novel shellac-yeast cells composite microcapsules programmed to release the cells upon change of pH in a narrow range. This was achieved by either spray drying or sprays co-precipitating dispersion of yeast cells in aqueous solution of ammonium shellac doped with a pH-sensitive polyelectrolyte. We also demonstrate that yeast cells retain their viability even when treated with aqueous solutions of low pH. In addition, the pH-triggered release of yeast cells from these composite microcapsules and their disintegration rates were investigated. We developed a theoretical model for the kinetics of yeast cells release from the microcapsules triggered by (i) pH change and (ii) the growth of the cells in a culture media.

In a separate strategy of microencapsulation of living cells, we used templates of Pickering emulsions stabilised with latex nanoparticles to fabricate colloidosomes loaded with viable probiotics. Depending on the method of transfer, we have shown that magnetic colloidosomes containing pH-sensitive polyelectrolyte loaded with living cells can be prepared using Pickering emulsion templates. In addition, we demonstrate two strategies to strengthen the stability of water-in-oil Pickering emulsion droplets by interlocking the adsorbed latex particle monolayer: by (i) using oppositely charged polyelectrolyte adsorption or (ii) using polyelectrolyte pre-coated yeast cells which act as cross-linkers inside the water-in-oil droplets.

Furthermore, we report the fabrication of 3 D multicellular cellosomes of living cells by using water-in-oil emulsion templates as intermediate. We have used two strategies to assemble yeast cells pre-coated with polyelectrolytes in water-in-oil emulsion

droplets stabilised with either surfactant or solid particles. The emulsion droplets containing oppositely charged yeast cells linked together by electrostatic interactions were shrunken to compact structures upon addition of dry octanol and subsequently transferred into water to fabricate cellosomes.

In summary, this thesis contributes an arsenal of new methods for microencapsulation of living cells for the purpose of their protection and triggered release. The results of this thesis can be used in the formulation of better probiotic products, protection and release of cells implants, tissue engineering and development of live vaccines.



## TABLE OF CONTENTS

<b>CHAPTER 1.</b>	<b>15</b>
<hr/>	
<b>1.1 General introduction and project aim</b>	<b>15</b>
<b>1.2 Encapsulation</b>	<b>15</b>
<b>1.3 Purpose of encapsulation process</b>	<b>17</b>
<b>1.4 Methods of microcapsules preparation</b>	<b>18</b>
<b>1.5 Materials used for microencapsulation</b>	<b>25</b>
<b>1.6 Encapsulation of cells and therapeutic drugs</b>	<b>27</b>
<b>1.7 Microencapsulation of probiotics</b>	<b>30</b>
1.7.1 Polymer Microspheres	33
1.7.2 Liposomes	33
<b>1.8 Lay out of the present thesis</b>	<b>34</b>
<b>CHAPTER 2.</b>	<b>36</b>
<hr/>	
<b>2.1 Materials and methods</b>	<b>36</b>
2.1.1 Materials	36
2.1.1.1 Water	36
2.1.1.2 Latex nanoparticles	36
2.1.1.3 Shellac	36
2.1.1.4 Sporopollenin microcapsules	36
2.1.1.5 Magnetic nanoparticles	37

2.1.1.6	Gelling agents	38
2.1.1.7	Oils	38
2.1.1.8	Alcohols	38
2.1.1.9	Surfactants	39
2.1.1.10	Polyelectrolytes	39
2.1.1.11	Buffers	39
2.1.1.12	General chemicals	40
2.1.1.13	Fluorescent dyes	42
<b>2.2</b>	<b>Methods</b>	<b>44</b>
2.2.1	Microscopy	44
2.2.1.1	Olympus BX51	44
2.2.1.2	Nikon Eclipse (Confocal) microscope	45
2.2.1.3	Scanning Electron Microscopy (SEM)	45
2.2.2	Haemocytometer	45
2.2.3	General equipments	46
2.2.4	Dispersing of yeast cells in milli-Q water	46
2.2.5	Preparation of culture media	46
2.2.6	Transfer of amidine latex nanoparticles into oil phase	47
2.2.7	Testing the viability of yeast cells using FDA solution	47
2.2.8	Coating yeast cells with polyelectrolytes	48
2.2.9	Preparation of magnetite nanoparticles	49
2.2.10	Preparation of sporopollenin microcapsules	49
2.2.11	Encapsulation of yeast cells in sporopollenin microcapsules	50
2.2.12	Growth process of yeast cells inside sporopollenin microcapsules using “in-gel” fermentation	50
		10

2.2.13	Encapsulation of magnetized yeast cells in sporopollenin microcapsules	51
2.2.14	Spray co-precipitating ammonium shellac solution/yeast cells formulation	51
2.2.15	Spray drying yeast cells/ammonium shellac solution formulation	52
2.2.16	Testing the viability of yeast cells inside the composite microcapsules	52
2.2.17	Disintegration of the microcapsules and triggered release of the cells	52
2.2.18	Preparation of Pickering emulsions stabilised with latex nanoparticles	53
2.2.19	Transfer of the w/o Pickering emulsion droplets into water	53
2.2.20	Preparation of w/o emulsion stabilised with oleic acid	54
2.2.21	Preparation of w/o emulsion stabilised by Span60	54
2.2.22	Fabrication of cellosomes from w/o Pickering emulsion templates	55
2.2.23	Transfer of w/o emulsion droplets into water using freezing process	56
2.2.24	Counting the numbers of released cells from composite microcapsules	56
<b>CHAPTER 3.</b>		<b>58</b>
<b>Encapsulation of living cells into sporopollenin microcapsules</b>		<b>58</b>
3.1.1	Introduction	58
3.1.2	Applications of sporopollenin microcapsules	60
3.1.3	Results and discussion	65
3.1.3.1	Growth of yeast cells in culture media	66
3.1.3.2	Yeast cells viability during the encapsulation process	66
3.1.3.3	Analysis of the cell intake of sporopollenin microcapsules	70
3.1.3.4	Encapsulation of magnetic yeast in sporopollenin	72
3.1.3.5	Examining cell activity inside sporopollenin microcapsules	74
3.1.4	Conclusions	77

**CHAPTER 4.** **78**

---

**Triggered Cell Release from Shellac-Cells Composite Microcapsules** **78**

4.1.1	Introduction	78
4.1.2	Results and discussion	80
4.1.2.1	Spray co-precipitating of yeast cells/ammonium shellac formulation into acetic acid	82
4.1.2.2	pH-triggered release of encapsulated living cells from the composite microcapsules	88
4.1.2.3	pH triggered release of cells from microcapsules based on doping of shellac with PAA.	94
4.1.2.4	Effect of pH on the disintegration time of shellac-yeast cells microcapsules and the cell viability	98
4.1.2.5	Growth triggered release of encapsulated living cells from composite shellac-yeast microcapsules in a culture medium	100
4.1.2.6	Fabrication of composite shellac/yeast cells microcapsules by spray co-precipitating with calcium chloride solution	103
4.1.2.7	Spray-drying of yeast cells/ammonium shellac formulation	105
4.1.2.8	Viability of yeast cells in acetic acid and calcium chloride solution	109
4.1.3	Conclusions	110

**CHAPTER 5.** **112**

---

**Fabrication of novel colloidosomes loaded with viable yeast cells** **112**

5.1.1	Introduction	112
5.1.1.1	Pickering emulsions as templates for colloidosomes	114
5.1.2	Results and discussion	123

5.1.2.1	Fabrication of gel-cored magnetic colloidosome from w/o Pickering emulsions templates	123
5.1.2.2	Transfer of the Pickering emulsion droplets into water	124
5.1.2.3	Viability of the yeast cells inside colloidosomes	125
5.1.2.4	Fabrication of colloidosomes interlocked with polyelectrolytes and polyelectrolyte pre-coated yeast cells	128
5.1.2.5	Transfer of w/o Pickering emulsion droplets into water using freezing process	135
5.1.3	Conclusions	140
<b>CHAPTER 6.</b>		<b>141</b>
<b>Fabrication of three dimensional living multicellular structures “Cellosomes”</b>		<b>141</b>
6.1.1	Introduction	141
6.1.2	Results and discussions	143
6.1.2.1	Fabrication of Cellosomes by templating w/o emulsions stabilised with oleic acid	144
6.1.2.1.1	Transfer of the fabricated multicellular structure from oil into water	147
6.1.2.2	Fabrication of cellosomes by templating w/o emulsions stabilised with Span60	151
6.1.2.2.1	Transfer of the shrunken water droplets containing bridged yeast cells to the water phase	153
6.1.2.3	Fabrication of cellosomes by adopting colloidosomes fabrication technique	155
6.1.2.4	Cellosomes based on water-in-octanol Pickering emulsions	161
6.1.3	Conclusions	164

**CHAPTER 7.** **165**

---

**Kinetics of triggered release of cells from composite polymer-cell microcapsules** **165**

7.1.1 Introduction 165

7.1.1.1 Theoretical Background 167

7.1.2 Results and Discussion 180

7.1.2.1 pH-triggered release of cells from shellac/cells microcapsules 180

7.1.2.2 Growth-triggered release of cells from shellac/cells microcapsules 184

7.1.3 Conclusions 186

**CHAPTER 8.** **187**

---

**Summary of main conclusions** **187**

**Future work** **190**

**Glossary** **191**

**References** **193**

# Chapter 1.

## 1.1 General introduction and project aim

The gastrointestinal microflora is an extremely complex ecosystem that coexists in equilibrium with the host.<sup>1</sup> Probiotics have beneficial effects for human being by prevention and treatment of specific pathological conditions.<sup>2</sup> Probiotic bacteria cannot survive harsh conditions such as low pH, and mechanical stress in the stomach. The aim of this PhD research project is to microencapsulate probiotic bacteria in various novel types of microcapsules to protect them from harsh conditions of low pH and mechanical stress, thus increasing their viability. We have developed and explored several methods for fabrication of microcapsules that can entrap the probiotics bacteria at low pH and release them at higher pH of approximately 8. In addition, we have used natural biomaterial sources to prepare and use naturally occurring sporopollenin microcapsules in encapsulation of probiotics.

## 1.2 Encapsulation

Encapsulation in general involves packaging of active ingredients such as dyes, proteins, vitamins, flavours and living cells inside a capsule or the pores of a gel or other porous media. Gibbs *et al.* defined encapsulation as a process which involves the coating or entrapment of a pure material or a mixture into another material. The coated or entrapped material is usually a liquid but can be a solid or a gas. It is also called core material, actives, fill, internal phase or payload, while the coating material can also be defined as capsule, wall material, membrane, carrier or shell.<sup>3</sup>

Vilstrup defined encapsulation as a process of creating a barrier to avoid chemical reactions and/or to enable the controlled release of the ingredients.<sup>4</sup> However, Champagne and Fustier defined encapsulation as a technology of packaging solid, liquid, and gaseous materials in small capsules that release their contents at controlled rates over prolonged of time.<sup>5</sup>

Encapsulation involves the incorporation of various ingredients within a capsule of approximately 5 to 300  $\mu\text{m}$  in diameter.<sup>6</sup> The accepted size range for capsules in order to be classified as microcapsules is not strictly recognised, but some researchers consider capsules smaller than 1  $\mu\text{m}$  as nano-capsules and capsules larger than 100  $\mu\text{m}$  as macrocapsules. Whereas, any capsules with size between 1- 100  $\mu\text{m}$  are called microcapsules.<sup>7</sup>

Encapsulation can have many different forms such as a membrane coating, a wall or a membrane of spherical or irregular shape, and multiwall structure.<sup>3</sup> The spherical geometry can have a continuous core region surrounded by a continuous shell, while an irregular geometry can contain a number of dispersed small droplets or particles of core material.<sup>4,7</sup> Capsules can be a solid as free-flowing powder or suspended in water, depending on the applications and the stability of the capsules and the encapsulated ingredients. They might have smooth or rough outer appearance too.

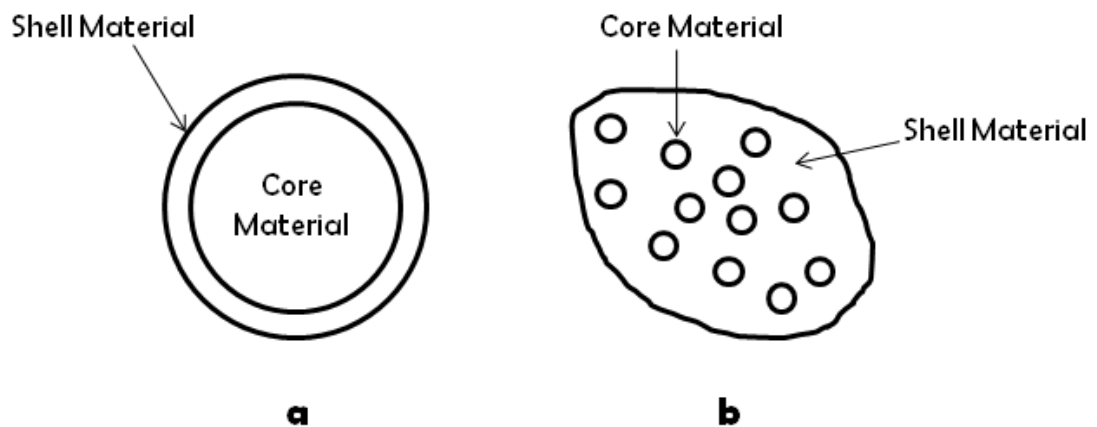


Figure 1.1: Schematic diagram of two representative types of microcapsules: (a) continuous core/shell microcapsule. (b) Multinuclear microcapsule. Reproduced from reference <sup>7</sup>



### 1.3 Purpose of encapsulation process

Gibbs *et al.* summarised the purpose of encapsulation as protection of its contents from the environment which can be destructive while allowing small molecules to pass in and out of the membrane.<sup>3</sup> Encapsulation can improve the retention time of the nutrient in food and allow controlled release at specific times, because some nutrient do not remain in food for a long time or may react with the other food components causing undesirable effects.<sup>8</sup>

Microcapsules should protect the active ingredient from its surrounding environment until an appropriate time or a triggering event. Then, the material escapes through the capsule wall by various means, including rupture, dissolution and changing pH and temperature. Microencapsulation offers many opportunities for exciting breakthroughs in medicine, cosmetic and industrial applications. It can be used in preventing chemical reactions, masking undesirable flavour, enhance stability of formulations, and to improve, control and delay delivery. It has been also used to encapsulate prescription drugs, over-the counter drugs, vitamins, living cells and minerals.<sup>3,9</sup> Varieties of core materials have been encapsulated in suitable microcapsules including adhesives, agrochemicals, live cells, active enzymes, flavours, pharmaceuticals and inks. Microcapsules are key components of all carbonless copy papers<sup>10</sup> and are present in oral and injected drug formulations. Microcapsules are also used for several long-acting commercial pesticide and herbicide products.<sup>7</sup>

Microencapsulation is becoming increasingly important for a wide variety of applications therefore, a versatile technique should be invented to produce capsules, whose size, permeability, mechanical strength and compatibility can be easily controlled. Control of the microcapsules size allows flexibility in applications and choice of encapsulated materials. Control of the permeability allows selective and timed release. Control of the mechanical strength allows the yield stress to be adjusted to withstand varying of mechanical loads and to enable release. Control of compatibility allows encapsulation of fragile and sensitive materials such as biomolecules and cells. Ideally, it should be feasible to construct microcapsules from

a wide variety of inorganic, organic or polymeric materials to provide flexibility in their uses.<sup>11</sup>

#### **1.4 Methods of microcapsules preparation**

Here we review in a brief format a variety of microencapsulation methods used in the literature to prepare microcapsules, several of which are applicable for microencapsulation of probiotics. To classify the methods of microcapsules preparation, one has to consider the nature of the phenomena that has been used to make the microcapsules. Generally the methods for preparing microcapsules are based on physical phenomena while, polymerisation reactions can be used to produce a capsule shell, or both physical and chemical phenomena can be combined together to prepare microcapsules. On that base some researchers classify methods of making microcapsules as chemical and mechanical process, whereas others just divide them into group A and group B processes.<sup>7</sup> Scientists have prepared microcapsules using both methods and variety ranges of chemical compounds including natural polymers have been employed.<sup>12</sup>

Chemical encapsulation (group A processes) can produce microcapsules which are found entirely in a liquid-filled stirred tank or tubular reactor; and itself can be classified into several subgroups. The first truly significant commercial product used microencapsulation was carbonless copy paper. The microcapsules for this product were made by complex coacervation, which involves the separation of a liquid phase of coating material from a polymeric solution and the wrapping of that phase as a uniform layer around the suspended core particles.<sup>10</sup>

Complex coacervation method is based on the capability of cationic and anionic water-soluble polymers to interact in water and form a liquid, polymer-rich phase called complex coacervate. This lays the foundations of complex coacervation process, which commonly uses gelatin as the cationic polymer and several other natural synthetic anionic water-soluble polymers interact with gelatin to form complex coacervates used for microencapsulation. The overall process includes several steps. The first step begins by dispersing the core material in an aqueous

gelatin solution this is normally done at 40-60 °C temperature range at which the gelatin solution is melted to liquid. After that the second step involves the addition of a polyanion or negatively charged polymer into the system. The pH and concentration of the polymer are adjusted in order that a liquid complex coacervate forms. Once the complex is formed, the system is then cooled to room temperature, and the gelatin in the coacervate gels and forms capsules with a very rubbery shell. Then the capsules are cooled further to 10 °C and treated with glutaraldehyde to increase the strength of the water swollen shell and create a thermally irreversible gel structure. The glutaraldehyde cross-links the gelatin by reacting with amino groups on the gelatin chain. In the final step, glutaraldehyde treated capsules can be dried in to a powder.<sup>7</sup>

The chemical understanding of the coacervation process is that the complex is in equilibrium with a dilute solution called the supernatant and this in return acts as the continuous phase while the complex coacervate acts as a dispersed phase. When a water-soluble core material is dispersed in the system and the complex coacervate wets this core material, each droplet or particle of dispersed core material is coated with a thin film of coacervate and when this liquid film is solidified, capsules are formed. The complex coacervation process has been used in the encapsulation of many water-immiscible liquids and is used in a variety of products, including inks for carbonless paper, perfume for industry inserts, and liquid crystals for display devices.<sup>7-8</sup>

The microcapsules produced by this technology are between 20-800 µm in diameter size range,<sup>3</sup> which contain 80-90 weight percent core material. The capsules are moisture sensitive. When stored at humidity above 70 % or immersed in water, the shell of the capsule swell greatly and facilitate the transport of material into or out of the capsules. Therefore, to reduce their moisture sensitivity, the capsules can be post-treated with urea and formaldehyde under acidic conditions.<sup>13</sup>

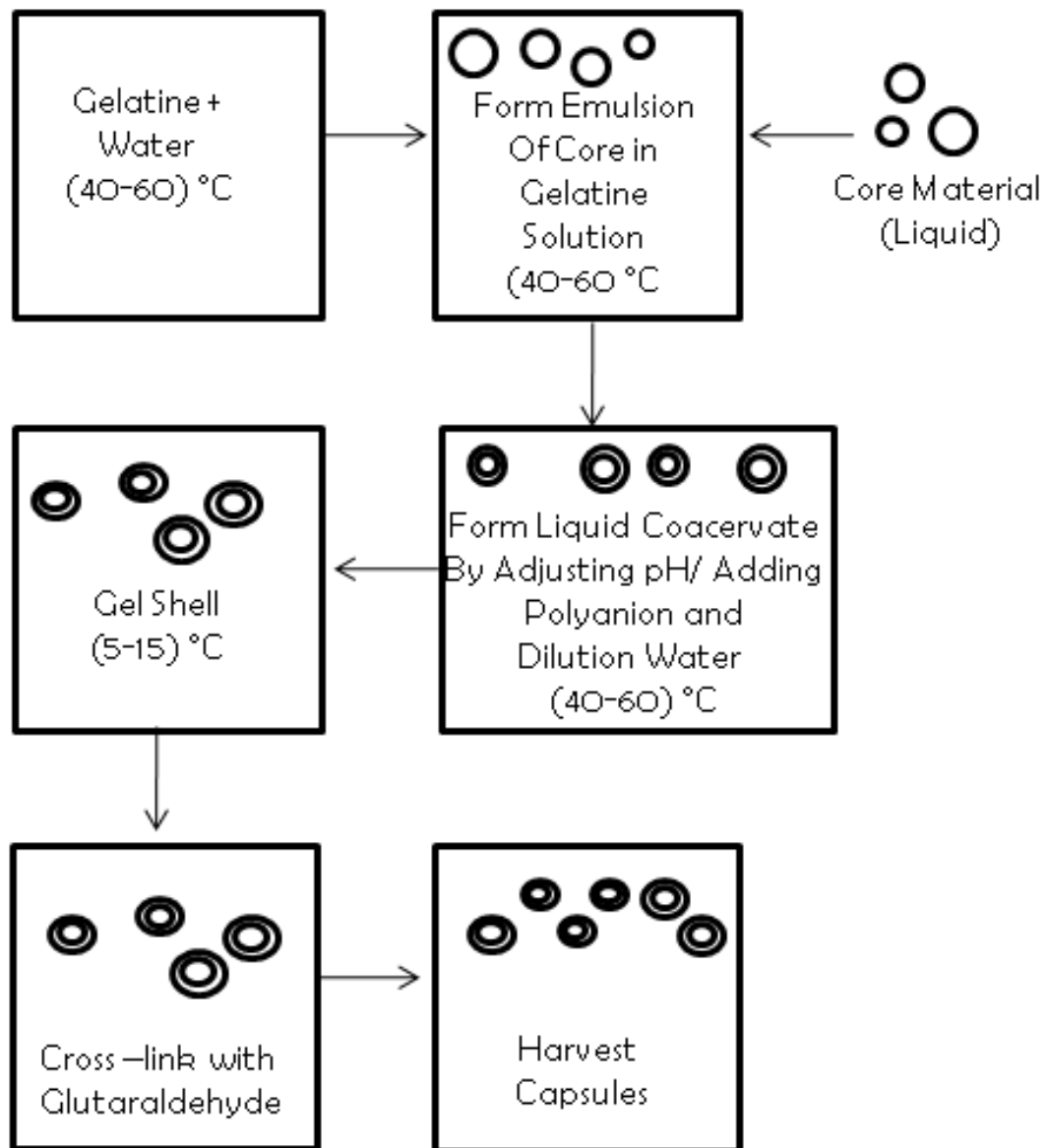


Figure 1.2: Schematic flow diagram of encapsulation process based on complex coacervation. Reproduced from reference <sup>7</sup>.

Polymer-polymer incompatibility method is based on incompatibility of two incompatible polymers which dissolve in a common solvent and do not mix in solution, as they essentially phase separate into two different liquid phases, one rich in one polymer, and the other phase is rich in the other polymer. This phenomenon can be exploited to make microcapsules by using one of the incompatible polymers to act as the capsule shell.<sup>7</sup> In a general example, the process starts with dispersing the core material in a hot (80 °C) solution of ethylcellulose in cyclohexane, and an addition of low molecular weight polyethylene into the system. Polyethylene is a polymer soluble in hot cyclohexane and incompatible with ethyl cellulose; this induces phase separation with formation of ethyl cellulose-rich phase and a polyethylene-rich phase, then a core material which is a solid unaffected by 80 °C cyclohexane is dispersed in this two-phase system. Ethyl cellulose is more polar than polyethylene; therefore, it adsorbs preferentially on the surface of the core material and produces a thin coating of the shell material around the particles of the core material. To solidify the ethyl cellulose solution and forming solid microcapsules, the system then cooled down to room temperature and the ethyl cellulose precipitates.<sup>7</sup>

Several commercially encapsulated pharmaceutical products are produced by this method.<sup>14</sup> Aspirin and potassium chloride are two examples of encapsulated pharmaceuticals based on polymer-polymer incompatibility technique. Polymer-polymer incompatibility process is generally performed in organic solvents and is used for encapsulation of solids with a degree of water solubility. The majority of capsules that have ethyl cellulose shell are irregularly shaped with 200-800 µm in diameter and are loaded with solid drug particles, or used for taste masking and increasing oral drug delivery.<sup>15</sup>

Interfacial polymerisation technique was evolved to be a versatile technology able to encapsulate a variety of core materials, including aqueous solution, water-immiscible liquids and solids. The particular feature of this technology is that the capsule shell is formed at or on the interface of droplets or particles by utilising polymerisation of reactive monomers. In this technique many types of interfacial polymerisation reactions are used. The process involves the dissolution of a multifunctional monomer in the liquid core material and then the solution is dispersed to the desired drop size in an aqueous phase that contains a dispersing agent. Then a rapid polymerisation

reaction at the interface generates the capsule shell by an addition of a co-reactant, usually a multifunctional amine into the aqueous phase. If the reaction uses isocyanate and an amine, then a polyurea capsule shell is produced, but if an acid chloride and an amine are used, then the result is a polyamide or nylon capsule.<sup>16</sup>

“*In situ*” polymerisation is another method which is closely related to interfacial polymerisation in a way that it involves the formation of capsules because of polymerisation of monomers added to the encapsulated reactor. However, with “*in situ*” polymerisation, reactive agents have not been added to the core material and polymerisation happens in the continuous phase and on the continuous phase side of the interface formed by the dispersed core material and continuous phase. When polymerisation begins, a low molecular weight pre-polymer is produced and this pre-polymer grows in size and deposits on the surface of the dispersed core material being encapsulated. As polymerisation with cross-linking continues to occur, it generates a solid capsule shell. Cakshae *et al.* in 1985 first reported the formation of microcapsules loaded with water-immiscible liquids with shells formed by the reaction of urea with formaldehyde in aqueous media at acidic pH.<sup>16b,c,17</sup>

The process of mechanical encapsulation method normally involves using mechanical phenomena to produce microcapsules loaded with designed core material; therefore, the principal means by which this type of microcapsules are made are centrifugal force, extrusion, co-extrusion, and formation of sprays. This type of encapsulation process is predating chemical encapsulation process as it was developed in 1930s.<sup>18</sup>

The first one to be invented was spray drying which generally involves the emulsification or dispersion of core material in a concentrated (40-60 weight percent solid) solution of shell material. The droplets produced normally have diameters of 1-3  $\mu\text{m}$ . The core materials can be water-immiscible liquids and the shell material is usually a soluble polymer. The emulsion droplets are then passed into the heated chamber of a spray drier, where they rapidly dehydrate and then produce dry capsules. The capsules are harvested in the bottom of the spray-drying chamber.<sup>7-8,16b,19</sup> Another form of spray drying includes atomising a liquid mixture in a vessel with a nozzle or spinning wheel and the solvent is then evaporated by contacting with hot air or gas. The resulting particles are then collected after their sedimentation.<sup>12,16d,20</sup>

Freeze-drying is performed by freezing probiotics in the presence of carrier material at low temperatures, followed by sublimation of the water under vacuum. In this way, water phase transition and oxidations are avoided. The addition of cryoprotectant helps to retain probiotics activity upon freeze-drying and stabilise them during storage. Vacuum drying is a similar process as freeze-drying but it takes place at 0-40 °C for 30 min to a few hours. The advantages are that the products are not frozen, which prevents freezing damage and energy consumption, and that the drying is fast.<sup>16d,19</sup>

In spray-cooling, a molten matrix with low melting point containing any bioactive compound is atomised through a pneumatic nozzle into a vessel. This process is similar to spray-drying with respect to the production of fine droplets. However, it is based on the injection of cold air into the vessel to enable solidification of the gel particles rather than on hot air which dries the droplets into fine powder particles. The liquid droplets solidify and entrap the bioactive product.<sup>5,12</sup>

Meanwhile, in fluidised bed coating a liquid coating material is sprayed through a nozzle over the core material in a hot environment. The film formation then begins, followed by successive wetting and drying or solidification stages which results in a solid, homogenous layer on the surface of a core. The small droplets of the sprayed liquid contact the particle surface, spread on the surface and coalesce. The spray liquid, also referred as shell, wall or coat material can be a solution, a suspension, an emulsion or a melt. Any edible material with a stable molten phase can be sprayed at high deposition rates, allowing coatings with a thickness of 100 µm up to 10 mm. The coating material can be injected from many angles and this influences the properties of the coating.<sup>3,7-8,12</sup>

In extrusion method a jet of core liquid is surrounded by a sheath of wall solution or melt. The liquid breaks into droplets core coated with wall solution as the jet moves through the air. The molten wall may be solidified or a solvent may be evaporated from the wall solution.<sup>7,12,16b,16d</sup> Extrusion is the oldest and most common method for making capsules with hydrocolloids.<sup>21</sup> In addition it is a simple and cheap method that uses a gentle operation which causes no damage to encapsulants.<sup>22</sup> (see Figure 1.3 for more details).

Emulsification Technique involves homogenising a mixture of small volume of the encapsulant in a polymer suspension into a larger volume of a vegetable oil to form a w/o emulsion. Then, the water soluble polymer is cross-linked to form tiny gel particles within the oil phase. The beads are collected by filtration later on. The method of cross-linking depends on the type of the supporting material used. The size of the beads can be controlled by the speed of homogenisation, and can range from 25  $\mu\text{m}$  to 2 mm.<sup>23</sup> (see Figure 1.4 for more details).

Lacroix *et al.* and Audet *et al.* have both used emulsification technique to successfully encapsulate lactic acid bacteria in both batch and continuous fermentation respectively.<sup>24</sup>

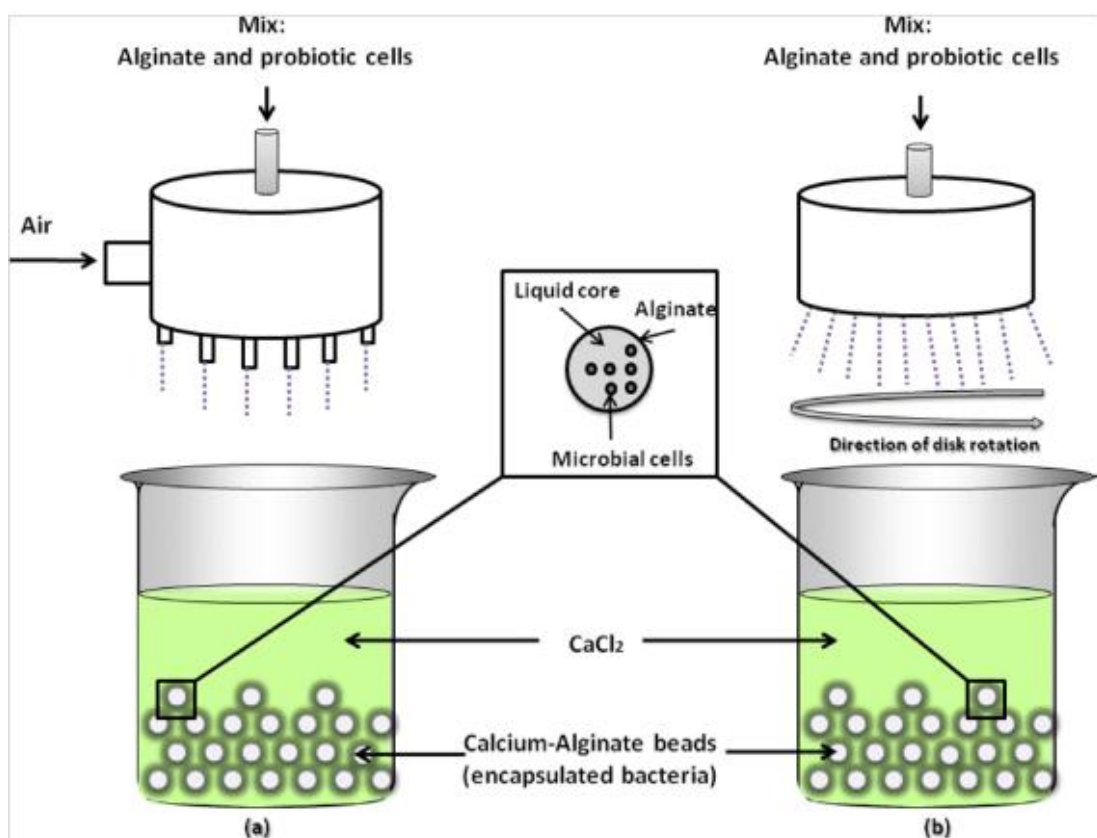


Figure 1.3: Extrusion technologies: simple needle droplet-generator that usually is air driven (a) and pinning disk device (b). The probiotic cells are added to the hydrocolloid solution and dripped through a syringe needle or a nozzle spray machine in the form of droplets which are allowed to free-fall into a hardening solution such as calcium chloride.<sup>16d</sup>



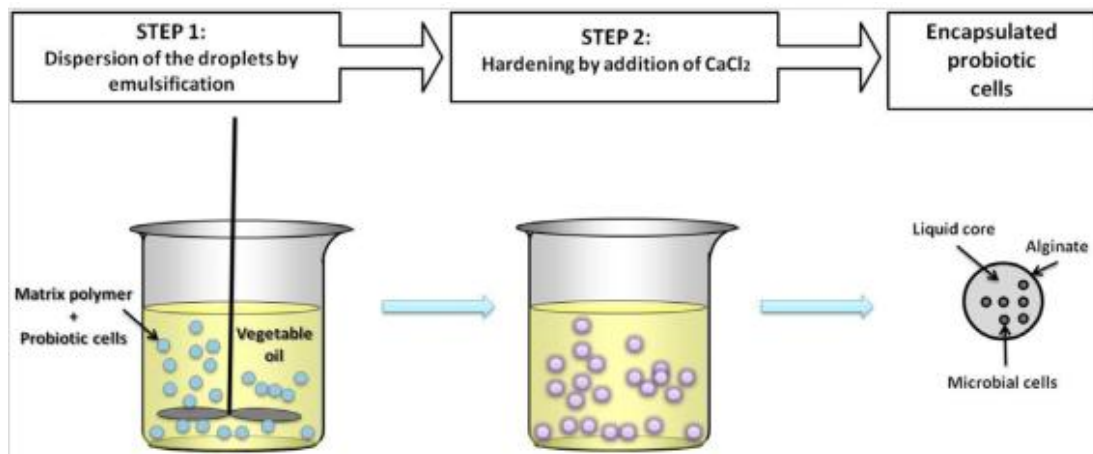


Figure 1.4: Schematic presentation of the emulsification procedure. A small volume of the cell-polymer suspension (i.e., the discontinuous phase) is added to a large volume of vegetable oil (i.e., the continuous phase). The mixture is then homogenized to form a water-in-oil emulsion. Once the water-in-oil emulsion is formed, the water-soluble polymer must be insolubilised to form tiny gel particles within the oil phase.<sup>16d</sup>

## 1.5 Materials used for microencapsulation

Sultana *et al.* incorporated Hi-Maize starch into alginate solution for the purpose of encapsulation of probiotic bacteria. They reported an improvement in the viability of probiotic bacteria compared to when the bacteria were encapsulated without the starch. The survival of the bacteria was also increased at  $-20\text{ }^{\circ}\text{C}$  by inclusion of glycerol ( cryo-protectant) with alginate mix.<sup>25</sup>

Alginates are naturally derived linear copolymers of 1, 4-linked  $\beta$ -D-mannuronic acid (M) and  $\alpha$ -L-guluronic acid (G) residues.<sup>16d</sup> Aqueous solutions of polysaccharides form hydrogel in the presence of divalent calcium ions via ionic interactions between the acid groups on G blocks and the bridging ions. As a result, calcium alginate gels are physically cross-linked polymers with mechanical and hosting properties dependent on the alginate composition.<sup>12</sup> Alginate hydrogel are extensively used in cell encapsulation.<sup>26</sup> Calcium alginate is preferred for encapsulation because it is simple, non-toxic, biocompatible, and cheap.<sup>22</sup>

Alginate hydrogel beads produced by mixing a suspension of the encapsulant with a solution sodium alginate solution, and then the mixture dripped into a solution of multivalent ions such as calcium chloride. The encapsulant is entrapped in the gel spheres instantaneously in a three-dimensional lattice of ionically cross-linked alginate.<sup>3,19,22,27</sup>

Cook *et al.* have produced alginate gels by external gelation, followed by subsequent dip-coating into chitosan solution. The polymers associated via electrostatic interactions between the acid and amine groups. The microcapsules are suitable for enteric delivery because the alginate microcapsules will form acid gels at low pH of (2-5). However, at higher pH values of approximately 7 in the intestine, and higher amount of phosphates should result in the dissolution of the microcapsules. Alginate microcapsules coated with chitosan improved the survival of *B. Breve* during exposure to stimulated gastric juice.<sup>28</sup>

Due to its favourable properties, such as good biocompatibility, biodegradability, and non-toxicity, chitosan is an important biomaterial in food and pharmaceutical applications.<sup>12,19</sup> Chitosan is a positively charged linear polysaccharide formed by deacetylation of chitin. It is soluble in water below pH 6 and forms a gel by ionotropic gelation. Chitosan, a polycation with amine groups, can be cross-linked by anions or polyanions, such as polyphosphates, polyaldehydic acid.<sup>16d,22,29</sup>

Talwalkar and Kailasapathy produced alginate-starch gel beads by dropping a mixture of alginate-starch-bacteria into a calcium chloride coagulation bath. They found that encapsulation prevented cell death from oxygen toxicity.<sup>30</sup> Starch is a polysaccharide consisting of large number of glucose units joined together by glucosidic bonds. It consists mainly of amylose. Resistant starch cannot be digested by pancreatic enzymes and can reach the colon where it will be fermented.<sup>19</sup> This property provides good enteric delivery characteristic of starch.<sup>3,16d</sup>

Other materials that have been used for microencapsulation include gelatine and  $\kappa$ -carrageenan which is a natural polysaccharide extracted from marine macroalgae and used as food additives. The polymer dissolves at high temperature (60-80 °C) in concentrations of (2-5 % wt.).<sup>31</sup>

The procedure for encapsulation using carrageenan includes adding the encapsulated slurry to heat-sterilised carrageenan solution at 40-45 °C (dependent on the type of the encapsulant). Gelation occurs by cooling to room temperature. Dropping the mixture of the encapsulant and the polymer into a solution of potassium chloride resulted in formation of the beads.<sup>19</sup>

## **1.6 Encapsulation of cells and therapeutic drugs**

Many diseases are closely tied with deficient or subnormal metabolic cell functions. Hemophilia, Parkinson's disease, diabetes and hepatic failure belong to this kind of degenerative and disability disorder. Milder forms of these diseases can be managed with treatments but it is complicated to mimic the precise regulation and the complex roles of the hormones, factors, or enzymes that are not produced by the body. Production of therapeutic drugs by encapsulated cells can be an answer for treatment of chronic diseases. Cell encapsulation technology is based on the immobilisation of cells within a semi permeable membrane. This membrane protects the cells from both mechanical stress and the host's immune system while allowing diffusion of nutrients, oxygen and waste as can be seen in Figure 1.5. This can result in a reduction or even lack of chronic administration of immunosuppressant, which is an important issue to be considered in organ transplantation. Encapsulation of cells allows the delivery of the product for a longer period of time as cells release the products continuously. Moreover, cell encapsulation allows the transplantation of non-human cells which could be considered as an alternative to the limited supply of donor tissue.<sup>32</sup>

Diaspro *et al.* have encapsulated single living yeast cells by the alternate adsorption of oppositely charged polyelectrolyte. They have demonstrated that after encapsulation, cells preserve their metabolic activities and they are still able to divide.<sup>33</sup>

Dusseault *et al.* described a method for microencapsulation of living cells in alginate-poly-L-lysine (PLL)-alginate membranes with covalent links between adjacent layers of microcapsules membranes, while preserving the desired membrane molecular weight cut-off and cell viability. They immobilised islets of Langerhans in alginate beads by using N-5-azido-2-nitrobenzoyloxy succinimide (ANB-NOS) as a cross

linker, where N-hydroxy succinimide ester group was covalently linked to PLL. The microcapsules are very unlikely to be damaged or destroyed in the environment found in the living body. In addition to protect the transplant from the recipient immune system, these microcapsules can protect the recipient from the risks associated with the transplant.<sup>34</sup>

In this present thesis we have used yeast cells as a model for probiotics cells because they are extremely important as model organism in modern cell biology research, and are the most thoroughly researched eukaryotic microorganism. They are robust, easily obtained and handled in research laboratories. They are classified in the kingdom of Fungi, and most of them reproduce asexually by budding. Yeast cells are unicellular, although some species with yeast forms may become multicellular through the formation of a string of connected budding cells. Yeast cell size can vary greatly depending on the species, typically measuring 3-4  $\mu\text{m}$  in diameter, although some yeast cells can reach over 40  $\mu\text{m}$ . Yeast is found in the stomach and the colon. The presence of yeast cells can only explain their resistance to pH variation. Most yeast cells can grow at pH 3, and some species can tolerate highly acidic conditions with a pH as low as 1.5.<sup>1</sup> The yeast species *Saccharomyces Cerevisiae* has been used in baking and fermenting of sugars for alcoholic beverages for thousands of years.

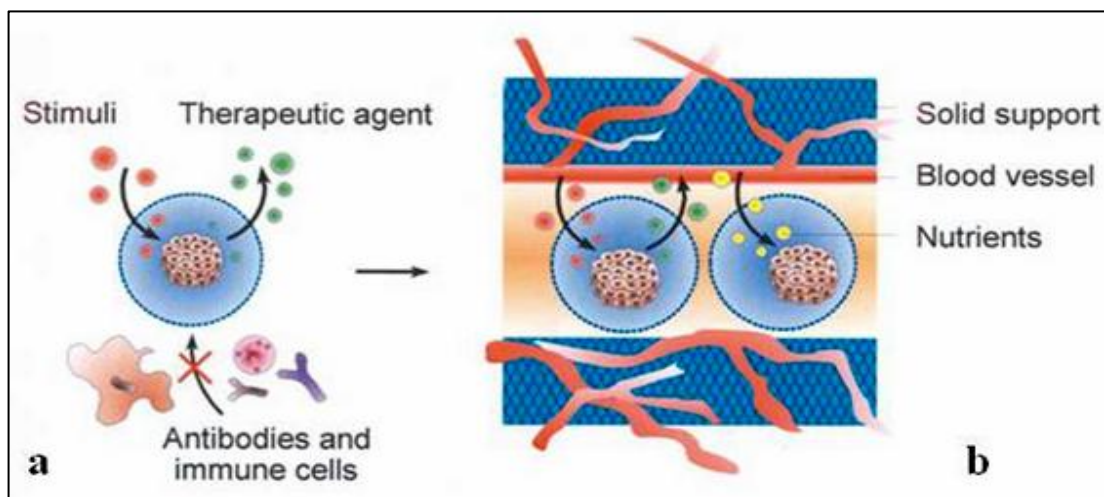


Figure 1.5: Cell microencapsulation. (a) Nutrients, oxygen and stimuli diffuse across the membrane, whereas antibodies and immune cells are excluded. (b) Pre-vascularised solid support system to facilitate optimal nutrition of the enclosed cells.<sup>35</sup>

Budding is the most common mode of vegetative growth in yeasts and multilateral budding is a typical reproductive characteristic of ascomycetous yeasts, including *Saccharomyces Cerevisiae*. Yeast buds are initiated when mother cells achieve a critical cell size at a time coinciding with the beginning of DNA synthesis. The ultimate goal of yeast cell division is to separate mother and daughter cells into two individual units with appropriately segregated sets of chromosomes, organelles and vesicles. Once all mitotic events have been completed, protein complexes at the division site act in a dynamic way to complete cell division. This is followed by a localized weakening of the cell wall and this, together with tension exerted by turgor, allows extrusion of cytoplasm into an area bounded by new cell wall material. The regulation of particular cell wall synthetic enzymes and transport of specific bud plasma membrane receptors are key steps in the emergence of a bud. Chitin forms a ring at the junction between the mother cell and forms the so-called bud scar and birth scar at the surface of the daughter. During bud formation, only the bud but not the mother cell will grow. Once mitosis is complete and the bud nucleus and other organelles have been migrated into the bud, cytokinesis commences and a septum is formed in the neck between mother and daughter. In *Saccharomyces cerevisiae*, cell size at division is asymmetrical with buds being smaller than mother cells when they separate.<sup>36</sup>

Meanwhile, encapsulation of therapeutic drugs into microcapsules provides several advantages over traditional formulations. Prior to release, the physical barrier provided by the encapsulation device protects the drug from degradation or premature metabolism. Release of the therapeutic products can be technologically controlled in order to achieve different kinetic profile. An ideal system should be able to achieve an effective drug concentration at the target tissue for an extended period of time. In addition, the system should provide a tight control over the device in case of side-effects. The small size (100-500  $\mu\text{m}$ ) of the capsules allows their implantation in close contact to the blood stream, which could be beneficial in specific applications for the long-term functionality of the enclosed cells due to an enhanced oxygen transfer into the capsules.<sup>32</sup>

## 1.7 Microencapsulation of probiotics

Probiotics have been defined by scientists in numerous ways such as being “mono or mixed cultures of live micro-organisms which, when applied to a man or animal, beneficially affect the host by improving the properties of the indigenous microflora”<sup>37</sup> or as viable microorganisms that when ingested have a beneficial effect in the prevention and treatment of specific pathological conditions.<sup>2</sup> Del Piano *et al.* believed that probiotics are living microorganisms which survive gastric, bile, and pancreatic secretions, attach to epithelial cells and colonise the human intestine.<sup>38</sup>

The population of living microorganisms in an adult human intestine was estimated to be more than 400 different bacterial species and approximately  $10^{14}$  bacterial cells.<sup>39</sup> The bacterial cells are classified into beneficial, neutral, and harmful, with respect to human health. Yeast are part of the residual microflora that makes up < 0.1 % of microbiota, but their diameter is 10 times larger than that of bacteria and they could represent a significant steric hindrance for bacteria.<sup>40</sup> The third most common genus in the gastrointestinal tract represented by *Bifidobacteria*, whereas, 86 % of the flora in the adult gut is predominantly *Bacteroides* followed by *Eubacterium*. Different factors such as weaning, ageing, stress, diet, drugs, bacterial contamination and constipation affect the intestinal microflora by decreasing the number of *Bifidobacteria* and increasing certain kinds of harmful bacteria.<sup>12</sup>

The beneficial effect and therapeutic applications of probiotic bacteria in humans claimed by scientists include maintenance of normal intestinal microflora, improvement of constipation, treatment of diarrhoea, enhancement of the immune system, reduction of lactose-intolerance, reduction of serum cholesterol levels, anticarcinogenic activity, and improved nutritional value of foods.<sup>16a,17,33,41</sup> The mechanism by which probiotics have their effect on the host may involve modifying gut pH, antagonising pathogens through production of antimicrobial and antibacterial compounds, competing for pathogen binding and receptor sites, as well as for available nutrients and growth factors, stimulating immunomodulatory cells and producing lactose.<sup>42</sup>

Probiotics products are available in the market in the form of milk, drinking and frozen yogurts, probiotic cheeses, ice-creams, spreads and fermented soya products. International standards require that products claimed to be probiotics products contain a minimum of  $10^7$  viable probiotic bacteria per gram of product.<sup>43</sup> Despite the important role of these probiotic bacteria, their beneficial effects is dependent on their survival in the harsh stomach conditions such as low pH of 2.5 to 3.5, presence of aggressive intestinal fluids ( e.g. bile and pancreatic juice), short transit time in duodenum, and mechanical stress which creates a hostile environment for probiotics survival. To protect probiotics from chemical and biological conditions in the GI tract and increase their viability, and provide sufficient amount of these probiotics in the lower intestine, a technique had to be developed.<sup>44</sup>

Microencapsulation technology has been invented and successfully applied to protect probiotics from such conditions caused by the external environment<sup>12</sup>. Different types of encapsulating materials have been used to trap probiotics bacteria. However, the most popular encapsulating material is alginate because it has the benefits of being nontoxic and being readily available. This method is routinely used to generate 20-30  $\mu\text{m}$  in diameter capsules loaded with pesticides and herbicides as well as that it has been used to prepare 3-6  $\mu\text{m}$  in diameter carbonless paper ink microcapsules.<sup>45</sup> Several microcapsules loaded with core materials of biological interest e.g. active enzymes have also been generated with this particular technique.<sup>46</sup>

Cook *et al.* produced alginate, and alginate-chitosan microcapsules loaded with dry probiotics in a matter of scalable and uniform, granular product by a drying method. The microcapsules were shown to improve the survival of the encapsulated probiotics during exposure to stimulated gastric juice.<sup>28</sup> Ding and Shah developed a method for applying an extra coating of palm oil and poly-L-lysine (POPL) to alginate (ALG) microcapsules to enhance the survival of probiotic bacteria. Eight strains of probiotic bacteria were encapsulated using both alginate alone and alginate with (POPL). The results were shown that alginate microcapsules can protect probiotic bacteria from acidic conditions and bile salts. However, POPL microcapsules provided better protection.<sup>45</sup>

Kailasapathy investigated the effect of incorporating microencapsulated probiotics cultures with encapsulant polymers such as alginate and starch and their effect on the survival of the probiotics cultures in yoghurt. The results showed that the addition of probiotics cultures either in the free or encapsulated forms tend to slow down the postacidification during storage of yoghurt. Microencapsulation enhanced the survival of probiotics cultures compared to free cells in yoghurt stored over 7 weeks. Addition of probiotics capsules didn't change the appearance, colour, acidity, flavour, and after taste attributes of the yoghurt, however, significantly altered the textural properties (smoothness) of yoghurt, which might occur because of the production of EPS (Exopolysaccharide) by the probiotics cultures, incorporation of sodium alginate and filler material (starch).<sup>47</sup> The other materials that have been used in the process of encapsulation of probiotics include,  $\kappa$ -Carrageenan, Chitosan.<sup>47</sup>

Probiotics in any food products from the time of production, processing and consumption need to be protected against: high temperature and shear, moisture, oxygen, most importantly degradation in the stomach especially the low pH, and bile salts. Several reviews<sup>3,16b,16d,19,22,38,43,48</sup> collected and presented the methods of probiotics encapsulation.

Natural examples of encapsulation include bird's egg shells, plant seeds, bacterial spores, skin and seashells.<sup>3</sup> However, various types of means for probiotic encapsulation have been developed artificially by using different types of natural and synthetic polymer materials, colloidal particles, lipids, and other organic and inorganic materials. Examples of those encapsulation vesicles are polymer microspheres, liposome, sporopollenin microcapsules, colloidosomes, and cellosomes. The definition, method of preparation, and applications of sporopollenin microcapsules, composite microcapsules, colloidosomes, and cellosomes are explained in chapters, 3, 4, 5, and 6 of this thesis, however, below we have briefly described polymer microspheres and liposome.



### 1.7.1 Polymer Microspheres

One of the methods of microsphere preparation is solvent evaporation method. The method depends on the hydrophobicity and hydrophilicity of the encapsulant. For hydrophobic active (drug) o/w emulsion method is widely used. This method includes four main steps, first the hydrophobic drug is dissolved in an organic solvent containing a polymer material, then the dispersed phase (organic) is emulsified into the continuous phase (aqueous). The third step involves the evaporation of the solvent in the dispersed phase through the continuous phase which transforms the droplets of the dispersed phase into solid particles. Finally, the microspheres recovered and dried to remove residual solvent. For hydrophilic drugs, alternative methods such as w/o/w double emulsion system has been proposed, where the aqueous solution of hydrophilic drug is emulsified with organic phase to yield w/o emulsion, which in return is dispersed into a second solution to prepare w/o/w double emulsion.<sup>49</sup>

PLGA (poly lactic-co-glycolic acid) is frequently used as the polymer for microsphere preparation by solvent evaporation, because of its biodegradable properties. Methylene chloride is the most used solvent, and the reason for that is because it is highly volatile and capable of dissolving many polymers.<sup>49a</sup>

### 1.7.2 Liposomes

Liposomes are single or multi-layered spherical lipid bilayers, which involve the complete enclosure of an aqueous phase within phospholipids, based membrane.<sup>50</sup> When phospholipids are dispersed in an aqueous media, liposomes spontaneously form.<sup>51</sup> The hydrophilic part of the phospholipids associated themselves with the aqueous media, and the hydrophobic groups interact with other hydrophobic moieties of other lipid molecules. A very stable capsule forms as the lipid bilayer sheet formed folds into a spherical shape. Separately, both aqueous and lipid-soluble materials can be entrapped in liposomes.<sup>3,8</sup> The size of liposomes can range from a few tens of nanometres to several microns.<sup>51</sup> Negatively charged phospholipids, lecithin, and cholesterol produce the most stable liposomes, which can be prepared by the dehydration-rehydration method as long as organic solvents are not used.<sup>3,8</sup> King *et al.* encapsulated ascorbic acid in liposomes with high efficiency and stability.<sup>52</sup> Liposomes have been used for delivery of vaccines, hormones, enzymes and vitamins into the body.<sup>53</sup>

## 1.8 Lay out of the present thesis

This thesis is presented in 8 chapters, and every chapter include a short introduction of the subject. In Chapter 2 all the different materials that have been used during this research project are described. In addition, Chapter 2 contains the detailed description of the methods associated with most of the work in this thesis; however, each separate chapter contains more specific details of the experimental procedures.

In Chapter 3, sporopollenin microcapsules were prepared in-house by alkaline extraction, and were also used for encapsulation of living yeast cells. The cell intake by the microcapsules was observed by using scanning electron, and confocal laser fluorescence microscopy. Viability of the encapsulated cells was tested by using “in-gel” growth experiment.

In Chapter 4, formulations of yeast cells/ammonium shellac solution in various ratios and concentrations were either spray dried or spray co-precipitated to fabricate composite shellac/yeast cells microcapsules. The morphology of the microcapsules was observed by optical, confocal and scanning electron microscopy. The viability of the yeast cells inside the composite microcapsules was tested by treating the cells with fluorescein diacetate (FDA) and live/dead kit and observing them by confocal and optical fluorescence microscopy. Meanwhile, the rate of microcapsules disintegration and release of the cells in aqueous solution of 0.1 M sodium bicarbonate at different pHs were examined. The kinetics of cells release upon pH-trigger and growth-trigger is also explored.

In Chapter 5, we encapsulated yeast cells in colloidosomes fabricated by templating w/o Pickering emulsions stabilised with amidine functionalised polystyrene latex nanoparticles. The water phase contained either native or polyelectrolyte pre-coated yeast cells. Various techniques were used to interlock the adsorbed nanoparticles at the interface, such as cross-linking with oppositely charged polyelectrolytes, or using anionic pre-coated yeast cells. To enhance the stability of the water droplets and hence, increase the efficiency of transferring w/o droplets from oil phase into water to yield colloidosomes, the aqueous core of the droplets contained either magnetic

nanoparticle to be manipulated by external magnetic field, or gelled up with the help of temperature sensitive gel such as agarose.

Chapter 6 includes the fabrication of three-dimensional multicellular structures of living cells resembling cellosomes by using w/o emulsion templated stabilised with either surfactant or solid nanoparticles. The w/o emulsion droplets which were used in the building blocks of the multicellular structures contained living yeast cells and transferred into water from the oil phase by using the freezing process.

In Chapter 7 we develop a theoretical model of the kinetics of cell release from composite shellac/cell microcapsules discussed in chapter 4.

Chapter 8 includes the summary of the main achievements and conclusions of this thesis.

## **Chapter 2.**

### **2.1 Materials and methods**

#### **2.1.1 Materials**

##### **2.1.1.1 Water**

Water was purified by reverse osmosis and by passage through a Milli-Q reagent water system (Millipore, UK). Surface tension was typically measured between (71.5 and 72.5 mN/ m) at 25 °C, and the measured resistivity always exceeded 18 m Ω/cm.

##### **2.1.1.2 Latex nanoparticles**

Cationic 0.3 μm (4 % w/v) polystyrene latex particles which have surface functionality of amidine (CH<sub>3</sub>C (NH)-NH<sub>2</sub>) groups were purchased from Invitrogen, Molecular Probes USA. They were transferred into oil by using ethanol as intermediate solvent.

##### **2.1.1.3 Shellac**

Shellac is biocompatible and biodegradable polyester produced from self-esterification of a mixture of polyhydroxy acids such as polyhydroxy polycarboxylic esters. It is insoluble in aqueous solution at neutral pH; therefore it was used in a soluble form of ammonium salt at pH > 7 which is commercially available as SSB Aqua Gold (solid content 25 % wt.). The alkaline solution was a gift from HARK Group, Germany.

##### **2.1.1.4 Sporopollenin microcapsules**

Sporopollenin microcapsules were prepared in house by phosphoric acid extraction from *Lycopodium Clavatum* pollen grains powder purchased from Fagron UK; the procedure was invented by Barrier *et al.*<sup>9a</sup>

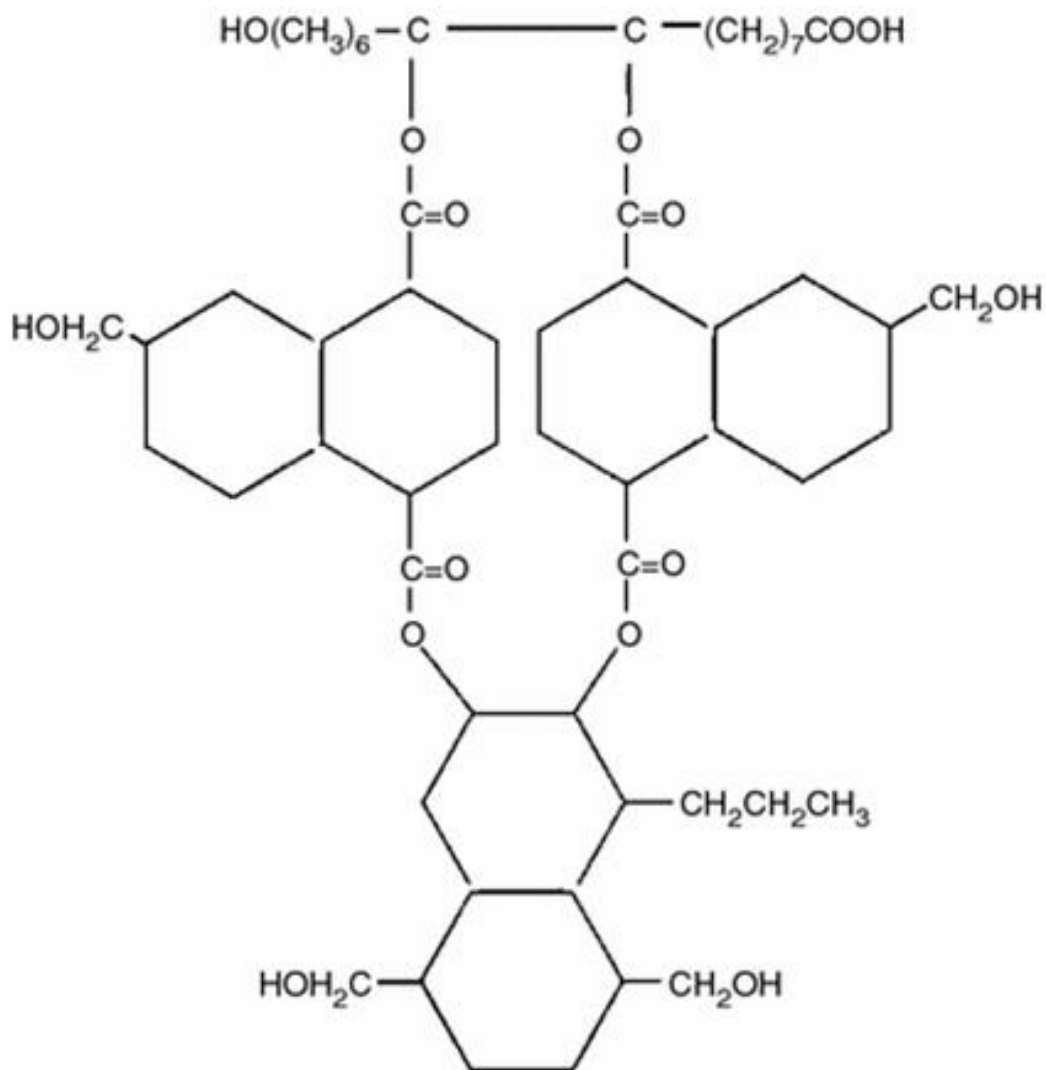


Figure 2.1: Simple structure of one of the main components of shellac.<sup>54</sup>

### 2.1.1.5 Magnetic nanoparticles

Magnetite nanoparticles were produced by the procedure published in a paper by García-Alonso *et al.*<sup>55</sup>. Iron (II) Chloride (99 %), and Iron (III) chloride (99 %) were used as purchased from Sigma-Aldrich; and ammonia (99.99 %) was purchased from Sigma-Aldrich.

### 2.1.1.6 Gelling agents

In some of the experiments gelling agents such as oxidised starch and agarose were used. Oxidised starch (Perfectamyl gel food grade modified starch E1404) was purchased from AVEBE in Netherlands. It was used in the process of in-gel growing encapsulated yeast cells inside *Lycopodium Clavatum* sporopollenin microcapsules. Agarose with low melting point for electrophoresis (CAS number: 9012-36-6) was used as purchased from Sigma in the experiment of fabrication gel-cored magnetic colloidosomes.

### 2.1.1.7 Oils

Various short and long chains hydrocarbons were used, some as oil phase to prepare water-in-oil emulsions.

Complete name	Purity	Supplier
Undecane	99 %	Aldrich
Tridecane	99 + %	Aldrich
Hexane	99 %	Sigma

Table 2.1: Specification of oils used in the emulsion templates.

### 2.1.1.8 Alcohols

All organic solvents and alcohols were used as received without further purification.

Complete name	Purity	Supplier
Ethanol “ ethyl alcohol”	Absolute 99 %	Bottled by the University of Hull
Isopropanol “ isopropyl alcohol, Propan-2-ol”	99.8+% (GLC) 0.785g/mL for analysis CertiFied AR	Fisher scientific
Hexanol	99 %	Avocado
Methanol	99.8 %	Aldrich
Octanol	99 %	Alfa Aesar

Table 2.2: Specification of alcohols used as solvents in our experiments.

### 2.1.1.9 Surfactants

Several different surfactants were used in stabilising water-in-oil emulsions. In addition aqueous solution of Tween20 was used to promote surface wetting of sporopollenin microcapsules in the encapsulation of living yeast cells.

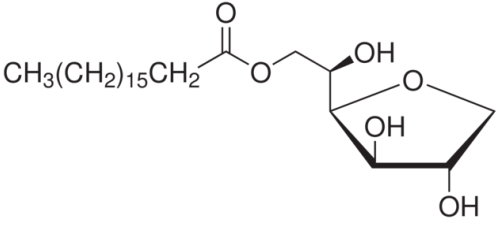
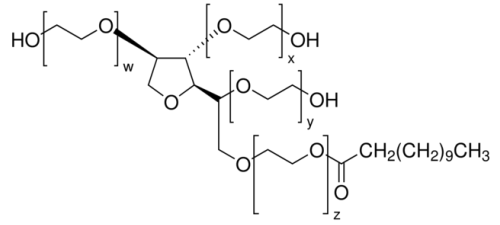
Complete name	HLB	Structure	Supplier
Span60 “Sorbitan monostearate”	4.7		Sigma
Tween20 “Polyethylene glycol sorbitan monolaurate ”	16.7		Sigma

Table 2.3: Specification of surfactants used in our experiments.

### 2.1.1.10 Polyelectrolytes

Polyelectrolytes were used for different purposes in some of the experiments, such as coating native yeast cells with cationic and anionic polyelectrolytes to enhance their surface charge. Sodium polyacrylate and carboxymethyl cellulose were integrated into ammonium shellac solution in order to enhance the disintegration of the produced composite microcapsules and create a pH-triggered release of the encapsulated yeast cells. (See table 2.4 for details).

### 2.1.1.11 Buffers

All buffers (0.1 M) were freshly prepared by mixing the components listed in the composition column in table 2.6. The pH was measured using a Fisher brand HydruS 400 pH meter. The pH of un-buffered solutions was adjusted by adding a few drops of 0.1 M sodium hydroxide or 0.1 M hydrochloric acid.

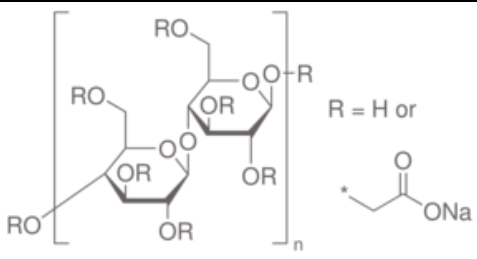
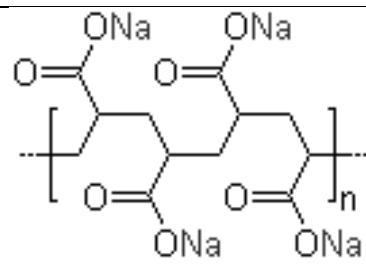
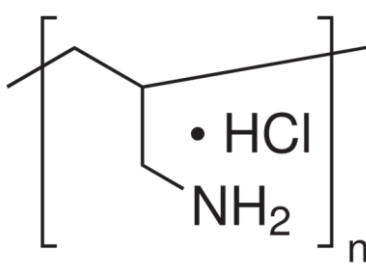
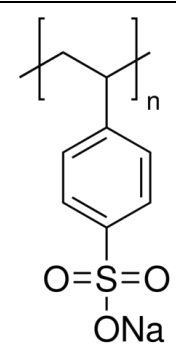
Complete name	Average MW	Structure	Supplier
Carboxymethyl cellulose sodium	Medium viscosity		Fluka
Sodium polyacrylate 86-92 % purity	5100 g/mol by GPC		Aldrich
Polyallylamine hydrochloride GPC vs. PEG std.	15,000 g/mol		Aldrich
Polystyrene sulfonate sodium salt 15-55 cP, 20 % at 25 °C	70,000 g/mol		Aldrich

Table 2.4: Specification of polyelectrolytes used in our experiments.

### 2.1.1.12 General chemicals

During this PhD research project a wide range of general chemicals were used. The following table summarises the characteristics of those chemicals.



<b>Complete name</b>	<b>Purity</b>	<b>Supplier</b>
Sodium chloride “pellets”	99.5 % wt.	VWR international Ltd
Ammonium sulfate	98.5 %	BDH Chemicals Ltd
Acetic acid “ glacial”	99 % specified	Fisher chemicals
Hydrochloric acid	1.16 S.G. 37 % for analysis CertiFied AR	Fisher chemicals
Calcium carbonate microparticles	Surface modified by fatty acid. Purity undetermined.	Socal® and Winnofil® Used as supplied
Glucose	99.5 %	Fisher chemicals
Yeast extract	-	OXIOD LP0021
o-phosphoric acid	99.99 %	Aldrich
Calcium chloride dihydrate	99 % for analysis certiFied AR	Fisher chemicals
Sodium hydroxide “ pellets”	98 % for analysis certified AR	Fisher chemicals
Sodium bicarbonate	99.5 % for analysis certified AR	Fisher chemicals
Lyophilised baker’s yeast powder	<i>Saccharomyces cerevisiae</i>	Purchased from local supermarket
Oleic acid	97 %	Fisher chemicals
Acetone	Absolute	Bottled by University of Hull
Sodium acetate trihydrate	99 %	Alfa Aesar
di-Potassium hydrogen orthophosphate, anhydrous “K <sub>2</sub> HPO <sub>4</sub> ”	99 + %	Fisher scientific
Potassium dihydrogen orthophosphate “KH <sub>2</sub> PO <sub>4</sub> ”	98-100 %	BDH Chemicals Ltd

Table 2.5: Specification of general chemicals used in our experiments.

Complete name	pH	Composition
Phosphate buffer	6.6	(38.1 mL of 0.1 M K <sub>2</sub> HPO <sub>4</sub> ) + (61.9 mL of 0.1 M KH <sub>2</sub> PO <sub>4</sub> )
Phosphate buffer	7	(61.5 mL of 0.1 M K <sub>2</sub> HPO <sub>4</sub> ) + (38.5 mL of 0.1 M KH <sub>2</sub> PO <sub>4</sub> )
Phosphate buffer	7.6	(86.6 mL of 0.1 M K <sub>2</sub> HPO <sub>4</sub> ) + (13.4 mL of 0.1 M KH <sub>2</sub> PO <sub>4</sub> )
Phosphate buffer	8	(94 mL of 0.1 M K <sub>2</sub> HPO <sub>4</sub> ) + (6 mL of 0.1 M KH <sub>2</sub> PO <sub>4</sub> )
Acetate buffer	5	(357 mL of 0.1 M acetic acid) + (643 mL of 0.1 M sodium acetate tri-hydrate)

Table 2.6: Specification of buffer solutions.

### 2.1.1.13 Fluorescent dyes

We have used several fluorescent dyes during this research project including fluorescein diacetate (FDA), Calcein-AM, and Propidium iodide to test the viability of the living cells. We have used Nile Red to pre-stain aqueous solution of ammonium shellac solution used in the preparation of shellac/yeast cells formulations. Fluorescein diacetate powder with 98 % purity (HPLC) was purchased from Fluka. Nile Red technical grade was purchased from Sigma. The following Figure 2.2 shows the structure of FDA and Nile Red.

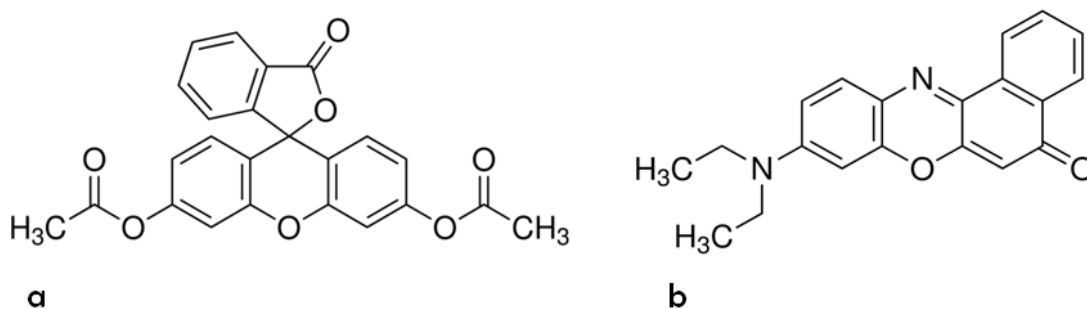


Figure 2.2: (a) Chemical structure of FDA, and (b) chemicals structure of Nile Red.

Live/Dead Cell Double Staining Kit was purchased from Sigma-Aldrich. The following specifications were taken from the supplier's website.<sup>56</sup> The Live/Dead Cell Double Staining Kit is utilized for simultaneous fluorescence staining of viable and dead cells. This kit contains Calcein-AM and Propidium iodide (PI) solutions, which stain viable and dead cells, respectively. Calcein-AM, acetoxymethyl ester of Calcein, is highly lipophilic and cell membrane permeable. Though Calcein-AM itself is not a fluorescent molecule, the Calcein generated from Calcein-AM by esterase in a viable cell emits a strong green fluorescence ( $\lambda_{\text{ex}}$  490 nm,  $\lambda_{\text{em}}$  515 nm). Therefore, Calcein-AM only stains viable cells. Alternatively, the nuclei staining dye PI cannot pass through a viable cell's membrane. It reaches the nucleus by passing through disordered areas of dead cell membrane, and intercalates with the DNA double helix of the cell to emit red fluorescence light ( $\lambda_{\text{ex}}$  535 nm,  $\lambda_{\text{em}}$  617 nm). Since both Calcein and PI-DNA can be excited with 490 nm light, simultaneous monitoring of viable and dead cells is possible with a fluorescence microscope with dual fluorescence filter set. Using  $\lambda_{\text{ex}}$  545 nm, only dead cells can be observed.

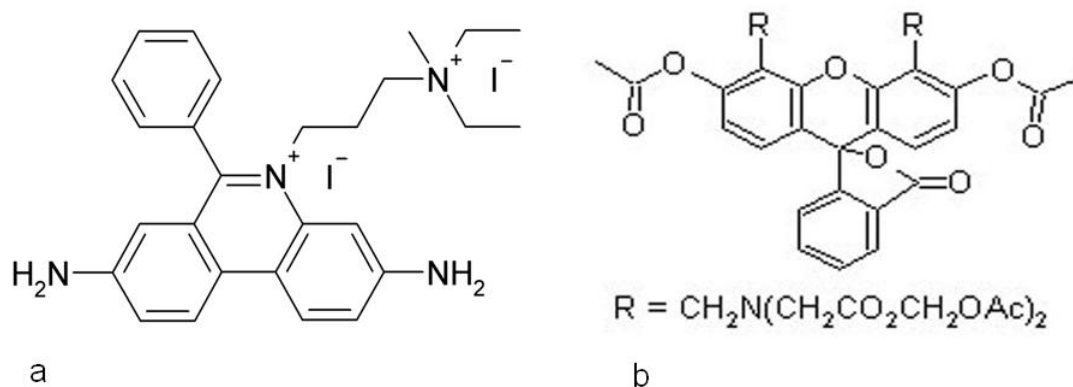


Figure 2.3: (a) Structure of Propidium iodide, and (b) structure of Calcein-AM.

## 2.2 Methods

Images were taken using a range of microscopes including confocal fluorescent and scanning electron microscopes.

### 2.2.1 Microscopy

#### 2.2.1.1 Olympus BX51

Optical and fluorescent images were taken by using Olympus microscope fitted with a digital camera system DP70 using a 1.5 million pixel CCD colour camera recording at 5.8-million pixel equivalent. Images were processed using Image Pro-plus software. This microscope is fitted with a series of filter sets corresponding to the absorption and emission wavelengths of specific dyes (table 2.8). It is used with a series of objectives 4x, 10x, 20x, 40x and 100x magnification.

Filter name	Description	$\lambda$ excitation (nm)	$\lambda$ emission (nm)	Fluorescent dye
U-MNUA2	Narrow-band with band pass barrier filter	360-370	420-460	Perylene
U-MWIBA2	Wide-band with band pass barrier filter	460-490	510 IF	FITC, Neuro-DiO, Fluorescein
U-MWIG2	Wide-band with interference barrier filter	520-550	580 IF	Rhodamine, Nile Red
U-M51004V2	FITC/TRITC filter set	~ 490-510 ~ 560-585	~ 525-545 ~ 600-635	FITC, Neuro-DiO, Rhodamine, Nile Red

Table 2.7: Characteristics of the different filter sets fitted on the Olympus fluorescence microscope and names of the corresponding dyes.

### 2.2.1.2 Nikon Eclipse (Confocal) microscope

Confocal images were obtained with a Nikon Eclipse TE 300 inverted microscope (Bio-Rad) using Kr/Ar gas laser (488 or 568nm excitation wavelengths) with the following objectives: 10x, 16.4x, and 40x.

### 2.2.1.3 Scanning Electron Microscopy (SEM)

SEM images were obtained using an Evo 60 field emission scanning electron microscope (Carl Zeiss, Gmbh). The samples were pre-coated with either carbon or gold monolayers to enhance their surface electro-conductivity.

## 2.2.2 Haemocytometer

The number of the yeast cells either grown or released from the shellac/yeast cells composite microcapsules were counted using a haemocytometer with 0.1 mm chamber depth, which was used as purchased from MARIENFELD. Figure 2.4 illustrates a micrograph of the grids of the haemocytometer used for counting the released cells.

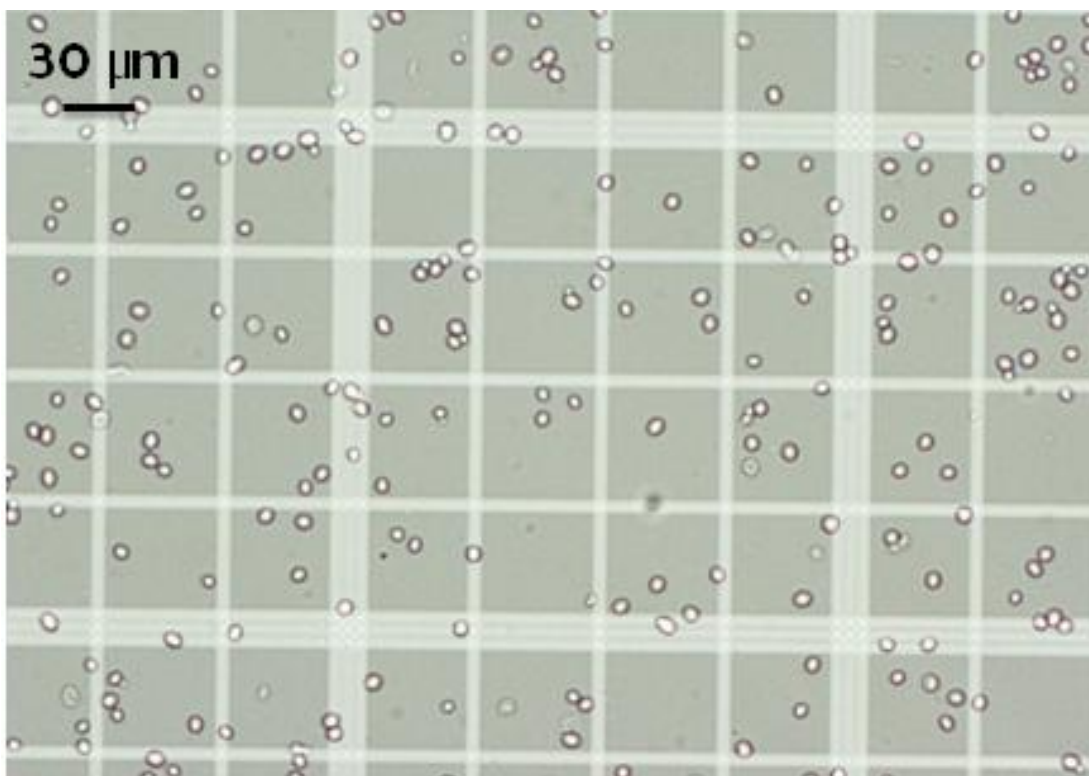


Figure 2.4: Number of released yeast cells from shellac/cells microcapsules counted using a Haemocytometer.

### 2.2.3 General equipments

Equipment	Make and model
Thermostat water bath A	Grant thermostat bath OLS200
Centrifuge A	Baird & Tatlock Auto Bench Centrifuge Mark IV
Centrifuge B	Eppendorf mini spin plus AG
Homogeniser	IKA® T25 digital ULTRA TURRAX®
Ultrasonic bath	Decon FS3006
Ultrasound	JENCONS scientific LTD VIBRA cell™
Magnetic stirrer	STUART SCIENTIFIC SM24
Diaphragm Vacuum pump	Vacuum brand MS 2C
pH meter	Fisher brand Hydrus 400
Micropipettes	Eppendorf research
Basic shaker	IKA® VIBRAX VXR basic
Mini shaker	IKA® MS 3 basic
Thermostat water bath B	Grant thermostat bath LTD6G

Table 2.8: Make and model of some the instruments used in this research project.

### 2.2.4 Dispersing of yeast cells in milli-Q water

Dry yeast powder was washed with milli-Q water several times; the suspension was centrifuged on 4,000 rpm for 5 minutes and then the supernatant was discarded after every wash. The yeast cells were finally redispersed in aqueous solutions depending on the type of the process.

### 2.2.5 Preparation of culture media

Yeast cells both free and encapsulated in microcapsules were exposed to culture media which was prepared by dissolving 2 g glucose, 0.3 g ammonium sulphate, 0.1 g sodium chloride and 0.5 g yeast extracts in 100 mL milli-Q water. The solution was sterilised by boiling at 100 °C for 1 hour and passed through 0.2 µm in diameter filter after it was cooled down to room temperature.

### **2.2.6 Transfer of amidine latex nanoparticles into oil phase**

Hydrophobic positively charged amidine latex nanoparticles were supplied in aqueous suspension 4 % wt. by the manufacturer. These cationic latex nanoparticles would electrostatically bind to anionic yeast cells (native or PAH/PSS pre-coated) in the water phase. Therefore, they were transferred into the oil phase in order to be used to stabilise water-in-oil Pickering emulsions. 1 mL of the latex aqueous suspension was centrifuged in an Eppendorf plastic tube using Eppendorf, mini Spin Plus centrifuge. The supernatant was discarded, followed by addition of 1 mL of absolute ethanol. The suspension was mixed on a shaker to disperse the latex particles. This procedure was repeated twice to transfer the latex particles into ethanol. Finally 1 mL ethanolic suspension of the amidine latex nanoparticles was transferred into 8 mL of oil using a similar procedure.

### **2.2.7 Testing the viability of yeast cells using FDA solution**

Fluorescein diacetate (FDA) solution was prepared by dissolving 10 mg powder in 1 mL acetone and the working solution was stored at  $-20\text{ }^{\circ}\text{C}$  and protected from sunlight by wrapping the sample tube in aluminium foil. The viability of the yeast cells was tested at various conditions such as extremely low pH, low temperature of ( $-20\text{ }^{\circ}\text{C}$ ), ethanol concentrations of (10, 20, and 40) % vol., aqueous solution of 0.5 M calcium chloride, and Tween20 solution (0.18 mM).

In all cases, the yeast cells were washed with milli-Q water several times after exposing them to the studied conditions and were redispersed in 490  $\mu\text{L}$  milli-Q water. Then 10  $\mu\text{L}$  of FDA working solution was added into the dispersion, which was shaken on a mini shaker for 20 minutes followed by washing with milli-Q water several times to remove the excess FDA. The stained cells were observed by optical fluorescence microscopy using FITC filter set. Stock suspension of 1 % wt. native yeast cells was prepared as follows: 0.01 g dry yeast powder was washed several times by using 5 mL in milli-Q water, and the suspension was centrifuged at 5,000 rpm for 5 minutes followed by discarding of the supernatant.

**(i) Freezing native yeast cells at  $-20^{\circ}\text{C}$ .** Yeast cells dispersion was frozen overnight in a freezer at  $-20^{\circ}\text{C}$ . The frozen dispersion was melted at room temperature and then the FDA test was performed to check the cells viability.

**(ii) Exposing native yeast cells to low pH and concentrated calcium chloride solution.** Prepared stock suspension of 1 % wt. native yeast cells was centrifuged and the supernatant was discarded. The sedimented yeast cells were redispersed in both 0.1 M hydrochloric acid and 0.5 M calcium chloride aqueous solutions separately and the suspensions were shaken for 30 minutes on a mini shaker. The dispersions were later centrifuged and washed with milli-Q water several times followed by the FDA test.

**(ii) Exposure of native yeast cells to aqueous ethanolic solution.** Yeast cells were washed with milli-Q water for several times and they were redispersed in aqueous ethanolic solutions in concentrations of (10, 20, and 40) % vol. the suspensions were shaken for one hour on a mini shaker followed by washing with milli-Q water and testing the yeast cells viability with FDA solution.

**(iv) Viability of native yeast cells in Tween20 aqueous solution.** A stock solution of 0.18 mM (3x CMC) Tween20 was prepared by dissolving 0.022 g Tween20 in 100 mL milli-Q water. Native yeast cells were redispersed in stock solution of Tween20. The dispersion was shaken on a mini shaker for one hour followed by washing with milli-Q water to remove excess Tween20. Finally, the yeast cells were treated with FDA solution for viability test.

## **2.2.8 Coating yeast cells with polyelectrolytes**

Dry yeast powder was washed with milli-Q water several times, by centrifugation at 5,000 rpm for 5 minutes and discarding of the supernatant. Aqueous dispersion of a known amount yeast cells was prepared by redispersing the washed yeast cells in milli-Q water. 0.02 g of (polyallyamine hydrochloride) PAH was dissolved in 4 mL milli-Q water. The solution was divided into 4 equal portions (1 mL each). 500  $\mu\text{L}$  of yeast dispersion was added dropwise into 1 mL of PAH solution with stirring on a magnetic stirrer, followed by stirring the dispersion for 5 more minutes after the complete mixing. All the portions of the PAH pre-coated yeast cells were mixed together and stirred at 700 rpm for 20 minutes on a magnetic stirrer. The final suspension was centrifuged at 4,000 rpm for 5 minutes and washed with water several



times to remove excess PAH, while the supernatant was discarded. The sedimented, PAH pre-coated yeast cells were redispersed in 1 mL milli-Q water. The same procedure was repeated using 0.02 g PSS dissolved in 4 mL milli-Q water divided into 4 portions. 500  $\mu$ L of the PAH pre-coated yeast cells were added dropwise into 1 mL of PSS solution with stirring. All the portions were mixed together and the suspension was stirred at 700 rpm for 20 minutes on a magnetic stirrer. The suspension was centrifuged and the PAH/PSS pre-coated yeast cells were washed with milli-Q water several times to remove excess PSS.

### **2.2.9 Preparation of magnetite nanoparticles**

Iron oxide magnetic ( $\text{Fe}_3\text{O}_4$ ) nanoparticles stabilised with PAH, magnetic nano-rods were produced following a procedure similar to that described elsewhere.<sup>57</sup>

2 mL of 1 M  $\text{FeCl}_3$  and 0.5 mL of 2 M  $\text{FeCl}_2$  aqueous solutions were mixed (a ratio 4:1, total volume 2.5 mL) and stirred vigorously. Then 25 mL of 1 M aqueous ammonia solution was added rapidly while stirring and the appearance of a dark iron oxide precipitate was immediately observed. After the subsequent incubation for 30 minutes the precipitate was separated using a permanent magnet and washed several times with water until pH~7 was detected in the supernatant. Aqueous suspension of magnetic nanoparticles was produced by using PAH as a stabiliser. 100  $\mu$ L of suspension of magnetic nanoparticles obtained as described above was diluted in 10 mL of 10 mg mL<sup>-1</sup> PAH aqueous solution and sonicated for 30 min at 50 % power of the Sonifier (Branson Digital Sonifier Model 450, 5 mm tip, 400 W maximal power) and immediately filtered with Milli-pore cartridge (pore size 0.2  $\mu$ m) which produced a stable aqueous suspension of magnetic nanoparticles.

### **2.2.10 Preparation of sporopollenin microcapsules**

Sporopollenin microcapsules were prepared from *Lycopodium clavatum* pollen grains by suspending 50 g dry pollen powder in 375 mL acetone. Then the pollen suspension was stirred under reflux for 4 hours. The de-fatted pollen was filtered off and treated with 375 mL 6 % wt. potassium hydroxide under reflux for 12 hours while the solution was filtered and replaced after 6 hours. Then the mixture was filtered through Whatman filter paper 20–25  $\mu$ m, washed with hot water and hot absolute ethanol on the filter. The solid residue was re-suspended in 375 mL 85 % wt. ortho-phosphoric

acid and stirred under reflux for 7 days. Then, it was filtered again and washed with water, acetone, 2 M hydrochloric acid and 2 M sodium hydroxide, water and acetone and finally washed with absolute ethanol and dried at 60 °C until constant weight.

#### **2.2.11 Encapsulation of yeast cells in sporopollenin microcapsules**

To encapsulate the yeast cells in sporopollenin microcapsules, a disc-like pellet was prepared by compressing 0.05 g loose dry sporopollenin powder with a mechanical press (15 tonnes) pressing force. The yeast cells were hydrated in Milli-Q water and subsequently washed several times. To infuse the cells into the sporopollenin microcapsules, the pellet was added into 1.5 g of freshly prepared dispersion of 30 % wt. concentrated yeast aqueous dispersion which contained either (i) a surfactant Tween20 (at concentration 0.18 mM, equivalent to 3 CMC) or (ii) ethanol (13 % wt. ). The mixture was immediately stirred for a few seconds to form a thick paste-like dispersion. The residual air trapped in the sporopollenin microparticles was evacuated by putting the sample under vacuum. The non-encapsulated yeast cells were washed off by replacing the supernatant with Milli-Q water ten times, after leaving the sporopollenin microcapsules to sediment under gravity. Finally, the sample was lyophilised at room temperature.

#### **2.2.12 Growth process of yeast cells inside sporopollenin microcapsules using “in-gel” fermentation**

Oxidised starch powder was dissolved in the prepared sterilised culture medium. For the purpose of the growth process of yeast cells encapsulated in sporopollenin microcapsules, four different samples were prepared in (14 mL Greiner® culture tube with screw on cap) as follows, sample (a) only contained the culture media and starch, sample (b) contained 1 % wt. native yeast cells dispersed in the culture media and starch, while, sample (c) composed of only 0.1 g of sporopollenin dispersed in the culture media and the starch, the last sample (d) was mainly 0.1 g sporopollenin with the encapsulated yeast cells inside, dispersed in the culture media plus the starch to act as the gel phase. All four samples were put together in a holder and then they were photographed with a digital camera, after which they were incubated at 37 °C in a Grant OLS200 thermostat bath, and then it was photographed at different time intervals to determine the effect of released carbon dioxide due to the cell growth.

### **2.2.13 Encapsulation of magnetized yeast cells in sporopollenin microcapsules**

Baker's yeast cells were washed several times with milli-Q water and then coated with polyelectrolytes using alternating deposition of PAH and PSS (from 10 mg/mL solution in 0.5 M NaCl) by the layer by layer methods. Since the hydrated yeast cells in water are negatively charged, they were coated first with PAH. 300  $\mu$ L of the cell suspension was combined with 1 mL of PAH (aqueous) solution during constant shaking, incubated during 10 min and then centrifuged. The remaining excess polyelectrolyte was removed and the cells were redispersed and washed three times with Milli-Q water. The cells were then combined with the PSS solution and the same steps repeated as before PAH coating. 100  $\mu$ L of PAH/PSS coated yeast cells were introduced into 1 mL of PAH-coated magnetic nanoparticles, incubated for 15 min and washed with water. The magnetised yeast cells were collected with a permanent magnet. 10 % wt. of magnetised yeast cells were encapsulated in sporopollenin microcapsules using the same procedure used for uncoated (native) cells in section 2.2.11.

### **2.2.14 Spray co-precipitating ammonium shellac solution/yeast cells formulation**

Baker's yeast cells were washed several times with milli-Q water and then re-dispersed in aqueous solutions of ammonium shellac at different concentrations. Three different shellac-yeast formulations were prepared: (i) shellac-yeast dispersion at pH 8; (ii) shellac-yeast dispersion doped with 0.52 % wt. carboxymethylcellulose at pH 8; The pH of the final dispersion was adjusted to 8 by adding (drop-wise) 0.01 M sodium hydroxide solution. (iii) shellac-yeast dispersion was doped with 4 % wt. sodium polyacrylate at pH 6.7 supported by acetate buffer. The spraying of the shellac-cells aqueous dispersion in all experiments was performed with push-sprayer with metal nozzle of internal diameter 380  $\mu$ m. The spraying frequency was 43 sprays per minute and each spray dose contained 0.03 g of shellac-cells dispersion. Each of the aforementioned dispersions was sprayed over either 3 % vol. aqueous acetic acid or 0.5 M aqueous calcium chloride solution, which produced composite "shellac-yeast cells" microcapsules. The microcapsules were stirred in the precipitating medium for 2 hours to test the viability of the yeast cells upon exposure to the acetic acid and calcium chloride solutions. Then they were isolated from these media by centrifugation and multiple washing with milli-Q water.

### **2.2.15 Spray drying yeast cells/ammonium shellac solution formulation**

Dispersions of yeast cells in ammonium shellac solution prepared as described in (section 2.2.14) (i)-(iii) were sprayed into an “in house” designed spray-dryer column in counter-flow of hot air. The produced microcapsules were collected in a Petri dish containing milli-Q water placed at the base of the column.

### **2.2.16 Testing the viability of yeast cells inside the composite microcapsules**

The viability of the yeast cells inside the microcapsules was tested by using fluorescence optical and confocal microscopy, by treating the aqueous suspension of yeast cells released from the microcapsules with a small amount (typically 1-2 drops of 10 mg/mL solution of fluorescein diacetate (FDA) in acetone per 10 mL of cell suspension). The same test was also performed on the encapsulated cells after the microcapsules were stirred in acetic acid or calcium chloride solutions for 2 hours. For determining the fraction of the dead cells, the suspension of the released yeast cells (200  $\mu$ L) was treated with 100  $\mu$ L of PI and shaken for 20 minutes at 37 °C. Then the cells were washed several times with milli-Q water and observed with TRITC filter optical fluorescence microscopy.

### **2.2.17 Disintegration of the microcapsules and triggered release of the cells**

The disintegration of the composite shellac-yeast microcapsules was monitored in 0.1 M aqueous phosphate buffer solution of various pHs, to mimic the physiological conditions in the stomach and the lower intestines; by transferring the microcapsules into the solution followed by stirring on 300 rpm with a magnetic stirrer at 37 °C. In all our experiments we have used the same beakers and magnetic stirrers, and kept the stirring speed constant. It is expected that without stirring, the results would have poor reproducibility. The disintegration processes was monitored by withdrawing small aliquots at regular periods and observing them using optical brightfield and fluorescence microscopy.

### 2.2.18 Preparation of Pickering emulsions stabilised with latex nanoparticles

Water-in-oil Pickering emulsions were stabilised with 300 nm amidine latex nanoparticles and the adsorbed particles monolayer was interlocked by using either PSS solution or PAH/PSS pre-coated yeast cells suspension in the water phase. The oil phases were prepared by dispersing amidine latex nanoparticles the procedure described in this thesis (section 2.2.6). The water phases were prepared as follows: (i) to interlock the particle monolayer with PSS in the w/o interface an aqueous suspension of 1 % wt. native yeast cells was prepared in 0.1 M sodium chloride solution which contained 1 % wt. PSS. (ii) To interlock the monolayer of the particles with PAH/PSS pre-coated yeast cells at the w/o interface a suspension of 15 % wt. yeast cells pre-coated with PAH/PSS was prepared in 0.1 M sodium chloride solution. The water phase was emulsified into the oil phase at 8,000 rpm for 30 seconds by using ultraturrax homogeniser.

### 2.2.19 Transfer of the w/o Pickering emulsion droplets into water

Colloidosomes were prepared by templating w/o Pickering emulsions droplets and subsequent transfer of the water droplets from the undecane phase to water phase by employing three different approaches as described below:

**(i) Exchange of the oil phase followed by centrifugation.** In this approach the undecane phase was replaced with 3 mL hexanol twice, and the emulsion droplets in hexanol were left to settle followed by removing the excess hexanol. 1 mL of the concentrated emulsion in hexanol was added on top of 5 mL milli-Q water, and then the mixture was centrifuged on 1,500 rpm for 3 minutes.

**(ii) Exchange of the oil phase followed by evaporation of the new oil phase.** In this method approach the undecane phase was replaced with hexane twice and the w/o emulsions droplets in hexane were left to settle. The excess hexane was removed and 1 mL of the concentrated emulsion in hexane was added on top of 5 mL of milli-Q water. The hexane phase was evaporated at 40 °C in a Grant thermostat water bath.

**(iii) Freezing process.** Calcium carbonate microparticles (0.2 g) were dispersed in 5 mL ethanol. The suspension was centrifuged on 5,000 rpm for 5 minutes followed by discarding of the supernatant. The calcium carbonate microparticles were redispersed in 1 mL ethanol and then 5 mL hexane was added into the suspension. The mixture was stirred to disperse the calcium carbonate microparticles properly. The undecane

phase of the original emulsion was replaced with hexane twice. The excess hexane was removed after the w/o emulsion droplets were settled and replaced by 5 mL of calcium carbonate microparticles suspension in hexane. The emulsion-calcium carbonate microparticles mixture was stirred to spread the microparticles homogeneously followed by freezing at -20 °C overnight. The frozen emulsion-microparticles mixture in hexane was filtered off and the frozen w/o emulsions droplets were redispersed in 3 mL cold aqueous solution of 1 % vol. glacial acetic acid to dissolve the calcium carbonate spacer microparticles. Finally the frozen-core of the colloidosomes was melted by increasing the temperature to 30 °C in a Grant thermostat water bath.

#### **2.2.20 Preparation of w/o emulsion stabilised with oleic acid**

3D multicellular cellosomes of living cells were prepared by templating w/o emulsion droplets stabilised with oleic acid. Both undecane and octanol equilibrated with water were used as an oil phase which was prepared by dispersing different amounts of oleic acid in the oil phases followed by vortexing the mixture for 20 minutes on a magnetic stirrer. The water phase was prepared by dispersing different amounts of yeast cells pre-coated with PAH in milli-Q water. Finally the water phase (1:9 ratios) was emulsified into the oil phase at 8,000 rpm for 30 seconds by using ultraturrax homogeniser.

#### **2.2.21 Preparation of w/o emulsion stabilised by Span60**

We used water-in-oil emulsion templates stabilised with Span60 to fabricate 3D multicellular living cellosomes by mixing and re-emulsifying two emulsions, one containing 10 % wt. PAH pre-coated yeast cells in the water droplets and the other containing 5 % wt. PSS solution in the water phase. The emulsions were prepared by emulsifying (1:9) ratio of the water phase into octanol equilibrated with water which contained 2 % wt. Span60 at 11,000 rpm for 30 seconds. In the case of water-in-octanol emulsion containing PSS solution in the water phase the emulsion was homogenised at 13,000 rpm for 1 minute by using ultraturrax homogeniser.

The two emulsions were mixed in a ratio of (50:50) and re-emulsified at 11,000 rpm for 30 seconds. The emulsion was left to settle for several minutes followed by shrinking the water emulsion droplets upon addition of dry octanol after removing the

original continuous phase. The shrinking procedure was repeated 3 times and the water-in-dry octanol emulsion droplets containing PAH pre-coated yeast cells linked together by PSS were transferred by using freezing process described in section 2.2.23.

### **2.2.22 Fabrication of cellosomes from w/o Pickering emulsion templates**

We have fabricated 3D multicellular living cellosomes by employing the colloidosomes fabrication strategy which includes using templates of water-in-oil Pickering emulsions stabilised with solid latex particles. Two Pickering emulsions were prepared, one containing yeast cells pre-coated with PAH and the other containing yeast cells pre-coated with PAH/PSS. The two emulsions were mixed and re-emulsified to yield a new Pickering emulsion containing both cationic and anionic yeast cells pre-coated with polyelectrolytes linked together by electrostatic interaction. Here, we have also used both undecane and octanol equilibrated with water as the oil phase which was prepared by dispersing 1 mL 300 nm amidine latex nanoparticles suspension in ethanol (4 % wt.) into 8 mL of the oil phase. The water phase contained 10 % wt. yeast cells pre-coated with either PAH or PAH/PSS in 0.5 M sodium chloride solution.

In all cases, the Pickering emulsions were prepared by emulsifying 1:9 ratio of water phase into the oil phase at 8,000 rpm for 30 seconds. The combination of the two Pickering emulsions was done by mixing 50:50 ratios of both emulsions and re-emulsifying the mixture at 8,000 rpm for 30 seconds. Finally, the cellosomes were prepared by transferring the w/o Pickering emulsions droplets containing both PAH and PAH/PSS pre-coated yeast cells from the oil phase into water phase by using the freezing process approach described in section 2.2.23.

### **2.2.23 Transfer of w/o emulsion droplets into water using freezing process**

Fabrication of the 3D multicellular cellosomes of living cells were achieved by transferring the w/o emulsion droplets from the oil continuous phase into water phase by using the freezing process. The w/o emulsions droplets were first shrunken upon addition of dry octanol and then they were transferred into water. Octanol is a long chain alcohol, and thus contains both a hydrophobic hydrocarbon chain and a hydrophilic end group. The solubility of water in octanol is  $2.2 \pm 0.2$  M at 25 °C.<sup>58</sup> The shrinking process gave closely packed yeast cells inside the water droplets and hence increased their stability to withstand the transfer process. This was done by leaving the emulsion droplets to settle and removing the excess oil, followed by replacing it with 5 mL dry octanol with gentle stirring. The emulsion in dry octanol was left for 30 minutes and then another 5 mL of dry octanol was added after the octanol phase was removed again. The octanol phase was replaced with 5 mL of calcium carbonate microparticles suspension in dry octanol prepared by dispersing 0.1 g calcium carbonate microparticles in 5 mL ethanol followed by centrifugation on 5,000 rpm for 3 minutes and discarding of the supernatant. The sedimented microparticles were redispersed in 0.5 mL ethanol and then 4.5 mL of dry octanol was added. The emulsion-microparticles mixture was vortexed for 30 seconds followed by freezing at - 20 °C overnight. The frozen w/o emulsion droplets were transferred from the octanol phase into water phase by removing the excess dry octanol and adding 100 µL of the concentrated frozen emulsion-microparticles mixture on top of 1 mL milli-Q water in an Eppendorf tube followed by centrifugation at 1,500 rpm for 3 minutes.

### **2.2.24 Counting the numbers of released cells from composite microcapsules**

We have prepared composite microcapsules which contained only shellac and yeast cells without any pH sensitive polyelectrolytes as follows: Baker's yeast cells were washed several times with milli-Q water and then re-dispersed in aqueous solutions of ammonium shellac 6 % wt. at pH 9; the pH of the final ammonium shellac/yeast cells formulation was measured to be 8. The spraying of the shellac-cells aqueous dispersion was performed with push-sprayer with metal nozzle of internal diameter 380 µm. The spraying frequency was 43 sprays per minute and each spray dose contained 0.03 g of shellac-cells dispersion. The dispersion was sprayed over 3 % vol.



aqueous acetic acid solution, which produced composite “shellac-yeast cells” microcapsules which were isolated from the acidic media by multiple washing with milli-Q water.

The disintegration of the composite shellac-yeast microcapsules was monitored in 0.1 M aqueous phosphate buffer solution of various pHs, to mimic the physiological conditions in the stomach and the lower intestines; by transferring the microcapsules into the solution followed by stirring on 300 rpm with a magnetic stirrer at 37 °C. In all our experiments we have used the same beakers and magnetic stirrers, and kept the stirring speed constant. It is expected that without stirring, the results would have poor reproducibility. The number of the released cells from the composite microcapsules was counted using a Haemocytometer which was observed by optical microscopy.

The growth of the encapsulated yeast cells inside the composite microcapsules were monitored by incubating the microcapsules in a culture medium of pH 5 containing 2 % wt. glucose, 0.5 % wt. yeast extract, 0.1 % wt. sodium chloride and 0.3 % wt. ammonium sulphate at 37 °C with stirring at 300 rpm on a magnetic stirrer. The number of released cells because of growth was counted in different times using a Haemocytometer which was observed by optical microscopy.

## Chapter 3.

### Encapsulation of living cells into sporopollenin microcapsules

#### 3.1.1 Introduction

The term sporopollenin was first coined by Zetzsche<sup>59</sup> to describe the material which essentially forms the major part of the outer highly resistant coat (exine) of pollen grains. Pollen powder consists of monodispersed pollen grains, which contains the sperm cells of seed plants. Each pollen grain contains vegetative (non-productive) cells and generative (reproductive) cells containing two nuclei, a tube nucleus and a generative nucleus. The group of cells are surrounded by a cellulose (intine) wall and the outer exine coat.

Sporopollenin has been recognised as one of the most resistant material of bioorganic origin<sup>60</sup> against both chemical and biological decay. Individual sporopollenin grains have been isolated from 500 million year old sedimentary rocks and also from Precambrian rocks dated up to about  $3.5 \times 10^9$  years in the form of microspores.<sup>61</sup> Pollen grains come in variety of morphologies, where the shapes, size and surface marking characteristics depend on the plant species. Most but not all are spherical, the smallest pollen grains are around 6  $\mu\text{m}$  in diameter. The spores of *Lycopodium clavatum* plant are shaped like a three-sided pyramid with distal face rounded triangular in outline and have particle size of about 28  $\mu\text{m}$  in diameter (see Figure 3.1a).<sup>62</sup>

Sporopollenin can be isolated from the pollens by consecutive alkaline and acidic solvent treatment, which remove the inner cellulose wall but morphologically preserve the exine. Although the exact chemical structure of sporopollenin is still debated, the analytical evidence suggest that at large it is an oxidised polymer of carotenoids and their esters.<sup>61f</sup>

Bohne *et al.*<sup>63</sup> investigated the structure and diffusion properties of sporopollenin microcapsules prepared from pine pollen. It was demonstrated that, sporopollenin exine formed from three main layers, two inner and an outer membrane. The external

membrane represents the part of the exine termed the sexine, while the two inner layers covering the lumen of the central microcapsule (endexine and foot layer) have been named nexine.<sup>64</sup> (See Figure 3.1b)

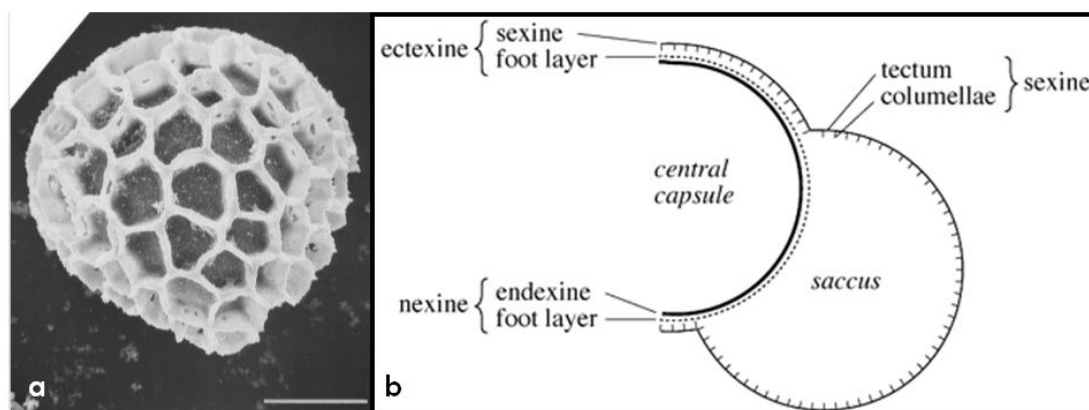


Figure 3.1: (a) Scanning Electron Microscopy image of the distal face of a *Lycopodium clavatum* spore.<sup>62</sup>, scale bar is 10  $\mu\text{m}$  in diameter (b) Schematic diagram of the sporopollenin strata of the pine exine, the two outer layers of the ectexine are detached from the foot layer, thus forming a saccus.<sup>63</sup>

The sexine is detached from the foot layer thus forming a saccus. The external wall of the sacci consists of a thin sporopollenin membrane (tectum), which covers a thick but macro-porous layer formed by honeycomb-shaped support structures, which are open to the lumen. The tectum is perforated by scattering pores of submicrometer size. The lumen of the central microcapsule is bordered by a continuous dense sporopollenin envelop. The pine nexine and sexine proved to be very different in terms of their permeability with respect to organic molecules. The nexine is an ultrafilter membrane, which is impermeable to most proteins, and its permeability to sugar is low indicating that the pores through the nexine are inhomogeneous with respect to their size and that most pores are too narrow for free diffusion of sugar molecules. The purified sexine at the external surface of the sacci is a micro-filter that is highly permeable for even larger polymer molecules and diffusible submicrometer particles. With respect of chromatography and immobilisation, the most interesting properties of the sacci are rapid polymer exchange, large and well accessible inner sporopollenin surface and high mechanical rigidity. The slow exchange of the central microcapsule for polymer and polyvalent anions might be of interest for controlled release applications.<sup>63</sup>

### 3.1.2 Applications of sporopollenin microcapsules

Sporopollenin microcapsules are monodispersed i.e. have the same particle diameter to within  $\pm 1 \mu\text{m}$ . This narrow size distribution makes sporopollenin a potential vehicle to encapsulate drugs. The spores and pollens are naturally occurring renewable materials, with very high resistance to highly acidic or alkaline conditions and are relatively elastic. This means they can pass into the stomach largely unchanged and therefore, protect any medically active ingredients that have been attached to, or contained within them, and would otherwise be destroyed in the stomach.<sup>9b,65</sup> Sporopollenin has the potential to be used as a drug delivery vehicle, because sporopollenin is capable of crossing the gut wall, largely intact, but is then destroyed within the blood stream, thereby releasing its contents.<sup>9b,65</sup>

Blackwell has investigated the process of absorption of both the raw spores of *Lycopodium clavatum* and their empty exines in man following oral ingestion. Patients were given the pollen or the exines randomly using a labelled envelope in a double blind trial where both the patient and the investigator were blind to the treatment given. Human volunteers from both sex aged between 20 to 59 years ingested an oral dose of approximately  $12.66 \times 10^6$  particles suspended in milk on different occasions. Quantification was determined by haemacytometry of the respective particles in venous blood taken from the arm of a volunteer at time intervals up to 1 hour following peroral administration. The volunteer's venous blood was examined and the particles were detected as rapidly as 5 minutes after ingestion and the counts reached a maximum at 15-30 minutes after ingestion.<sup>9b</sup> Confocal microscopy also confirmed the presence of exine particles in the recovered blood plasma and pellet samples.<sup>9b</sup> (see Figure 3.2).

The effect of the sporopollenin vehicle on cells has been investigated by adding the sporopollenin microcapsules into a culture of growing human endothelial cells. Proliferation, apoptosis and necrosis were assessed, together with direct microscopic examination. No differences were seen at any concentration of sporopollenin used, suggesting that no direct toxic effect of the vehicle was present.<sup>9b</sup> Sporopollenin microcapsules have the advantage of being non-toxic and non-allergenic, because they do not have proteins or carbohydrates on their surface.

The exine shells appear to have nano-sized holes running through them<sup>63</sup> which allow their core to be removed and replaced by a suitable active compound or nutraceutical. Certain surface active substances such as ethanol greatly enhance the sporopollenin filling rate.

Mackenzie *et al.*<sup>9a-c,66</sup> has developed chemical and physical methods by which a large variety of chemical entities including peptides, nucleotides and metals can be attached or encapsulated within the empty exine coating of sporopollenin. Large sporopollenin microcapsules > 25 µm in diameter, do not transfer into the blood stream, and therefore, can be used to release their contents over a period of time lower down in the lower intestine and thus deliver nutraceutical and other food additives such as probiotics. The active ingredient which it is to be encapsulated must be in liquid form, either naturally or in solution, other materials such as proteins, vitamins or enzymes are dissolved in aqueous or organic solvents, which can be evaporated or simply filtered off after encapsulation.

The potential use of sporopollenin exine to enhance medical imaging was reported by Lorch *et al.*<sup>65</sup> and the principle behind this process is, the exine coatings concentrate a contrast material in a particular part of the body, where it then shows up brightly within the scanner. Sporopollenin has also been used as a novel natural taste masker for materials such as sunflower oil, and cod liver oil. The exine could be loaded with high amount of the material and still remain as dry as powder and retain flavour masking.<sup>9a</sup> The high loading, taste masking and anti-oxidant properties of sporopollenin exine, therefore, make this technology ideal for the delivery of unpleasant tasting, easily oxidisable substances such as fish oil.

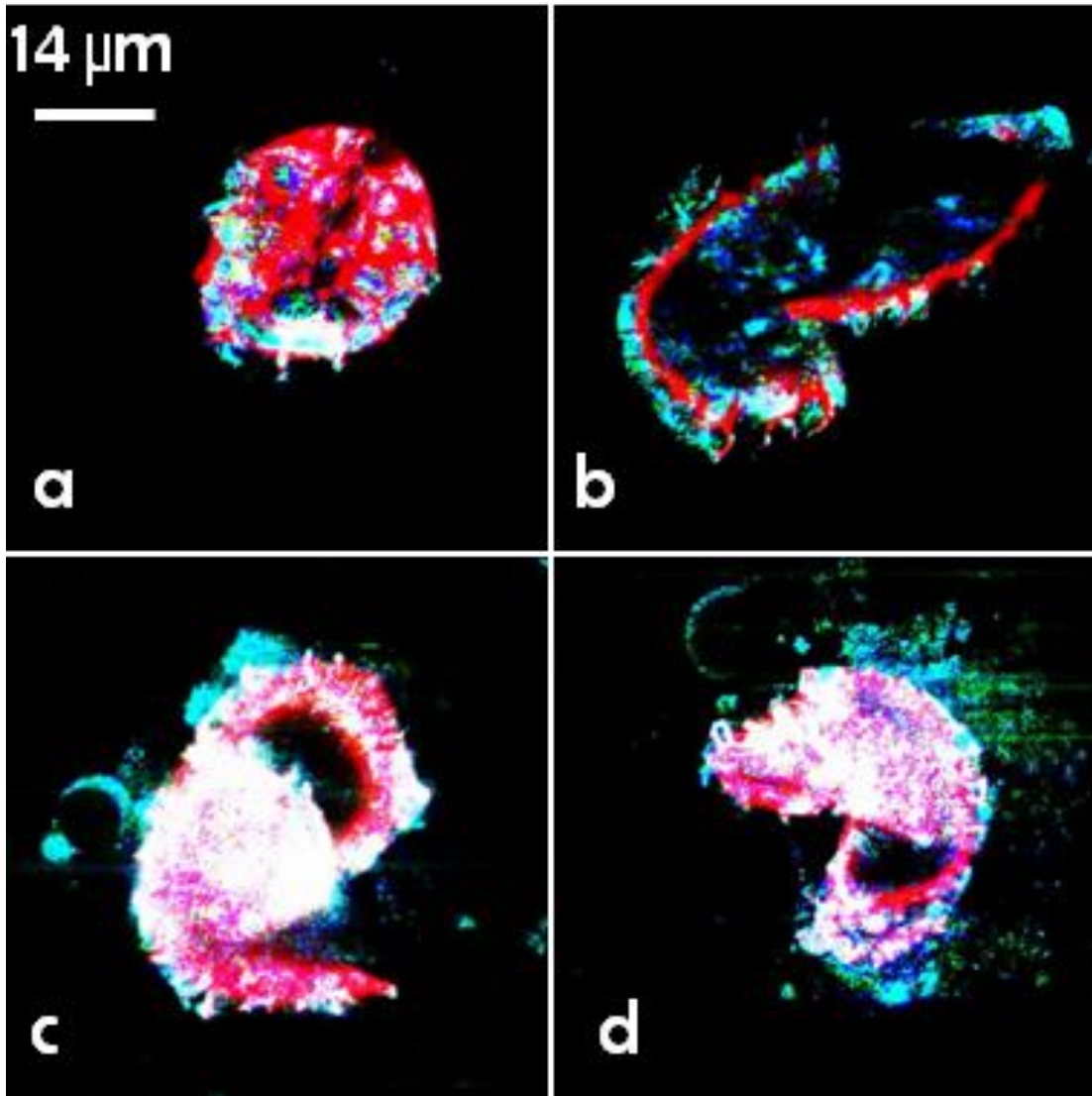


Figure 3.2: Confocal images of exines recovered in blood after 5 minutes in plasma (a), 45 minutes in plasma (b), 5 minutes in lysed blood pellet (c) and 30 minutes in lysed blood pellet (d). Image reproduced from the reference<sup>9b</sup>

Paunov *et al.*<sup>67</sup> reported a simple and robust method for loading sporopollenin exine of *Lycopodium Clavatum* with inorganic and organic nanoparticles synthesised in situ. The technique uses sporopollenin microcapsules as chemical micro-reactors where a chemical reaction is generating a large amount of the product (e.g. of low solubility) inside the microcapsule shells. The procedure begins by loading the microcapsules with a solution of the reagent (A) or a mixture of soluble reagents.

The loaded microcapsules can be filtered off quickly and washed with pure solvent on the filter to remove the excess of the reagent (A) and then redisperse the microcapsules in a solution of reagent (B) to conduct a chemical reaction.  $A + B = C$ , where (C) is a product of low solubility. Filtering and washing the “filled” sporopollenin with a pure solvent to remove the excess of reagent (B), followed by re-dispersion in water. In case of a chemical reaction producing nano-particles of average diameter larger than the pore size, the particles remain trapped in the capsules but the solvent can still access them through the sporopollenin pores. This method has been used to load sporopollenin with variety of chemical compounds including fabricated magnetic sporopollenin nanoparticles ( $Fe_3O_4$ ), which brought the idea of using the prepared microcapsules for direct drug delivery by using an external field. This can be done by loading the magnetic sporopollenin with additional component (e.g. drug, vaccine, food supplements).<sup>67</sup> In this chapter we describe novel technique for encapsulation and protection of living cells into sporopollenin microcapsules.

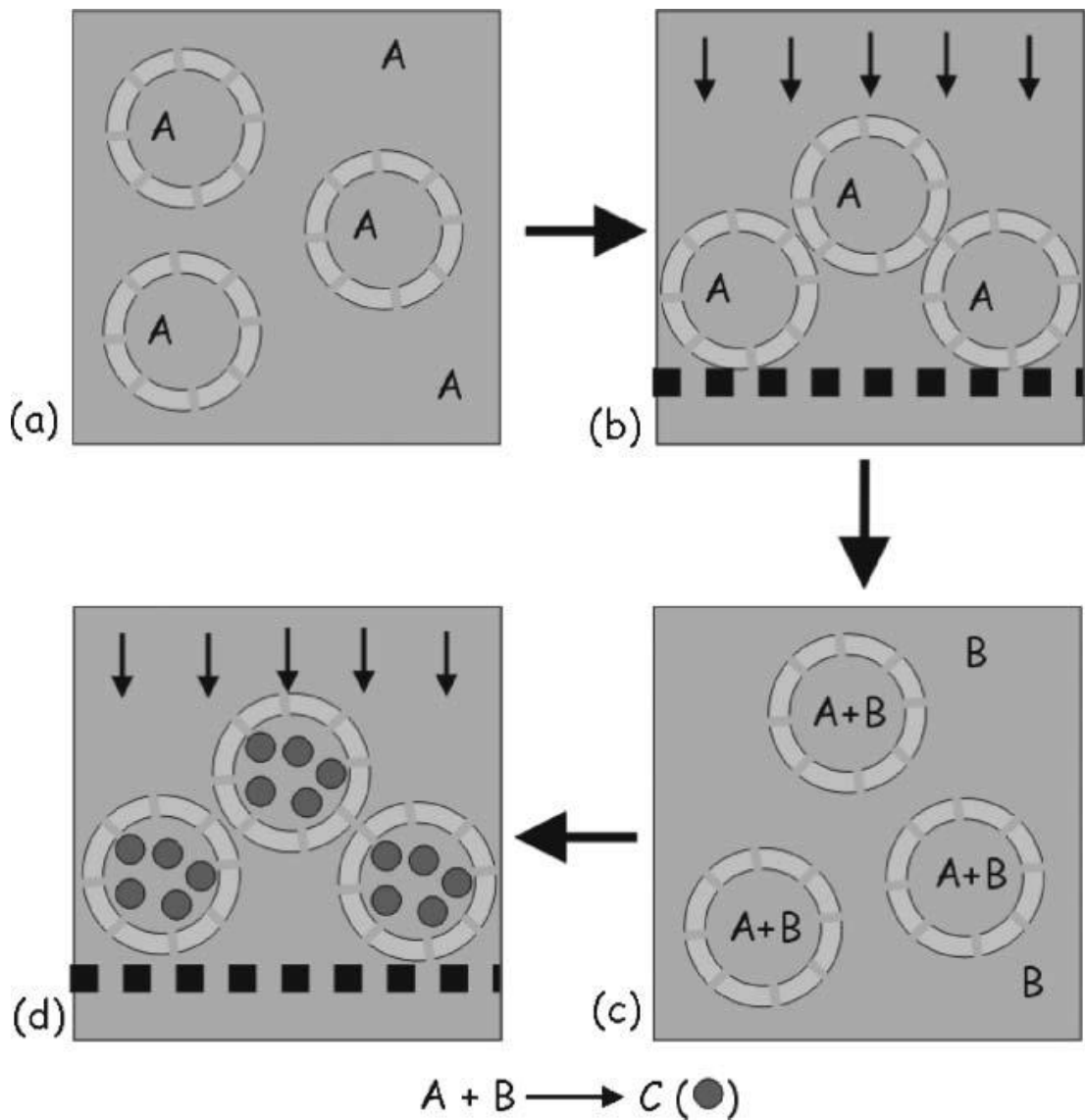


Figure 3.3: Schematic representation of the method for loading sporopollenin microcapsules with nanoparticles as a result of a chemical reaction. (a) A compressed tablet of sporopollenin is dispersed in a solution of reagent A to load the capsules with this solution. (b) The sporopollenin capsules loaded with solution A are filtered and quickly washed with pure solvent to remove the excess of reagent A in the continuous phase followed by their redispersion in a solution of reagent B. (c) The chemical reaction  $A + B$  gives a product C of low solubility which results in the formation of nanoparticles growing inside the sporopollenin. (d) The loaded capsules are filtered and washed on the filter with a pure solvent to remove the excess of reagent B, followed by redispersion in water.<sup>67</sup>



### 3.1.3 Results and discussion

In this chapter, hollow sporopollenin microcapsules prepared in-house from *Lycopodium Clavatum* plant powder by a consecutive alkaline and acidic extraction. This leads to the removal of the cellulosic inner intine but morphologically preserved the outer robust exine shell. Baker's yeast cells *Saccharomyces cerevisiae* which are used as model for living cells, and probiotics culture, were selected for this study because they are robust and resilient microorganism, easy to obtain and handle in laboratory. Similar results are expected with most commonly used probiotic cultures. The method of encapsulating of yeast cells has been demonstrated on the basis of the fact that each pollen micro-particle from *Lycopodium clavatum* has a trilite scar on its surface which also exists in the sporopollenin microcapsules produced from this material. Upon compression, the sporopollenin particles are "squashed" which opens their trilite scars.

In this experiment the sporopollenin powder was compressed into a thin pellet which was then incubated into a concentrated aqueous suspension of living cells in the presence of a surface active agent. The latter is needed to promote wetting of the sporopollenin by the liquid phase. The capillary effect causes an influx of liquid through the opened trilite scars of the compressed sporopollenin and facilitates their closure after they are fully "re-inflated" with the liquid media (See Figure 3.4 for more information). This liquid influx drags some of the cells from the suspension into the sporopollenin microcapsules where they remain trapped after the microcapsules re-inflates and can be grown further in a suitable culture medium. This process, for example, can be used for encapsulation and protection of probiotics upon food processing and storage. This procedure could also find applications in oral delivery of live vaccines as the sporopollenin shells have been reported to cross the gut wall but the living cells encapsulated inside them may remain isolated from the body's immune system.

Although, yeast cells can be encapsulated in sporopollenin using passive filling over a period of 2 hours, however, vacuum enhanced filling has been employed to ensure the efficient encapsulation. The vacuum treatment de-gases the empty microcapsules and this in return should enhance the influx of the cells into their core through the opened scars.

### **3.1.3.1 Growth of yeast cells in culture media**

The most common mode of vegetative growth in yeasts is by a process called budding which is a typical reproductive characteristic of ascomycetous yeasts, including *Saccharomyces cerevisiae*.<sup>36</sup> Native unprotected yeast cells were incubated at different temperature using a culture media which is suitably prepared for yeast cells growth from materials that contained glucose, a source of nitrogen and some inorganic salts.( see chapter 2 for the preparation procedure) Figure 3.5a-c demonstrates the growth of native yeast cells, where (a) is 1 % wt. yeast cells dispersed in milli-Q water before incubation, while (c, and d) show the yeast cells after 19 hours of incubation in the media at 25 and 37 °C, respectively. It is clearly demonstrated that the cells can grow faster in the same media at higher temperature of 37 °C.

### **3.1.3.2 Yeast cells viability during the encapsulation process**

The viability of unprotected yeast cells has been tested by using fluorescence microscopy after treating the cells with FDA. The test is based on the fact that FDA is a non-fluorescent derivative that readily diffuses through the cell membrane, where intracellular FDA is hydrolyzed by nonspecific de-esterases resulting in release of fluorescein which accumulates into living cells if their lipid membrane is intact and can be detected by fluorescence microscopy. Fluorescein diacetate appears to be passively transported through the cells membrane and because fluorescein accumulation depends upon an intact membrane and active metabolism, only active living cells should fluoresce.<sup>68</sup>

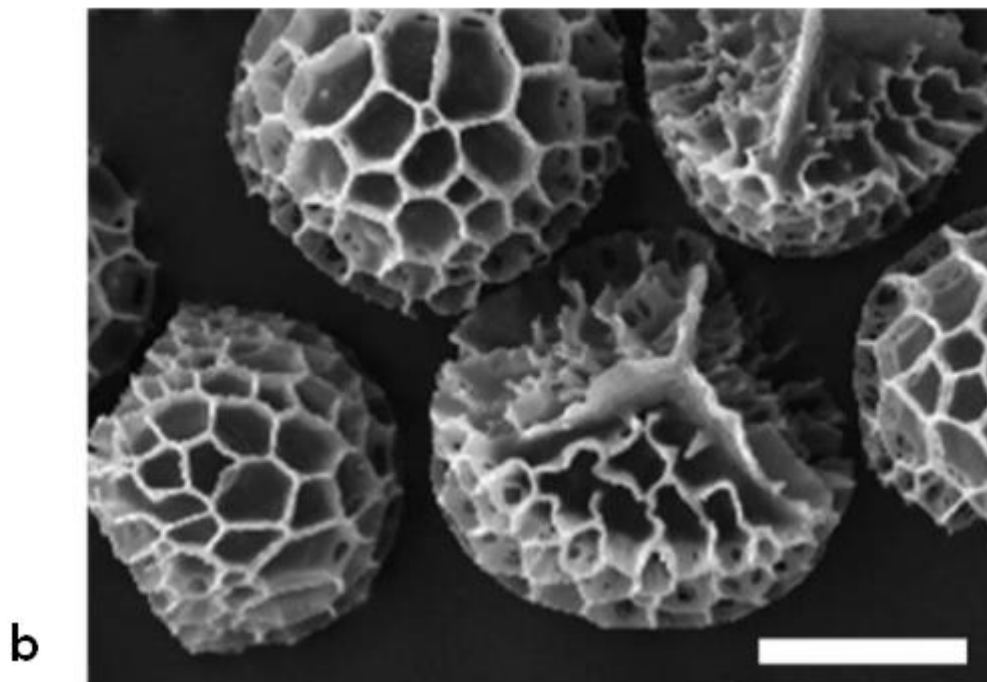
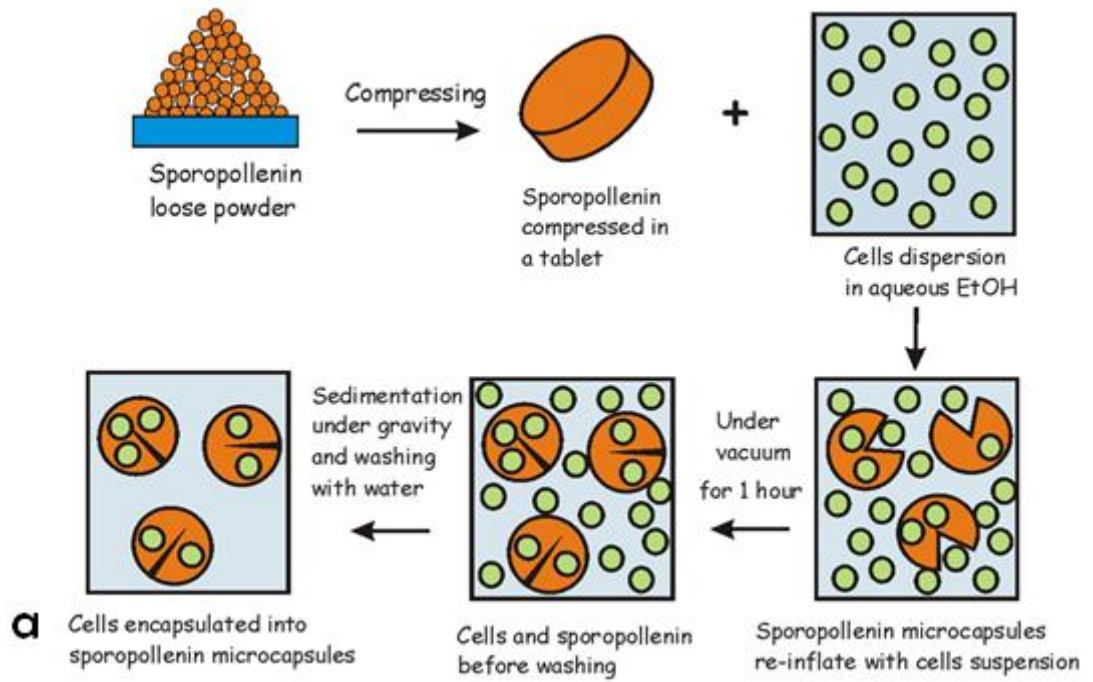


Figure 3.4: (a) Schematic representation of the process of encapsulating yeast cells into sporopollenin microcapsules. (b) Scanning electron microscopy images of sporopollenin from *Lycopodium clavatum* pollens. Each sporopollenin particle is hollow and has a trilete scar which can be opened upon compression. Scale bar is 15  $\mu\text{m}$ .

The work described in this chapter, involves using two different types of surface active agents to promote wetting of the sporopollenin surface by the cell dispersion. Here both a low molecular weight alcohol (food grade) and a classical non-ionic surfactant (Tween20) at low concentration (3 times CMC) were used. These surface active agents might have an effect on the viability of the cells at a particular concentration, therefore, investigation of the yeast cells viability in both aqueous solutions, was performed. First, the viability of yeast cells in water–ethanol mixture at various ethanol concentrations was tested, where the cell dispersion was kept in the water ethanol solution for one hour and then was treated with a solution of 1 mM fluorescein diacetate (FDA). Then the cells were washed with Milli-Q water to remove the excess FDA and observed by fluorescence microscopy with FITC filter set.

We demonstrated with the FDA test that the yeast cells did not have their viability impaired after short time exposure to the alcohol solution at concentration of up to 20 % vol. while our experiments using 40 % vol. ethanol in water mixture resulted in completely destruction of all yeast cells. The use of ethanol as a wetting agent is not essential for the cell encapsulation process and other biocompatible surface active agents could also be good for this purpose, as similar results have been obtained using 0.18 mM Tween20 solution which is equal to 3 times the CMC of this surfactant, therefore it is not necessary to use ethanol, as the latter is presented here only as an example. Other surface active agents, such as sodium dodecyl sulfate, natural surfactants like saponins, at concentrations close to their CMC can also be used to achieve the same effect. Higher concentrations of surfactants, however, could be toxic for the cells as they interact adversely with the cells membranes.

Figure 3.5d-f shows the fluorescence microscopy image of the individual yeast cells stained with FDA after being treated with aqueous solution of ethanol (d, and e) and Tween20 (f) before their encapsulation into the sporopollenin capsules. The results show that short time incubation in the aqueous solution of either ethanol or Tween20 does not show an adverse effect on the yeast cells and does not significantly impair their viability. Unfortunately, direct observation of the fluorescence from the FDA-stained cells encapsulated inside the sporopollenin cannot be achieved due to the natural fluorescence of the sporopollenin material which is much stronger than the fluorescence signal from the entrapped yeast cells.

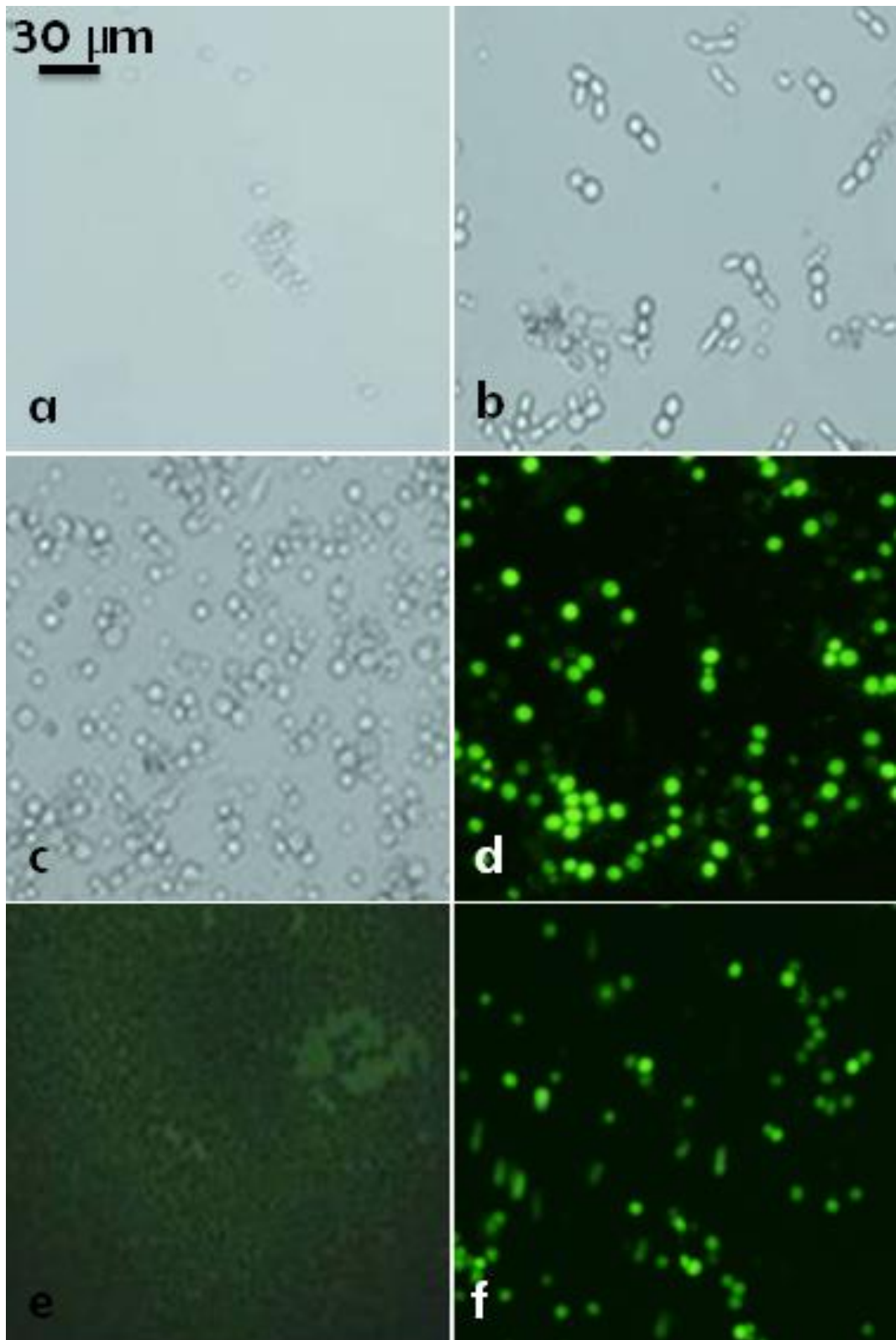


Figure 3.5: (a) 1 % wt. native yeast cells before growing in culture media, (b) the cells incubated in culture media for 19 hours at 25 °C, (c) cells incubated at 37 °C, (d) native yeast cells exposed to 20 % vol. ethanol for one hour, (e) 40 % vol. ethanol was used, (f) the cells were dispersed in 3 times CMC Tween20 solution for one hour.

### 3.1.3.3 Analysis of the cell intake of sporopollenin microcapsules

Direct observation of the encapsulated yeast cells inside the sporopollenin microcapsules using optical or even fluorescence microscopy was found to be technically very challenging. Therefore, other means has to be employed to study the cell intake by the microcapsules. Several methods have been used; one of them was using Scanning Electron Microscopy to observe the cells in cracked-open microcapsules. For this purpose a sample of sporopollenin loaded with yeast cells was treated with liquid nitrogen to make it brittle and then grinded by pestle and mortar to crack the microcapsules open. The cracked open shells with encapsulated cells were visualised using scanning electron microscopy. Figure 3.6 and 3.8 show typical SEM images of cracked-open sporopollenin from *Lycopodium clavatum* with encapsulated yeast cells. The SEM images show that the sporopollenin contains a significant number of cells which can be grown further on the inside of the microcapsules if the yeast is exposed to a suitable growth medium.

In our experiments we remove all the non-encapsulated cells outside the sporopollenin microcapsules before grinding the sample to prevent them from moving into the inside of the microcapsules after they were cracked open. To remove the non-encapsulated yeast cells the sample was excessively washed with milli-Q water and then left still until the microcapsules and the encapsulated yeast cells inside sedimented under gravity, after which, the dispersion of the non encapsulated cells was decanted. This has achieved because the non-encapsulated yeast cells are smaller in size and lighter than the sporopollenin microcapsules, therefore, the microcapsules will sediment much faster than the non-encapsulated cells. Figure 3.7 illustrates several steps in the removal of non-encapsulated yeast cells.

The sporopollenin loaded with live yeast cells was also examined by using confocal fluorescence microscopy following the exposure of the sample to a solution of fluorescein diacetate. A series of fluorescence images of the cross-section of a sporopollenin in Figure 3.9 shows clusters of fluorescing cells which indicates that the yeast cells remain viable after a successful encapsulation process.

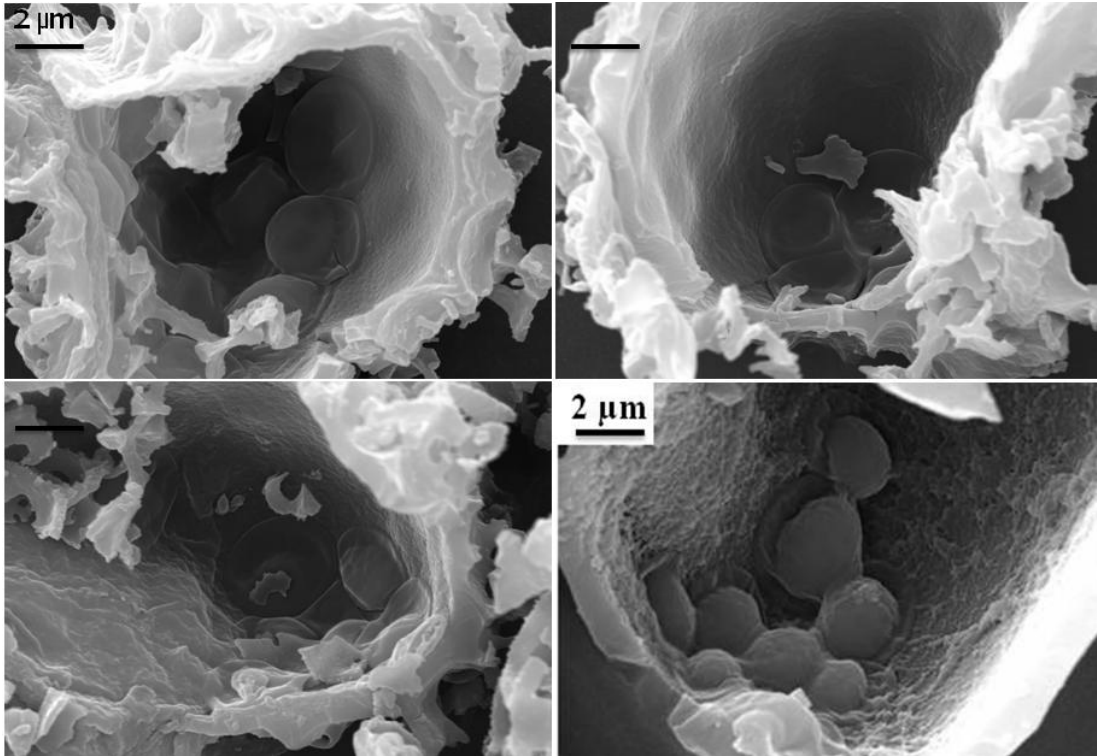


Figure 3.6: Scanning electron microscopy images of encapsulated yeast inside sporopollenin microcapsules (28  $\mu\text{m}$  in diameter) prepared from *Lycopodium clavatum* pollens using 20 % vol. ethanol water mixture as a surface active agent. The sample was treated with liquid nitrogen and then the microcapsules were cracked open by pestle and mortar.

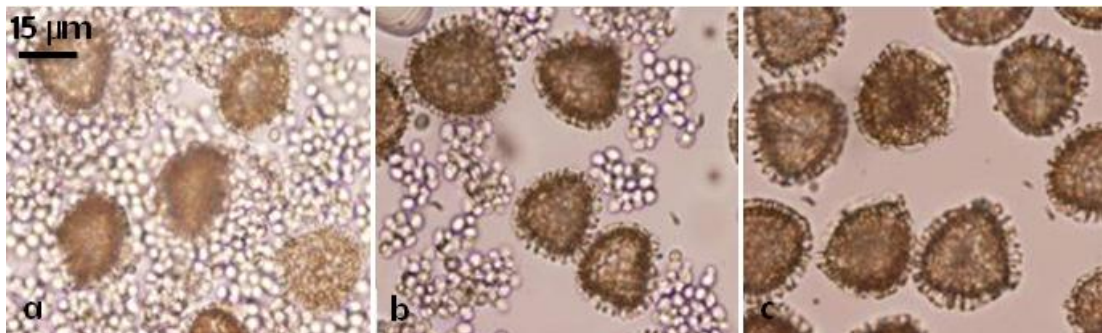


Figure 3.7: Optical microscopic images of a mixture of non-encapsulated yeast cells with *Lycopodium clavatum* sporopollenin microcapsules loaded with yeast cells. (a) represents before washing, (b) represents after 3 times washing, and (c) is after 10 times washing and sedimenting the microcapsules under gravity.

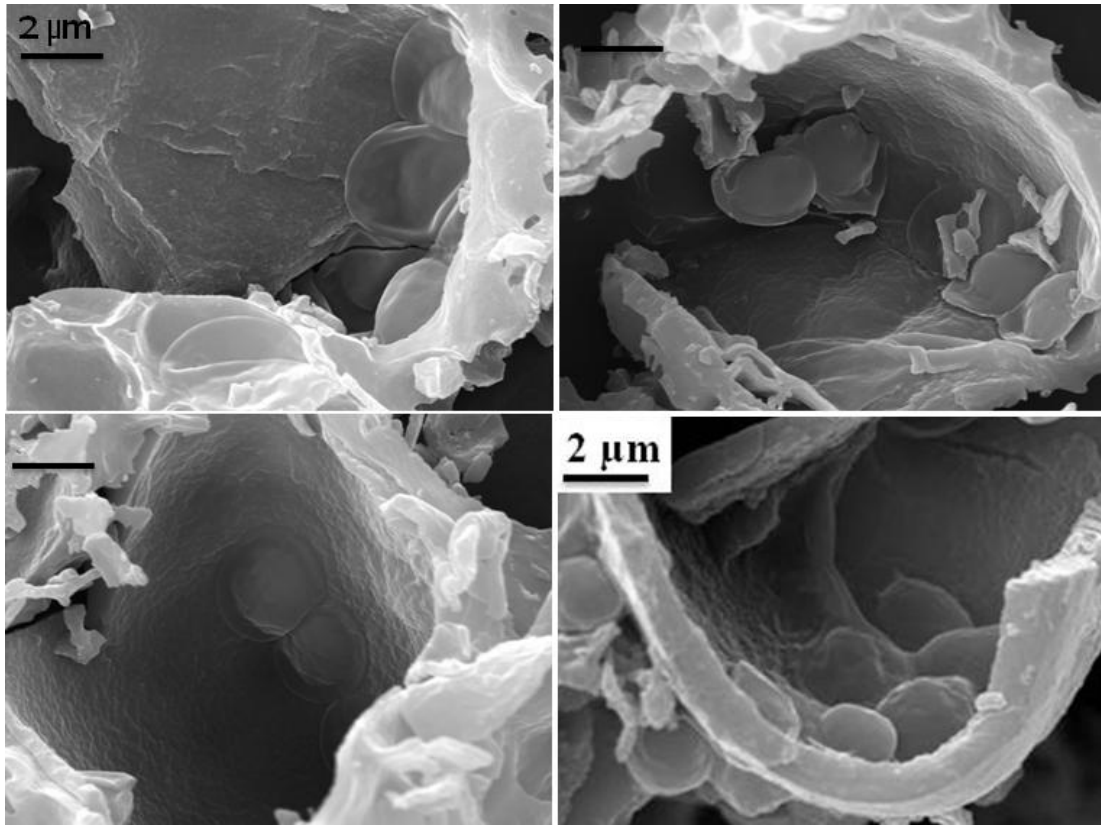


Figure 3.8; Scanning Electron Microscopy images of yeast cells encapsulated inside sporopollenin microcapsules (28  $\mu\text{m}$  in diameter) using aqueous solution of Tween20 as surface active agent. The Tween20 concentration was 3 times CMC (0.18 mM).

#### 3.1.3.4 Encapsulation of magnetic yeast in sporopollenin

One relatively novel method of targeted delivery of active ingredients is based on using magnetic particles encapsulated within a delivery vehicle. This way the cost preparation of such materials can be reduced and the drug toxicity can be minimised as the active compound can be transported directly to the purposed location in the body. The following experiment was designed for two purposes; one was for targeted deliveries of living cells especially live probiotics into lower intestines by conjugating the cells with magnetic nanoparticles and using a magnetic field for external manipulation. The other purpose of this experiment was to confirm the presence of encapsulated yeast cells in the sporopollenin microcapsules. Yeast cells were magnetically functionalised by coating them with magnetic nanoparticles as described by Fakhruhin *et al.*<sup>69</sup> and then encapsulated in sporopollenin microcapsules as an aqueous dispersion with the non-ionic surfactant Tween20 (at concentration 3 times



the CMC). The sporopollenin suspension was washed off thoroughly by multiple cycles of sedimentation and replacement of supernatant to remove the non-encapsulated yeast cells which yielded a result similar to the sample shown in Figure 3.7. The presence of magnetised yeast cells inside the microcapsules was confirmed by using an external magnet by which we were able to collect the suspension of the sporopollenin with encapsulated cells which indicates that the magnetically functionalised yeast cells are entrapped inside the microcapsules as it is shown in Figure 3.10.

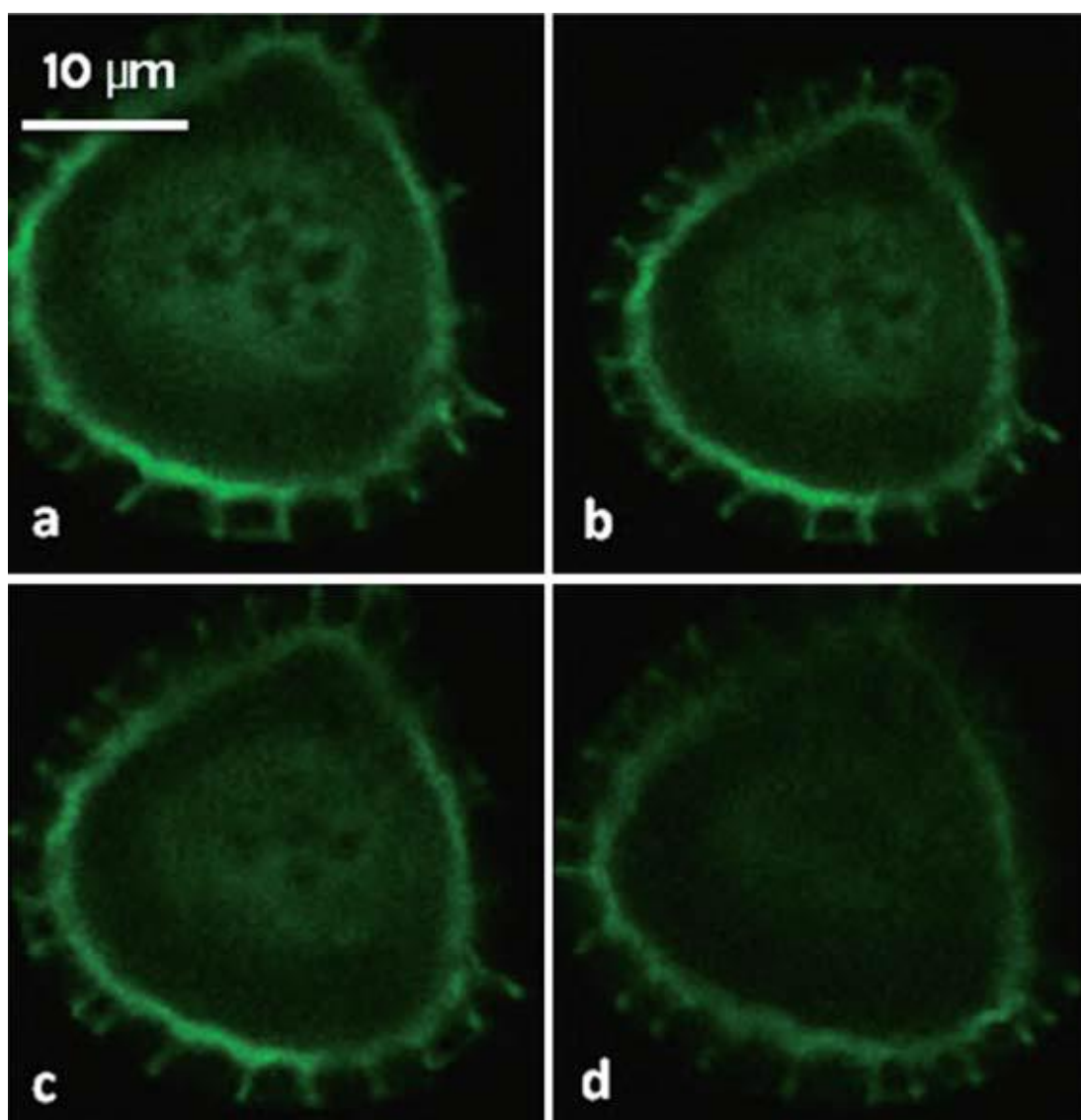


Figure 3.9: Confocal fluorescence microscope image of a cluster of encapsulated yeast cells inside a sporopollenin microcapsule. Each micrograph shows different depths in the Z position as follows: (a) 13.1  $\mu\text{m}$ , (b) 13.6  $\mu\text{m}$ , (c) 14.0  $\mu\text{m}$ , and (d) 15.8  $\mu\text{m}$ .

### 3.1.3.5 Examining cell activity inside sporopollenin microcapsules

To check whether the cells can grow and function inside the sporopollenin microcapsules, a fixed amount of the sporopollenin loaded with yeast cells was added into an aqueous gel prepared from oxidised starch containing sterilised yeast growth media. 3 control experiments were conducted where yeast cells alone and sporopollenin alone were encapsulated into the gel.

Figure 3.11 presents the results of the biological activity of the yeast cells encapsulated in the sporopollenin microcapsules which is indicated by the carbon dioxide released during the growth. This was detected by breaking (puffing) of the starch gel in which the sporopollenin was dispersed. The top image of Figure 3.11 corresponds to the beginning of the experiment and the bottom image shows the results of the biological activity of the cells. To make the experiment rigorous 3 control experiments were conducted, (the first 3 tubes, (a)–(c)) which contain only the starch gel (a), the yeast alone in a starch gel (b) and the sporopollenin alone in a starch gel (c). As it becomes clear from the images, only the yeast alone (b) and the yeast in the sporopollenin (d) puff the gel, hence the yeast in the sporopollenin is biologically active. The top marks on tubes (b) and (d) indicate the position of the expanded gel due to the carbon dioxide produced by the yeast cells.

It is worth mentioning that although the direct observation of the cells encapsulated in sporopollenin was challenging one can see that, microencapsulation of yeast cells inside sporopollenin was successfully achieved. The mechanism of this process can be summarised as follows. The trilite scars on the sporopollenin microcapsules opens up by compressing the dry sporopollenin powder into a tablet. This is then exposed to a concentrated dispersion of cells in the presence of a surface active agent such as aqueous solution of Tween20 or ethanol, which enhances the wetting of the interior of the dry sporopollenin microcapsules by the aqueous suspension of the cells. This process allows the microcapsules to be re-inflated by infusing them with significant amount of cells in their cavities before their trilite scars are closed.

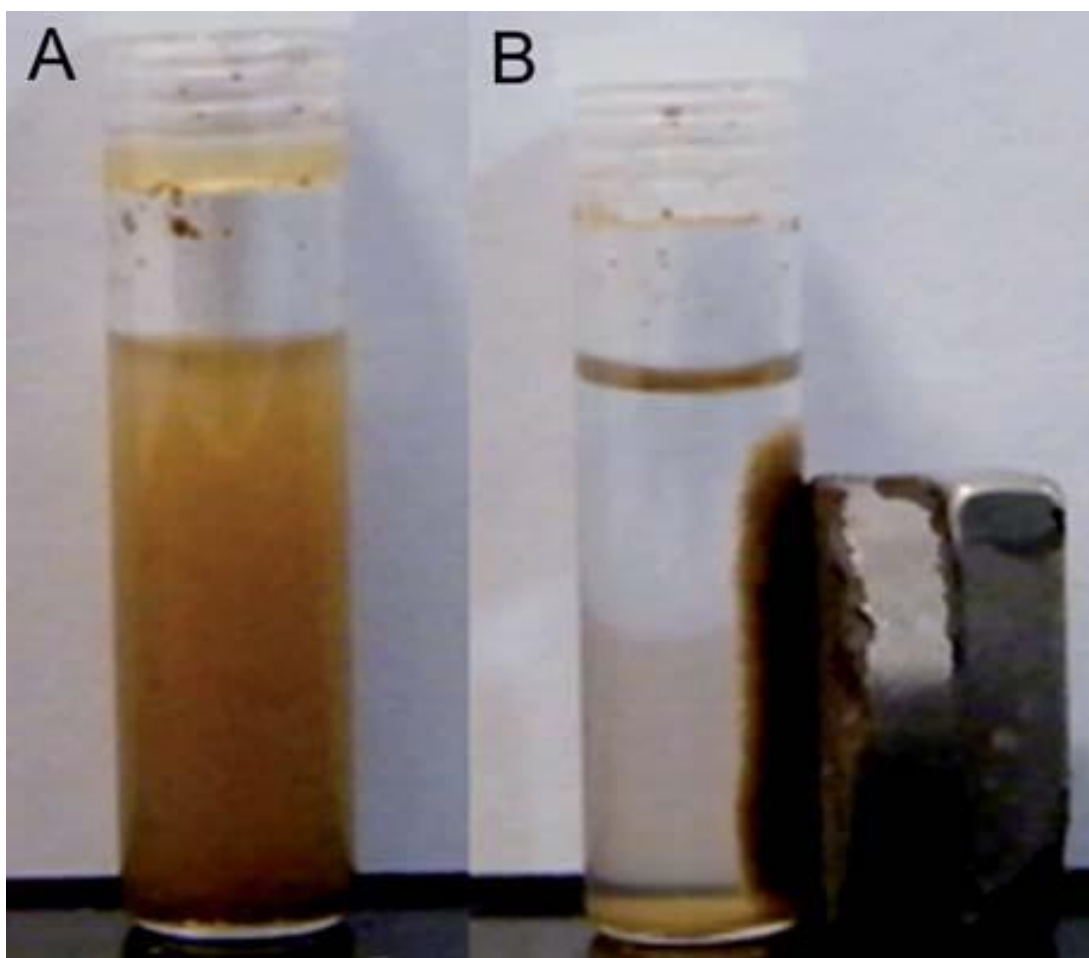


Figure 3.10: (A) Re-dispersed suspension of sporopollenin with entrapped magnetic yeast cells; (B) the sporopollenin particles are attracted to the external magnet due to the presence of magnetically functionalised yeast cells inside the capsules.

The process is driven by the wetting action of the surface-active agent. As the sporopollenin fills in with the aqueous media, the original volume of the sporopollenin pellet in the solution increases up to five fold and the trilite scars close up as the sporopollenin capsules re-inflate which gives rise to trapping the yeast cells inside the capsules. It has been found that the method works efficiently only if the sporopollenin tablet is exposed to a minimal amount of concentrated suspension of cells. Another significant point is that, after mixing the yeast dispersion and the sporopollenin disc, the mixture has to be stirred for a few seconds until a paste is produced and then put under vacuum for at least an hour. The later helps to evacuate the trapped air from the inside of the sporopollenin, facilitates the closing of the trilite scars and results in efficient cells encapsulation.

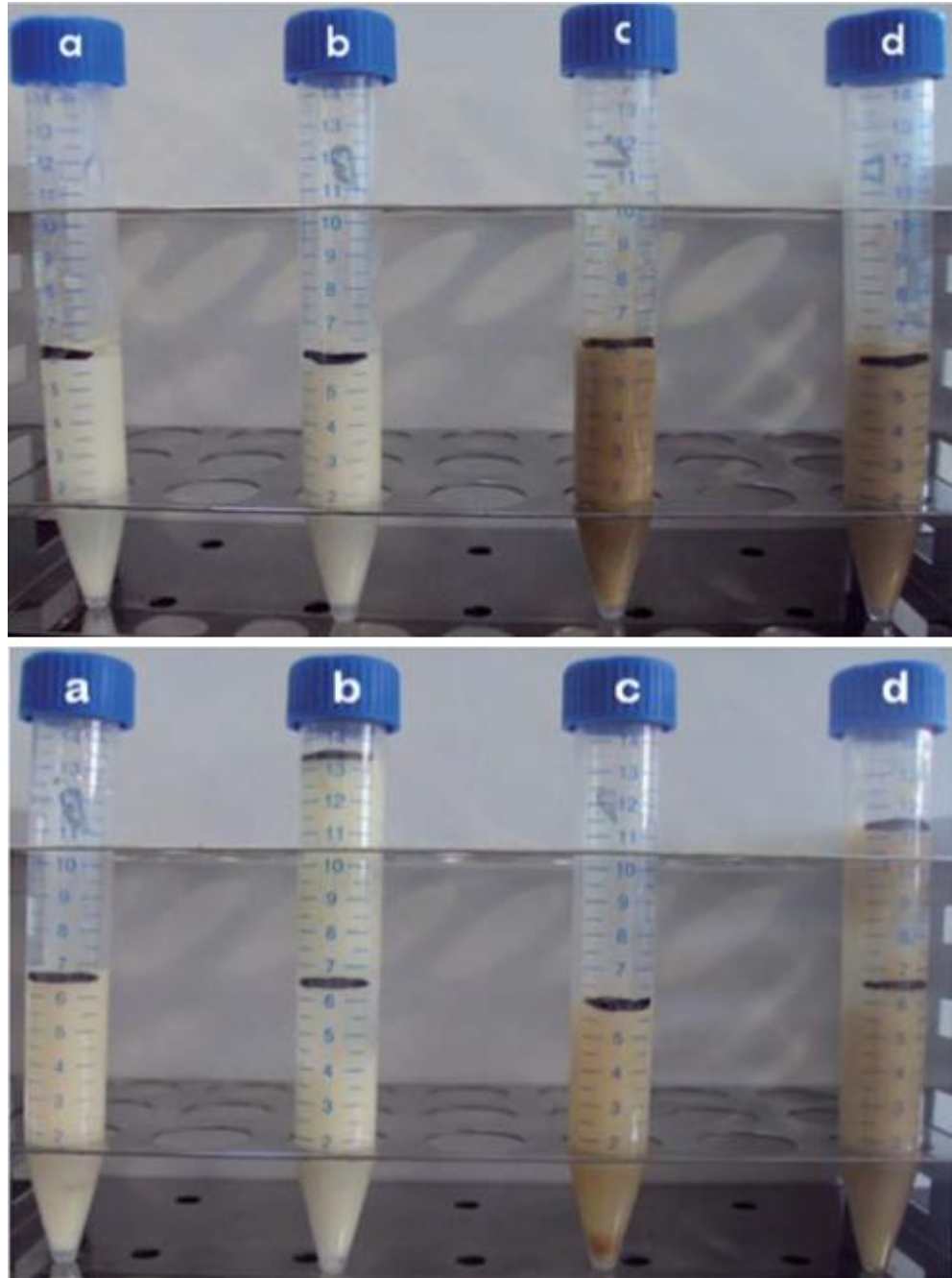


Figure 3.11: Top image: the culture medium was sterilised by boiling at 100 °C for 1 hour and then cooled down to room temperature, after which the starch powder was dissolved in it before incubation at 37 °C for 24 hours; here (a) is just starch gel with the culture medium, (b) starch gel with the culture medium and 1 % wt. native yeast cells, while, (c) 0.1 g sporopollenin in the culture medium with starch gel and (d) 0.1 g sporopollenin with yeast cells encapsulated inside with starch gel. Bottom image: the samples were incubated at 37 °C in a Grant thermostat for 24 hours. Samples (a, and c) which are controls and contain no yeast cells are not grown but samples (b and d) which contain yeast cells are grown and carbon dioxide gas has puffed the gel.

### 3.1.4 Conclusions

In summary, encapsulation of living yeast cells into the exine of pollens from *Lycopodium Clavatum* plant has been achieved. The sporopollenin particles produced from this plant are approximately 28  $\mu\text{m}$  in diameter and have trilite scars on their surface which can be opened up after compression which allowed us to encapsulate live cells inside the sporopollenin microcapsules cavities. For efficient encapsulation, the sporopollenin powder needs to be compressed into a pellet so as to force the trilite scars to open up. Exposing the dry sporopollenin pellet to a concentrated aqueous dispersion of cells in the presence of a surface active agent helps the process of efficient encapsulation by facilitating the capillary suction of cells suspension inside the compressed sporopollenin microcapsules, inducing their ‘‘re-inflating’’ with the cells dispersion and closing the opened trilite scars. The viability of the cells was demonstrated after the encapsulation procedure and it was shown that the sporopollenin microcapsules contain a significant amount of entrapped cells.

We were successful in growing encapsulated cells further inside the sporopollenin by placing the loaded sporopollenin into a culture medium. The latter is possible due to the fact that nano-pores of the sporopollenin allow nutrient transport across its membrane. The cells inside the pollens can grow until they fill all the space, after which their growth will be impaired. This could be used for controlling the rate of fermentation reactions or for using sporopollenin as bioreactors to generate and load the active ingredient in situ. The encapsulation of living cells inside sporopollenin can be used for many different applications in the food and pharmaceutical industries, including protection of probiotics in food formulations and delivery of live vaccines for pharmaceutical applications.

In addition, by using the method developed previously the pollens could be loaded with magnetic nanoparticles and live cultures simultaneously. This can allow remote manipulation, like fixation, removal or targeted delivery of such bio-reactors. Yet another potential application of this method could be to encapsulate two or more symbiotic cells forming a food chain inside the pollen grains and study their growth and behaviour.

## Chapter 4.

### Triggered Cell Release from Shellac-Cells Composite Microcapsules

#### 4.1.1 Introduction

Shellac is biodegradable and renewable resin of the insect (*Kerria Lacca*)<sup>70</sup> formed by self-esterification of a mixture of polyhydroxy acids<sup>71</sup> such as polyhydroxy polycarboxylic esters, lactones and anhydrides, and the main components are aleuritic and shellolic acids.<sup>72</sup> Shellac can be purified from its source “a natural polymer” called Lac, the resinous secretion of the insect found on several species of trees in Asian countries such as India, Thailand and China. The physico-chemical properties of shellac are variable depending on the strain of insect, host trees and refining methods. Because of its natural origin, shellac is an acceptable coating material for food supplement products. In general, shellac possesses good resistance to gastric fluid, suggesting its use for enteric coating purposes.<sup>73</sup> Shellac is soluble in ethanol and insoluble in water but it can be dissolved in alkaline solution above pH 7, below this pH starts to precipitate. Shellac has density around 1.0619 g/mL close to the density of water and refractive index of 1.367.

Changes in the mechanical and physicochemical properties of shellac have been observed by partial hydrolysis. Films prepared from hydrolysed shellac are more flexible and soft than those prepared from native shellac. Meanwhile, the solubility of shellac was increased to pH 7 and the ability of the hydrolysed shellac to form ammonium salt has been enhanced. Treating shellac with alkaline solutions should be an easy approach for modifying shellac that possesses better enteric properties.<sup>73b</sup> Successful fabrication of food-grade shellac micro-rods which contained a range of micro-particle inclusions to use as efficient foaming agent and production of shellac micro-rods with yeast cells “lumps” to improve steric stability of food-grade foams have been reported by Campbell *et al.*<sup>74</sup>

Encapsulation using shellac was recently reported by Law *et al.* which include stabilisation and targeted delivery of Nattokinase (NKCP) in shellac beads prepared by cross-linking aqueous solution of ammonium shellac salt with divalent calcium ion.<sup>70</sup> While, more recently a systematic study of the mechanical properties of thin-walled liquid-filled pectinate capsules and the influence of the addition of shellac to the polymer solution was made. The measurements showed that precipitation of shellac under acidic conditions increased the flexibility and softness of the capsules against deformations.<sup>75</sup>

In two separate studies Xue *et al.*<sup>76</sup> prepared and characterised calcium-shellac microspheres loaded with carbamide peroxide (CP) as tooth whitening agent. In their first study they used extrusion technique based on dropping aqueous ammonium shellac solution into calcium chloride solution, whereas, emulsifying aqueous solution of ammonium shellac in sunflower oil with calcium chloride powders, followed by gelation between shellac and calcium resulted in preparation of micro-spheres loaded with (CP) in their subsequent study.

The most important work involving encapsulation of probiotics using shellac was carried out by Stummer *et al.* by coating individual fluid-bed dried bacterial species with formulation of shellac and various plasticisers such as glycerol, sodium alginate and polyvinylpyrrolidone. The enteric coating has increased elasticity, and solubility of shellac was increased at pH 7.5. In addition the enteric coating provided protection for the individual microorganisms against acidic pH of stimulated intestinal fluid.<sup>73a</sup>

Despite the efforts made to use shellac as a protective cover for microorganisms especially probiotics, coating and protecting the bulk of such microorganism in a suitable composite microcapsule made out of shellac derivatives, which has ability to transfer viable probiotics to the lower intestine and release them through disintegrating in pH of approximately 8 has not been reported to our knowledge. Therefore, in this chapter, we report the fabrication and subsequent disintegration of composite shellac/yeast cells microcapsules by manipulation of spraying techniques. Here yeast cells have been used as a model for probiotics because they are the most researched, robust and easy to obtain and handle microorganisms in laboratory.

The fabrication process of the desired composite microcapsules that can protect the probiotics from the mechanical stress of the stomach and low pH of gastric juice, has been accomplished by two spraying techniques, which have been employed as follows: dispersion of native yeast cells in ammonium shellac solution was either spray co-precipitated in acetic acid or calcium chloride solutions or spray dried in a designed spray dryer of hot air at 80 °C. Improving the ability of the composite microcapsules to disintegrate at pH nearby 8 provided the idea of doping the ammonium shellac solution with both carboxymethylcellulose and sodium polyacrylate solutions separately.

#### **4.1.2 Results and discussion**

Composite shellac-yeast cells microcapsules were fabricated by either spray drying or spray co-precipitating a dispersion of yeast cells in ammonium shellac solution as shown in Figure 4.1. Dispersions of 10 % wt. yeast cells in aqueous solutions of different concentrations of ammonium shellac were co-precipitated by either pH change (to acidic pH) or by using calcium chloride solution. In both cases, rigid and stable composite microcapsules were fabricated, which were capable of disintegrating at pH greater than 7.

The spherical aqueous droplets of yeast cells dispersed in ammonium shellac solution produced by the spray co precipitation method faced a rapid precipitation upon their contact with the solution of the precipitating agent (acetic acid or calcium chloride), which allowed them to retain their shape upon contact with the solution.



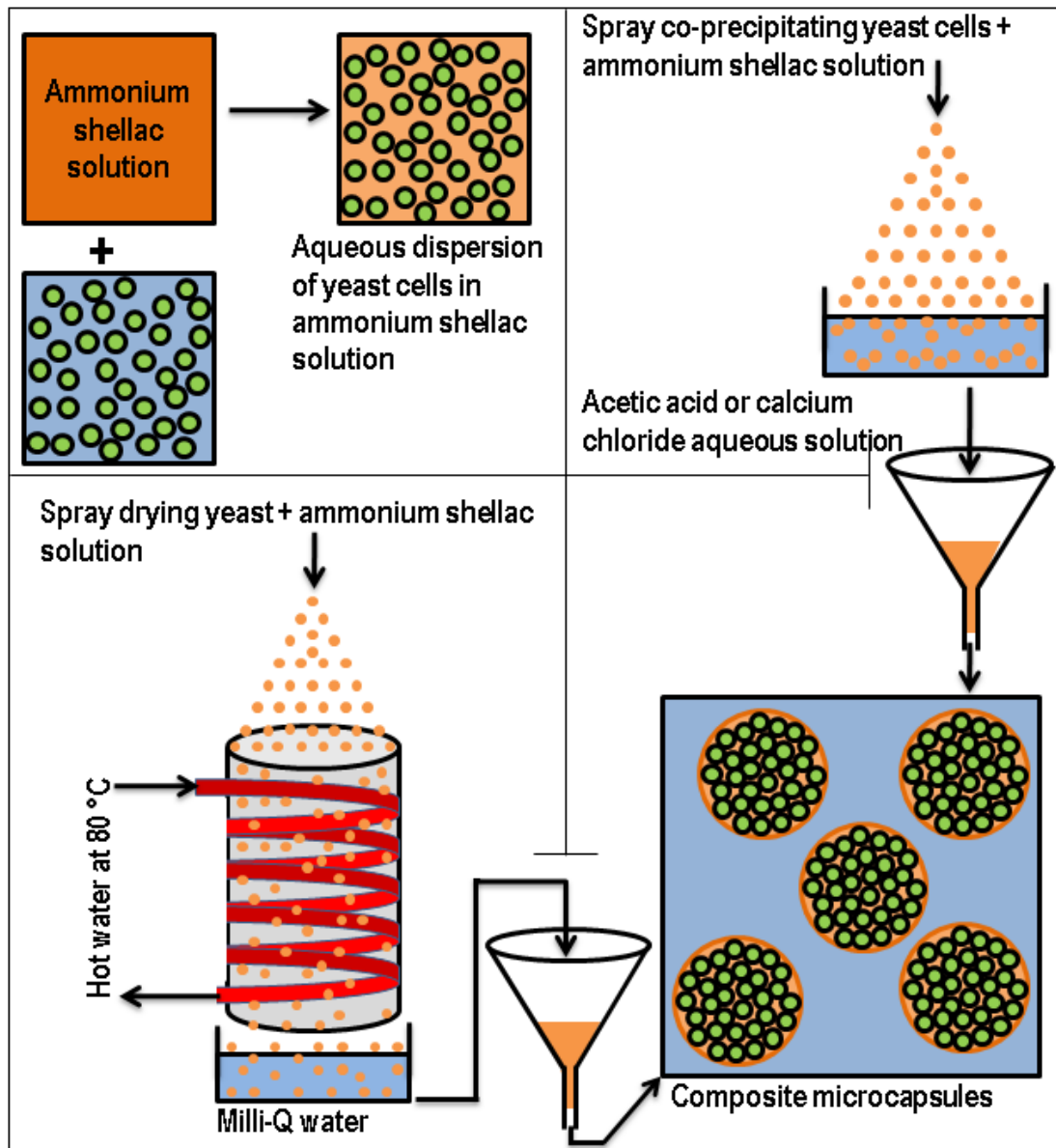


Figure 4.1: Schematic diagram of fabricating composite shellac-cells microcapsules by spray drying and co-precipitating of aqueous dispersion of yeast cells in ammonium shellac solution. The aqueous cell dispersion was doped with pH sensitive polyelectrolytes to control the rate of cells release from the microcapsules in aqueous media at specified pH.

#### **4.1.2.1 Spray co-precipitating of yeast cells/ammonium shellac formulation into acetic acid**

Rigid, and stable composite microcapsules were fabricated by spray co-precipitating aqueous dispersion of 10 % wt. yeast cells in 7 % wt. ammonium shellac solution into 3 % vol. acetic acid solution. The microcapsules were stirred in the acidic medium for 30 minutes then they were filtered off and washed with milli-Q water several times to be characterised by optical and fluorescence (confocal) microscopy. Figure 4.2 shows optical microscopy images of the obtained composite microcapsules from a range of ammonium shellac concentrations which are reflected in the capsule morphology. We found that 7 % wt. ammonium shellac in the initial dispersion was the optimal concentration yielding rigid microcapsules of sufficient integrity, mechanical stability and consistent size range. Some of the microcapsules had semi-spherical shape as the micro-drops shape was “arrested” upon impact with the precipitating solution. The inner structure of the fabricated microcapsules was revealed using confocal fluorescence microscopy by imaging the fabricated microcapsules after staining the ammonium shellac solution with traces of Nile Red ( $10^{-4}$  M) before it was used in the spraying process, while the yeast cells inside the fabricated microcapsules were treated with FDA solution.

Positive FDA test indicates that the yeast cells membranes are intact and the enzymes in the cell interior are active. Typical images of composite microcapsules observed by fluorescence confocal microscopy are shown in Figure 4.3. One can see that the co-precipitated shellac is enclosing the yeast cells producing linking bridges between the individual cells. As shown in Figure 4.3, the red domains represent the pre-stained co-precipitated shellac with traces of Nile Red and the green spheres are the live yeast cells stained with FDA. The confocal microscope images also confirm the viability of the yeast cells inside the microcapsules after exposing them to 3 % vol. acetic acid. These tests combined with FDA staining of cells obtained from the disintegrated microcapsules (see the following pages) confirm that the encapsulated yeast cells are still viable and survive the experimental conditions of the microcapsule fabrication.

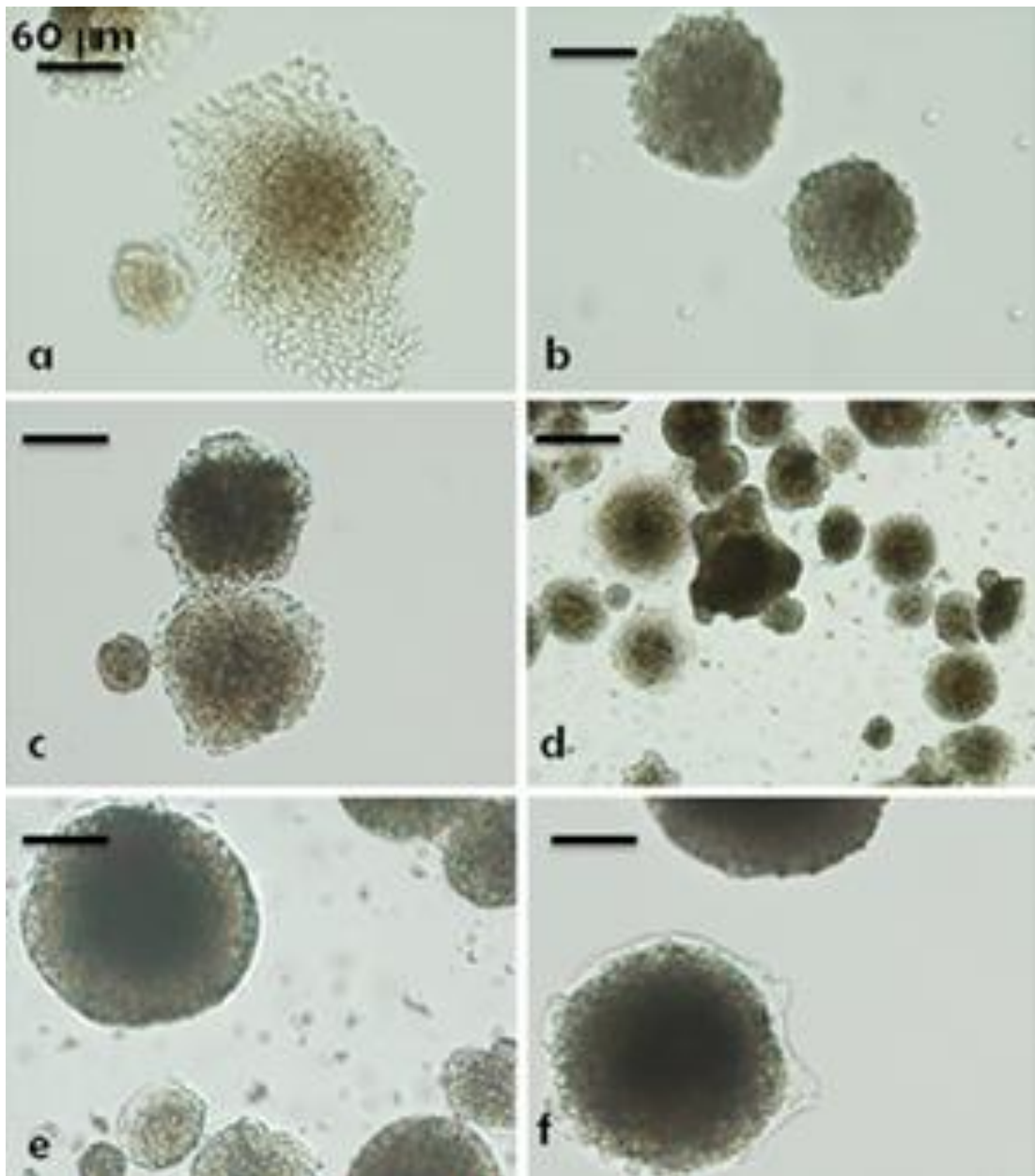


Figure 4.2: Composite shellac-yeast cells microcapsules fabricated by spray co-precipitating a dispersion of 10 % wt. yeast cells in 3 % vol. acetic acid where different concentrations of ammonium shellac solution at pH 8 used as follows, (a= 3.5, b= 5, c= 6 , d, and e = 7, f= 14 ) % wt. All scale bars are 60  $\mu\text{m}$ .

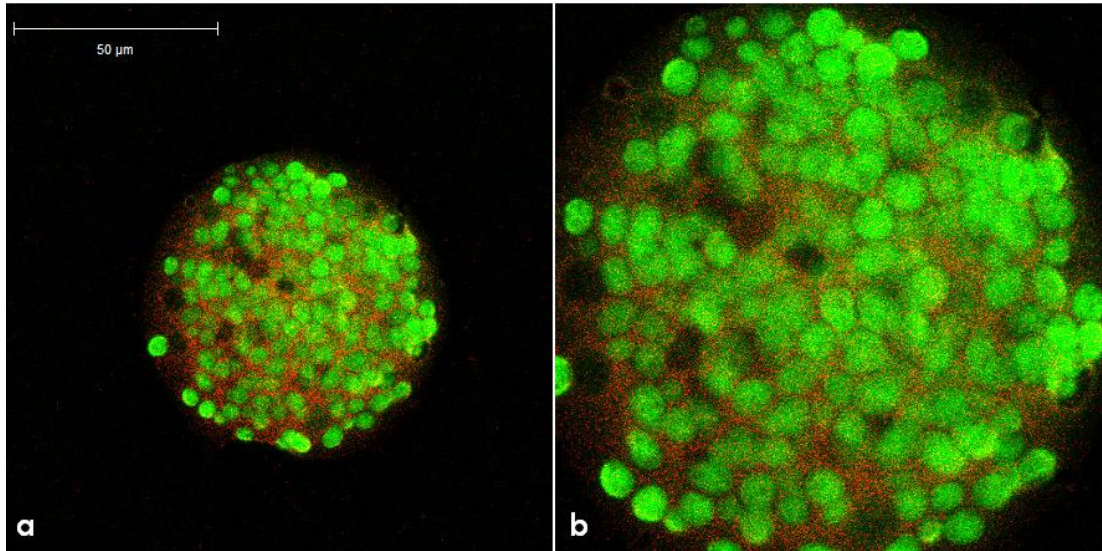


Figure 4.3: Confocal fluorescence microscope images of composite shellac-yeast microcapsules fabricated by spray co-precipitating 10 % wt. yeast cells dispersion in 7 % wt. ammonium shellac solution using 3 % vol. acetic acid solution. The images (a, and b) show a microcapsule observed by confocal fluorescence microscopy with the simultaneous fluorescence by the shellac matrix (doped with Nile Red) and the cells (treated with FDA) at different resolutions.

We also tested the viability of the microencapsulated yeast cells upon exposure to 0.1 M hydrochloric acid at pH 1, which is close to the acidity in the stomach. Native unprotected yeast cells were used as control samples. The results of this experiment, shown in Figure 4.5, confirm that the encapsulated cells can survive exposure to pH 1 without loss of viability, while the mortality of the unprotected cells is 100%.

Scanning Electron Microscopy (SEM) images of the composite shellac-yeast microcapsules showed several typical types of composite microcapsules with diverse morphologies and size distributions. Figure 4.6a-b show typical microcapsules with “mushroom”-like morphology of diameter approximately 100 μm. This reveals fast precipitation of the drops of dispersion of ammonium shellac and yeast cells upon contact with the acetic acid solution. Another example of composite shellac-yeast microcapsule of diameter of approximately 60 μm and different morphology is shown in Figure 4.6c where high percentage of coated yeast cells are exposed on its rough surface. In contrast, smaller microcapsules (around 30 μm in diameter) possessed smoother surface without exposed yeast cells (Figure 4.6d).

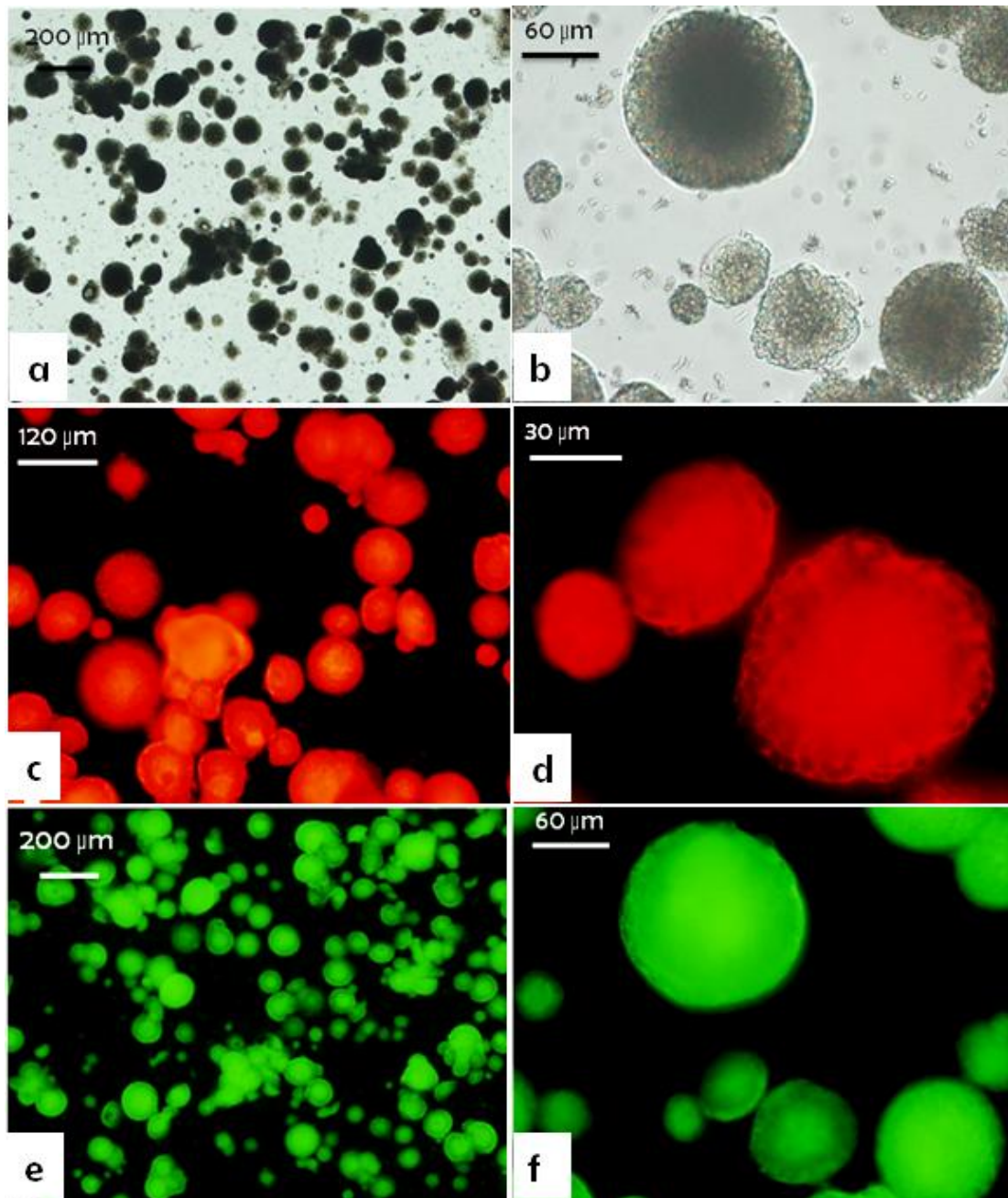


Figure 4.4: Composite shellac/yeast cells microcapsules fabricated by spray co-precipitating a dispersion of yeast cells 10 % wt in ammonium shellac solution 7 % wt. at pH 8 using 3 % vol. acetic acid solution placed in a Petri dish. Micrographs (c, d) microcapsules observed by TRIC fluorescence microscopy, while, in (e, f) FTIC filter was used.

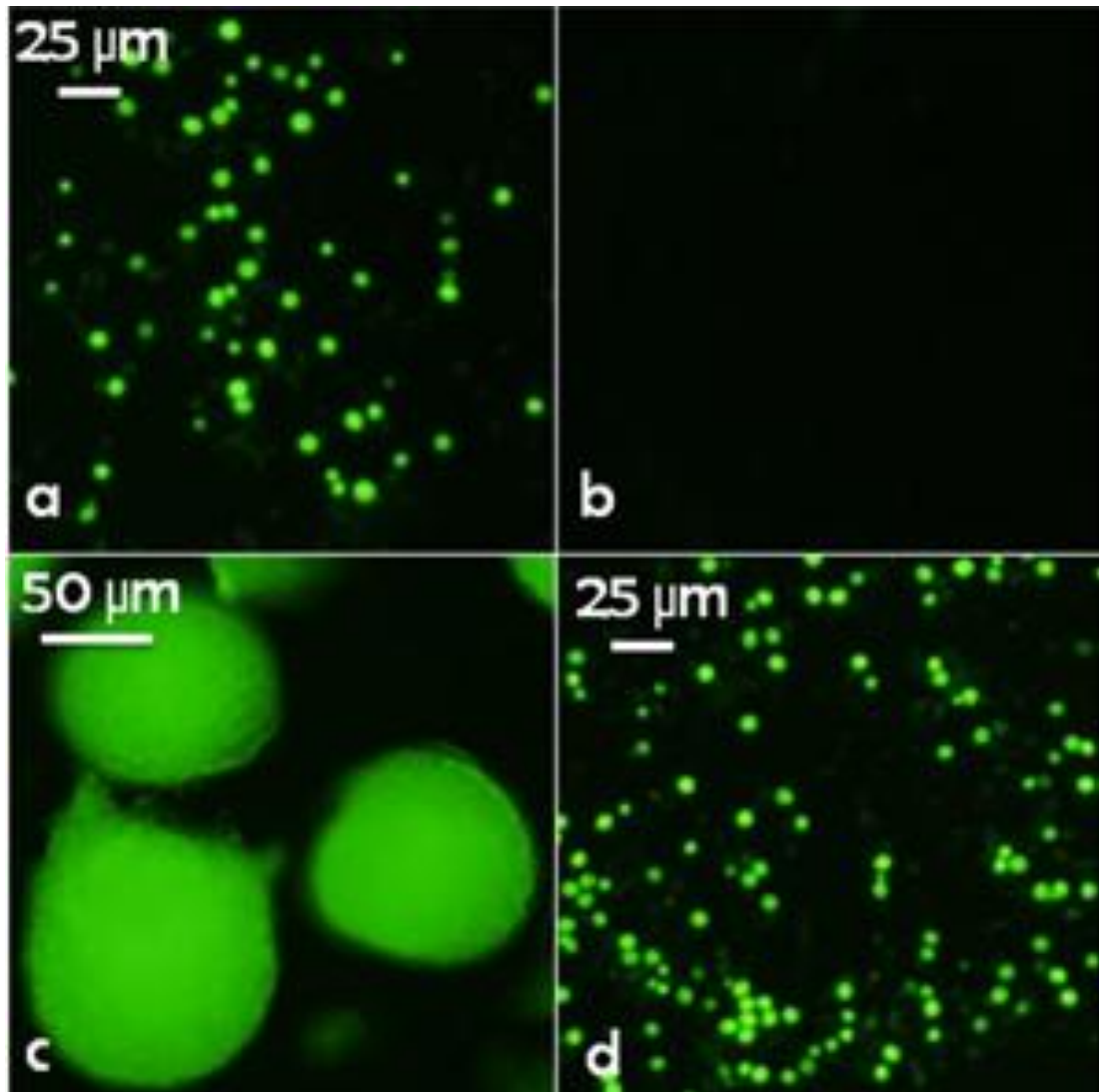


Figure 4.5: Fluorescence microscopy image of native unprotected yeast cells at (a) pH 7 and (b) after being exposed to 0.1 M HCl solution at pH 1 for 30 minutes and then tested for viability with FDA. (c) Composite shellac-yeast cells microcapsules exposed to 0.1 M HCl solution at pH 1 for 30 minutes then washed with milli-Q water and incubated with FDA. (d) Fluorescence microscopy image of the released yeast cells from composite microcapsules incubated at pH 1 for 30 minutes followed by their complete disintegration at pH 8 and incubating with FDA solution.

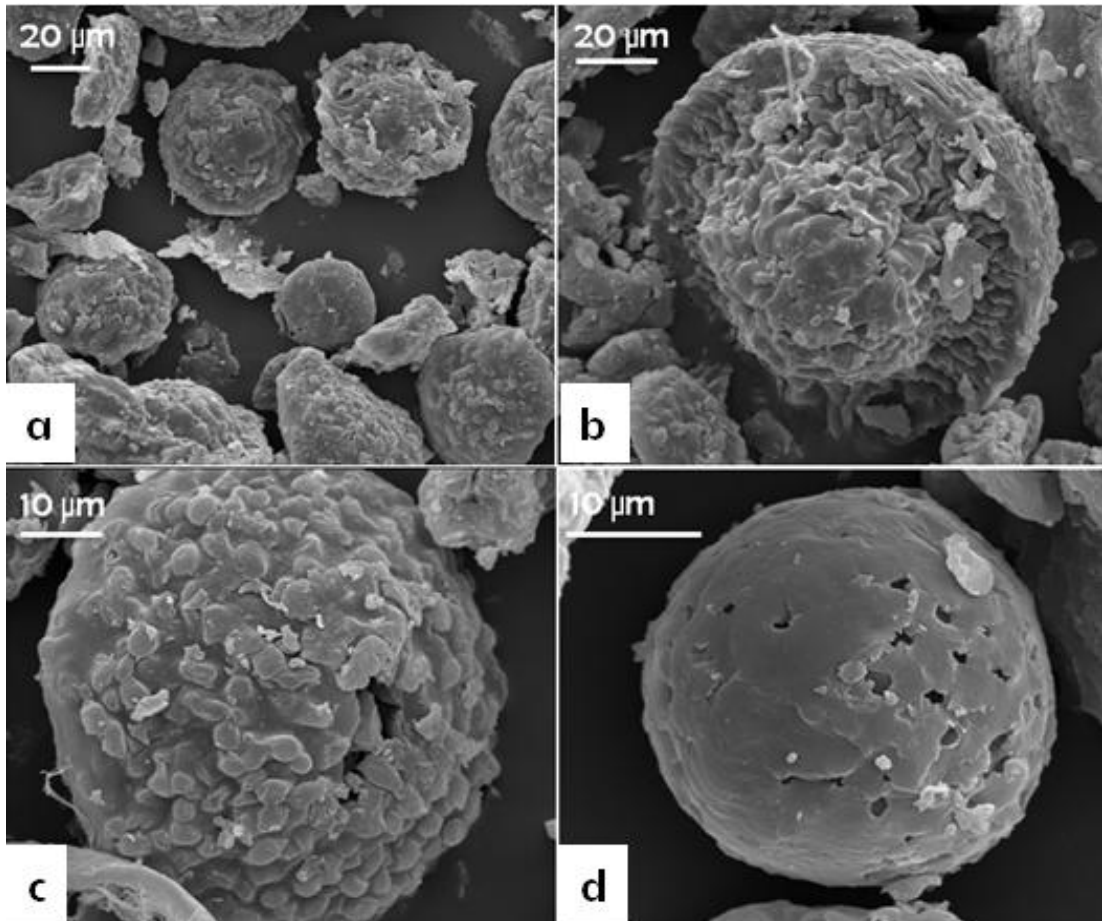


Figure 4.6: SEM images of composite shellac/yeast cells microcapsules fabricated by spray co-precipitating dispersion of 10 % wt. yeast cells in 7 % wt. ammonium shellac solution at pH 8 using 3 % vol. acetic acid placed in a Petri dish. Micrographs (b-d) show microcapsules with different size and morphology.

#### **4.1.2.2 pH-triggered release of encapsulated living cells from the composite microcapsules**

Shellac dissolves at  $\text{pH} > 7$  and starts to precipitate in lower pH; therefore it is a good candidate to be used in the production of protective cover for probiotics against low pH values and mechanical stress. Microcapsules fabricated from spray co-precipitated dispersions of yeast cells in ammonium shellac at low pH should consequently disintegrate at  $\text{pH} > 7$  and release their payload of yeast cells. In a series of experiments we studied the disintegration profile of the composite microcapsules after transferring them into an aqueous solution of 0.1 M sodium bicarbonate at pH 8 to mimic the physiological condition of the lower intestines.

It was found (see Figure 4.7) that the disintegration process of the composite shellac-yeast microcapsules was surprisingly slow as it took up to several hours for their complete disintegration to occur. Therefore, to control the disintegration rate we doped the ammonium shellac solution with hydrophilic pH sensitive polyelectrolytes. It was expected that such polyelectrolyte inclusions would produce voids in the structure of the shellac-yeast microcapsules upon swelling and subsequently accelerate their breakdown to smaller fragments and individual cells.

In one series of experiments, the shellac solution was doped with carboxymethylcellulose sodium salt (CMC). Below 0.5 % wt. CMC, the spray co-precipitation also resulted in stable and rigid composite shellac-yeast microcapsules. These microcapsules were capable of much faster disintegration and release of the yeast cells at pH 8 as shown in Figures 4.8, and 4.9 the microcapsules started to disintegrate first by losing their spherical morphology and producing a lump of aggregated yeast cells, and then the individual yeast cells started to separate from each other because the precipitated shellac which interconnected the yeast cells started to dissolve.



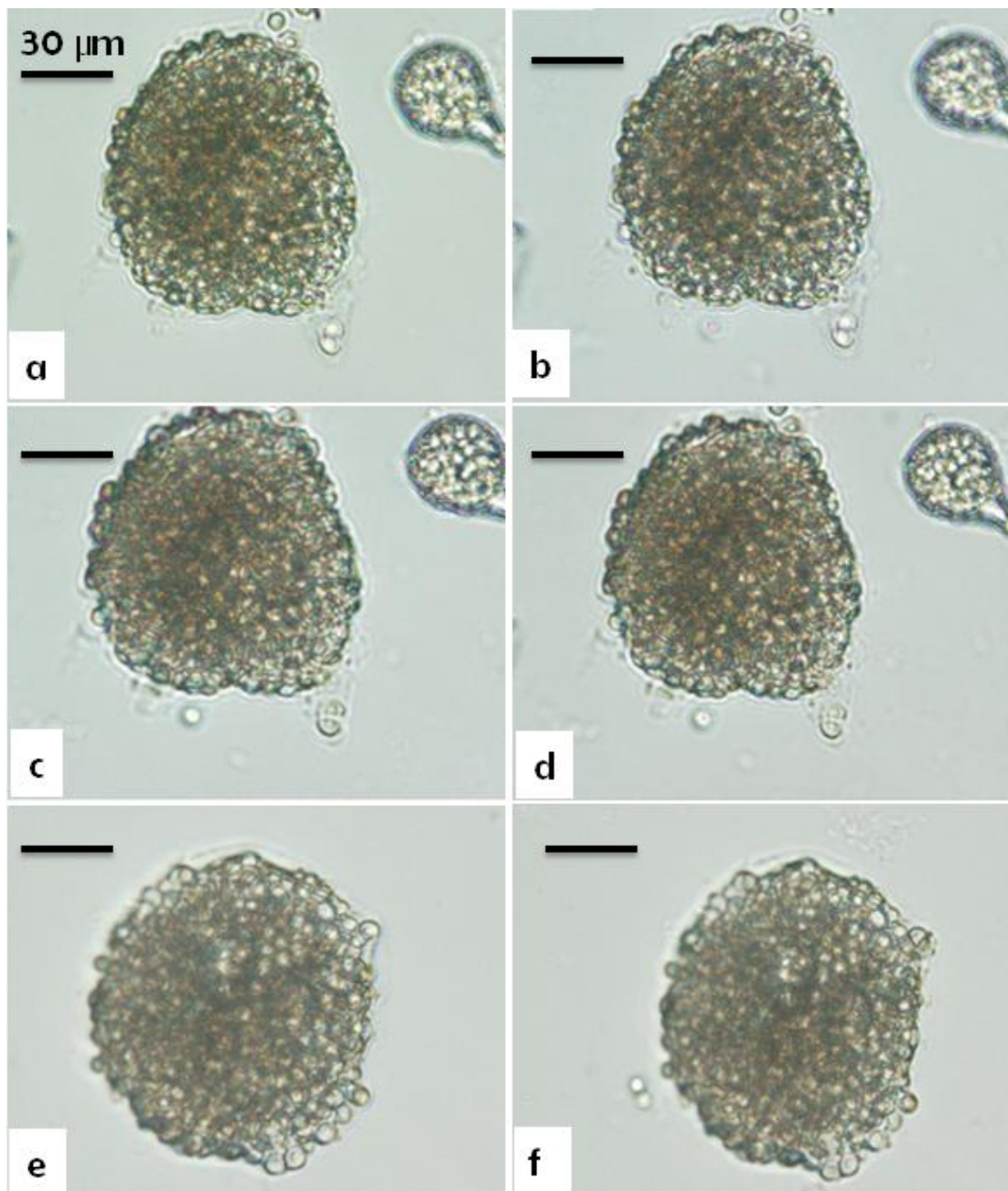


Figure 4.7: Composite shellac/yeast microcapsules fabricated by co-precipitating 10 % wt. yeast cells dispersion in 7 % wt. ammonium shellac solution transferred to aqueous solution of 0.1 M sodium bicarbonate at pH 8 for (1, 2, 3, and 4) hours in (a, b, c, and d) respectively, and at pH 10 for ( 1 and 2 ) hours in ( e-f) respectively.

In Figure 4.8 and 4.9, where 7 % wt. ammonium shellac solution was used, the composite microcapsules start to disintegrate after stirring them in the aqueous solution of sodium bicarbonate for 20 minutes and as the stirring times increase, more microcapsules disintegrate until after approximately 90 minutes of stirring all the microcapsules successfully disintegrated and released the yeast cells. The disintegration process was shortened by doping the ammonium shellac solution with 0.52 % wt. carboxymethyl cellulose. The idea is, when carboxymethyl cellulose starts to swell at  $\text{pH} > 7$ , it would produce voids in the structure of the microcapsules by co-swelling them and this increase the speed of disintegration, because the microcapsules will be more accessible for the aqueous solution.

The disintegrated microcapsules (released yeast cells) washed with milli-Q water and then treated with FDA solution to test the viability of the released yeast cells by fluorescence microscopy. Figure 4.10e-f shows the released yeast cells from the disintegrated composite shellac/yeast microcapsules are still viable.

Using images similar to those in Figures 4.9 and 4.10, the numbers of the remaining microcapsules counted and then the data was used to plot a graph ( see Figure 4.11) to illustrate the trend of the triggered release of the yeast cells inside the fabricated microcapsules in different stirring times. For example according to Figure 4.9b , approximately 19 microcapsules were remaining intact at 0 min of transferring the microcapsules into the aqueous solution of sodium bicarbonate, whereas, when the microcapsules stirred for further 10 min in Figure 10b , the number of the remaining intact microcapsules decreased to approximately 10. Then as the microcapsules was further stirred in the alkaline solution, an extra number of the remaining microcapsules disintegrated, and then after 90 min of stirring the suspension, the number of remaining microcapsules decreased to approximately one in Figure 4.10d.

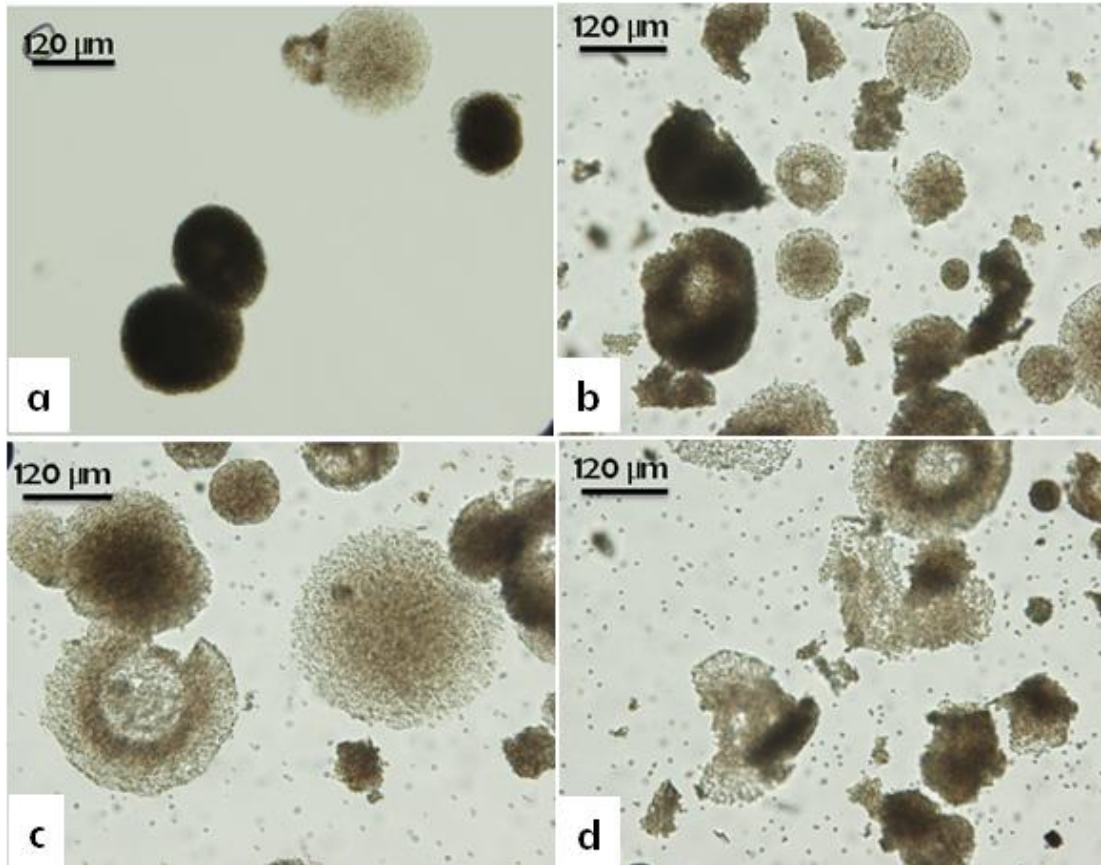


Figure 4.8: Disintegration of composite shellac/yeast cells microcapsules fabricated by co-precipitating a dispersion of 10 % wt. yeast cells in 5 % wt. ammonium shellac solution doped with 0.52 % wt. carboxymethylcellulose using acetic acid solution. Micrographs (b, c, and d) represent the microcapsules after 20, 40, and 60 minutes passed over stirring them in the alkaline medium respectively.

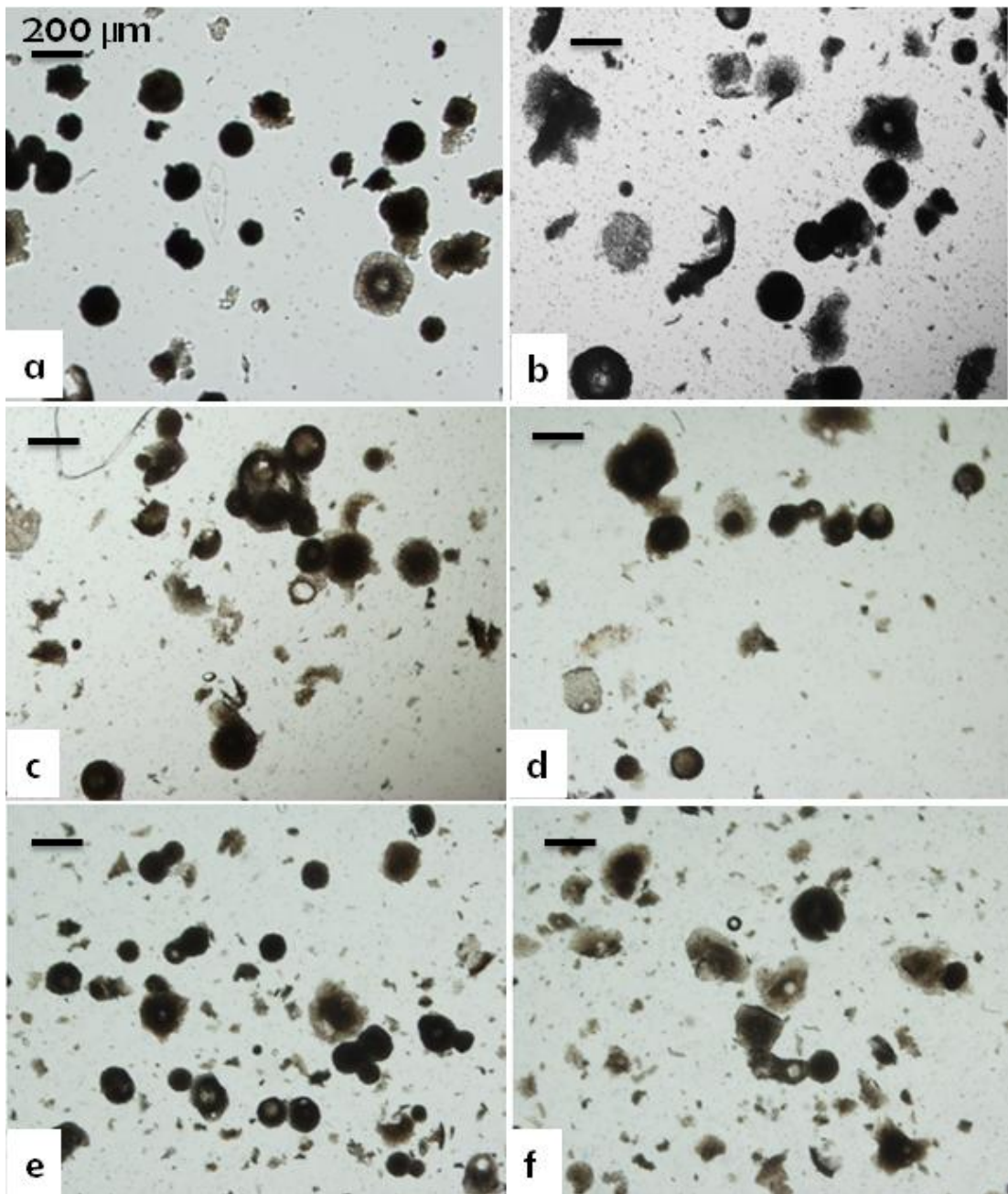


Figure 4.9: Disintegration of composite shellac/yeast microcapsules fabricated by spray co-precipitating dispersion of 10 % wt. yeast cells in 7 % wt. ammonium shellac solution doped with 0.52 % wt. carboxymethylcellulose using acetic acid solution. The microcapsules transferred followed by stirring in aqueous solution of 0.1 M sodium bicarbonate at pH 8 for 0, 10, 20, 30, 40, and 50 minutes in a-f.

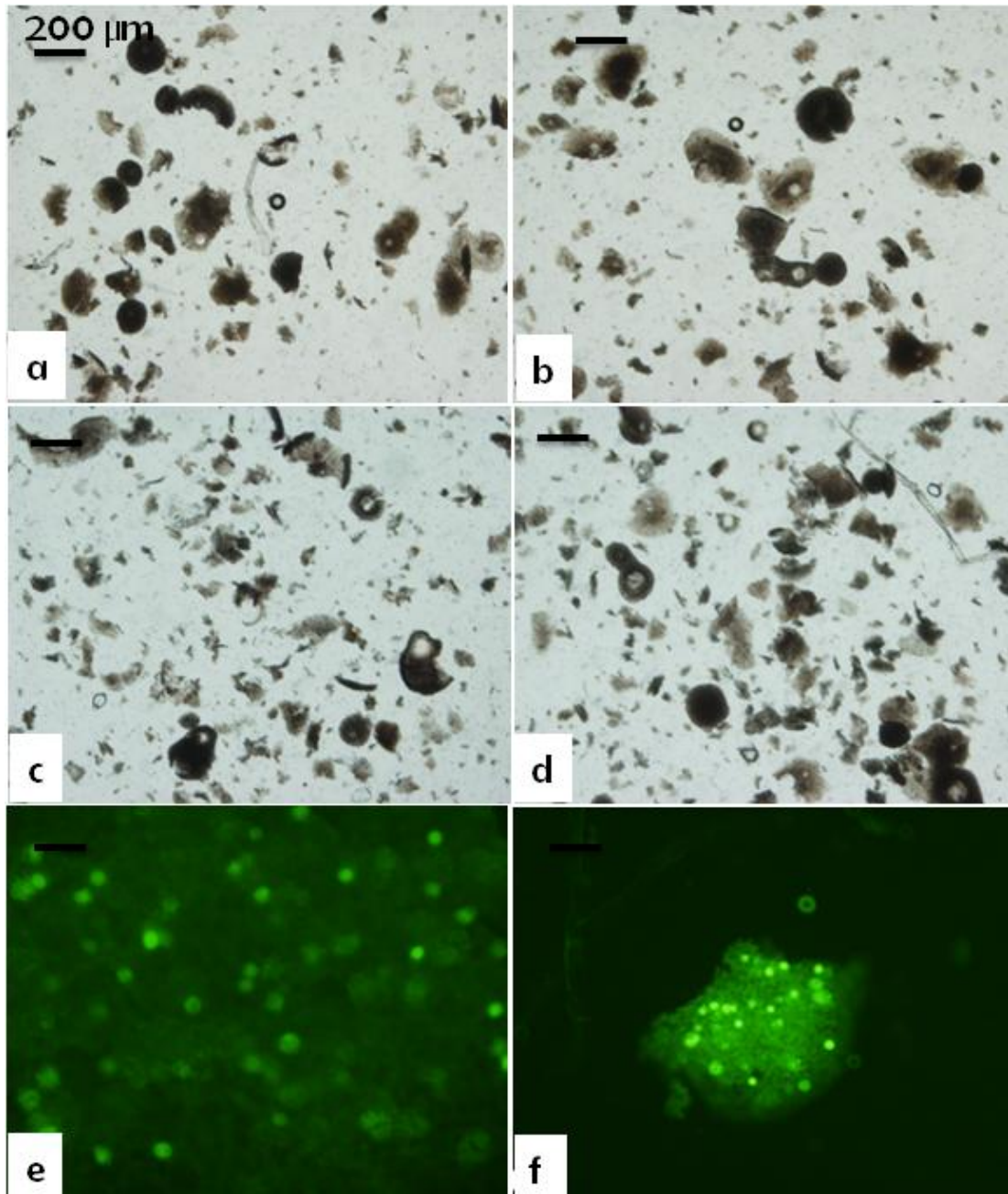


Figure 4.10: Disintegration of composite shellac-yeast microcapsules fabricated by spray co-precipitating dispersion of 10 % wt. yeast cells in 7 % wt. ammonium shellac solution doped with 0.52 % wt. carboxymethyl cellulose sprayed over 3% wt acetic acid aqueous solution. The microcapsules were transferred in a solution of sodium bicarbonate at pH 8 with stirring. Images were taken after: (a) 0 min, (b) 20 min, (c) 40 min, (d) 60 min. (e) 70 min, and (f) 80 min, while (g) and (h) show the viable yeast cells released from the disintegrated microcapsules, using fluorescence microscopy after treating them with FDA solution.

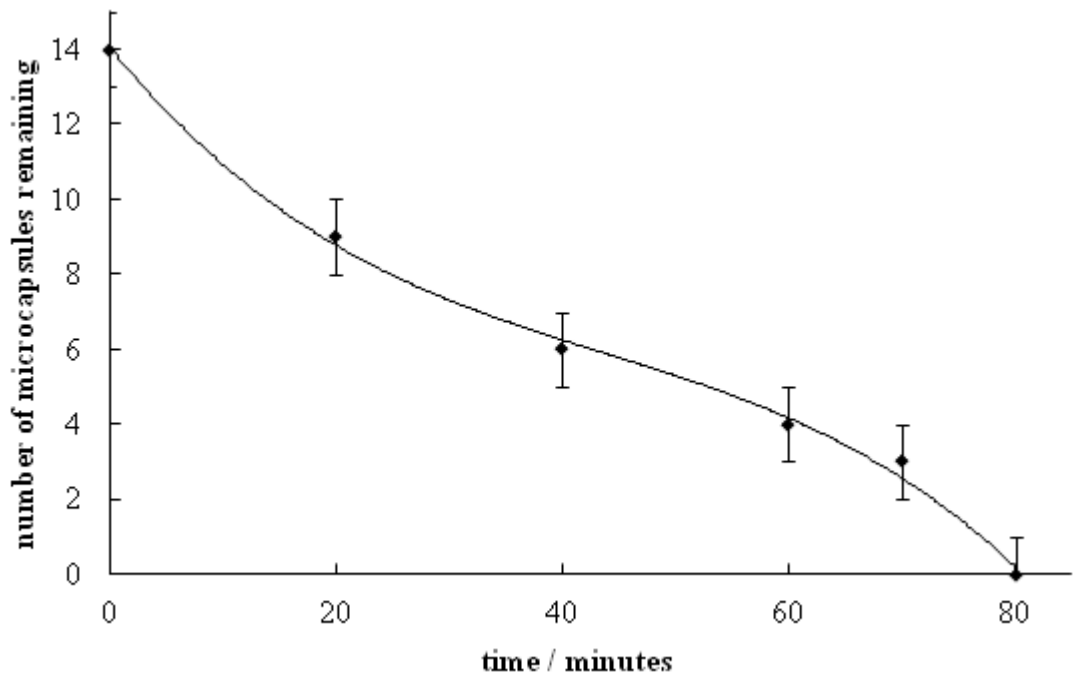


Figure 4.11: The relationship between remaining composite shellac-yeast cell microcapsules and time of transferring and stirring them in 0.1 M aqueous solution of sodium bicarbonate at pH 8.

#### 4.1.2.3 pH triggered release of cells from microcapsules based on doping of shellac with PAA.

Our attempts to accelerate the disintegration of the microcapsules by increasing the CMC content did not produce microcapsules with sufficient integrity as the CMC interfered with the spray precipitation of the shellac at the production stage. Due to this restriction we replaced CMC with sodium polyacrylate (PAA) which as we demonstrate below in a proof of concept study showed dramatically better results with pH induced cell release. PAA is an anionic polymer which swells in aqueous solutions above pH 7-7.5 and can absorb water up to 400 times its own weight. High salt levels swell the polymer more by causing the formation of globular structures, which holds ions and increase the possibility of entanglement.<sup>77</sup>

In this experiment 5 % wt. aqueous solution of ammonium shellac was doped with 4 % wt. PAA and then the native yeast cells were dispersed in the mixture at pH 6.7 supported by acetate buffer and the dispersion was spray co-precipitated in 3 % vol. acetic acid. The produced composite microcapsules were tested for swelling upon exposure to aqueous sodium bicarbonate solution. Figures 4.12 and 4.13 show microcapsules exposed to a drop of 1 M sodium bicarbonate which show a profound and rapid swelling as the composite shellac microcapsules started to dissolve.

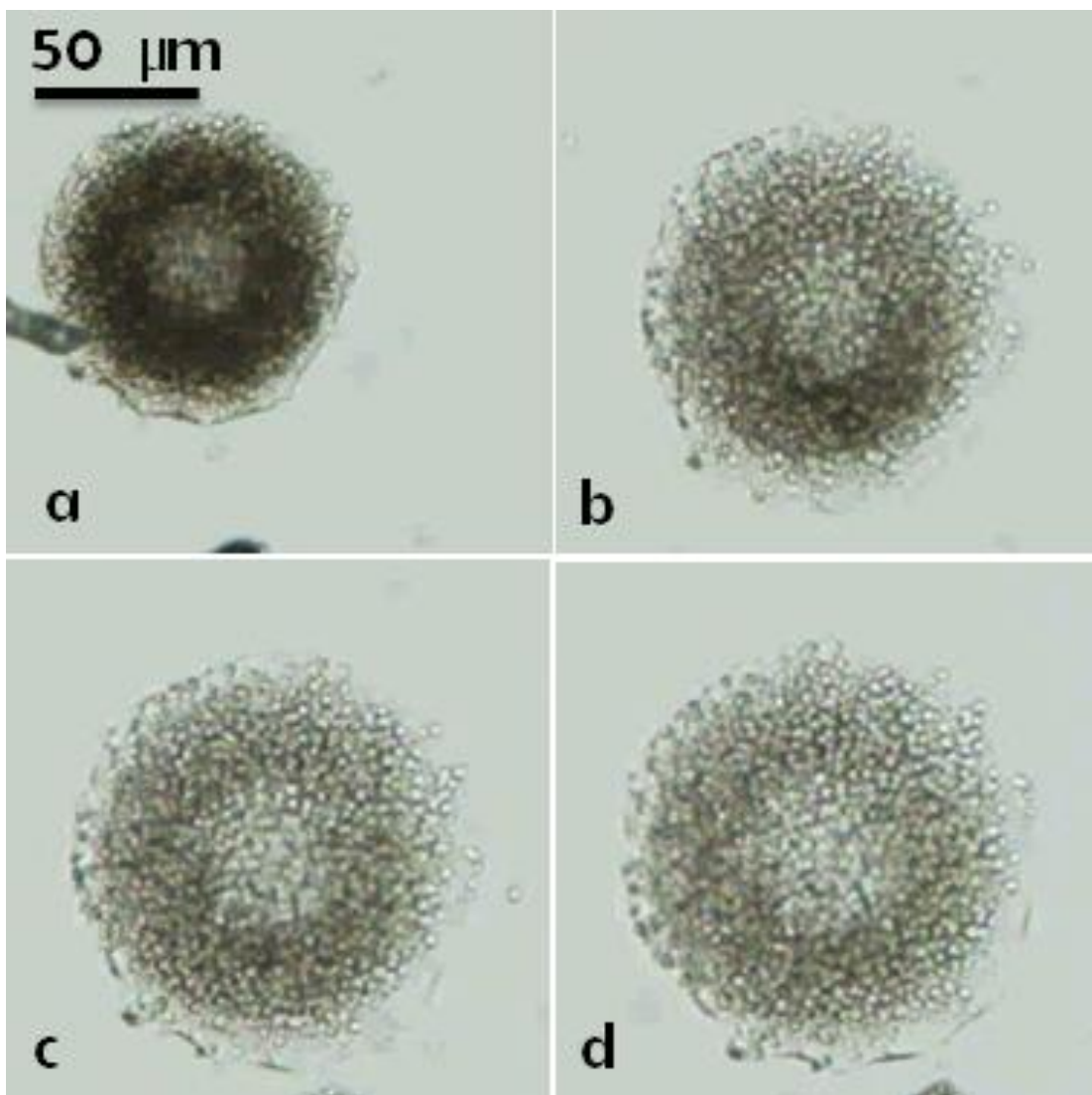


Figure 4.12: The composite shellac-yeast cells microcapsules fabricated by spray co-precipitating yeast cells in ammonium shellac solution doped with 4 % wt. sodium polyacrylate in 3 % vol. acetic acid. The microcapsules swelled and started to disintegrate with slow release of cells, a-d show different times.

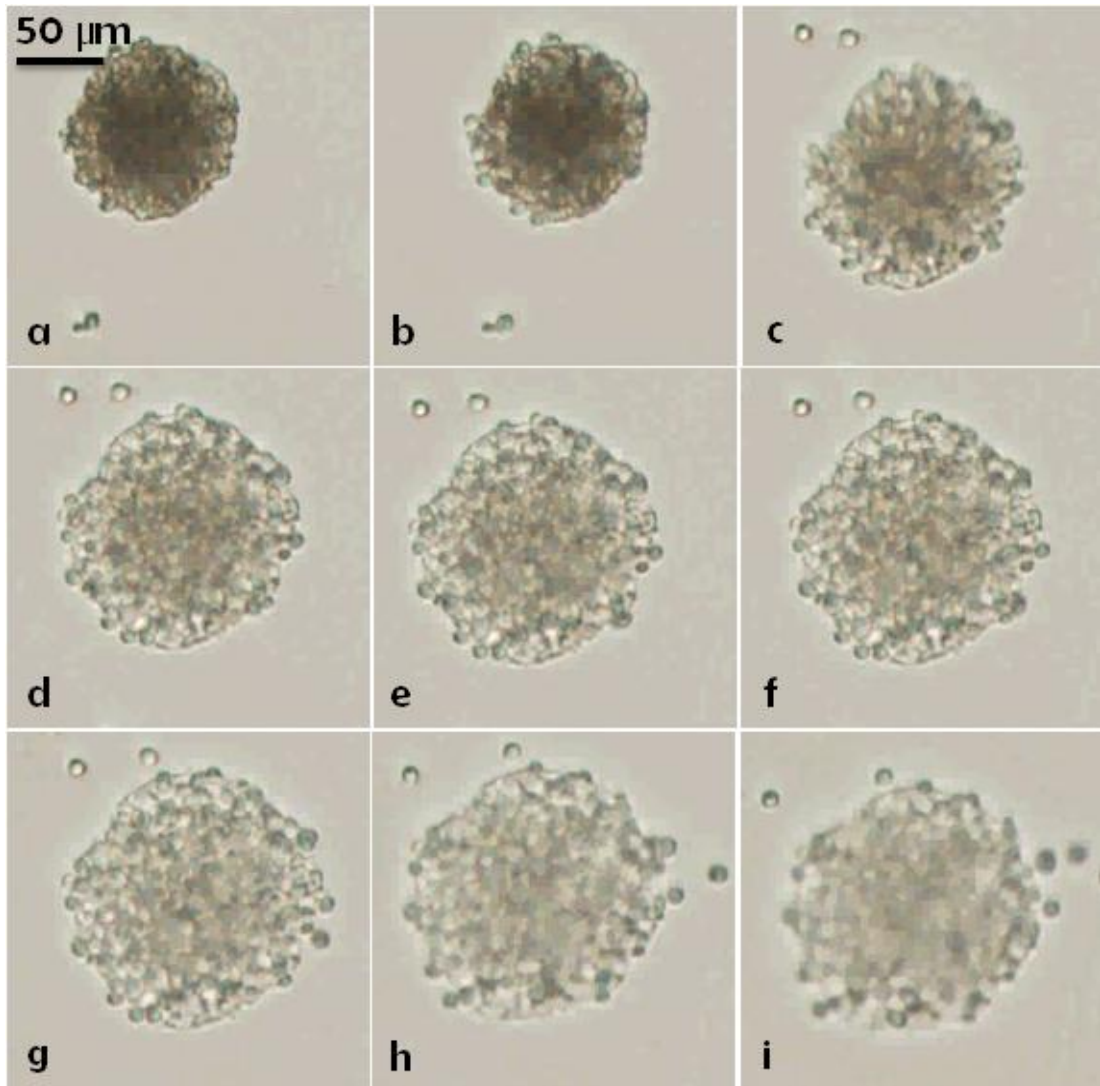


Figure 4.13: The composite shellac/yeast cells microcapsules fabricated by spray co-precipitating yeast cells in ammonium shellac solution doped with 4 % wt. sodium polyacrylate in 3 % vol. aqueous solution of acetic acid. The micrographs are captured in different times showing the microcapsules swelled at pH 8 when exposed to a drop of 1 M sodium bicarbonate and they started to disintegrate and release the yeast cells.

Figure 4.14 illustrates the disintegration process of the microcapsules within 20 minutes time period as they were transferred into a beaker containing 0.1 M sodium bicarbonate aqueous solution with stirring, while small aliquots were examined by optical microscopy. The results show that the disintegration process is much faster than in the case of bare shellac-yeast and CMC doped shellac-yeast microcapsules. Figure 4.14e shows the results of the FDA test on the released cells which confirm that the shellac and the PAA have no visible adverse effects on their viability.



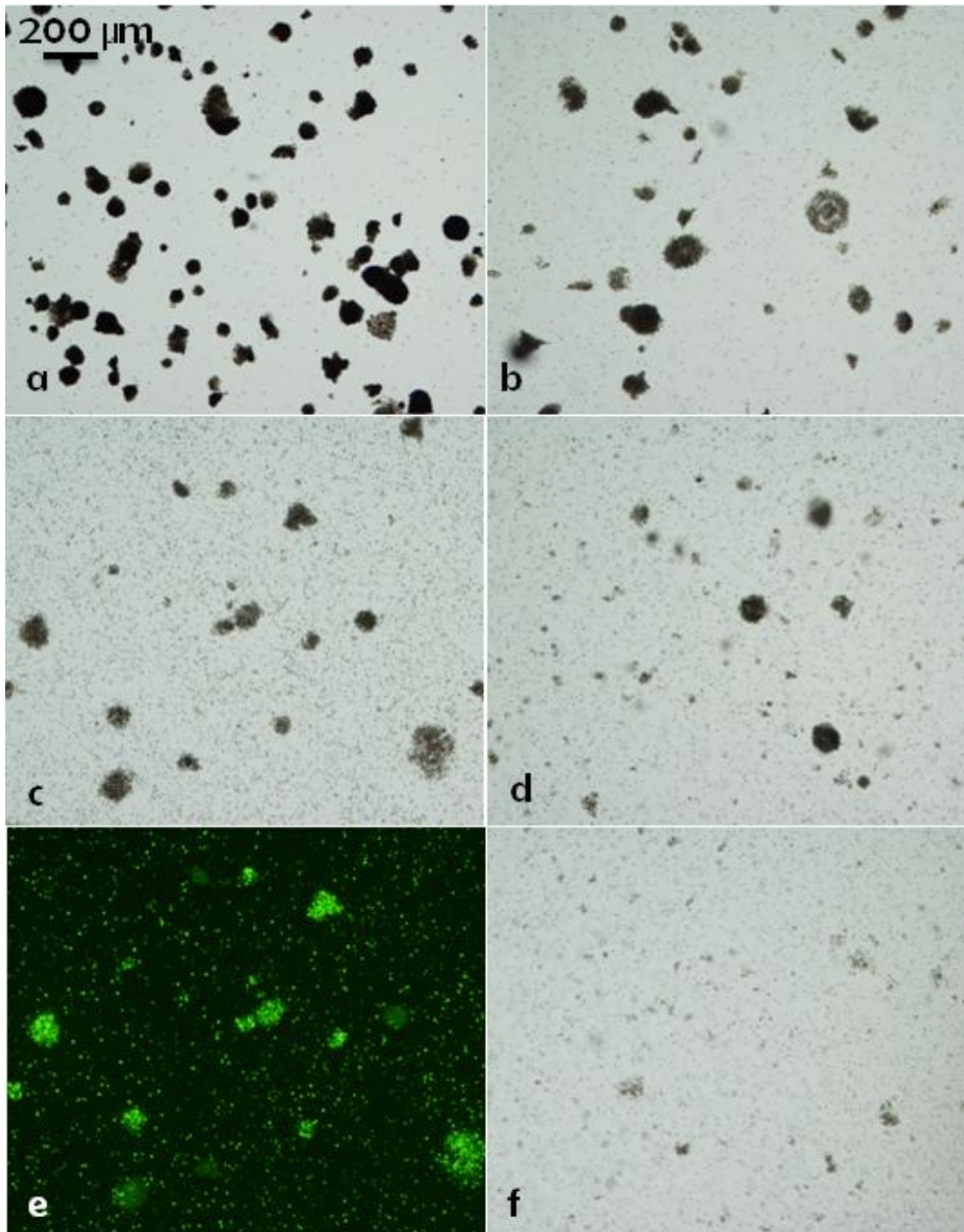


Figure 4.14: Disintegration of composite shellac-yeast cell microcapsules fabricated by spray co-precipitating dispersion of 10 % wt. yeast cells in 5 % wt. ammonium shellac solution doped with 4 % wt. sodium polyacrylate in 3 % vol. acetic acid solution. The washed microcapsules were stirred in a solution of 0.1 M sodium bicarbonate at pH 8 for (a) 0 min, (b) 10 min, (c) 15 min, (d) 20 min, (e) 15 min (same as (c) but with FITC fluorescence filter), and (f) 118 min. (e) shows a fluorescence microscopy image of viable yeast cells released from the disintegrated microcapsules after treatment with FDA.

#### 4.1.2.4 Effect of pH on the disintegration time of shellac-yeast cells microcapsules and the cell viability

The fabricated composite shellac-yeast cells microcapsules were transferred into 0.1 M phosphate buffer solutions of different pH values at constant stirring and small aliquots were taken and checked by optical microscopy to study the disintegration profile in the pH range of 5-9. Figure 4.16 shows the microcapsules after a certain time elapsed over stirring them in the buffer solutions of different pH. The pH of the medium was constantly monitored while the microcapsules were disintegrating because of the possible buffering effect of the dissolving shellac. However, no measurable pH change was observed in the solution during the microcapsules disintegration in all studied cases. Figure 4.15 represents the time (in hours) required for the shellac/PAA/yeast composite microcapsules to completely disintegrate as a function of pH of the medium. One sees that the disintegration time is increasing sharply as the pH decreases. This experiment shows that disintegration times of the order of 2-3h can be achieved at pH of the medium of around 7-7.5

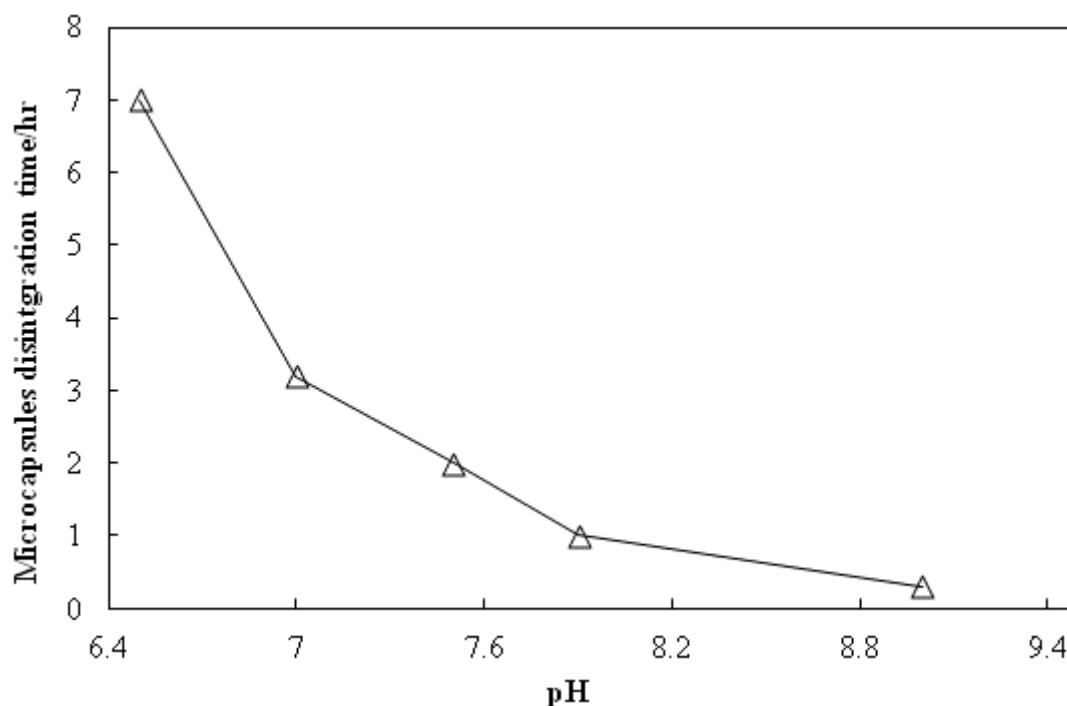


Figure 4.15: Relationship between the times it takes for the complete disintegration of the composite shellac-yeast cells microcapsules at different pH values.

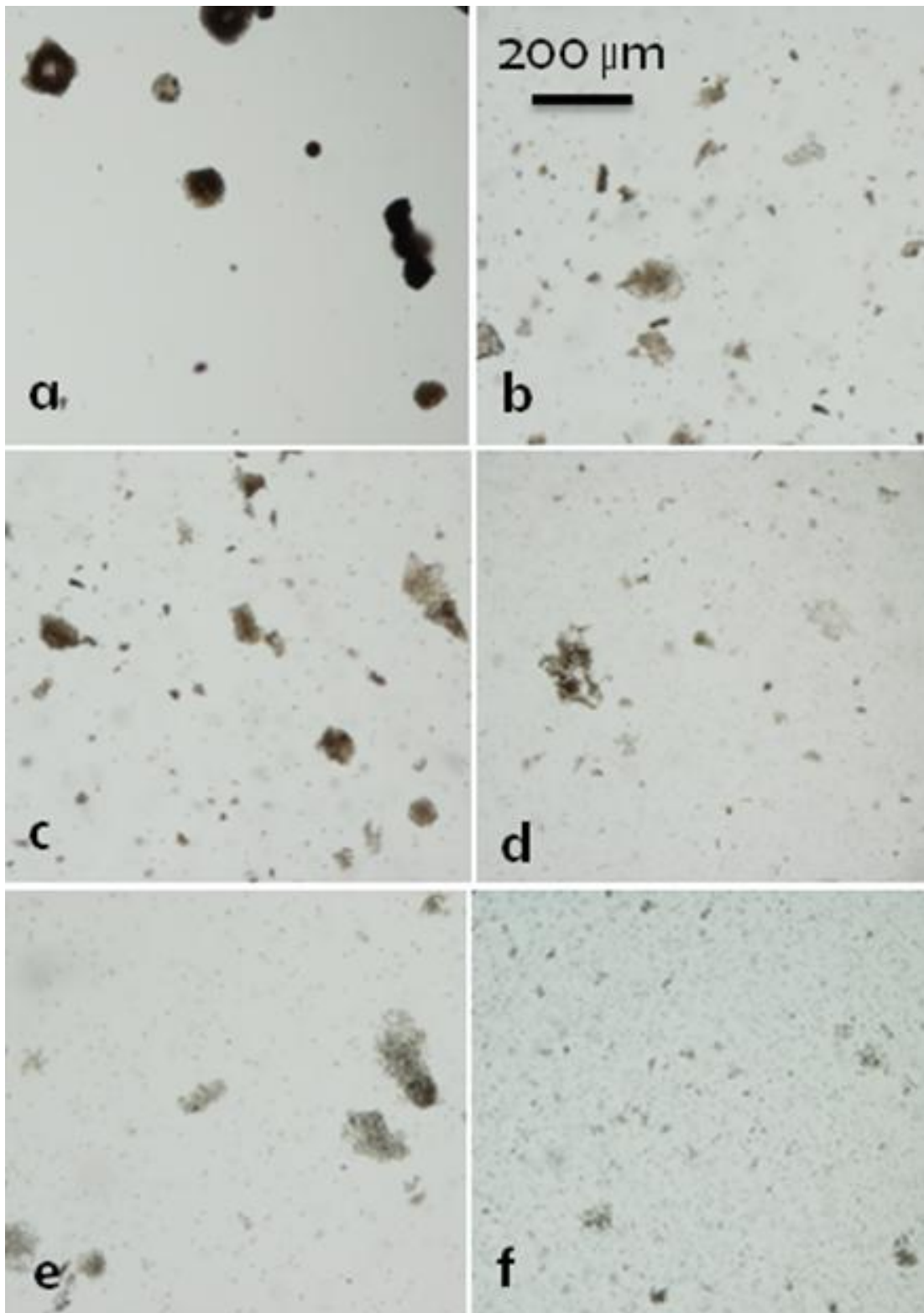


Figure 4.16: Composite microcapsules of shellac-yeast cells transferred into 0.1 M of phosphate buffer solutions at different pH and stirred on a magnetic stirrer while aliquots were withdrawn at regular intervals and checked by optical microscopy. The above micrographs illustrate the time it takes for the complete disintegration of the microcapsules at different pH. (a is after 24 hours at pH = 5, the microcapsules remained intact), (b is after 7 hours at pH = 6.5) (c is 3.2 hours at pH = 7), ( d is 2 hours at pH = 7.5), (e is 1 hour at pH = 7.9) , ( f is 0.3 hours at pH = 9).

#### **4.1.2.5 Growth triggered release of encapsulated living cells from composite shellac-yeast microcapsules in a culture medium**

The growth and viability of the encapsulated yeast cells inside the composite microcapsules were tested by incubating the microcapsules in a culture medium of pH 5 containing 2 % wt. glucose, 0.5 % wt. yeast extract, 0.1 % wt. sodium chloride and 0.3 % wt. ammonium sulphate at 37 °C in a thermostat. The yeast growth was monitored for over 48 hours. Figures 4.17 and 4.18 show the evolution of the cells with time, which confirm that the yeast cells are still viable as they grow through a budding process and the microcapsules gradually started to crack as the cells growing on their surface expand. Figure 4.18c-f shows a large number of individual yeast cells released from the microcapsules after 48 hours of incubation of the sample in the culture medium. The viability of the released cells was reconfirmed by staining them with FDA and observation using fluorescence microscopy. This includes both the released and the grown cells into the medium. This procedure is a demonstration of an alternative way of triggered release of living cells from composite microcapsules, i.e. cell growth triggered release.

The growing process in this experiment was performed at pH 5 to preserve the integrity of the shellac microcapsules where the cell release is triggered only by the growth of the yeast cells. We tested the viability of the encapsulated cells inside the composite microcapsules by dispersing a sample of microcapsules (washed with milli-Q water) in a culture medium at pH 5, which was sterilised at 100 °C for 1 hour and cooled down to 37 °C. A gel of 10 % wt. of oxidised starch was prepared in culture medium and after adding a sample of the composite microcapsules to it the gel was incubated at 37°C for 12 hours to observe the effect of the release and growth of the encapsulated yeast cells. The carbon dioxide produced from the growing yeast cells, released from the microcapsules consequently puffed up the gel as it is evident from the Figure 4.17. A blank sample (a2) containing only culture medium and starch was also prepared, while, tube (b1) contained the microcapsules. The results of this experiment reconfirm that the yeast cells inside the composite microcapsules have preserved their viability hence as they are released in the culture medium and grow, they produced carbon dioxide gas which break up the gel. In contrast, the blank sample shows no growth, since it does not contain yeast cells.

In addition to this experiment, we performed a DNA test with a live/dead cells kit (purchased from Sigma) on the yeast cells sample produced after growth triggered release from the disintegrated shellac-yeast microcapsules incubated in a culture medium. The results are presented in Figure 4.18e-f where the cells treated with Propidium Iodide (PI). Since the later intercalates with the DNA of dead cells by crossing through their open membrane only the dead cells fluoresce in red. As one can see in Figure 4.18f, only a very small fraction of the total cell population is fluorescent hence most of the cells are viable, which is also confirmed by the FDA test, as presented in Figure 4.18d.

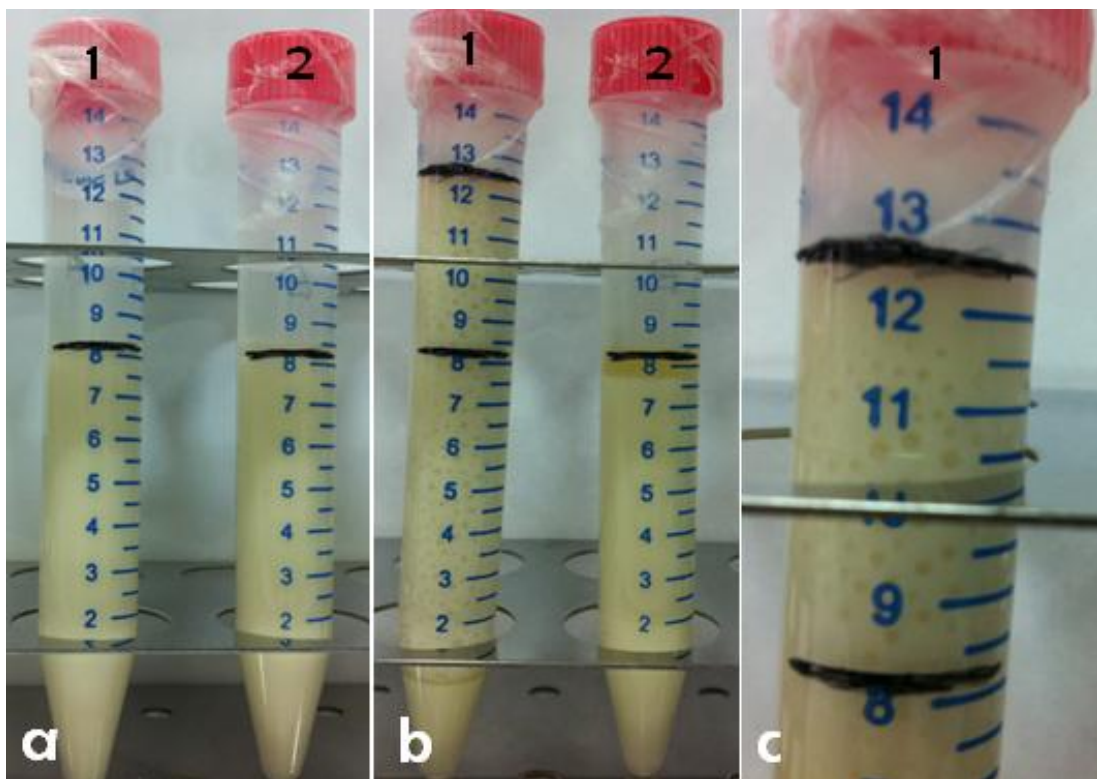


Figure 4.17: The culture medium was sterilised by boiling at 100 °C for 1 hour and then cooled down to 37 °C. Micrograph (a) represents the gel systems before incubation. (a1) composite microcapsules were dispersed in the sterilised culture medium after they were washed with milli-Q water several times. A gel was prepared from the suspension of the microcapsules in culture medium by dissolving starch powder. (a2) Starch powder was dissolved in the sterilised culture medium without the composite microcapsules. Micrograph (b) shows the gel systems after incubation at 37 °C for 12 hours; only (b1) which contained encapsulated yeast cells is grown, while (c) is a zoomed in image of (b1).

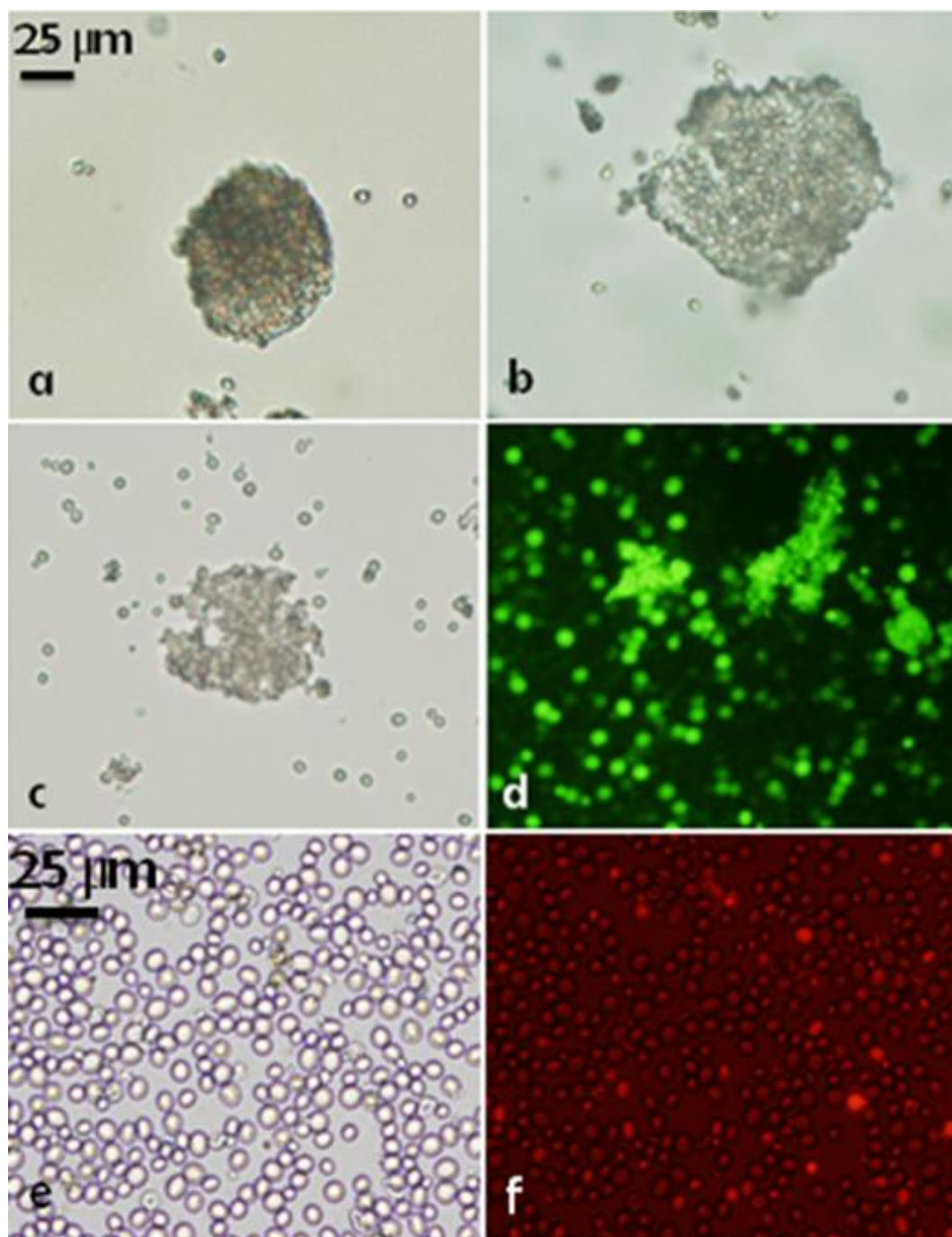


Figure 4.18: The composite shellac-yeast cells microcapsules transferred and incubated in a culture medium at 37 °C, at pH 5 for over 48 hours. Micrographs (a-d) show the disintegration of the microcapsules at 0h, 10h, 24h, and 36h. Micrographs (e, and f) the released yeast cells (at 48 hours incubation) were treated with Propidium Iodide (PI) solutions to stain the dead cells. (e) is an optical image of (f). PI, a nuclei staining dye, cannot pass through a viable cell membrane. It reaches the nucleus by passing through disordered areas of dead cell membrane, and intercalates with the DNA double helix of the cell to emit red fluorescence (excitation: 535 nm, emission: 617 nm). With 545 nm excitation, only dead cells can be observed. The image (f) is a superposition of the fluorescence image and the brightfield image which helps to compare the non-fluorescent cells (darker) with the fluorescent ones (bright red). One sees only a small fraction of dead cells (bright red).

#### **4.1.2.6 Fabrication of composite shellac/yeast cells microcapsules by spray co-precipitating with calcium chloride solution**

Previously calcium–shellac microspheres with encapsulated carbamide peroxide (CP) have been made by emulsification to generate an emulsion including shellac ammonium salt aqueous solution with soluble CP dispersed in sunflower oil with calcium chloride powder, followed by gelation between shellac and calcium.<sup>76a</sup> Meanwhile, it has been reported that Calcium-shellac spheres were successfully prepared using an extrusion technique based on dropping aqueous ammonium shellac solution into calcium chloride solution.<sup>76b</sup> Nevertheless, the fabrication of composite shellac/yeast cells microcapsules by co-precipitating dispersion of yeast cells in ammonium shellac solution using calcium chloride precipitation approach has not been tried before. Therefore, attempts to prepare such microcapsules by using spray co-precipitation method were made. The process essentially includes spraying a dispersion of known amount of yeast cells in known concentration of ammonium shellac solution into a Petri dish which contained known concentration of calcium chloride solution.

The spray co-precipitation method with 0.5 M calcium chloride as a precipitating agent yielded hemi-spherical, rigid, and relatively stable composite shellac-yeast cell microcapsules. Figure 4.19 shows the results of the spray co-precipitating a dispersion of 10 % wt. yeast cells at different concentrations of ammonium shellac solution at pH 8. The microcapsules with higher shellac content had substantially longer disintegration times. Although good results were achieved in co-precipitating yeast cells and ammonium shellac solution using acetic acid solution, unfortunately, it cannot be concluded that the same results were achieved for fabricating microcapsules by spray co-precipitating yeast cells in ammonium shellac solution using calcium chloride solution, especially when 5 % wt. ammonium shellac solution was used. Although microcapsules still fabricated, but they had stability issues, and the cells were separated from each other as it is shown in Figure 4.19a, high percentage of yeast cells surrounded a small stable microcapsule inside another less stable one.

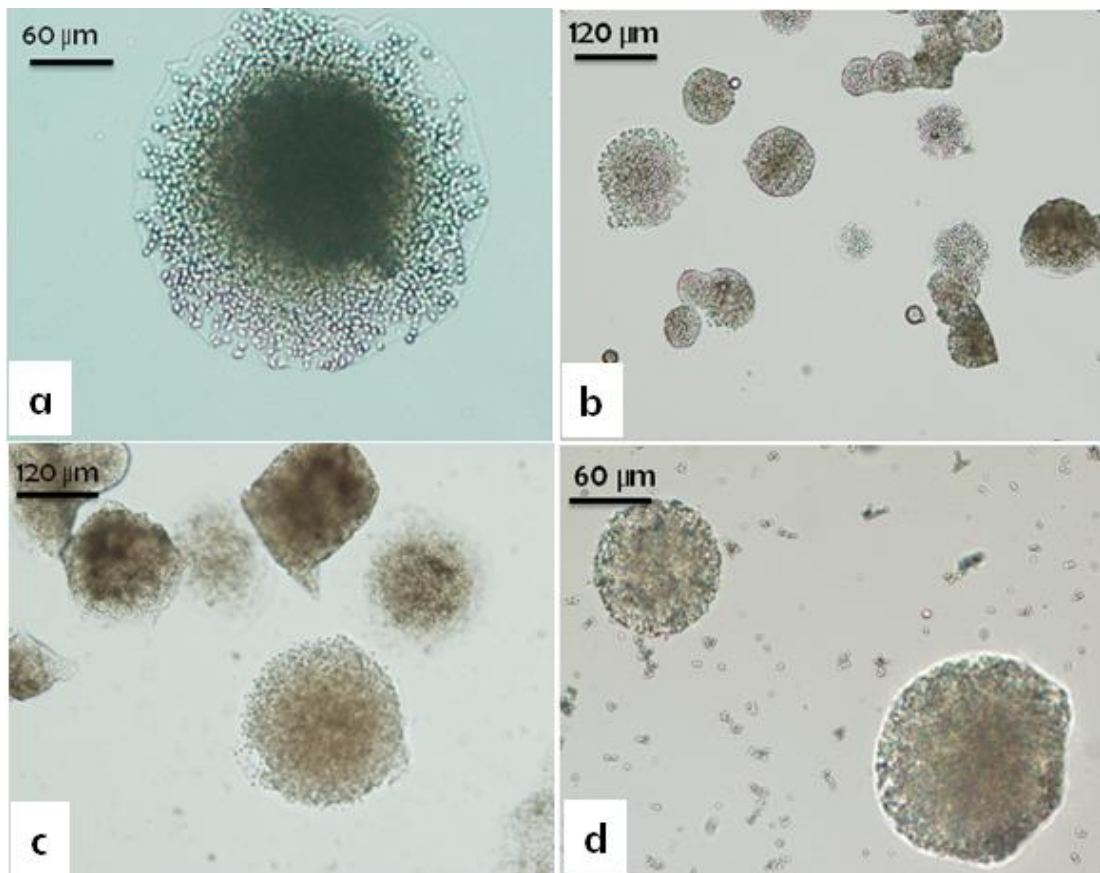


Figure 4.19: Composite shellac-yeast microcapsules prepared from a dispersion of 10 % wt. yeast cells at pH 8 and different concentrations of ammonium shellac: (a, b, c, and d) represent (5, 6, 7, and 14) % wt. ammonium shellac solution, respectively. The dispersion was spray co-precipitated in 0.5 M calcium chloride solution.

The falling composite microcapsules were filtered off and dried at 50 °C and then coated with gold nanoparticles to be observed by Scanning electron microscopy. Figure 4.20 shows the SEM images obtained from the filtered and dried microcapsules which demonstrate hemi-spherical morphologies similar to those of acetic acid co-precipitated dispersion.



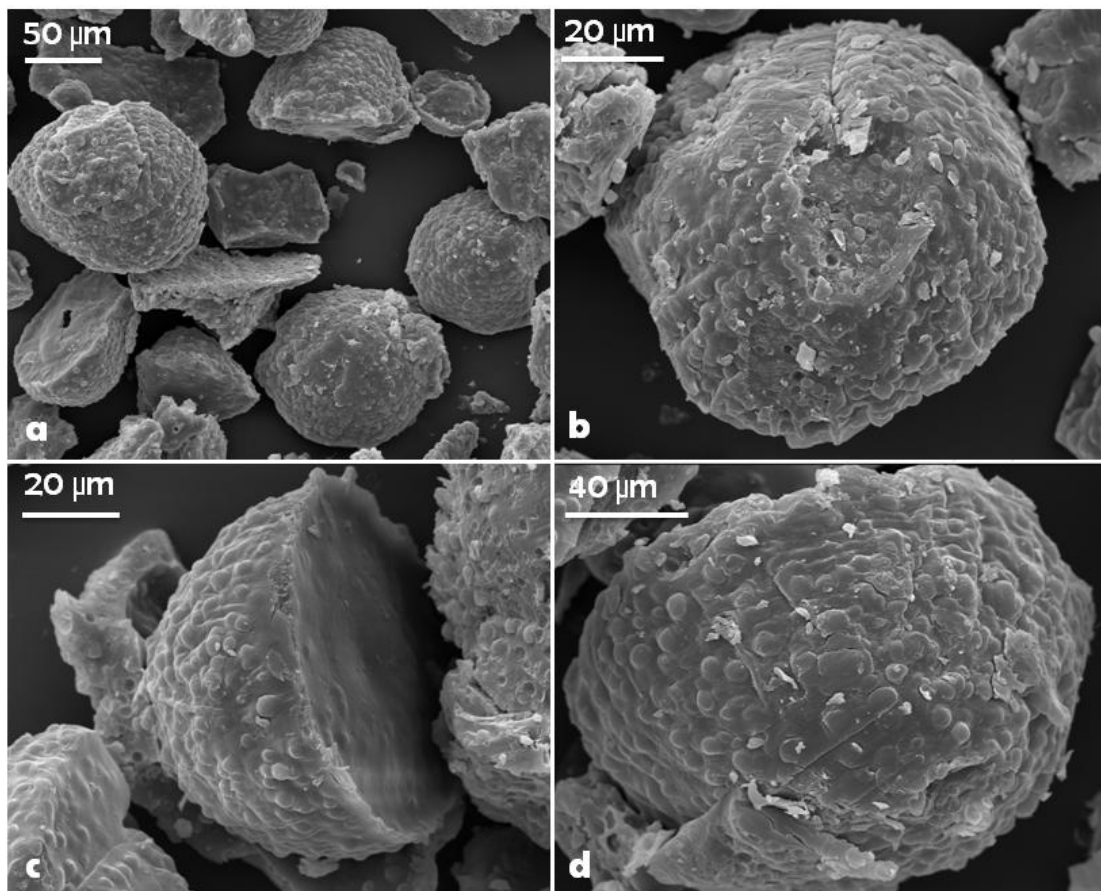


Figure 4.20: SEM images of dried composite shellac-yeast microcapsules fabricated by spray co-precipitating dispersion of 10 % wt. yeast cells in 7 % wt. ammonium shellac solution using 0.5 M calcium chloride solution.

#### 4.1.2.7 Spray-drying of yeast cells/ammonium shellac formulation

To wrap up probiotic and protect them from harsh GI tract conditions of mechanical stress and extremely low pH, various types of microcapsules have been designed but the most successful microcapsule should be capable of disintegrating in pH of lower intestines ( $\text{pH} > 7$ ). We developed novel magnetic “shellac-yeast” microcapsules suitable for directed delivery of cells by using external magnetic field, which are capable of disintegrating at  $\text{pH} > 7$  and release their load.

Magnetically directed delivery would allow significant amount of cells to be positioned at a targeted location inside the host. This may reduce amount of cells to deliver, prevent side effects and minimise the amount of materials used. Here we show our results with magnetically functionalised microcapsules loaded with yeast cells which can be manipulated with an external magnetic field. If a dispersion of yeast in ammonium shellac solution was sprayed through a column with hot air, the water content of the droplets start to evaporate and the droplets dry up which result in the increase of the concentration of the shellac solution which starts to precipitate and produce microcapsules loaded with high percentage of yeast cells with dried solid shellac.

We collected the falling dry microcapsules in a Petri dish which contains milli-Q water at the base of the spray-drying column. Figure 4.21 includes images of such stable and rigid magnetised microcapsules fabricated by using this strategy. We demonstrated that they can be collected and manipulated by an external magnetic field as shown in Figure 4.21f. Figure 4.21c and 4.21e show that the encapsulated yeast cells preserved their viability. Magnetite particles were produced as described in ref. 17 and mixed with the aqueous shellac solution. Magnetic shellac-yeast microcapsules were produced by spray drying 10 % wt. yeast cells in 7 % wt. ammonium shellac solution doped with 1 % wt. magnetite nanoparticles.<sup>20</sup> (see Figure 4.1 for more details).

The microcapsules were transferred into an aqueous solution of sodium bicarbonate at pH 8 followed by stirring, and then samples were collected from the medium after washing with milli-Q water and examined by optical microscopy. Figure 4.22 shows the morphology of the microcapsules after stirring them for 2 hours in the alkaline solution at pH 8. The microcapsules started to open up which provided more access of their surface to the aqueous solution which continued until their complete disintegration after stirring in the solution for 2 hours.

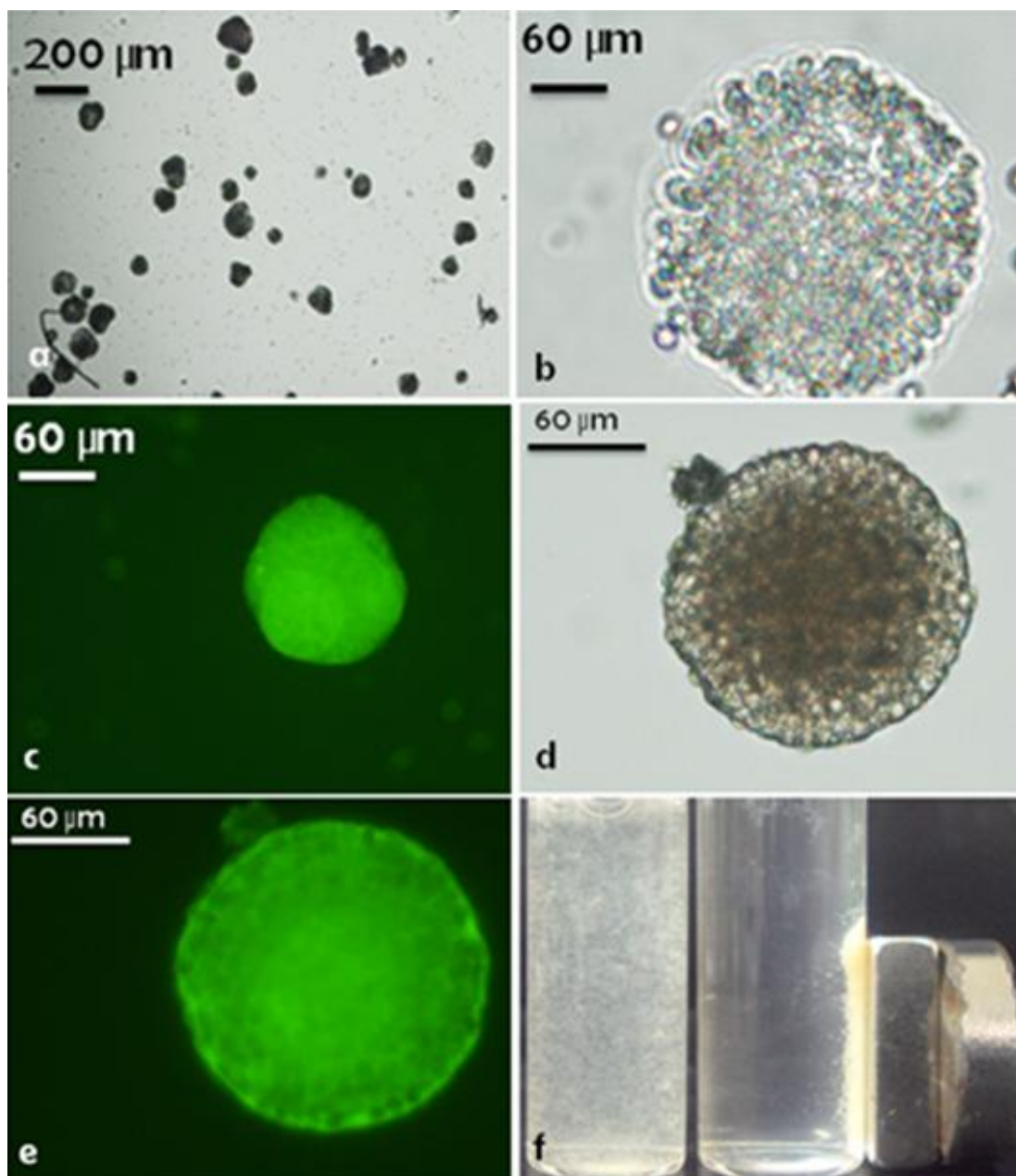


Figure 4.21: Composite shellac-yeast microcapsules fabricated by spray drying a dispersion of 10 % wt. yeast cells in 7 % wt. ammonium shellac aqueous solution. The yeast cells inside the microcapsules were treated with FDA solution and observed by fluorescence microscopy with FITC filter set in micrographs (c) and (e). Micrographs (d) and (f) show magnetised microcapsule containing 1% vol. magnetite nanoparticles.

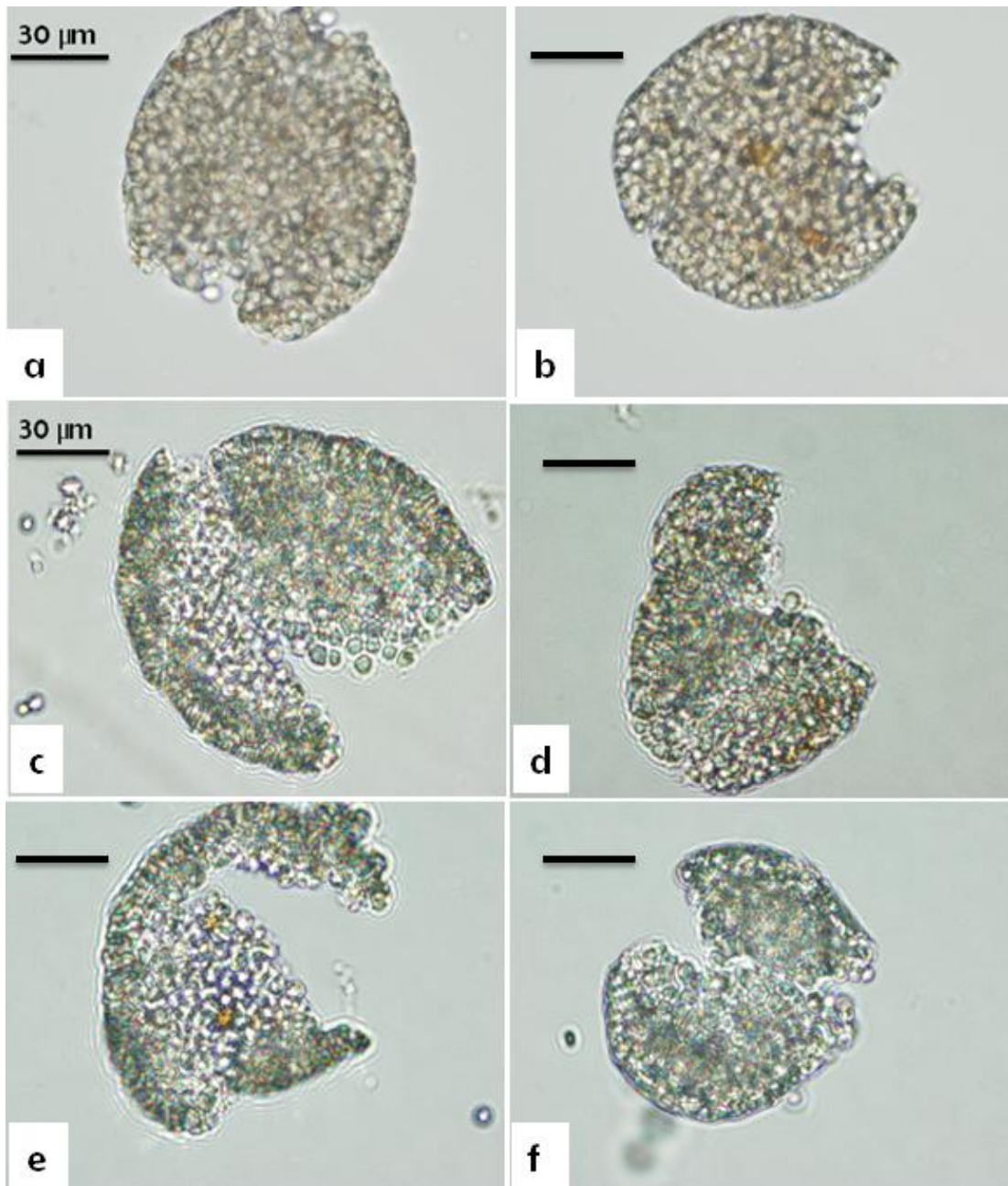


Figure 4.22: The magnetised composite shellac-yeast microcapsules transferred into 0.1 M aqueous solution of sodium bicarbonate at pH 8 and stirred for one hour in (a, and b) and two hours in (c-f) then small samples were collected to be imaged by optical microscopy.

#### 4.1.2.8 Viability of yeast cells in acetic acid and calcium chloride solution

Yeast cells washed with milli-Q water several times, and they were centrifuged and the supernatant was discarded after every wash. The sedimented yeast cells were re-dispersed in either 3 % vol acetic acid solution or 0.5 M calcium chloride solution, and the dispersions were shaken on a mini shaker for one hour, then the yeast cells were washed again with milli-Q water then FDA viability test was done for each sample and the result showed that in case of transferring the yeast cells in acetic acid solution almost every single cell has died but in the case of dispersing the cells in 0.5 M calcium chloride solution the chance of survival was higher and relatively high percentage of yeast cells still viable as it is illustrated in Figure 4.23.

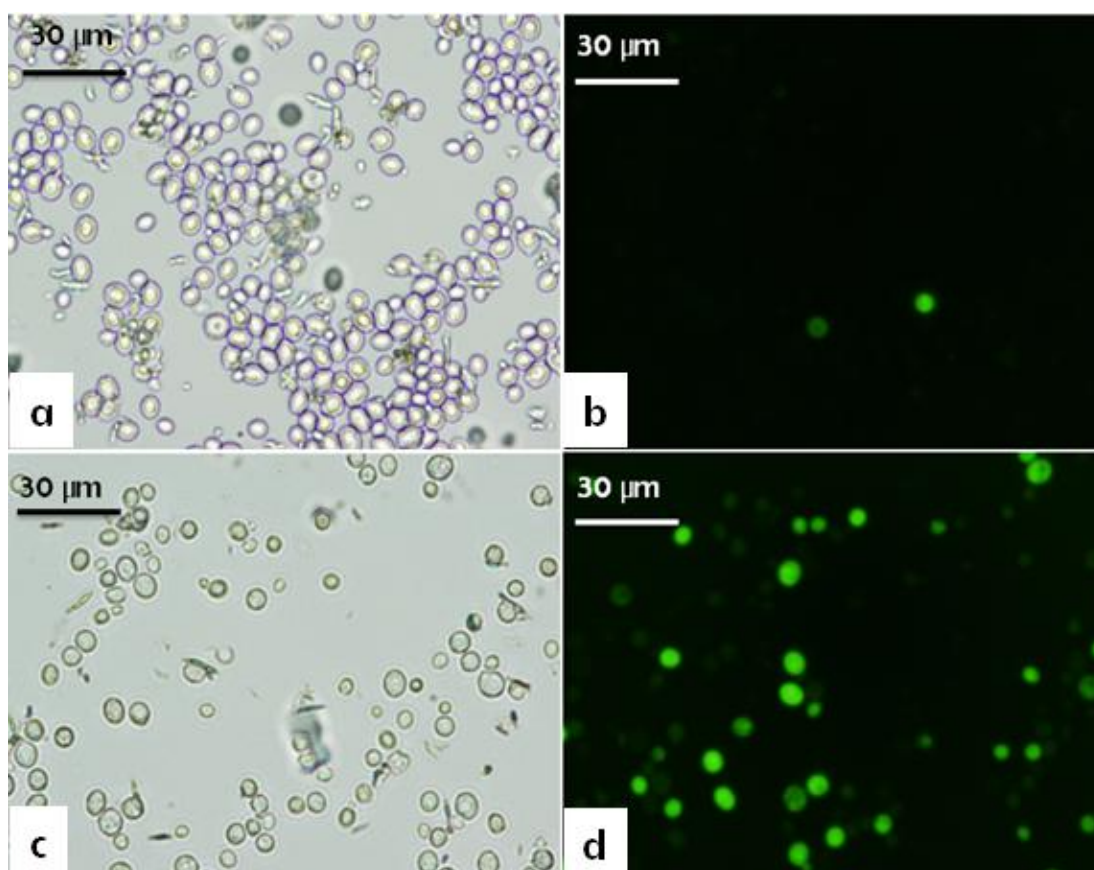


Figure 4.23: Yeast cells dispersed in a solution of 10 % vol. acetic acid solution for one hour in micrographs (a and b), while in micrographs (c and d) the yeast cells dispersed in a solution of 0.5 M calcium chloride for one hour, then the samples were washed and the yeast cells were treated with FDA solution and observed by optical and FTIC fluorescence microscopy.

### 4.1.3 Conclusions

Composite microcapsules of shellac and yeast cells were fabricated by both spray co-precipitating and spray-drying dispersions of yeast cells in ammonium shellac solution. Two alternative techniques were used: (i) spray co-precipitating a dispersion of yeast cells in aqueous solution of ammonium shellac at  $\text{pH} > 7$ , into either acetic acid or calcium chloride aqueous solution; or (ii) spray-drying the shellac-yeast dispersion. Different concentrations of ammonium shellac solution were used to produce rigid and stable microcapsules which can disintegrate at  $\text{pH} > 7$  for specified time interval and release viable cells into the solution. The pH trigger for cell release and the time of disintegration were controlled by (a) the shellac concentration and (b) doping the solution with pH sensitive polymers.

We demonstrate as a proof of concept how carboxymethylcellulose and sodium polyacrylate can be used to trigger the cell release from the microcapsules at neutral and higher pH and to speed up the shellac-cell microcapsule disintegration process. Doping of the shellac solutions with carboxymethylcellulose significantly enhanced the rate of releasing the yeast cells from the composite microcapsules at neutral and higher pH. The inclusion of sodium polyacrylate in the shellac resulted in much faster disintegration of the microcapsules upon increase of the pH above 7 and in some cases instant cell release. We show that the released and encapsulated yeast cells have preserved their viability during the microencapsulation and the release process. The produced composite microcapsules were capable of protecting the cells at extremely low pH (pH 1) and still produce viable cells upon disintegration at neutral and higher pH. We discovered that shellac-cell microcapsules can produce triggered release of cells upon exposure to growth media, i.e. growth induced release.

We also produced magnetically functionalised shellac-cell microcapsules which can be used for delivery of encapsulated cells directed by an external magnetic field. We demonstrate the robustness and versatility of shellac as microencapsulating material for protection of cells in acidic environments. The composite shellac-cell microcapsules reported here could be used in formulations for protection and delivery of probiotics and other cell cultures with programmed and triggered release of the encapsulated cells by using a variety of pH sensitive food grade polymers as cell

release triggers. Such microcapsules could also be used in other application involving triggered release of the encapsulated cells in cell implants, including stem cell delivery and live vaccines release.

## Chapter 5.

### Fabrication of novel colloidosomes loaded with viable yeast cells

In this chapter, we explored the possibilities of fabricating novel colloidosomes microcapsules loaded with viable yeast cells as a model for probiotics. Colloidosomes have been fabricated from various materials including polymers and gel beads. Here we have developed two main strategies to fabricate colloidosomes depending on the mode of triggered release, the type of emulsion templates, and the method of transfer of the templated emulsion drops from oil into water. The first strategy includes fabrication of magnetic colloidosomes with gel-cores which contains pH-sensitive and swellable polyacrylate. The second method involves fabrication of colloidosomes structures interlocked with either anionic polyelectrolytes or yeast cells pre-coated with anionic polyelectrolytes.

#### 5.1.1 Introduction

Spherical shells of micron-sized colloidal particles can be formed by introducing colloidal particles to emulsion templates. The particles adsorbed and self-assemble on the surface of the droplets in order to minimise the total interfacial energy forming Pickering emulsion drops as precursor of colloidosomes, which are mainly prepared from w/o emulsion templates stabilised by solid particles.<sup>78</sup> Although the term colloidosomes was first used by Dinsmore *et al.*<sup>11</sup> but Velev *et al.* were considered to be the first to produce colloidosomes-like structures. In a series of papers<sup>78</sup> on assembly of latex particles by using emulsion droplets as templates, they prepared spherical shell-like supraparticles and ball-like composite assemblies (see Figure 5.1).

In the first paper, ordered empty latex balls were prepared by assembling lysine-functionalised sulfate latex particles in octanol-water emulsion droplets. The particles were locked in the interface by adding casein solution which gently binds them together within the shells of the droplets. Then the octanol core of the droplets was dissolved by using ethanol to produce the empty shells of latex particles. The strength of this bridging was not sufficient to protect the superparticle structures during the



dissolution of the core; therefore, a mixture of hydrochloric acid and calcium chloride was used to coagulate the latex particles in the interface.<sup>78a</sup>

In the second paper, octanol in water emulsion droplets were stabilised by SDS-treated amidine latex particles, and the particles were locked inside the droplets by addition of casein solution. Then the octanol core was dissolved by injecting ethanol but the droplets/particle complexes could not withstand the ethanol extraction, therefore, more SDS solution was added to coagulate the particles within the octanol droplets, which were removed from the surrounding environment by centrifuging, washing and suspending the aggregates in the casein/SDS solution. Meanwhile, to prepare composite supraparticles, an octanol in water emulsion stabilised with SDS-treated amidine latex particles was homogenised with a suspension of lysine-sensitised sulfate latex particles. The sulfate particles were fixed within the droplets by adding casein solution. Then hydrochloric acid and calcium chloride were used to induce the coagulation of the sulfate latex shells, and “fortify” the composite supraparticles, which were finally removed from the environment by dissolution of the octanol core using ethanol extraction.<sup>78b</sup>

Dinsmore *et al.*<sup>11</sup> produced colloidosomes by emulsifying a suspension of the materials to be encapsulated in an immiscible fluid containing colloidal particles that adsorb on the surface of the emulsion droplets. After the droplet surface was completely covered by particles; the adsorbed particles were interlocked together to form an elastic shell. This interlocking is essential to ensure that the capsules remain intact when they are transferred to a water phase. It was further reported that the interlocking of the adsorbed particles monolayer around the water droplets can be achieved by either lightly sintering the particles or electrostatically binding a polyelectrolyte of the opposite charge to the particles. Upon heating to the polystyrene glassifying temperature ( $T_g$ ), the particles partially bridged thus creating approximately 150 nm diameter bridges or “necks” between them. The resultant colloidosomes, therefore, contained a precise array of uniform pores in an elastic shell.<sup>11</sup>

In a separate formulation the bridging is done by using a polyelectrolyte such as poly-L-lysine or polystyrene sulfonate that will adsorb onto the particles at the interface; the polyelectrolyte molecules bridge neighbouring particles and lock them together. The adsorption of polyelectrolyte significantly enhances the elastic properties of the colloidosomes. The final step of the assembly process involves removing the fluid interface by exchanging the continuous phase (oil) with one that is miscible with the fluid inside the colloidosome (water). This ensures that the pores in the elastic shell control the permeability by allowing exchange by diffusion across the colloidosome shell. This fluid exchange step can readily be accomplished by transferring the capsules from the oil to the water phase by gentle centrifugation of the Pickering emulsion over a water phase. The resultant colloidosome structures provide a rigid elastic shell that serves as a protective coating for the interior material. Colloidosomes can be used to efficiently encapsulate and provide a rigid shell of controllable elasticity and permeability. An important feature of colloidosomes which makes them promising as encapsulants, is the wide variety of potential mechanisms for release. Constant release through the controlled pores is the most direct release mechanism. Although as they are elastic shells, release may be triggered by rupture through shear stress.<sup>11</sup>

#### **5.1.1.1 Pickering emulsions as templates for colloidosomes**

Finely divided solid particles can act as emulsifiers for o/w or w/o emulsions by residing at the interface. The credit being usually given to Pickering hence, the name Pickering emulsions.<sup>79</sup> Pickering emulsions can be remarkably stable to coalescence due, in part, to the high energies of detachment for particles adsorbed at liquid-liquid interfaces.<sup>80</sup> Low molar mass surfactants and surface-active polymers can form a variety of aggregated structures in aqueous or non-aqueous media and are commonly employed as emulsifiers in the preparation of emulsions and as stabilisers in the preparation of foams. Solid particles can function in similar ways to surfactants but certain differences in behaviour are noticeable. Individual solid particles do not assemble to give aggregates in the same way that surfactant molecules form micelles. For surfactant present in oil and water mixtures, the system of hydrophilic-lipophilic balance (HLB) is the most important variable in determining whether aggregated surfactants, micelles or microemulsion droplets reside in water, oil or a third phase.<sup>81</sup>

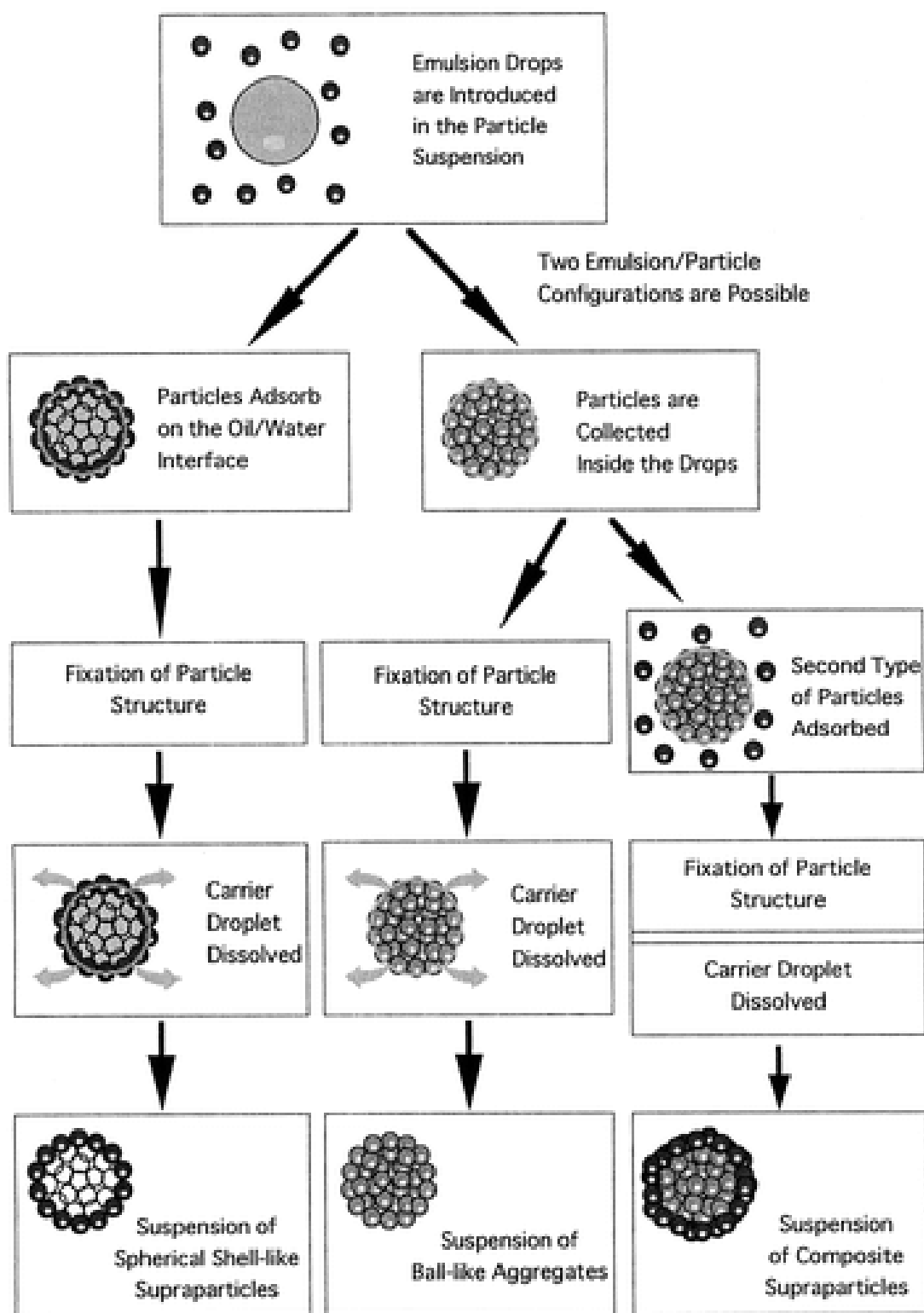


Figure 5.1: Possible modifications of the “emulsion template” method for supraparticle assembly. Schematic was used as it has been published in reference<sup>78a</sup>.

For hydrophilic surfactants, the area per head group is larger than that of the chain and the monolayer curve around oil resulting in o/w micro and macroemulsions. For lipophilic surfactants the area per chain exceeds that of the head group and water becomes the dispersed phase in w/o macroemulsions. For conditions in which the head group and chain areas are similar, monolayers have a net curvature of zero and new aggregates form including lamellar phases and bicontinuous microemulsion.<sup>80-82</sup>

In case of spherical particles which adsorb to interfaces (water-air or water-oil) the relevant parameter is thought to be the contact angle  $\theta$  which the particle makes with the interface (see Figure 5.2). For hydrophilic particles e.g. metal oxides,  $\theta$  measured through the aqueous phase is normally  $< 90^\circ$  and a larger fraction of the particle's surface resides in the water than in the non-polar phase. For hydrophobic particles e.g. suitably treated silica nanoparticles,  $\theta$  is generally greater than  $90^\circ$  and the particle resides more in air or oil than in water. By analogy with surfactant molecules, the monolayers will curve in a way that larger area of the particle surface remains on the external side, giving rise to air in water aqueous foams and o/w emulsions ( $\theta < 90^\circ$ ) and water in air aerosols or w/o emulsions ( $\theta > 90^\circ$ ).<sup>82</sup>

If a spherical particle (s) with radius (r) is initially totally in phase ( $\alpha$ ) and subsequently adsorbed to the ( $\alpha\beta$ ) interface, the interfaces ( $s\alpha$ ,  $s\beta$ ,  $\alpha\beta$ ) have interfacial tension ( $\gamma$ ) associated with them, adsorption of the particle at the interface results in an area of the ( $s\alpha$ ) interface being lost but being replaced by an equal area of the ( $s\beta$ ) interface. More importantly, an area of the ( $\alpha\beta$ ) interface is also lost due to the presence of the particle and this area depends on ( $\theta$ ).<sup>81</sup>

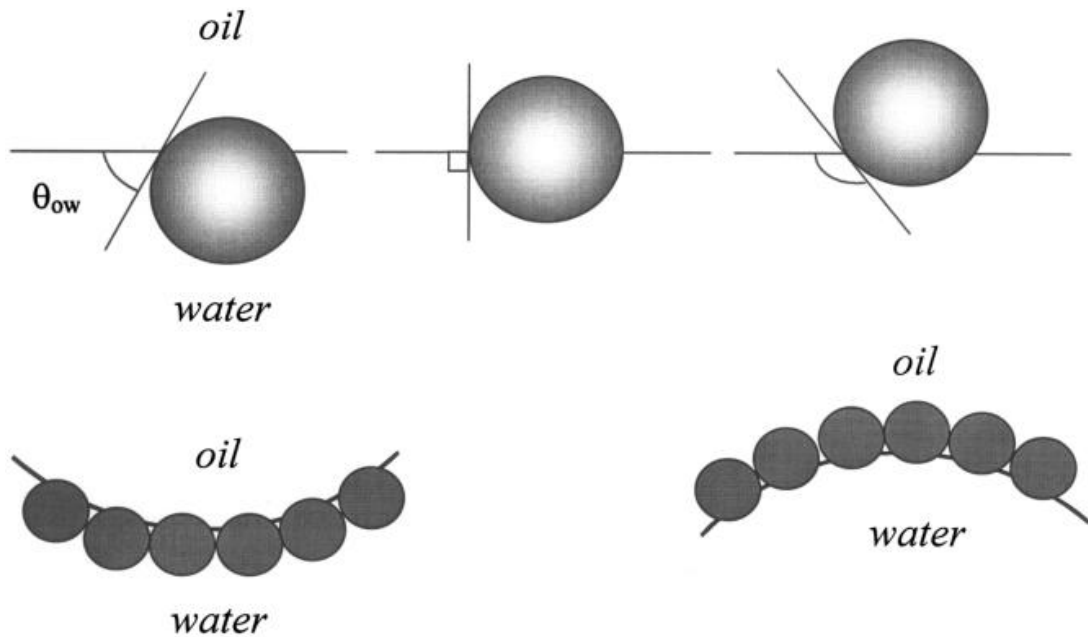


Figure 5.2: Position of a small spherical particle at a planar oil–water interface for a contact angle (measured through the aqueous phase) less than  $90^\circ$  (left), equal to  $90^\circ$  (centre) and greater than  $90^\circ$  (right). (Lower) Corresponding probable positioning of particles at a curved interface, for  $\theta < 90^\circ$ , solid stabilised o/w emulsions may form (left), for  $\theta > 90^\circ$  solid-stabilised w/o emulsions may form (right).<sup>83</sup>

The energy of attachment of a particle to a fluid–fluid interface is also related to the tension of the interface ( $\gamma_{\alpha\beta}$ ). Assuming the particle is small, so that the effect of gravity is negligible, the energy  $\Delta E$  required to remove the particle from the interface is given by

$$\Delta E = \pi r^2 \gamma_{\alpha\beta} (1 \pm \cos\theta)^2 \quad (5.1)$$

In which the sign inside the bracket is negative for removal into the water phase and positive for removal into the air or oil phase. If the energy of attachment of particle to interfaces is higher than the thermal energy ( $kT$ ), then the particles adsorb to the interface effectively irreversibly. This is in a sharp contrast to surfactant molecules which adsorb and desorb on a relatively fast timescale. Since  $\Delta E$  depends on the square of the particle radius, it decreases markedly for smaller particles.<sup>82</sup>

Aveyard *et al.*<sup>84</sup> found out that at air-water surface, compression of the monolayer leads to the formation of rafts of hexagonally packed particles and addition of salt to the aqueous phase causes 2-D clusters to form. By contrast, at an octane-water interface, particle monolayers remain highly ordered as a result of long-range repulsion even on concentrated salt solution. The enhanced lateral repulsion was attributed to electrostatic interactions, through the oil phase, of residual surface charges at the particle-octane interface. The difference between the behaviour at the two interfaces was argued to be due to a change in the “wettability” of the particles, in that they were more hydrophilic at air-water surface and hence a smaller area of the particles was exposed to air resulting in reduced repulsion.<sup>84</sup> Since close-packed arrays of particles can form at a planar oil-water interface, the possibility exists that similar arrays occur around curved interfaces such as those in emulsions. The properties of latex particles in oil solvents are dependent on whether the solvent is “good” (particle solvent interactions are favourable) or “poor” (interactions are unfavourable).<sup>80</sup>

Aveyard *et al.*<sup>83</sup> studied the effect of electrolyte on colloidal particles and found out that, since the majority of colloidal particles in aqueous dispersions are charged, addition of salt not only reduces their surface potentials but can also lead to coagulation of the particles into flocs. It is known that good emulsion stabilisation was achieved when the particles were weakly flocculated (by salt in the case of o/w or by surfactant in the case of w/o); less stable emulsions resulted when the particles were completely flocculated. The appearance of flocculated particles initially enhances the emulsion stability. Further increase in salt concentration results in destabilisation. It may be that small flocs if formed at low salt concentration adsorb to drop interfaces resulting in stabilisation, whereas at higher salt concentration the flocs size and extent may be larger and adsorption is reduced. A theoretical description of the adsorption of charged particles to charged liquid surfaces concludes that adsorption is favoured in the presence of salt as particles become more hydrophobic.<sup>83</sup>

Paunov *et al.*<sup>85</sup> developed a new method to fabricate colloidosomes from emulsion templates stabilised by either polymeric microrods or polystyrene latex particles and gelling the water core to give the droplets extra stability and thus transfer them into water with high efficiency. They developed a new method to produce novel “hairy” colloidosome microcapsules with shells of polymeric microrods. The work included the emulsification of hot aqueous solution of agarose in tricaprylin in the presence of SU-8 microrods, and then the system was cooled off to set the agarose gel. The obtained suspension of aqueous gel microcapsules was diluted with ethanol and centrifuged to separate them from the supernatant. In the final step, the microcapsules were washed with ethanol and water and redispersed in water.<sup>85a</sup>

Furthermore, they reported that their technique allows preparation of colloidosomes with diameters between several tens to several hundreds of micrometers. Also it was emphasised that, the function of the gel cores is to support the particle shells and to give the microcapsules enough stiffness to be separated from the oil phase by centrifugation. More importantly, the potential use of these capsules as delivery vehicles and for control release of drugs, cosmetics and food supplements has been mentioned.<sup>85a</sup>

In another subsequent work of Paunov's group<sup>85b</sup> the fabrication of novel colloidosome microcapsules with aqueous gel core has been proved. In this work they were mimicking the recently developed “gel trapping technique”<sup>86</sup>. Except this time monodispersed surfactant-free white aliphatic amine latex particles with average diameter of 3.9  $\mu\text{m}$  were used instead of polymeric microrods. It was also mentioned that the cross-linking of the monolayer of the latex particles around the gelled emulsion drops with glutaraldehyde was made to increase the stability of the drops so as to sustain therein transfer into water. Meanwhile, it was found that the polystyrene (PS) latex particles do not undergo notable swelling when in contact with sunflower oil at temperature 75 °C. That is why sunflower oil has been used as oil phase in a series of experiments.<sup>85b</sup>

In addition, Paunov's group also tested the effect of the aqueous gel core on the mechanical stability of the templated emulsion drops upon transfer into water.<sup>85b</sup> This was done by preparing the same emulsion template without using gelling agent. However, it was discovered that, upon transfer into water the shells of colloid particles collapsed due to the treatment with ethanol even after cross-linking with glutaraldehyde. Moreover, it was revealed that, if tricaprylin was used as oil phase, the latex particles in the colloidosome membrane partially swell and form a membrane of swollen polystyrene on the capsule surface. The process was controlled by varying the temperature and the degree of exposure of the emulsion template to tripcaprylin, which allows the pore size of the colloidosome membrane to be controlled independently of the size of the colloidal particles.<sup>85b</sup>

In 2004 Ashby *et al.* produced giant pendant colloidosomes by displacing pendant water drops coated with a monolayer of monodispersed sulphate polystyrene latex particles (220 nm) through a planar oil-water interface.<sup>87</sup> Their method is based on forming a pendant drop of an aqueous suspension of latex particles in the oil phase and then produced a closely packed particles monolayer adsorbed on the drop surface by multiple infusion and withdrawal of the particles suspension through the capillary in the oil phase. Finally, the pendant water drop in oil, densely coated with adsorbed particles, was transferred through a planar oil-water interface to produce giant colloidosome. Furthermore, Ashby reported that, in their method no partial fusion of the particles is required, as the integrity of the particle monolayer is supported by the oil film. They also explained that their methodology can produce colloidosomes attached to a capillary which allows the properties of the colloidosome membrane, like membrane tension and elasticity, to be studied as a function of the number of adsorbed particles, as this can be easily controlled by changing the volume of the inner aqueous phase.<sup>87</sup>

Duan *et al.*<sup>88</sup> for the first time fabricated magnetic colloidosomes by directing self-assembling of magnetite ( $\text{Fe}_3\text{O}_4$ ) nanoparticles at the interface of w/o droplets. Magnetite nanoparticles of different size capped with 2-bromo-2-methylpropionic acid were dispersed in toluene, which emulsified with water phase by vigorous shaking for a few minutes. The colloidosomes were collected by external magnetic field, followed by three times washing with ethanol. The stability of the water-in-oil



droplets was improved by gelation of the aqueous phase with 1.5 % wt. agarose gel, which was set at room temperature. The colloidosomes with agarose gel core exhibit greatly improved mechanical stability, indicated by the fact that they keep spherical shape and don not collapse upon drying for a longer time, as compared to those without gelled cores.

Kim *et al.* used colloidal particles that have size range from nm to  $\mu\text{m}$  to cover the surface of temperature-sensitive microgels to fabricate temperature responsive colloidosomes. They demonstrated that these types of colloidosomes can control permeability through the size of the adsorbed colloidal particles, the thickness of the particle shell, obtained by buckling the microgel surface, or through the use of deformable particles.<sup>89</sup>

To overcome the limitations of some experimental conditions that have been mentioned in the previous methods, Routh and Laib developed a new method to produce stable colloidosomes at low temperatures for the encapsulation of thermally sensitive compounds. This method lacks the use of aggressive chemicals, gelling agents or filling the capsules through the pores of the shell and more importantly uses low temperature conditions. In this technique, the aqueous suspension of poly(styrene-co-butylacrylate) latex particles (180 nm) with a low transition temperature (  $T_g$ ) of 42 °C was mechanically mixed with an oil media ( dodecane or sunflower oil) possibly containing surfactant or electrolyte to produce w/o emulsions, and then the copolymer particles have been partially fused by heating them slightly above their ( $T_g$ ). To transfer the water droplets into fresh water to produce colloidosomes, Routh and Laib, tried different approaches, one of them was centrifugation method and the second was filtration and redispersing in water. The third and the most effective method of transfer was sedimentation for several days, although, low transfer yield was still reported in all of the transfer approaches according to their results.<sup>90</sup>

Prestige and Simovic<sup>91</sup> investigated the self-assembly of hydrophobic silica nanoparticles at the surface of charged submicrometer triglyceride droplets aiming to optimise the preparation of stable colloidosomes. They concluded that in controlling hydrophilic silica nanoparticles interactions, the droplet charge, oil phase volume

fraction, droplet/particle ratio and salt concentration play important roles. This was reflected in the colloidosome zeta potential, stability and interfacial structure. They subsequently proved that silica nanoparticle interactions with negatively charged droplets are weak while, silica nanoparticles strongly covered the positively charged triglyceride droplets and undergone charge reversal at specific droplet/particle ratio and electrolyte concentration. They also claim that in their work stable 1-3  $\mu\text{m}$  colloidosomes were phase separated from hetero-coagulates of droplets and nanoparticles.<sup>91</sup>

Shah *et al.* presented a novel technique to fabricate monodispersed stimuli-responsive colloidosomes using stimuli-sensitive microgel particles as building blocks. The microgel particles self-assemble themselves along the oil-water interface. According to the authors, the technique is highly versatile, as it can be used in conjunction with microfluidic devices to produce highly monodispersed colloidosomes, or with any other bulk-emulsification techniques to produce colloidosomes in large quantities.<sup>92</sup>

Thompson and Armes have prepared covalently cross-linked colloidosomes from templating o/w Pickering emulsion stabilised by near-monodisperse sterically-stabilised with poly (glycerol monomethacrylate) polystyrene latex particles. The o/w droplets were covalently stabilised by cross-linking the hydroxy-functional stabiliser chains at the inner surface of the latex particles adsorbed onto the oil droplets using toluene 2, 4-diisocyanate-terminated poly (propylene glycol) as a cross-linker. The cross-linked colloidosomes are significantly more stable than o/w Pickering emulsion droplets, as judged by their treatment with either excess alcohol or a non-ionic surfactant.<sup>93</sup>

Alternatively Walsh *et al.* have used commercially available steric stabiliser poly (ethylene imine) (PEI) to produce polyamine-functionalised polystyrene latexes, which were used to stabilise o/w Pickering emulsions and they were covalently cross-linked at the oil droplet interface using commercially available polymeric cross-linkers, PPG-TDI, PPG-DGE, and PEG-DGE. In each case the internal oil phase was removed by washing with excess alcohol.<sup>94</sup>

Yuan *et al.* reported the preparation of colloidosome microcapsules using sterically stabilised PS latex particles through emulsion droplet templates by either thermally annealing the adsorbed particles which have a shell formed by adsorption of thermally responsive and pH-responsive polymer chains of PDMA-*b*-PMMA (poly[2-(dimethylamino)ethylmethacrylate]-*b*- poly[methylmethacrylate]), or chemically cross-linking of the polymer chains from within the emulsion droplets using cross-linking agent BIEE (1,2-Bis(2-iodoethoxy)ethane).<sup>95</sup>

Nomura and Routh fabricated water-core colloidosomes at room temperature from Pickering emulsions stabilised by poly (methylmethacrylate-co-butylacrylate) latex nanoparticles. Adding small amount of ethanol caused the particle aggregation due to the diffusion of ethanol into the aqueous latex suspension, which resulted in creating an irreversible shell for the colloidosomes.<sup>96</sup> While, using the above technique Keen *et al.* have recently encapsulated viable Baker's yeast cells in colloidosomes, where use of harsh chemicals and high temperature has been avoided.<sup>97</sup>

## **5.1.2 Results and discussion**

### **5.1.2.1 Fabrication of gel-cored magnetic colloidosome from w/o Pickering emulsions templates**

In this part of the chapter, we demonstrate the fabrication of magnetic colloidosomes loaded with living cells. Yeast cells as model for living probiotic cells were encapsulated in gel-cored magnetic colloidosome containing a fixed amount of sodium polyacrylate which can expand 400 times its original size at pH > 7. This can program the loaded colloidosomes to trigger release the cells at pH > 7. All Pickering emulsions in our study in this chapter were stabilised by amidine latex particles approximately 300 nm in diameter, which were initially dispersed in the oil phase (tridecane).

In addition the colloidosome cores contained magnetic nanoparticles so that they can be manipulated by an external magnet, and facilitate the transfer of the w/o emulsion droplets from the oil continuous phase into water and produce colloidosome. Other than adjusting the trigger release of the cells, polyacrylate is an anionic polyelectrolyte which can bind to the cationic amidine latex nanoparticles from inside the droplets and as a result lock the particles in the interface permanently, which in return made the transfer process relatively easier. The whole process of fabricating gel-cored pH-responsive, magnetic colloidosomes has been illustrated in Figure 5.3.

Amidine latex particles can stabilise water in oil emulsions in which the water phase contains dispersed yeast cells. The important point to consider here is that, the latex particles should be dispersed in the oil phase to avoid their adsorption on the yeast cell's membrane, which can destroy the cells. Although, amidine latex particles are hydrophobic with hydrophilic amidine functional groups, they are not easily dispersible in oil, because they are water based from production. The latex needed to be centrifuged out of the water then redispersed them in sufficient amount of ethanol twice to remove traces of water if any was left, then they were centrifuged out of the excess ethanol and redispersed in minimum amount of ethanol, afterwards it was mixed with the oil, this way a homogeneous dispersion of the amidine latex particles in oil was produced. Water droplets in oil stabilised by amidine latex particles are very stable and can be considered a novel method to encapsulate yeast cells in their water core. Figure 5.4 shows w/o emulsion droplets in tridecane, after the emulsion was cooled down at 4 °C to set the Agarose gel. The droplets observed by optical microscopy, which indicates that they have average droplet diameters of 200 µm.

#### **5.1.2.2 Transfer of the Pickering emulsion droplets into water**

The produced droplets were transferred from the tridecane phase into water to yield the colloidosomes, by using external magnet approach. The process included removing the excess oil in the emulsion and then adding concentrated emulsion on top of milli-Q water phase in a sample tube which was in return fixed on a permanent magnet. As the emulsion droplets hit the water surface they were dragged downward with the force of the permanent external magnet and settled at the bottom of the tube.

The oil phase was separated on the top of the water phase. See Figure 5.5 which demonstrates the fabricated colloidosome after transferred into water.

### 5.1.2.3 Viability of the yeast cells inside colloidosomes

The whole idea of microencapsulation of living cells is to protect them from harsh conditions; therefore, we have performed some viability tests for the encapsulated yeast cells. After the colloidosomes were washed several times with milli-Q water, the yeast cells inside were treated with both FDA and Calcein-AM/Propidium iodide live/dead kit solutions simultaneously. The FDA test shows the yeast cell membrane is intact and the enzymes in the cell interior are active (see Figure 5.6b).

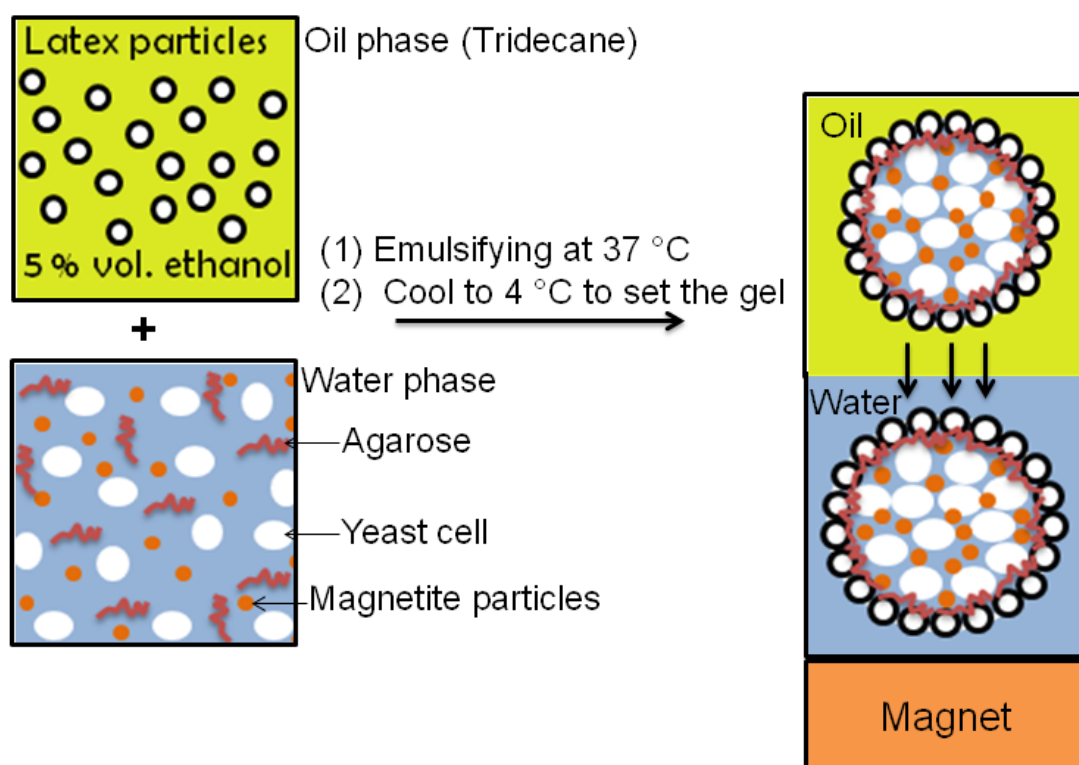


Figure 5.3: Schematic diagram of the fabrication of gel-cored magnetised colloidosome by templating w/o Pickering emulsions droplets.

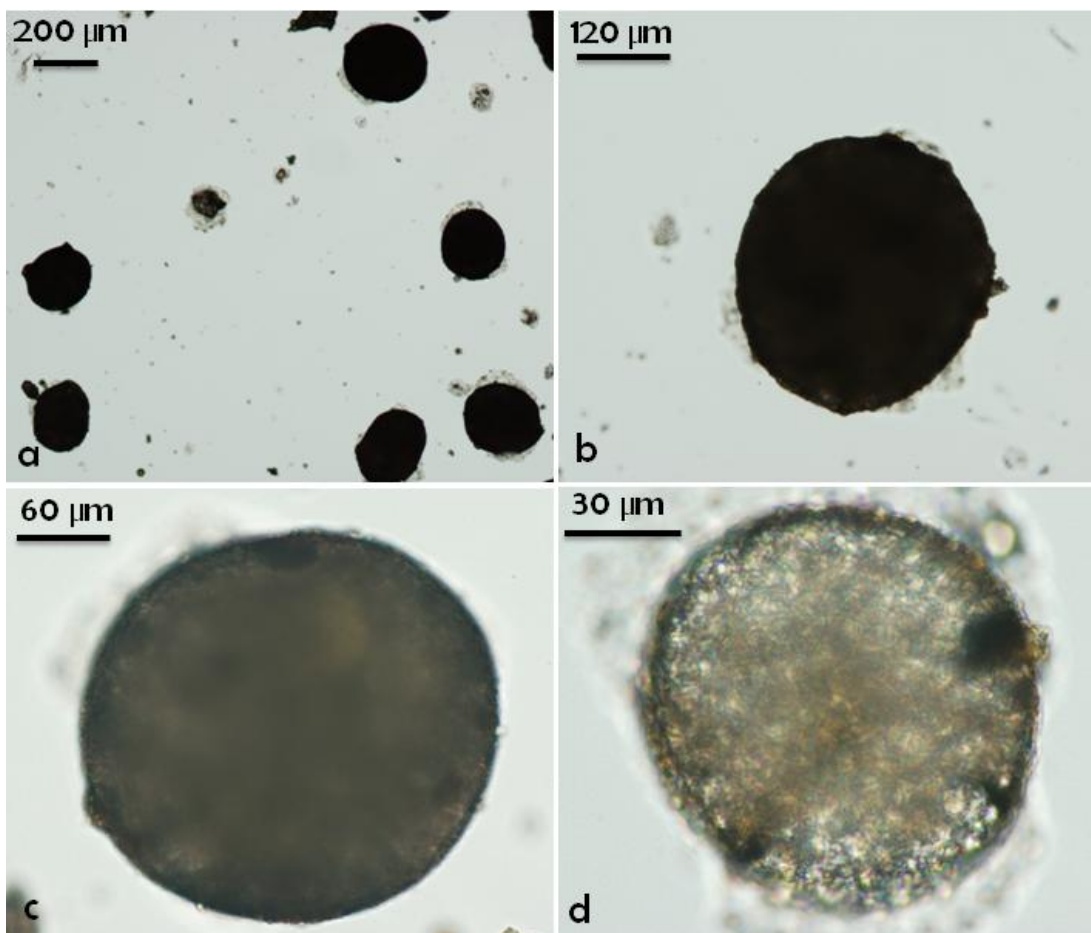


Figure 5.4: Emulsion (w/o) droplets stabilised with 300 nm amidine functionalised polystyrene latex nanoparticles in tridecane. The water phase contained 10 % wt. native yeast cells and 4 % wt. sodium polyacrylate, 0.5 % wt. magnetic nanoparticles, and 1 % wt. agarose gel.

In addition to the FDA test, we performed a Calcein/Propidium iodide test with live/dead cells kit on the yeast cells encapsulated inside the colloidosomes. The results are presented in Figure 5.6c-d, where in (c) the stained cells were observed with dual fluorescence filter set of FITC/TRITC and as one can see only the green fluorescence is visible, indicating the viability of the encapsulated cells. With dual fluorescence filter set of FITC/TRITC both dead (red) and live (green) cells can be observed. But with 545 nm excitation which is TRITC filter set only the dead (red) cells can be observed as it has shown in Figure 5.6d. There is limited number of cells showing in red colour which indicates that high percentage of the encapsulated cells is still viable. Calcein-AM works on the same principle as FDA.

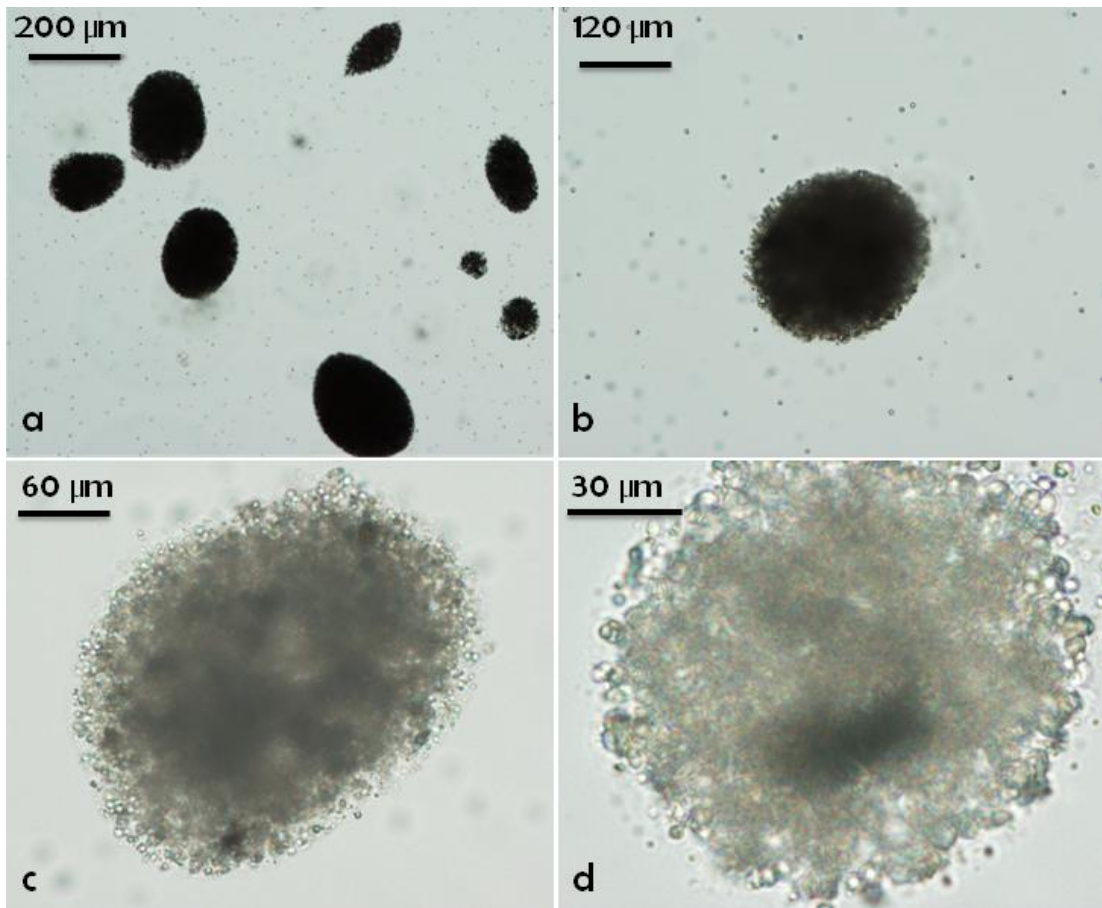


Figure 5.5: Colloidosomes transferred to water by using external magnet and fabricated by using water-in-tridecane emulsion templates stabilised with amidine functionalised polystyrene nanoparticles.

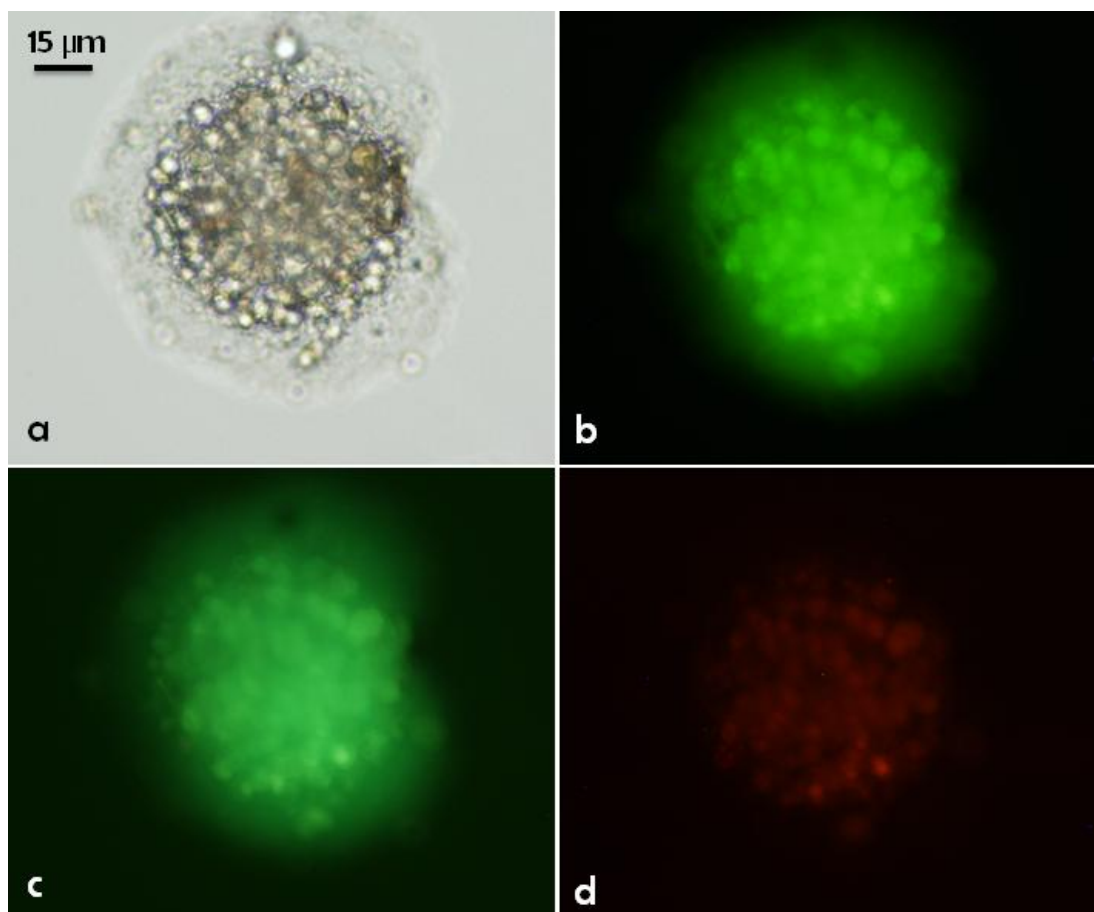


Figure 5.6: The yeast cells encapsulated inside colloidosomes were treated with Calcein-AM/Propidium iodide live/ dead kit as well as FDA and were observed by optical fluorescence microscopy to test the viability of the cells. (a) is an optical image, (b) is observed using FITC filter, (c) is dual filter of FITC and TRITC, while, (d) is only TRITC filter set.

#### 5.1.2.4 Fabrication of colloidosomes interlocked with polyelectrolytes and polyelectrolyte pre-coated yeast cells

In the second part of this chapter, we report the fabrication and *in situ* encapsulation of yeast cells in colloidosome microcapsules from w/o Pickering emulsion templates stabilised by 300 nm polystyrene latex particles functionalised with amidine functional groups. The stability of the emulsion droplets was achieved by interlocking the adsorbed particles monolayer at the w/o interface with either (i) oppositely charged polyelectrolyte adsorption or (ii) using polyelectrolyte pre-coated yeast cells which acts as cross-linker ( see Figures 5.7, and 5.8). These two approaches are the base of two strategies of preparation of cells containing colloidosomes.



We have enhanced the surface charge of yeast cells by using layer-by-layer polyelectrolyte adsorption technique using both (PAH/PSS). PSS is anionic polyelectrolyte which can cross-link the monolayer of the adsorbed amidine particles at the w/o interface by electrostatically binding to the positively charged latex particles, while yeast cells are slightly negatively charged and can adsorb a layer of cationic polyelectrolyte such as PAH. This will result in producing positively charged yeast cells which in turn can adsorb a layer of anionic polyelectrolyte (PSS) and produce strongly negatively charged yeast cells. We have also designed a strategy where the strongly negatively charged yeast cells act as a cross-linker to the amidine latex particles monolayer at the interface of the w/o Pickering emulsion. Increasing the stability of the w/o Pickering emulsion droplets by cross-linking the monolayer of the adsorbed amidine latex particles at the w/o interface helps the successful transfer of emulsion droplets from the oil phase into water phase and hence produce colloidosomes.

First of all, to optimise the amount of yeast cells to be encapsulated in the water-in-undecane droplets, a series of experiments were performed, in which all the conditions were kept constant except the amount of yeast cells. To start with, no yeast cells were used as it is shown in (Figure 5.9), the emulsion is relatively stable and the droplets are polydisperse with relatively narrow size range, and mean diameter of 85  $\mu\text{m}$ . In the next experiment 1 % wt. yeast cells was added into the water phase. The produced water-in-undecane emulsion was still stable but the droplet size is dramatically decreased and went down from approximately 85  $\mu\text{m}$  to approximately 48  $\mu\text{m}$ . Upon further increase of the yeast cells concentration the emulsion drops diameter started to increase slowly as the amount of yeast cells increased. From 1 to 30 % wt. yeast cells at which the largest droplets were obtained and the emulsion was at its highest stability. Hence, the droplets size increases with the amount of yeast cells in the water phase as illustrated in Figure 5.10-11.

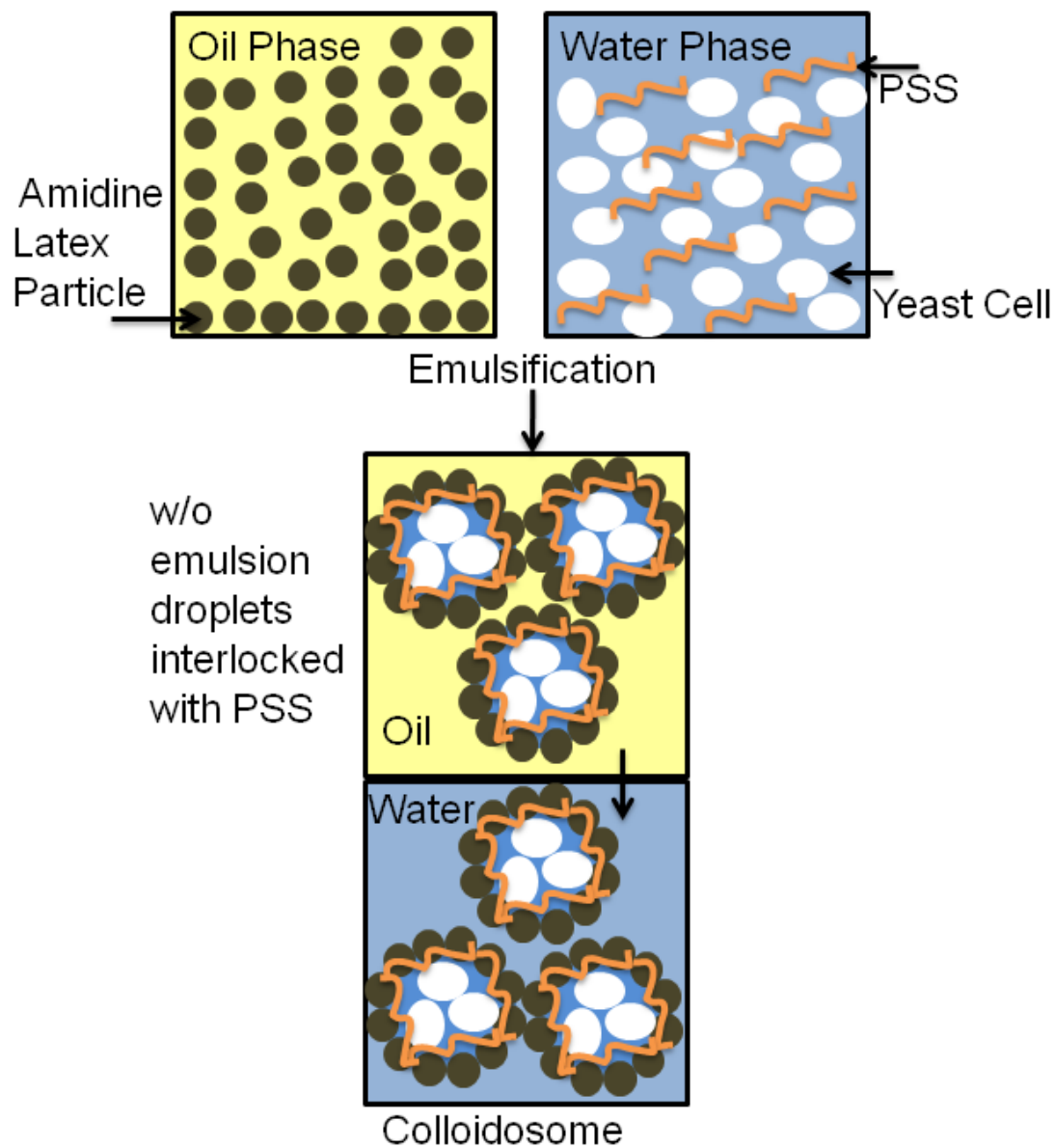


Figure 5.7: Strategy (i) aqueous suspension of yeast cells in the presence of negatively charged polystyrene sulfonate emulsified with oil phase (undecane) containing 300 nm amidine latex particles. Stable water droplets in undecane were produced after they were interlocked with PSS, then the droplets were transferred into water to produce colloidosome using freezing process.

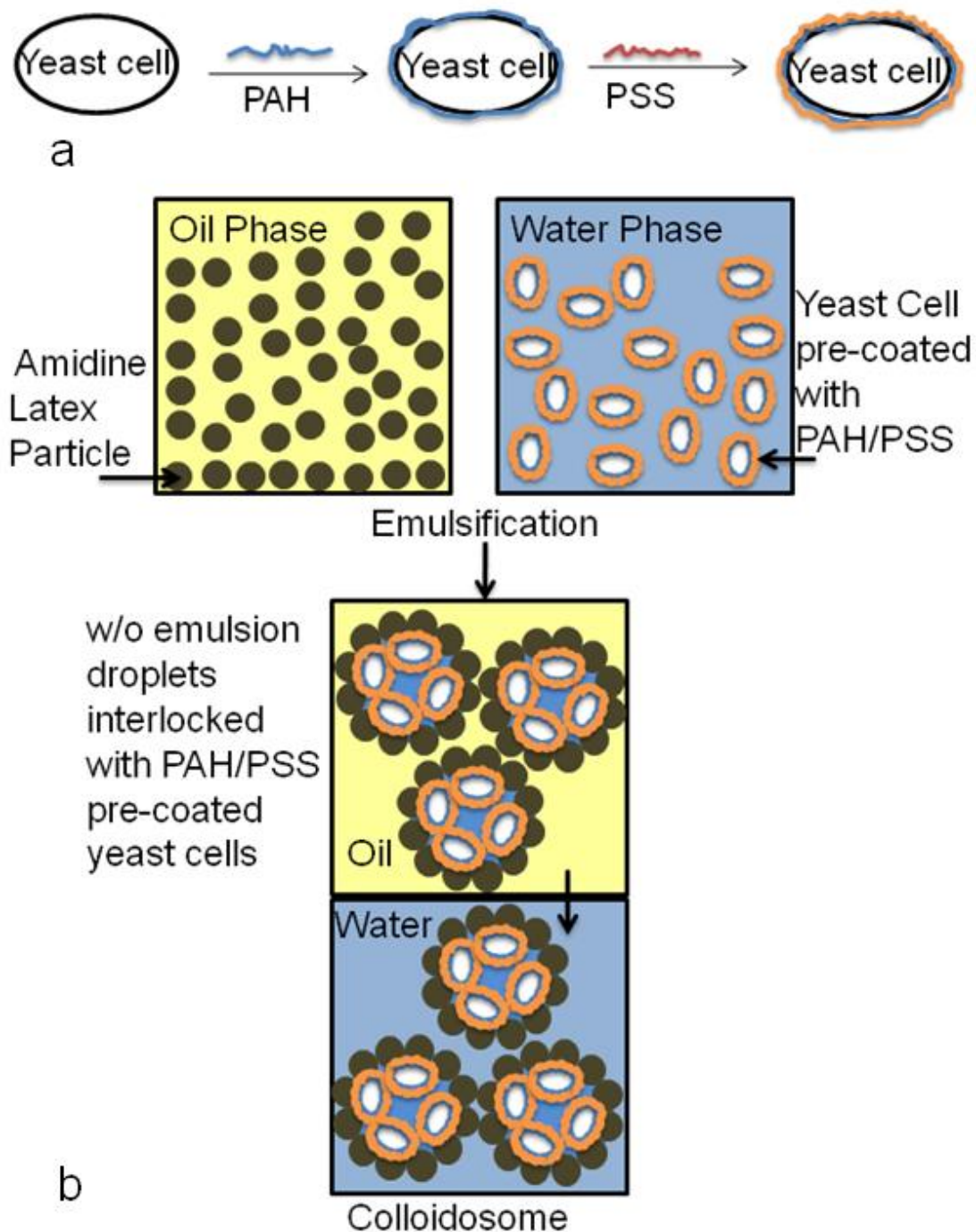


Figure 5.8: Strategy (ii) (a) schematic diagram of coating yeast cells with polyelectrolytes. (b) Schematic diagram of aqueous suspension of anionic pre-coated yeast cells emulsified in oil which contained 300 nm amidine latex particles to produce water in oil emulsion droplets. The stability of the w/o emulsion droplets increased by cross-linking the monolayer of the adsorbed particles at w/o interface using PAH/PSS pre-coated yeast cells. The droplets were transferred into water using a freezing process to produce colloidosome.

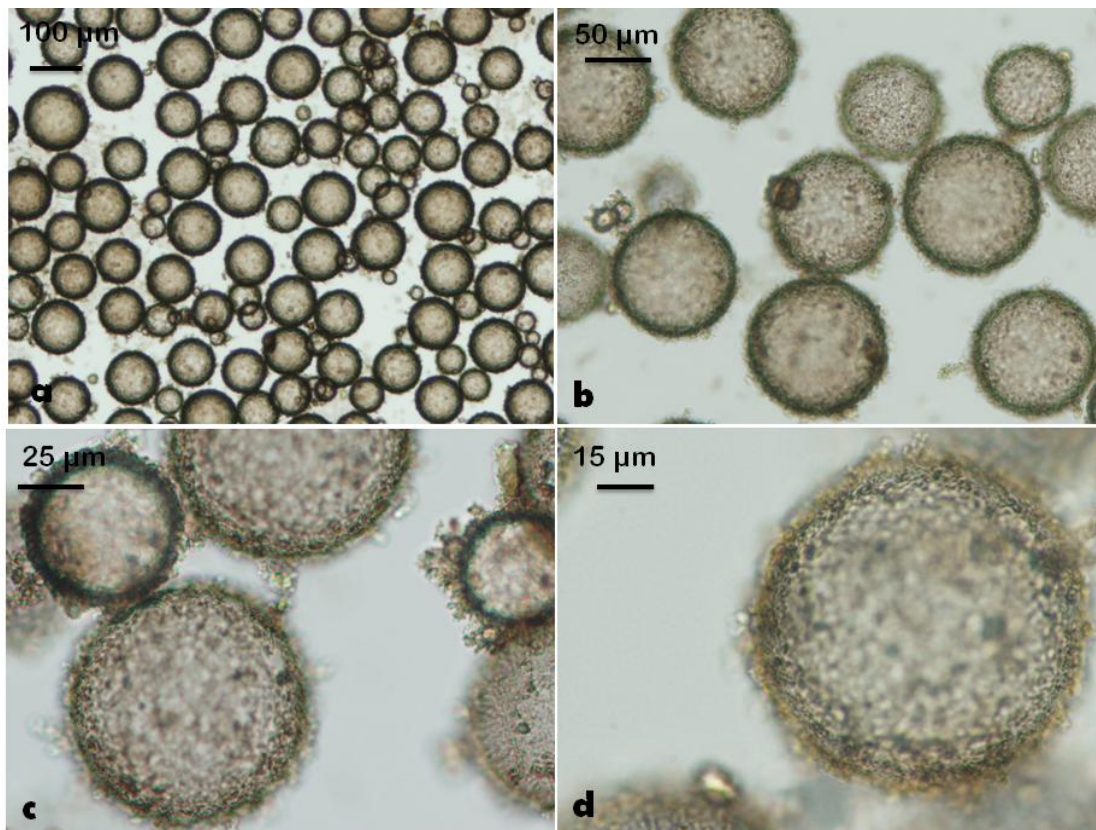


Figure 5.9: Water-in-undecane emulsion stabilised with 0.5 % wt. 300 nm amidine latex particles for 30 seconds at 10,000 rpm using 18 mm head IKA® T25 Digital Ultra Turrax homogeniser. The water phase contained 1 % wt. PSS dissolved in 0.1 M sodium chloride solution. The ratio of water phase to undecane phase was 1:9, a-d represent different magnifications.

The reason could be related to the fact that the yeast cells are slightly negatively charged and when there is a minimum amount of them available in the water phase, they might contribute into building the monolayers of particles around the water droplets, therefore, more particles would be available to adsorb at the w/o interface at higher yeast cells concentration and therefore, produced more droplets with smaller average size. Consequently, when the amount of yeast cells increased to 10 % wt., then the cells are not used in building the membrane anymore i.e. the excess cells do not adsorb at the interface and will remain in the water phase and they start to bulk up the droplets due to random packing in the bulk of the drops.

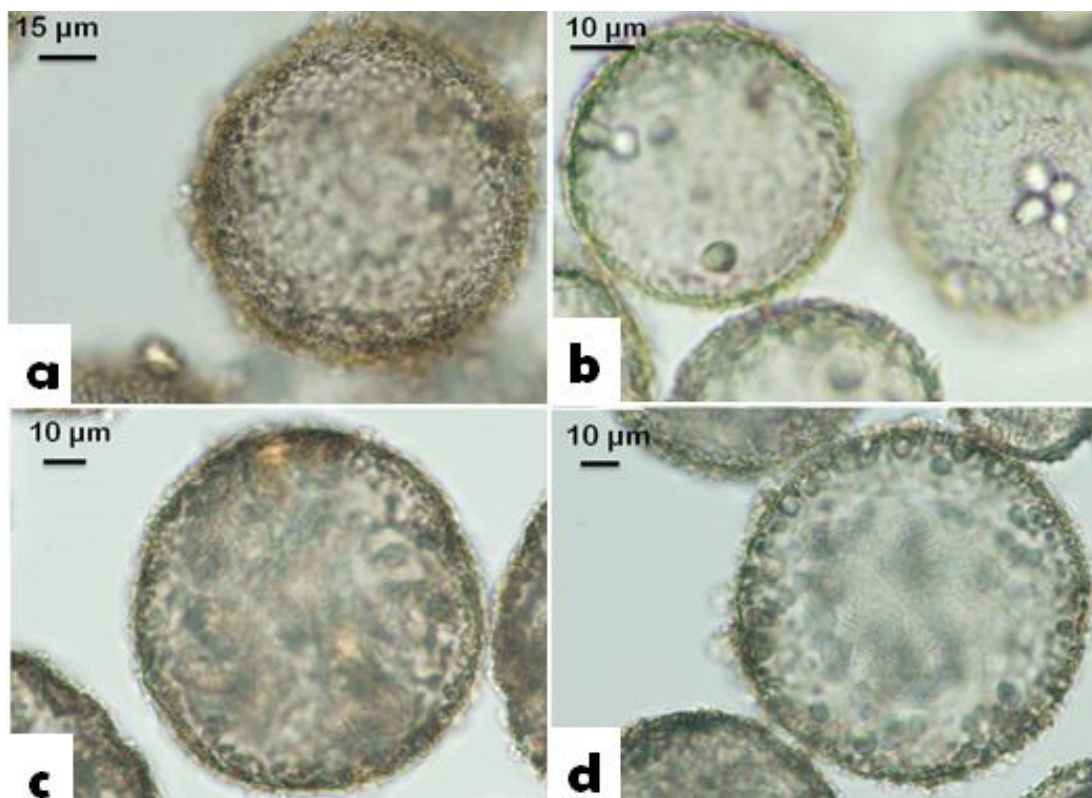


Figure 5.10: Aqueous suspension of native yeast cells was emulsified in undecane in the presence of 0.5 % wt. 300 nm amidine latex particles for 30 seconds at 10,000 rpm using 18 mm head IKA® T25 Digital Ultra Turrax homogeniser. (a) is no yeast cells in the water phase, (b) is 1 % wt. yeast cells, (c) is 10 % wt. and (d) 20 % wt. yeast cells. In all cases the volume fraction of the water phase was 10 % vol.

Yeast cells are slightly negatively charged therefore, when cells mixed with a saturated aqueous solution of polyelectrolyte such as polyallylamine hydrochloride a layer of positively charged polyelectrolyte will adsorb on the cell surface and making the cells positively charged. Meanwhile, a layer of anionic polyelectrolyte such as polystyrene sulfonate can absorb on top of the layer of PAH which gives rise to negatively charged yeast cells. Negatively charged yeast cells coated with layers of polyelectrolyte can be used to increase the stability of water droplets in undecane stabilised by amidine latex particles as it is outlined in this work. The coated cells are negatively charged, hence they attach themselves to the positively charged amidine functional group on the latex particles by electrostatic interaction which is relatively strong, therefore it will held the water droplets in the oil together more strongly and then produce very stable and relatively large size droplets of up to 500 μm compared to the droplets that produced from interlocking the adsorbed particles monolayer with

(PSS) which produced droplets around 100  $\mu\text{m}$ . The produced water-in-undecane emulsion droplets can be transferred into water successfully but the process is very sensitive and extra care need to be taken to prevent their destruction. Nevertheless it is feasible, but with limited yield of colloidosomes transferred into the water phase, the rest would be destroyed in the process as reported by authors of alternative techniques.<sup>11,90</sup>

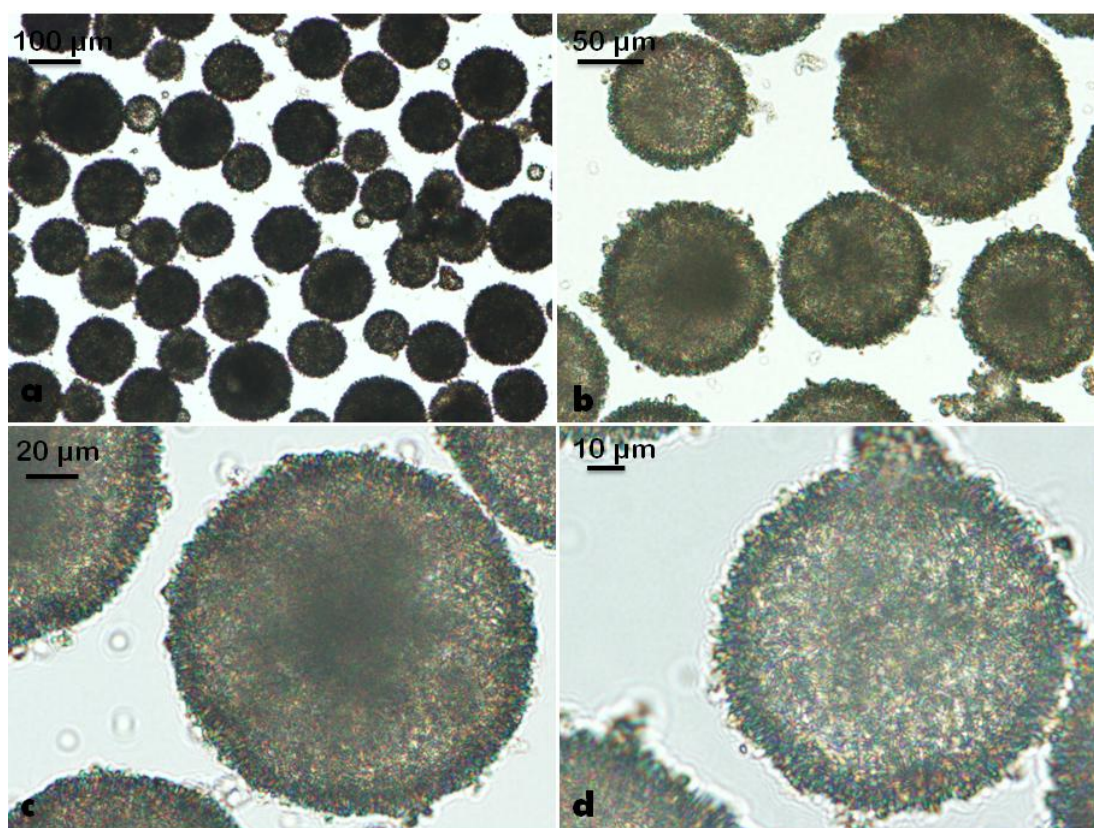


Figure 5.11: Aqueous suspension of native yeast cells (30 % wt.) was emulsified in undecane in the presence of 0.5 % wt. cationic amidine latex nanoparticles (300 nm) for 30 seconds at 10,000 rpm using 18 mm head IKA<sup>®</sup> T25 Digital Ultra Turrax homogeniser. The volume fraction of the water phase was 10 % vol.

#### **5.1.2.5 Transfer of w/o Pickering emulsion droplets into water using freezing process**

To transfer the water droplets from oil to water and hence producing stable colloidosomes, three strategies were taken. In one of these methods the emulsion was poured on top of a known amount of water which contained ethanol to reduce the surface tension and then gently centrifuged to settle the colloidosomes to the bottom. Although it has been reported<sup>11</sup> that a number of colloidosomes should be seen in the water phase by this particular strategy, on this occasion the transfer process was unsuccessful as no colloidosomes were seen. Attempts were also made to transfer the droplets into water by evaporation method in which the undecane was replaced with hexane twice and then removed the excess hexane and poured the concentrated emulsion on top of water and evaporated the hexane at 40 °C in order to move the droplets into the water phase. Unfortunately, this process produced aggregates which were not dispersible in water, which indicates that the droplets were aggregated together during the evaporation process and produced a bulky mass which was not easily observable by optical microscope.

One of the successful strategies used to transfer the droplets was a freezing method which we developed. Here the emulsion was frozen in a freezer for 2 days after adding a known amount of calcium carbonate microparticles which were playing the role of a spacer in the oil between the water droplets. The frozen water droplets were filtered off and redispersed in fresh milli-Q water to produce stable colloidosomes. The encapsulated yeast cells inside the colloidosomes were treated with fluorescein diacetate and observed by fluorescence microscopy; bright green colour indicates the viability of the yeast cells. In case of stabilising droplets with amidine latex particles and polyelectrolyte coated yeast cells, the droplets are larger and the transfer process from oil to water is more efficient as more colloidosomes were visible in the water phase compared to the ones the droplets with amidine particle monolayer cross-linked with polystyrene sulfonate.

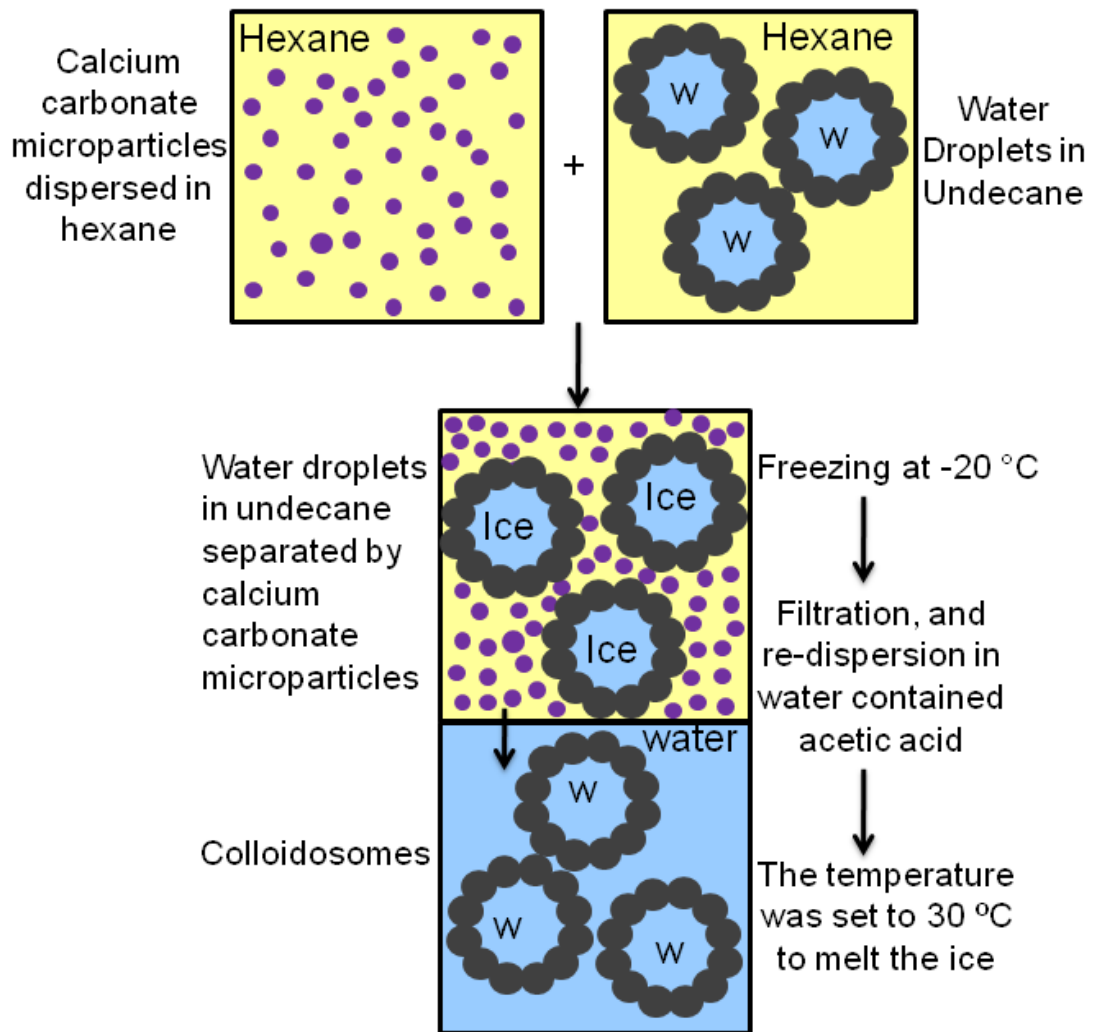


Figure 5.12: Schematic diagram of freezing process. Calcium carbonate microparticles dispersed in hexane which was then mixed with w/o Pickering emulsion. The mixture was frozen at  $-20\text{ }^{\circ}\text{C}$  overnight and then the frozen w/o emulsion droplets were redispersed in water containing acetic acid (1 % vol.) after it was filtered off.

Without addition of calcium carbonate microparticles as spacers between the droplets during the freezing process, droplets lost their spherical shape and aggregated together and formed solid block of ice which was not easy to redisperse them in water as it can be seen in Figure 5.16d. To prove the viability of yeast cells at very low temperature, a sample of yeast cells was frozen overnight in the freezer at  $-20\text{ }^{\circ}\text{C}$ . The frozen yeast cells were left to melt at room temperature followed by treating them with FDA solution and checking their viability by fluorescence microscopy.



As it can be seen from Figure 5.16c, the cells are still viable and can withstand temperature as low as  $-20\text{ }^{\circ}\text{C}$ . This confirms the fact that the yeast cells encapsulated inside the colloidosomes can preserve their viability and withstand freezing at such low temperature for approximately 12 hours. Similar green fluorescence signal can be detected from intact yeast cells treated with FDA.

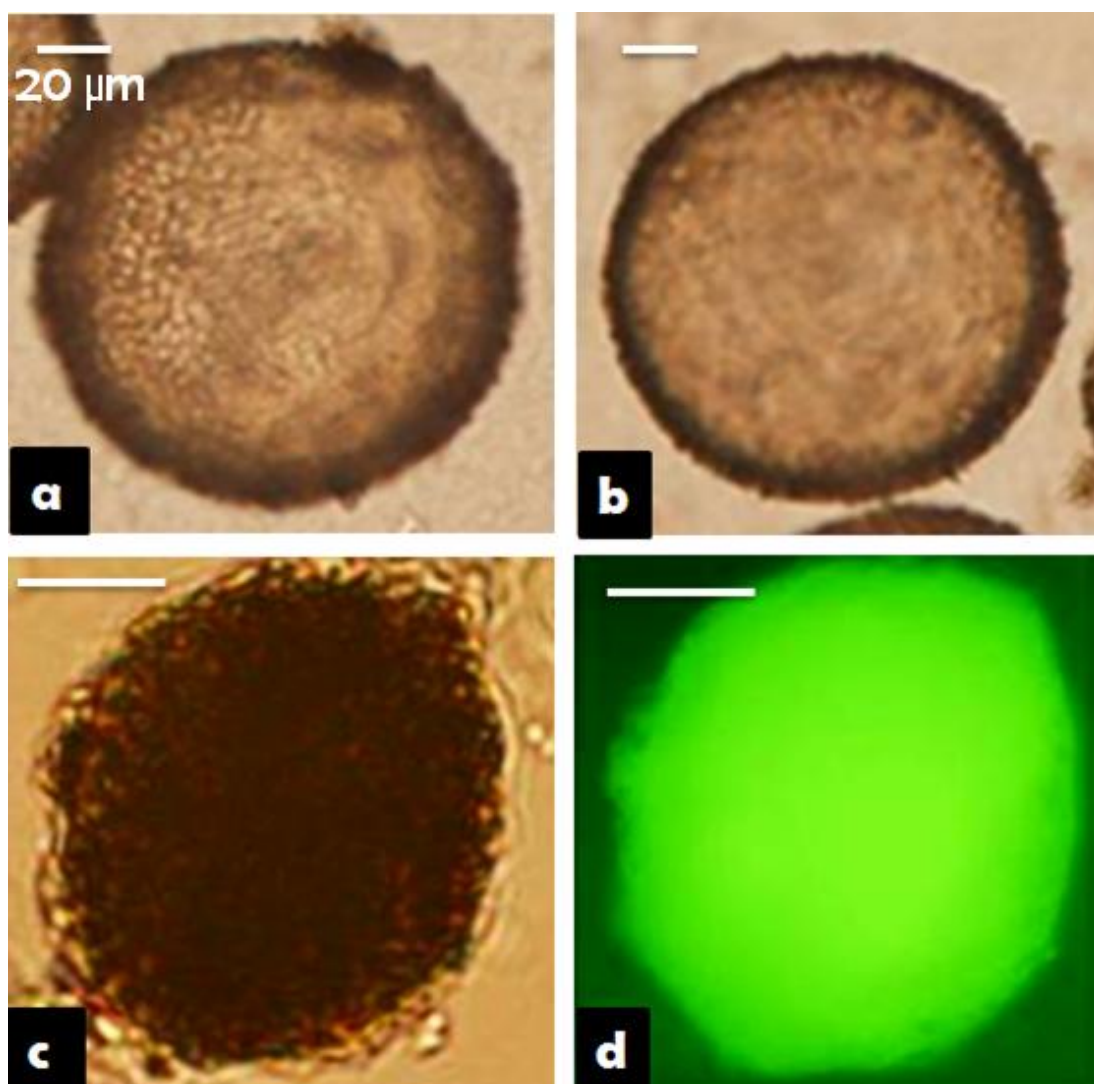


Figure 5.13: Water droplets in undecane stabilised with 300 nm amidine latex particles, the adsorbed monolayer of the particle was interlocked together with PSS( a and b). While (c and d) shows the colloidosomes produced from transferring such droplets into water by a freezing process, in (d) the encapsulated yeast cells inside the colloidosomes were treated with FDA and observed by fluorescence microscopy, whereas, (c) is a brightfield optical microscopy image of a colloidosome obtained by this method.

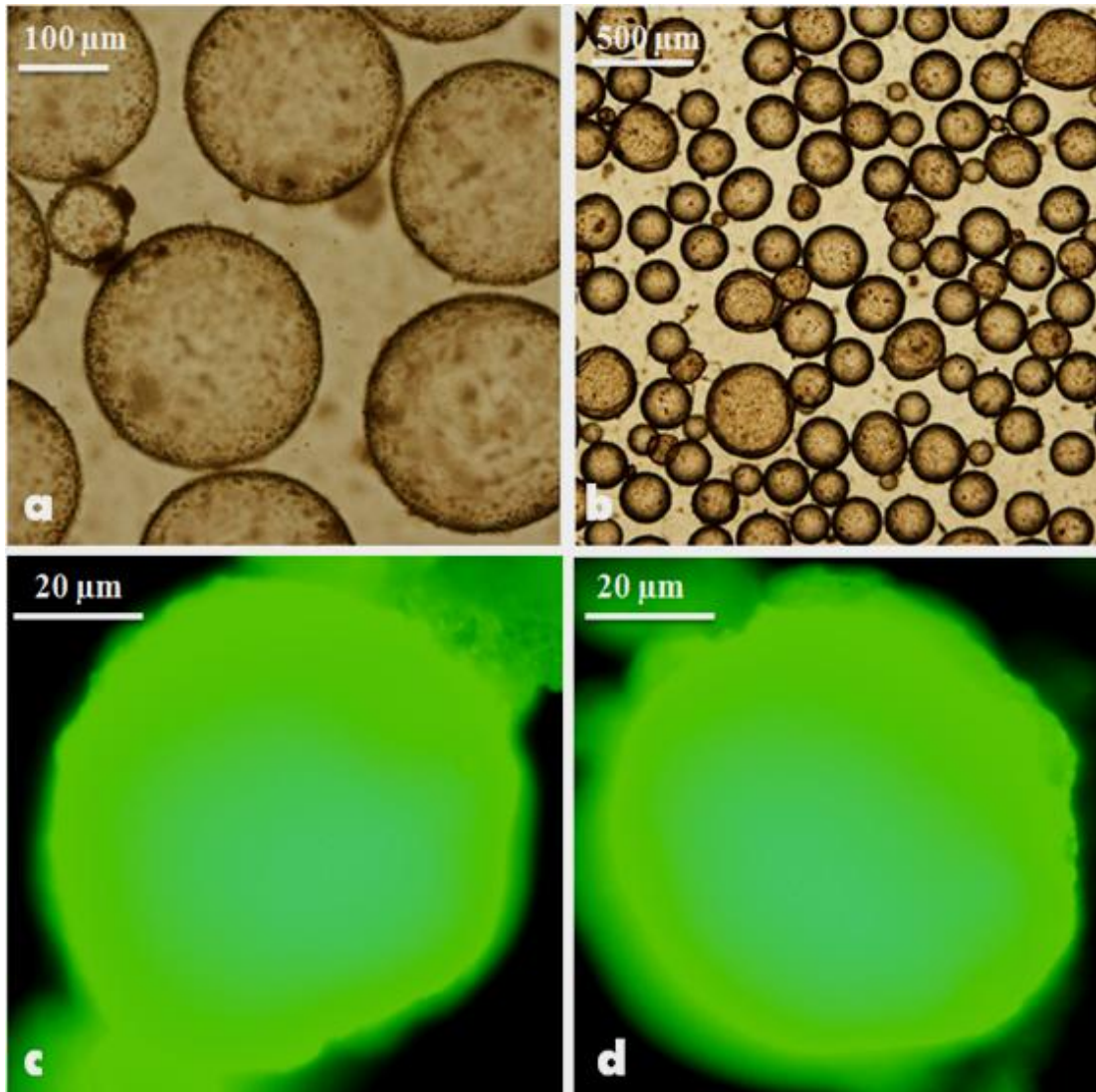


Figure 5.14: (a and b) show water droplets in undecane stabilised with 300 nm amidine latex particles and the stability of the droplets was reinforced by using yeast cells coated with polyelectrolytes. While (c and d) are colloidosomes fabricated from such emulsion templates. The droplets were transferred into fresh water by freezing process and the colloidosomes were stained with FDA and observed under fluorescence microscopy.

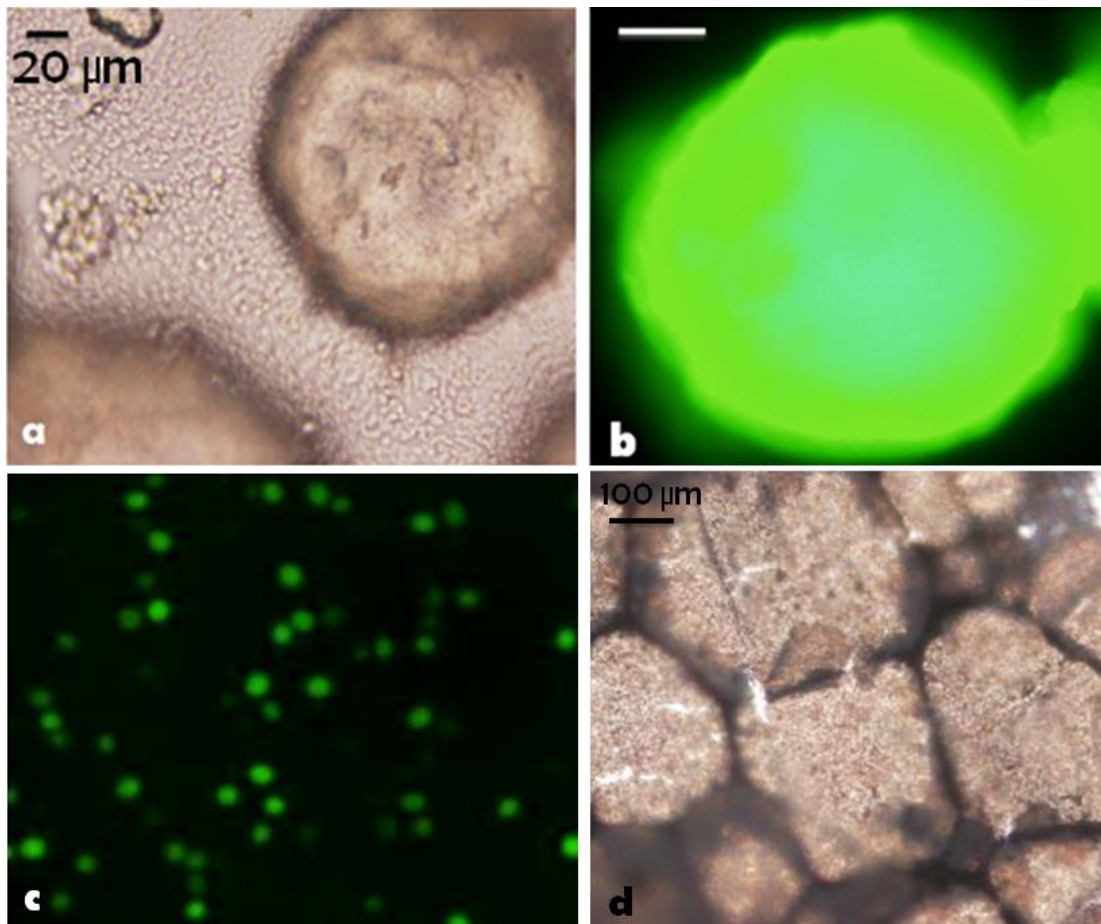


Figure 5.15: (a) shows calcium carbonate microparticles in between the water droplets in undecane (b) The encapsulated yeast cells inside the colloidosome were treated with FDA solution and observed by fluorescence microscope. (c) Yeast cells dispersion was frozen at  $-20\text{ }^{\circ}\text{C}$  overnight, followed by treating them with FDA solution. (d) Frozen w/o emulsion droplets at  $-20\text{ }^{\circ}\text{C}$  without addition of calcium carbonate microparticles.

### 5.1.3 Conclusions

Live yeast cells were encapsulated in novel colloidosomes prepared from Pickering emulsion templates which were stabilised by 300 nm cationic amidine latex nanoparticles. Two strategies were used to fabricate and interlock the structure of the Pickering water droplets in oil. (i) The first was to integrate magnetic nanoparticles in a gelled water phase with an agarose gel for its successful transfer from oil into water. In addition, known amount of polyacrylate was used for two purposes of both pH trigger release of the yeast cells upon increasing pH and to electrostatically bind to the cationic amidine latex nanoparticles at the w/o interface. (ii) The second approach to increase droplet stability was achieved by interlocking the adsorbed amidine latex particles monolayer at the w/o interface with either (a) polystyrene sulfonate from the inside of the droplets or (b) utilising anionic polyelectrolyte pre-coated yeast cells to electrostatically bind to the cationic amidine latex nanoparticles from the inside of the droplets.

Water droplets produced from stabilised Pickering emulsions were successfully transferred into water to produce colloidosomes for encapsulation of living yeast cells. Two main strategies were taken; first was using an external magnetic field to collect the magnetic colloidosomes at the bottom of a sample tube and the other was by freezing the emulsion after addition of calcium carbonate microparticles followed by filtration and redispersing in water which contained acetic acid to dissolve the calcium carbonate. Furthermore, viability test for the encapsulated cells were performed using both FDA and live/dead cells kit, which indicated viable cells inside the colloidosomes. The produced colloidosomes show that living cells like probiotics or cell implants can be successfully encapsulated and protected from the environment/ the results from this chapter can be used not only in protection of probiotics but also in development of live vaccine formulations, and cell implants.

## Chapter 6.

### Fabrication of three dimensional living multicellular structures

#### “Cellosomes”

##### 6.1.1 Introduction

In this chapter we report the fabrication of three-dimensional living multicellular structures, which are named cellosomes in analogy with colloidosomes.<sup>57</sup> Cellosomes are novel multicellular assemblies, which consist of a spherical monolayer of living cells held together by colloidal interactions. The term yeastosomes which is an alternative name for cellosomes from yeast cells was first described by Brandy *et al.*<sup>98</sup>. The idea in their study was based on templating microbubbles with cells coated with cationic polyelectrolyte using the layer-by-layer technique. Cellosomes not only resemble colloidosomes but also spherical colonial multicellular microorganisms such as *Volvox aureas*.<sup>98</sup>

Fakhrulin *et al.*<sup>99</sup> have reported the development of colloidosomes as hollow microcapsules whose membrane consist of a single monolayer of living cells. By analogy with colloidosomes they have been named cellosomes. Other than spherical colloidosomes, non-spherical structures were fabricated by these authors by immobilising yeast cells pre-coated with PAH and CMC on the surface of calcium carbonate microcrystals of rhombohedral and needle-like morphologies which were coated with several layers of PAH/PSS. Finally, hollow multicellular structures were obtained by dissolving the sacrificial calcium carbonate particles.<sup>99</sup>

Cellosomes may find practical applications in the area of developing biological microcontainers, tissue engineering of hollow transplants and in other areas of biotechnology, as the yeast cells can be replaced by either plant or mammalian cells. To facilitate the separation of the cellosomes from the excess of cells a monolayer of magnetic nanoparticles embedded in the polyelectrolyte layer which allows the cellosomes to be extracted and further manipulated by an external magnetic field. The development of the first primitive multicellular organisms might have been facilitated

by non-specific adsorption of individual cells onto particles of non-biological origin which might have been later digested by the by-products of the cell activity.<sup>98-100</sup>

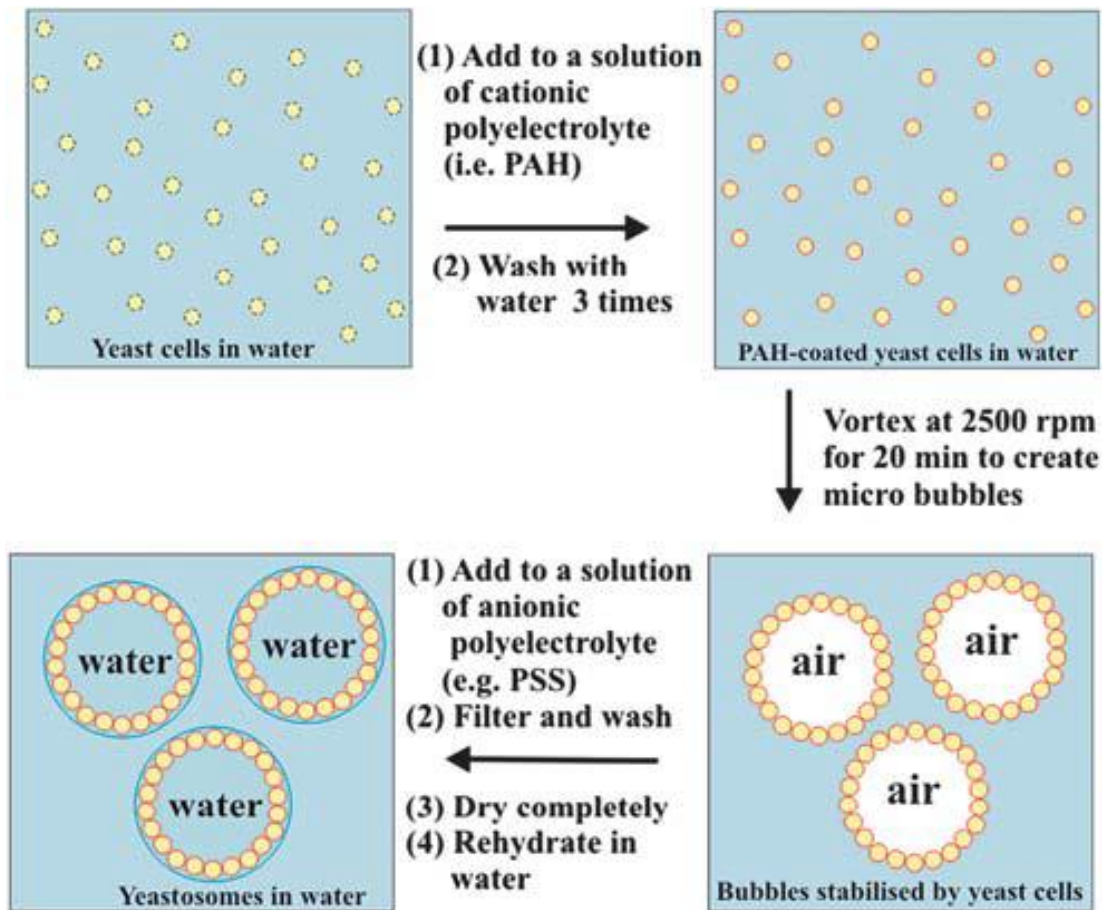


Figure 6.1: Schematics of the assembly of living yeast cells into living hollow shell structures (yeastosomes) by using air bubbles as templates. The bare cells are suspended in water and coated with a cationic polyelectrolyte (e.g. PAH) followed by vortexing to create microbubbles which act as templates for the cationic cells. The cell-coated microbubbles are sealed by further addition of an anionic polyelectrolyte (e.g. PSS). These structures are filtered out and rehydrated to produce yeastosomes.<sup>98</sup>

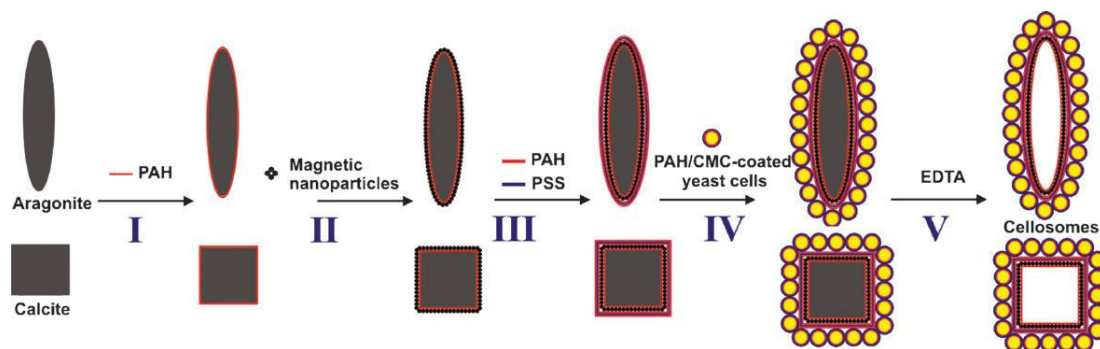


Figure 6.2: Schematic representation of the process of fabrication of magnetic cellosomes. I – coating of microcrystals with PAH; II – formation of MNPs layer on microcrystals; III – coating of PAH–MNP-coated microcrystals with additional layers with PAH/PSS/PAH; IV – immobilization of PAH–CMC-coated yeast cells on the surface of modified microcrystals; V – dissolution of CaCO<sub>3</sub> cores resulting in formation of hollow magnetic cellosomes.<sup>57</sup>

### 6.1.2 Results and discussions

In this chapter we report the fabrication of multicellular structures by using w/o emulsion templates as intermediate. Different approaches were taken to produce intermediate w/o emulsions which were used as templates to produce the final multicellular assemblies. We have used two main strategies to assemble yeast cells pre-coated with polyelectrolytes in water droplets in various oils stabilised with either surfactant or solid particles. In the first strategy, an aqueous dispersion of yeast cells coated with cationic polyelectrolytes<sup>69</sup> was either emulsified in oil using either anionic surfactants such as oleic acid or non-ionic surfactant such as Span60 to produce intermediate stable water droplets loaded with coated yeast cells.

Our second strategy included preparation of two water-in-oil (w/o) emulsions stabilised with latex nanoparticles, each emulsion contained oppositely charged yeast cells coated with polyelectrolytes encapsulated in the water droplets. The two emulsions containing cells pre-coated with oppositely charged polyelectrolytes were mixed and re-emulsified, followed by shrinking the water droplets in dry octanol and subsequently transfer the shrunken droplets into water to fabricate 3D structures of cells packaged by a monolayer of latex particles. The cellosomes produced by this strategy were transferred from the oil to the water phase by freezing and filtering off the oil phase.

### 6.1.2.1 Fabrication of Cellosomes by templating w/o emulsions stabilised with oleic acid

Oleic acid is a mono unsaturated omega-9 fatty acid found in various animal and vegetable sources. It is a weak acid with pKa around 5, so it is negatively charged in aqueous solution at pH 7. To fabricate 3D living assemblies of yeast cells pre-coated with polyelectrolyte through templating w/o emulsions, we have used oleic acid as the surfactant to stabilise the water droplets. The hydrophilic head of oleic acid which is partially dissociated when in aqueous solutions will electrostatically attract the cationic polymer/modified yeast cells and produce stable water droplets in oil. These water droplets were transferred into water and produced 3D multicellular assemblies (cellosomes). The schematic diagram of the overall process has been outlined in Figure 6.3.

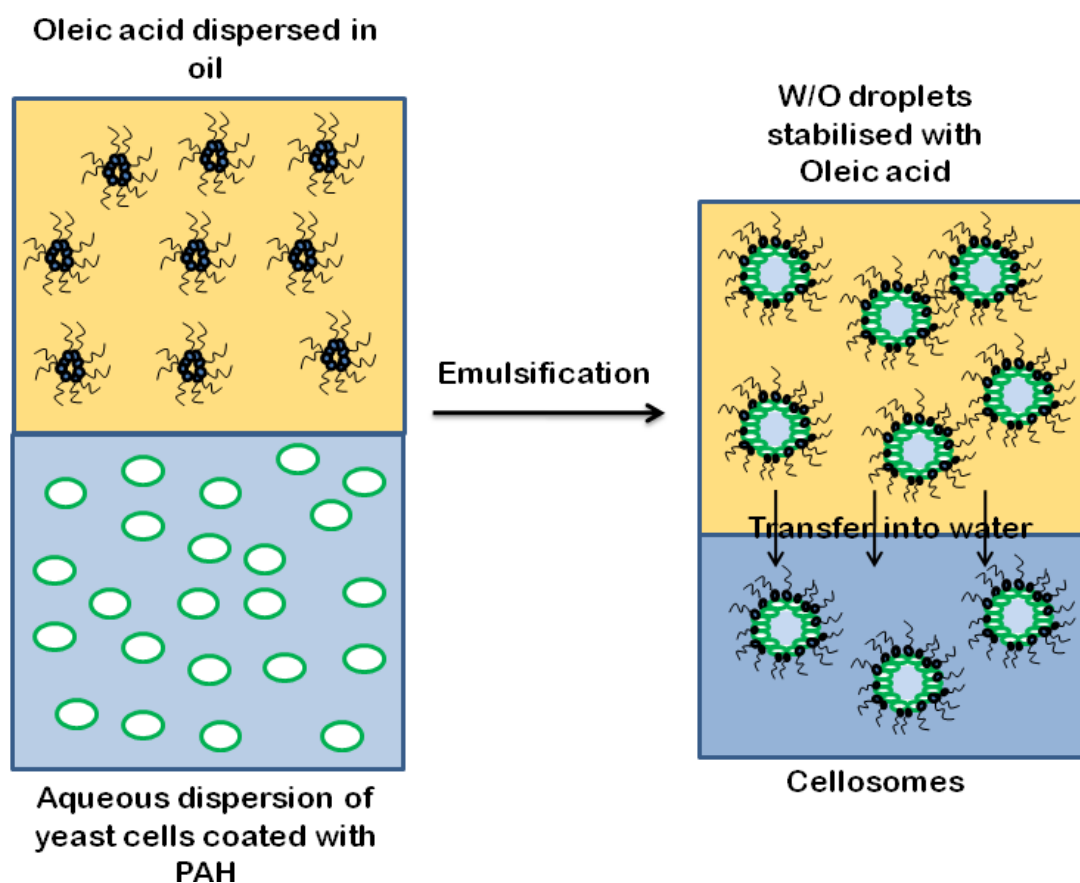


Figure 6.3: Schematic diagram shows the fabrication of cellosomes by templating w/o emulsions stabilised with oleic acid.



We optimised the concentration of the oleic acid to prepare the intermediate emulsions with highest stability, and desirable size droplets. Therefore, a series of emulsions prepared with different concentrations of oleic acid (1, 2,5,10 and 15) % vol. (see Figure 6.4). Meanwhile, the weight percentage of yeast cells to be encapsulated was assessed by preparing yet another series of emulsions containing different concentrations of pre-coated yeast cells. We found that using 15 % wt. oleic acid produced emulsions with relatively high stability and suitable average droplet size for a successful transfer into the water phase.

Figure 6.4 shows different emulsions prepared by using different concentrations of oleic acid and encapsulating different amount of yeast cells pre-coated with PAH. In all cases the pH of the water phase was fixed to neutral by using milli-Q water to disperse the pre-coated cells. Using (10 or 20) % wt. PAH coated yeast cells produced relatively stable emulsions with appropriate droplet sizes. Note that not all the yeast cells were encapsulated inside and in the interface of the water droplets; some cells were spreaded out in the oil phase in the form of cell clusters. (See Figure 6.5 for more details).

To increase the rigidity of the droplets and pack a higher amount of pre-coated yeast cells, the concentration of cells was increased to 30 % wt. which produced smaller droplets with diameters approximately around 50  $\mu\text{m}$ . As shown in Figure 6.6, highly stable emulsion has been produced and the exact position of the yeast cells was located by staining them with FDA through the oil phase and observing them by fluorescence optical microscopy, which showed that most of the yeast cells were situated at the interface, (see Figure 6.6d).

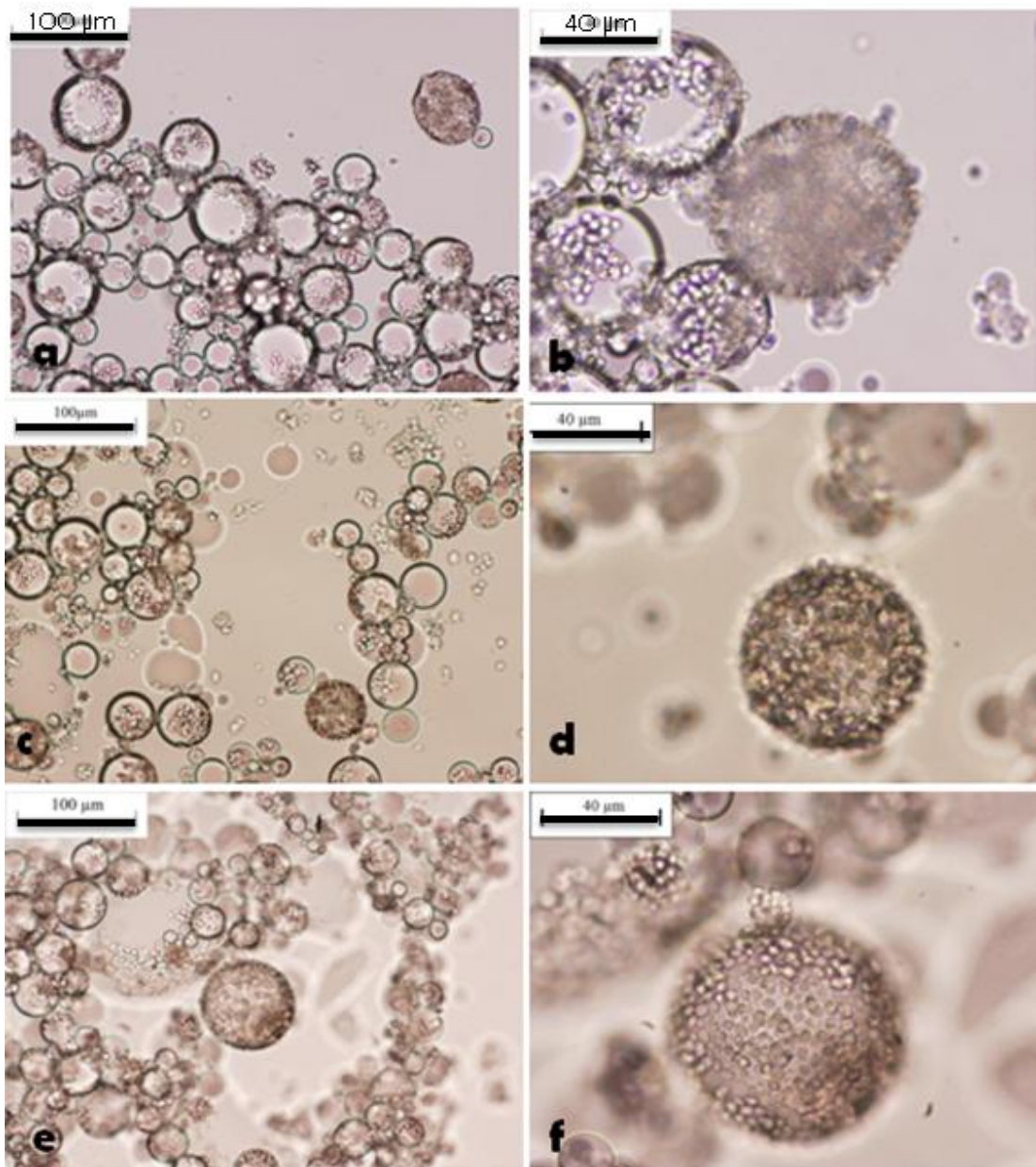


Figure 6.4: w/o emulsion droplets stabilised with oleic acid, the water phase contains PAH coated yeast cells; (a, b) contained 6 % wt. PAH coated yeast cells, where the emulsion was stabilised with 3 % vol. oleic acid, while, (c, d) contained 10 % wt. PAH coated yeast cells and 5 % vol. oleic acid was used to stabilise the emulsion, and (e, f) the water phase contained 10 % wt. PAH coated yeast cells and 10 % vol. oleic acid.

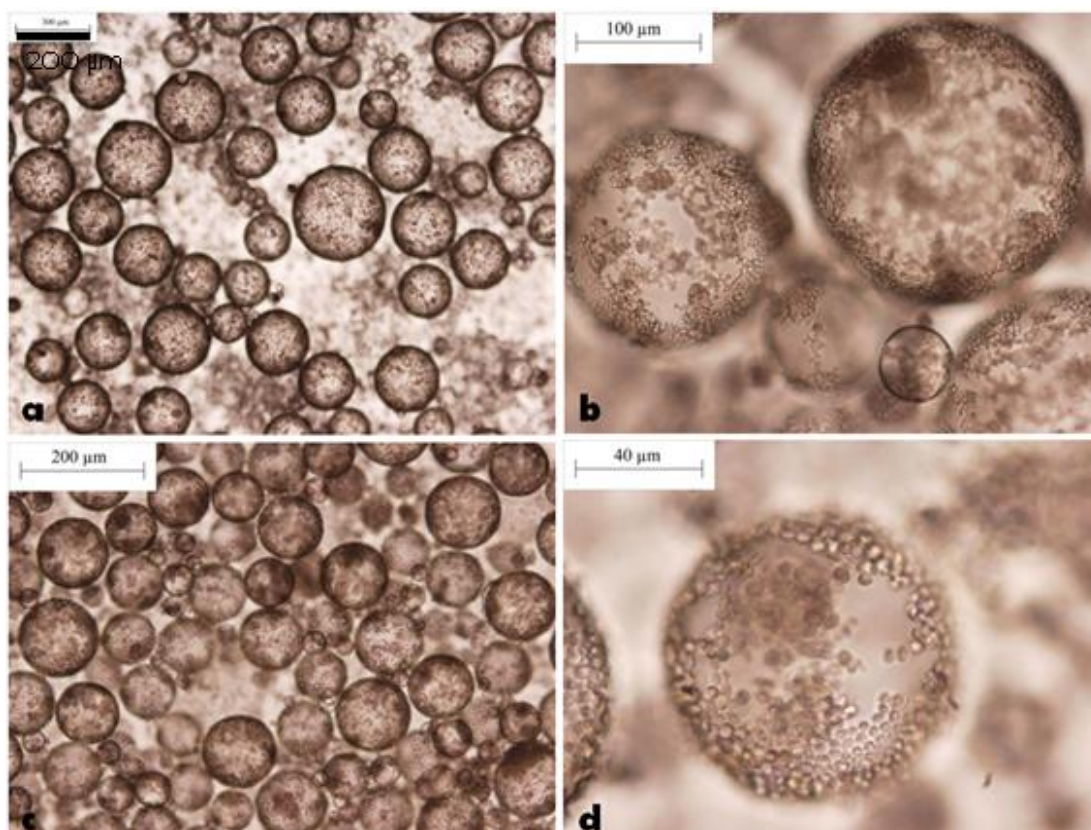


Figure 6.5: Emulsions (w/undecane) stabilised with 15 vol % oleic acid, (a, and b) the water phase contains 10 wt % yeast cells coated with PAH; water phase contains 20 wt % PAH coated yeast cells in (c and d).

#### 6.1.2.1.1 Transfer of the fabricated multicellular structure from oil into water

We have successfully transferred the fabricated cellosomes from oil into water by using two different approaches; one was an adopted so-called freezing process where fabricated cellosomes transferred from the oil phase into water, the other was replacing the oil phase (undecane) with dry octanol to shrink the water content of the droplets. By doing so, one can decrease the size of the droplets and closely pack the cells together and the result is fabrication of more stable cellosomes which can withstand the transfer from the oil phase into water phase. However, addition of dry octanol made the droplets lose their spherical shape into “potato-shaped” droplets as it can be seen in (Figure 6.7 a-b).

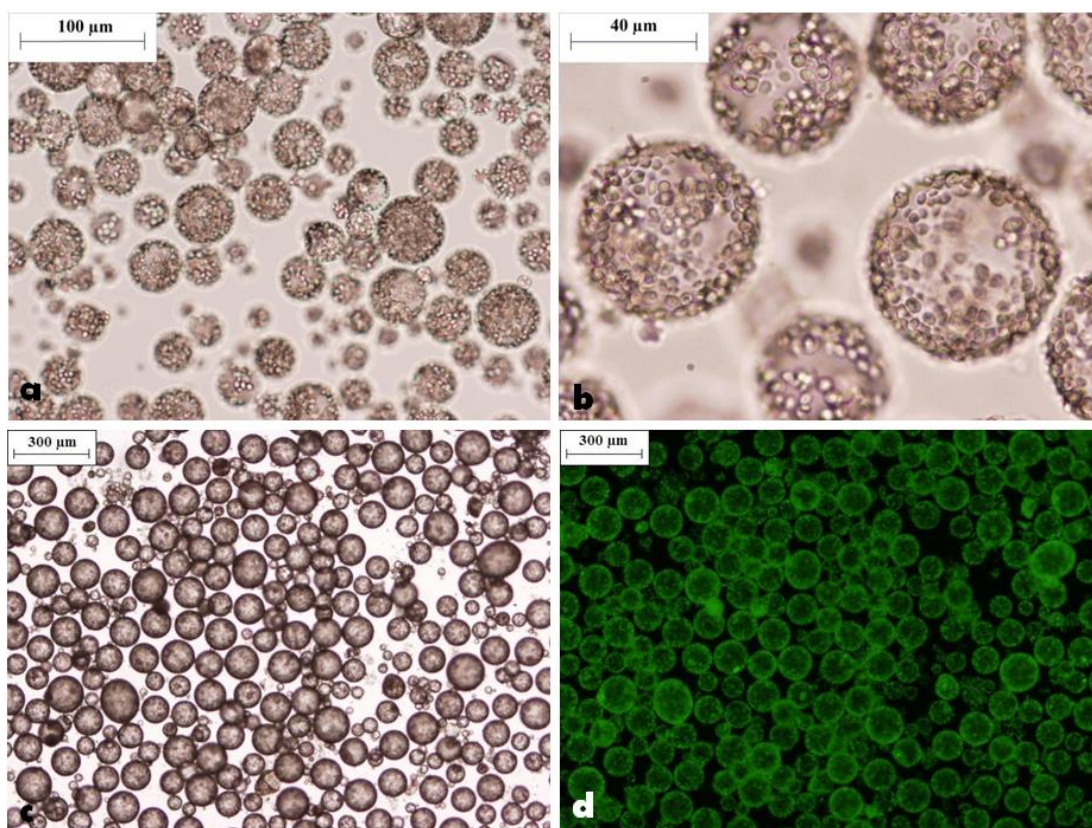


Figure 6.6: w/o emulsion stabilised with 15 % vol. oleic acid and the water phase contained 30 % wt. yeast cells pre-coated with PAH. (d) Shows the stained yeast cells with FDA observed by fluorescence optical microscopy to locate the position of the encapsulated cells.

The reason for this behaviour could be that the pre-coated yeast cells are relatively surface active and the energy of their attachment to the interface is affected by the type of the oil. We have therefore, used octanol saturated with water as the oil phase to fabricate the intermediate emulsions, rather than undecane, this way we could prevent the change of oil phase and hence the energy attachment of the polyelectrolyte coated cells at the interface can be fixed. Despite the fact that some of the droplets lost their spherical shape and some even completely destroyed, we prepared relatively stable emulsion droplets, which were subsequently shrunken upon addition of dry octanol, and transferred from the dry octanol into water to fabricate the final multicellular structures.

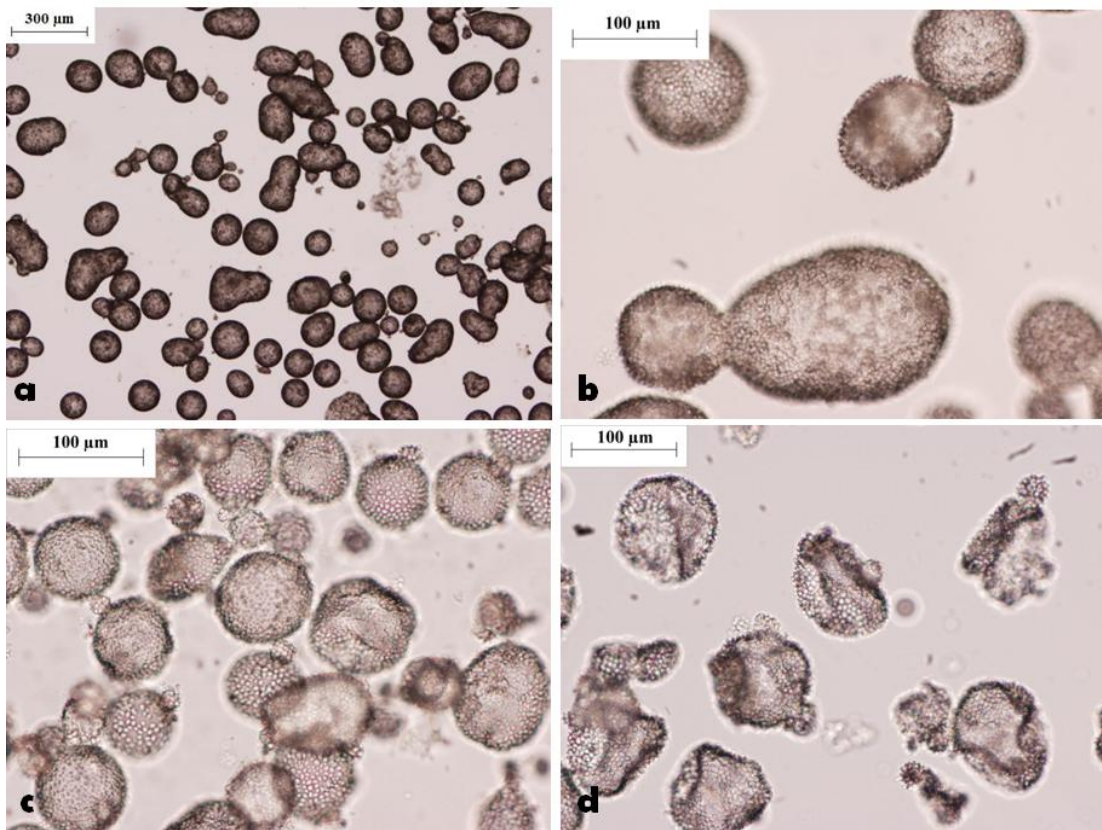


Figure 6.7: (a) w/o emulsions containing 30 % wt. PAH pre-coated yeast cells stabilised with 15 % vol. oleic acid in undecane, (b) after replacing undecane with dry octanol. (c) w/octanol saturated with water emulsion containing 30 % wt. PAH pre-coated yeast cells and 15 % vol. oleic acid before shrinking and (d) after shrinking the droplets in dry octanol.

We have fabricated and transferred 3D multicellular structures by templating w/o emulsions stabilised with oleic acid in undecane. The emulsion was frozen at  $-20\text{ }^{\circ}\text{C}$  after addition of 2 % wt. calcium carbonate microparticles to the oil phase which in return acted as spacers between the water droplets and prevented them from fusing together. The frozen emulsion was later added on top of 5 mL of milli-Q water in a sample tube and centrifuged. The presence of cellosomes in the water was observed and confirmed by optical microscopy (see Figure 6.8). The calcium carbonate microparticles were pre-treated with oleic acid to make them hydrophobic and dispersible in the oil phase.

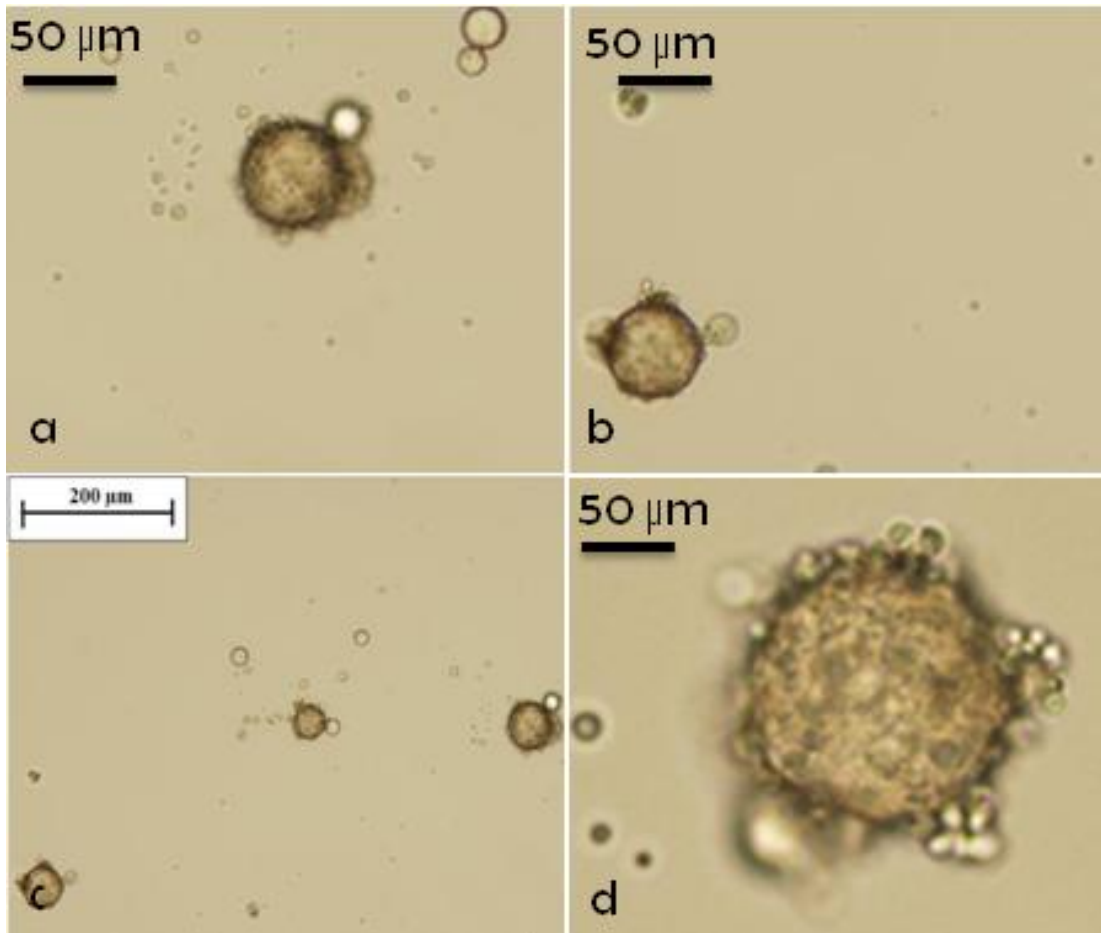


Figure 6.8: Cellosomes (multicellular structure) observed by optical microscopy containing 30 % wt. PAH pre-coated yeast cells fabricated by templating w/o emulsion stabilised with 15 % vol. oleic acid in undecane. The fabricated cellosomes transferred from undecane to water by freezing the emulsion followed by centrifugation.

### **6.1.2.2 Fabrication of cellosomes by templating w/o emulsions stabilised with Span60**

In this part of the chapter, we have demonstrated that multicellular assemblies of cells in cellosomes can be fabricated by templating w/o emulsions stabilised by non-ionic surfactant Span60 (sorbitan monostearate) which is an ester of sorbitan (a sorbitol derivative) and stearic acid. It is primarily used as a surfactant for stabilising water-in-oil emulsions. Sorbitan monostearate is used in the manufacture of food and healthcare products, and is a non-ionic surfactant with emulsifying, dispersion, and wetting properties. We have introduced span60 as an active emulsifier to prepare two emulsions in octanol saturated with water, one containing yeast cells pre-coated with cationic polyelectrolytes, the other containing concentrated solution of PSS. The two emulsions were mixed and re-emulsified together, which caused merging water droplets containing PAH/pre-coated cells with water droplets containing PSS.

First, we prepared a blank emulsion by emulsify water saturated with octanol into octanol saturated with water 1:9 ratios using 2 % vol. Span60 without adding any yeast cells. Figure 6.9a shows the stable emulsion droplets prepared which had spherical morphologies and droplet diameters ranging from a few micrometers to approximately 20  $\mu\text{m}$ . Furthermore, we have prepared two additional emulsions; one containing 10 % wt. yeast cells pre-coated with PAH (Figure 6.9c-d), and another one, containing only 5 % wt. PSS (Figure 6.9b), which produced very small water droplets contained concentrated solution of PSS. The latter was mixed and re-emulsified with the first emulsion which contained PAH coated yeast cells, and was used to “inject” PSS solution into the larger droplets (containing PAH pre-coated yeast cells). This electrostatically bound “cationic” yeast cells by the anionic PSS solution sustain the cell structure (see Figure 6.10). The water phase used in all cases was water saturated with octanol to prevent mass transfer of either octanol or water from one phase to another.

The water droplets which contained electrostatically bound yeast cells were prepared to be transferred from the octanol into water to produce the final 3D cellosomes structures by shrinking them up on addition of dry octanol which solubilised the water content of the droplets and closely packed the yeast cells in the cores. Although the shape of the droplets have not changed to indicate the shrinking, the size of the droplets visually decreased and the cells seemed to be closely packed together after the emulsion was diluted with dry octanol and leaving it for 2 hours (Figure 6.11).

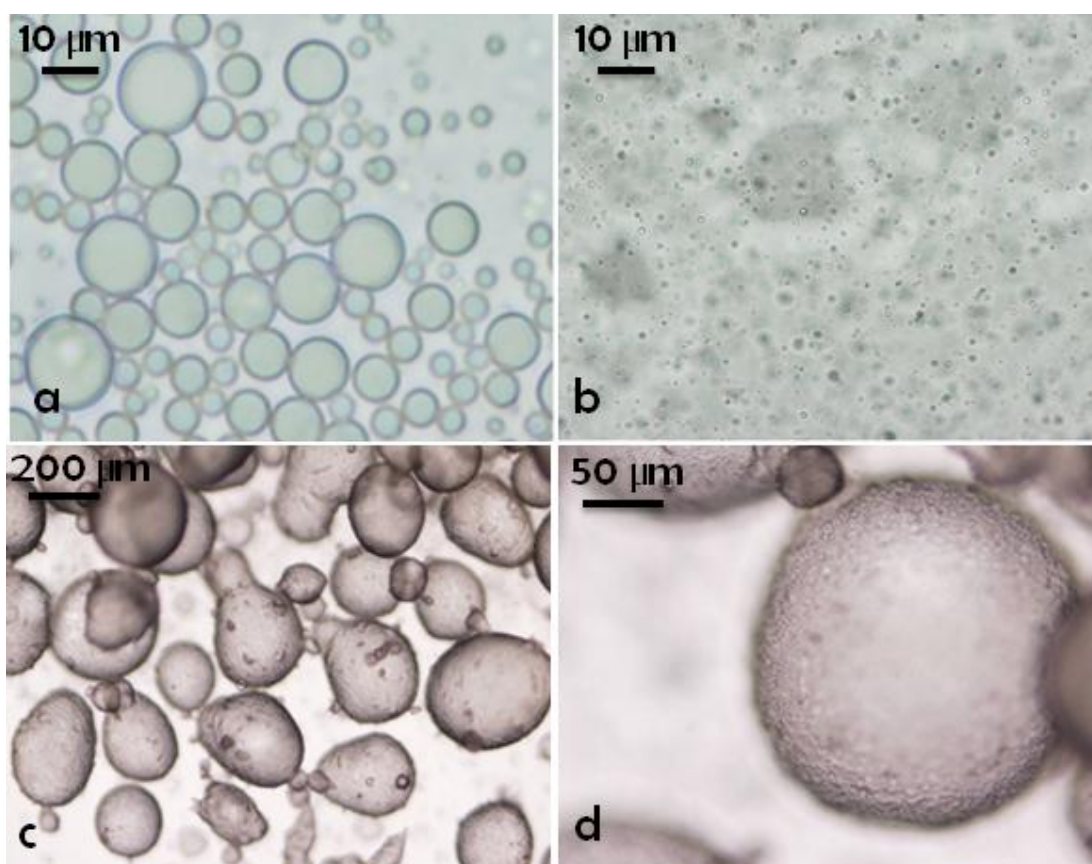


Figure 6.9: Water in octanol emulsion stabilised with 2 % vol. Span60, octanol phase was equilibrated with the water phase. (a) Without yeast cells. (b) The water phase contained 5 % wt. PSS solution. (c, and d) The water phase contained 10 % wt. yeast cells pre-coated with PAH.



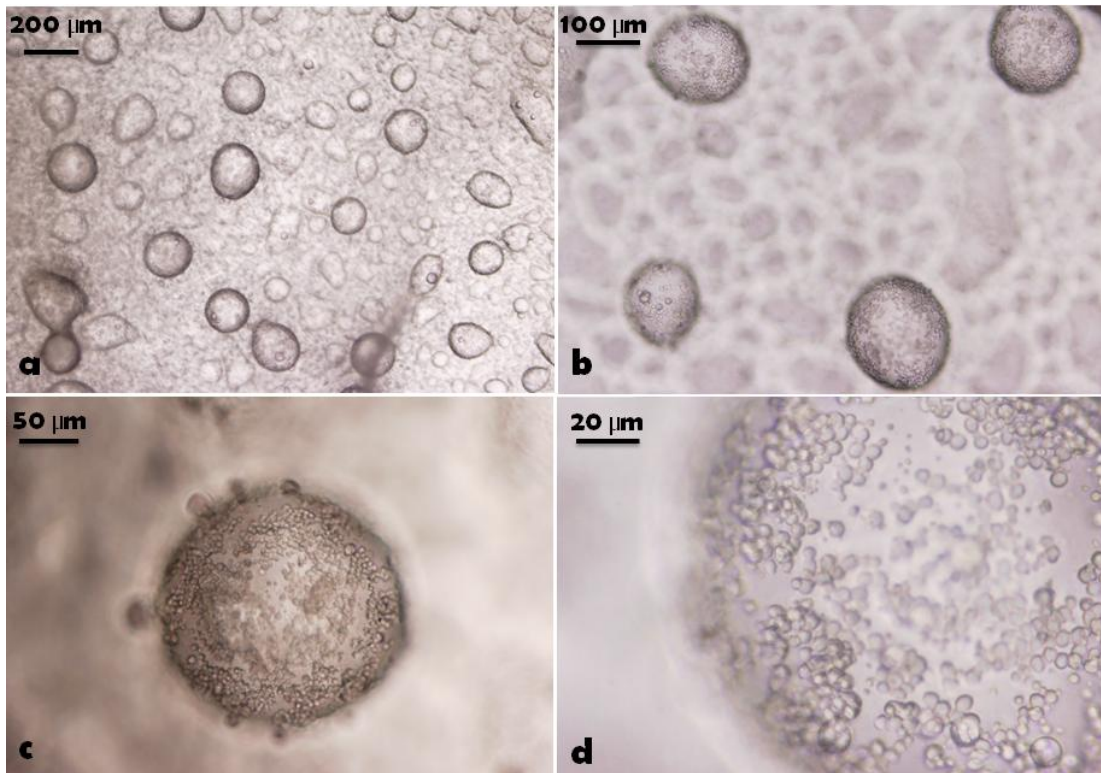


Figure 6.10 : Recombined emulsion prepared from mixing and re-emulsifying the two w/o emulsions, one contained PAH pre-coated yeast cells and the other concentrated PSS solution.

#### 6.1.2.2.1 Transfer of the shrunken water droplets containing bridged yeast cells to the water phase

We have tried different approaches to transfer the fabricated cellosomes from the oil to the water phase. For example, adding a fixed amount of concentrated emulsion with shrunken water droplets following the treatment with dry octanol on top of water layer which contained PSS followed by centrifugation. However, by this method we were not able to successfully transfer the cellosomes into the water phase. We also tried another approach by dissolving the oil phase (octanol) in ethanol after the excess octanol was removed but this strategy was also proved to be unsuccessful as all the droplets were disintegrated and the cells were spread out in the ethanol. We have successfully transferred the shrunken emulsion droplets into water and produce the cellosomes by adding calcium carbonate microparticles into the shrunken w/o emulsion and then filtering it off and redispersing the shrunken droplets back in water which contained 1 % vol. acetic acid to dissolve the calcium carbonate microparticles.

The process proved to be successful since a high yield of transferred cellosomes were observed in the water phase. Calcium carbonate microparticles separated the shrunken water droplets from each other and prevented them from fusing together in the process of filtration and transfer, (see Figure 6.12).

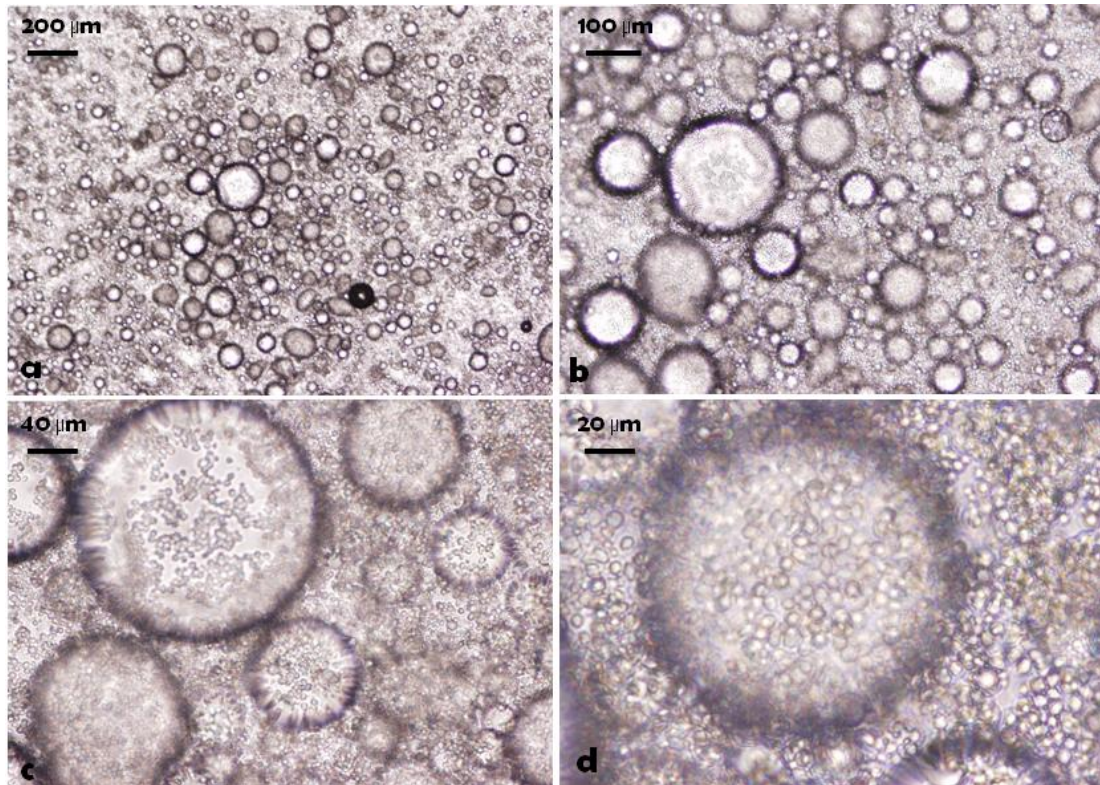


Figure 6.11 : Water droplets containing PAH treated yeast cells electrostatically linked together by using PSS. The droplets were shrunken upon addition of 5 mL dry octanol and left for 2 hours.

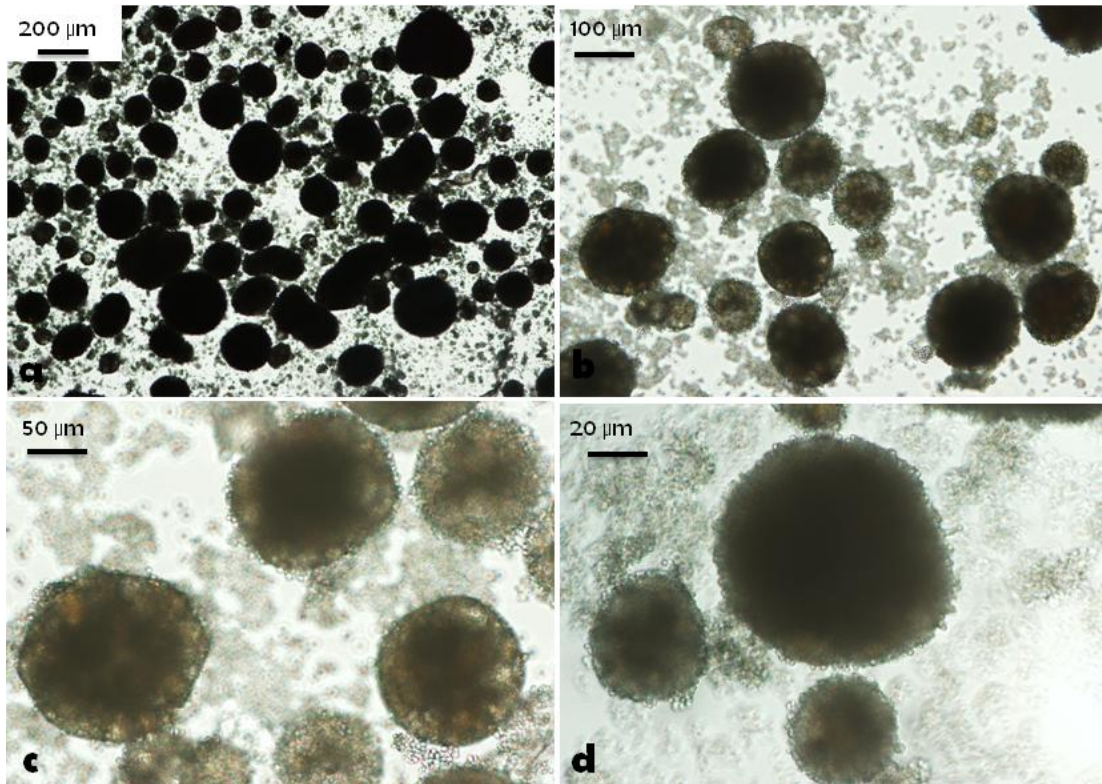


Figure 6.12 : Cellosomes transferred in water by using a freezing process. These cellosomes were assembled by using electrostatically bridged yeast cells coated with PAH and linked together through PSS.

### 6.1.2.3 Fabrication of cellosomes by adopting colloidosomes fabrication technique

In a conventional method, colloidosomes can be prepared from templating Pickering emulsions.<sup>11</sup> We have employed similar strategy in this part of the chapter to fabricate three dimensional living multicellular structures of yeast cells. We have prepared two Pickering emulsions, (i) one contained cationic yeast cells pre-coated with PAH, and (ii) another emulsion containing water droplets with anionic cells pre-coated with PAH/PSS. Both emulsions were stabilised by 300 nm polystyrene latex nanoparticles with amidine groups on their surfaces. The polystyrene latex particles were transferred to the oil phase before emulsification by using ethanol dispersion.

The emulsions were mixed and re-emulsified together to yield another Pickering emulsions which contained both cationic and anionic pre-coated yeast cells fused together by electrostatic interactions, as illustrated in Figure 6.13. The process has increased the stability of the droplets and hence facilitated their transfer from the oil phase into water phase to produce cellosomes. We have used different concentrations of yeast cells pre-coated with only PAH and PAH/PSS to optimise the conditions for preparation of highly stable emulsion. First 10 % wt. PAH or PAH/PSS pre-coated yeast cells were dispersed in the water phase.

Figure 6.14 shows w/o emulsions of water droplets in undecane stabilised with 300 nm amidine latex nanoparticles, where the water droplets contained 10 % wt. of both PAH and PAH/PSS pre-coated yeast cells, and the volume fraction of water phase was 10 % vol. The droplets were relatively stable and had diameters in the range of 150-200  $\mu\text{m}$ . The pre-coated cells were mainly residing inside the water core. However, when we dispersed 20 % wt. pre-coated yeast cells in the water phase, less stable emulsion was produced and most of the cells were aggregated and transferred from the water drops to the oil phase ( see Figure 6.15).

Transferring the multicellular structures (Cellosomes) from the emulsion into water was done by first shrinking the water content of the droplets which was achieved by removing the excess oil and adding 5 mL dry octanol. As it can be seen in Figure 6.17 the addition of dry octanol into the emulsion was successfully shrunken the water droplets and closely packed the yeast cells together. This structures the droplets with extra stability to withstand their transfer from the emulsion into the water phase.

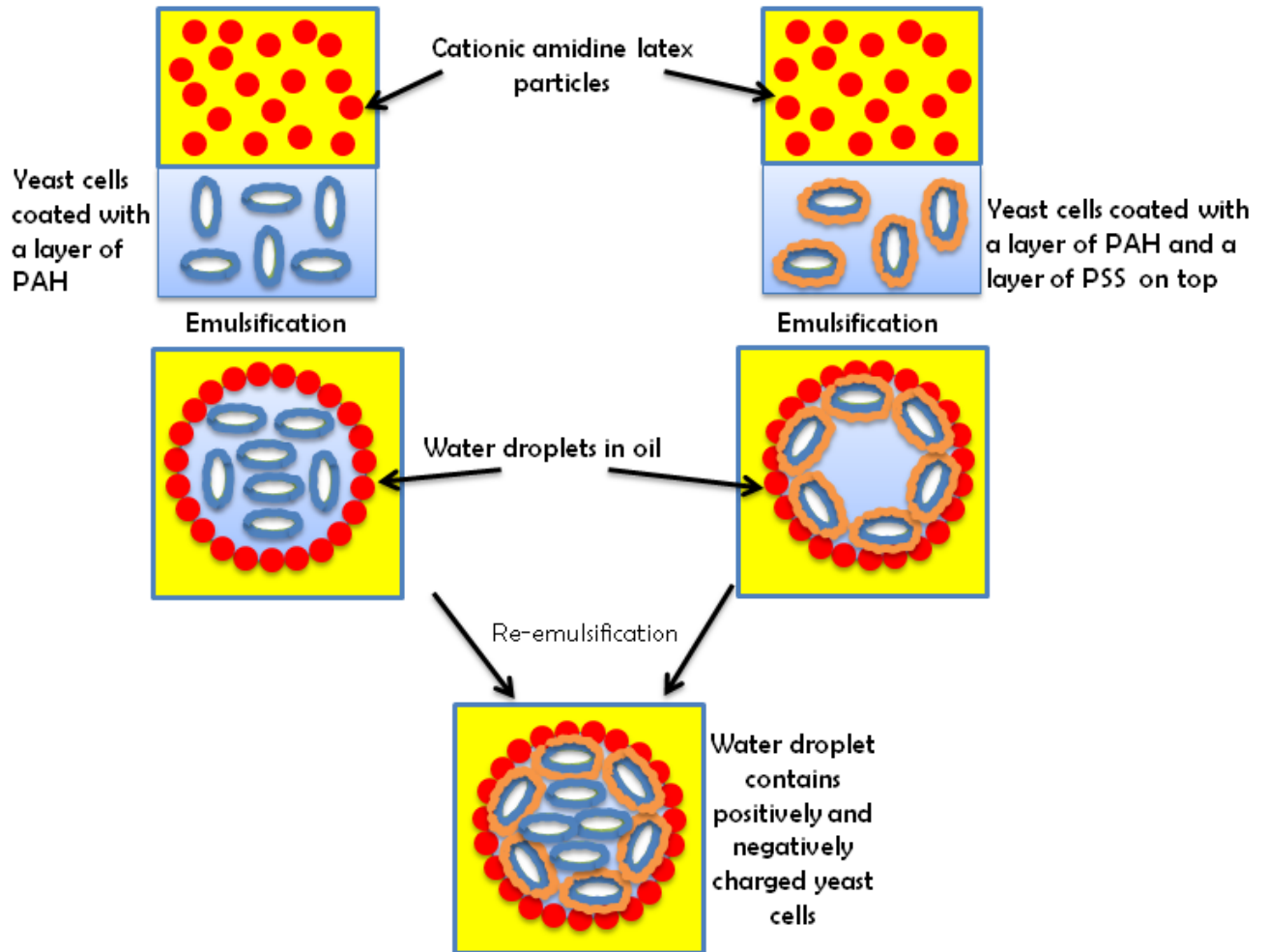


Figure 6.13: Schematic diagram of fabrication of cellosomes loaded with both cationic and anionic pre-coated yeast cells by using Pickering emulsions templating technique.

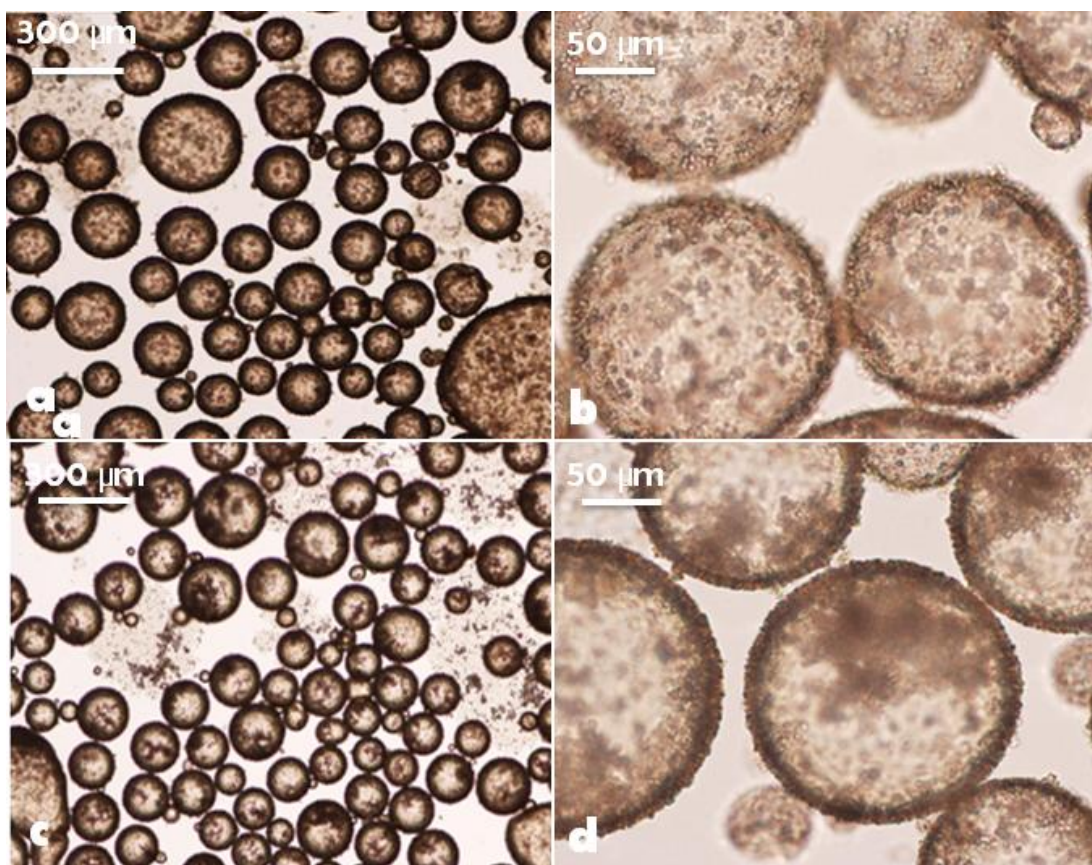


Figure 6.14: Water-in-undecane emulsions stabilised with 300 nm amidine latex particles, the water phases were aqueous suspension of 10 % wt. PAH pre-coated yeast cells in (a and b), and 10 % wt. PAH+PSS pre-coated yeast cells in (c and d). The volume fraction of the water phase was 10 % vol.

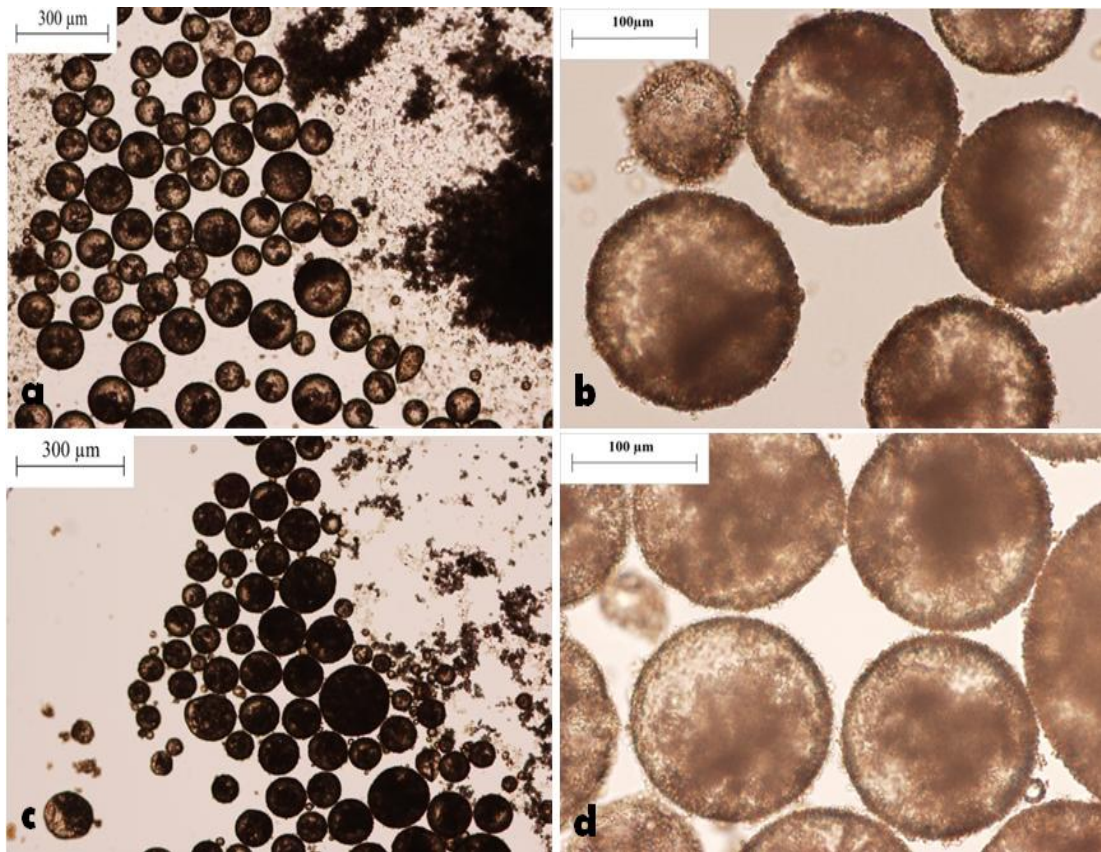


Figure 6.15: Water-in-undecane emulsions stabilised with 300 nm amidine latex particles, the water phases contained aqueous suspension of 20 % wt. PAH pre-coated yeast cells in (a and b), and 20 % wt. PAH+PSS pre-coated yeast cells in (c and d). the volume fraction of water phase was 10 % vol.

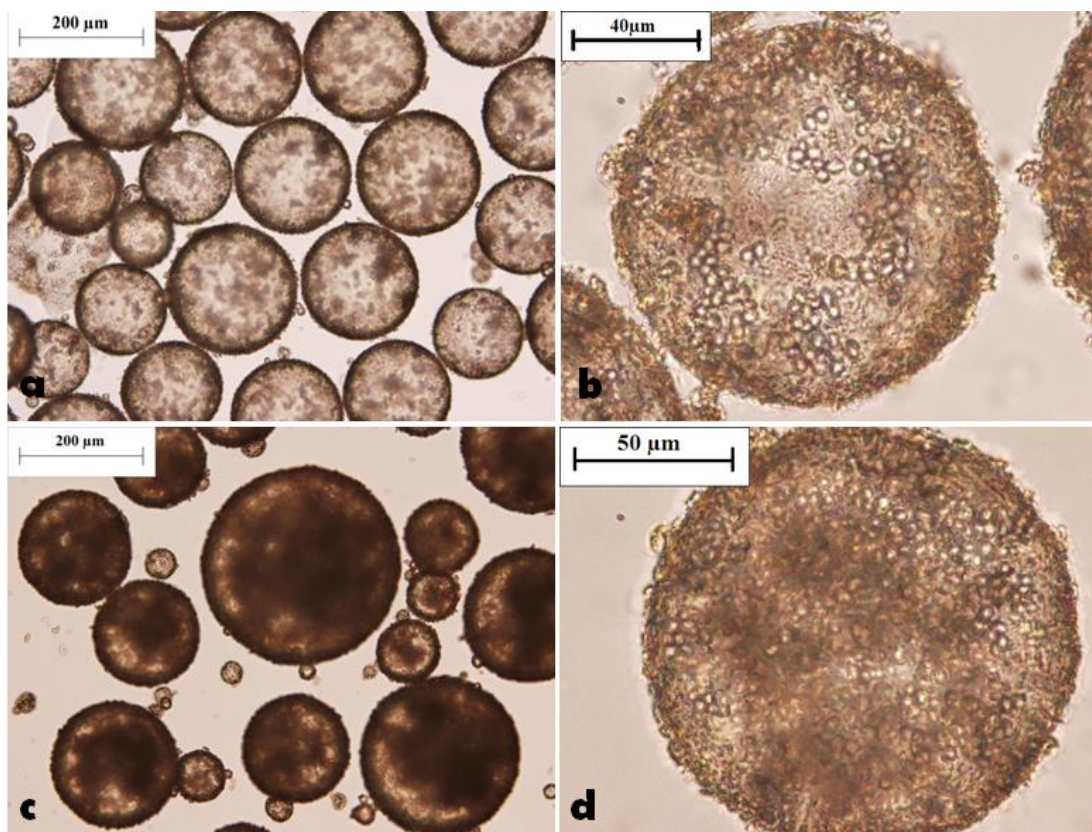


Figure 6.16: The two water-in-undecane emulsions containing PAH pre-coated cells and PAH+PSS pre-coated cells after being mixed and re-emulsified to yield a new Pickering emulsion which contained both cationic and anionic pre-coated yeast cells fused together by electrostatic interactions. The weight percentage of yeast cells initially used was 10 % wt. in micrographs (a, and b), while, in micrographs (c, and d) 20 % wt. yeast cells were dispersed in water initially. The volume fraction of water phase was 10 % vol.



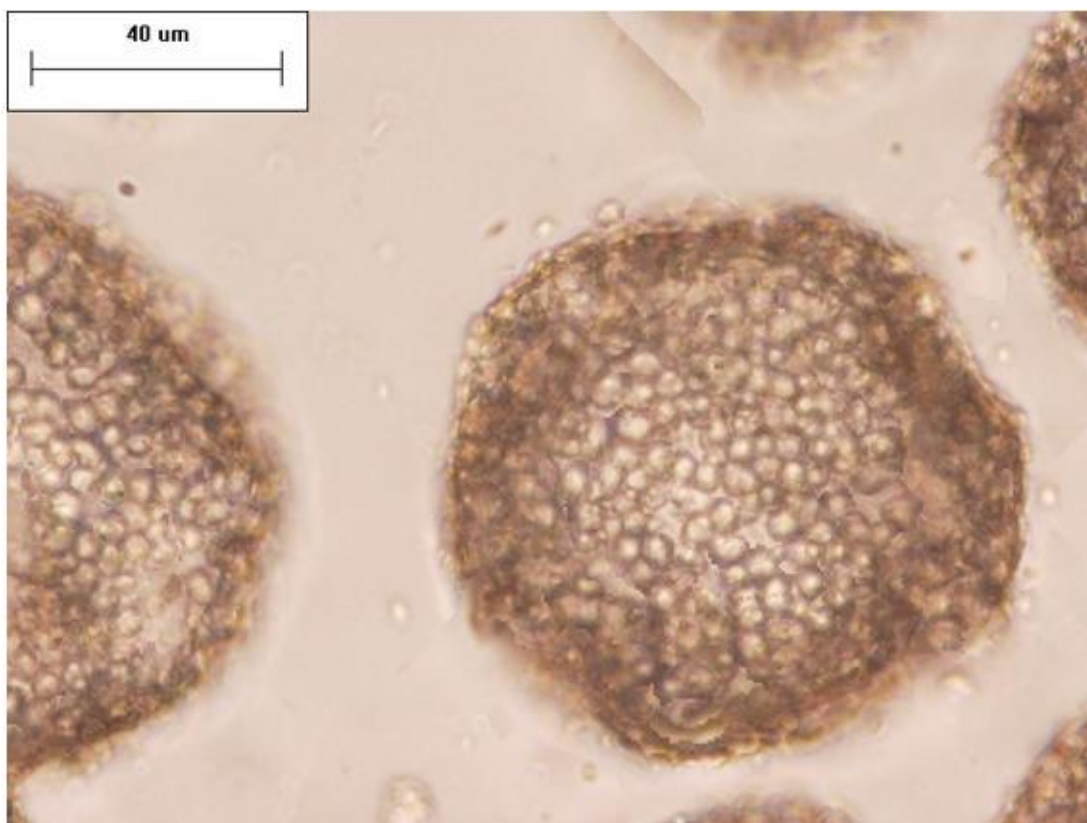


Figure 6.17: Water droplet in octanol contains both cationic and anionic pre-coated yeast cells, after being shrunk upon addition of dry octanol which partially solubilise the water inside the droplets.

#### 6.1.2.4 Cellosomes based on water-in-octanol Pickering emulsions

We have used octanol as the oil phase in preparation of the intermediate Pickering emulsions and followed the procedure exactly as in the case of undecane. We have noticed that water droplets containing yeast cells pre-coated with PAH/PSS layers were relatively spherical with average diameters of approximately 200  $\mu\text{m}$ , whereas, water droplets contained PAH pre-coated cells are much smaller with average diameters of approximately 100  $\mu\text{m}$  with many non-spherical morphologies shown in Figure 6.18. The prepared Pickering emulsions containing the aqueous suspension of the oppositely charged yeast cells emulsified in octanol were mixed together and re-emulsified, and the process resulted in the formation of water droplets of irregular or ellipsoidal shape.

Generally, the emulsion prepared by using octanol is less stable than the emulsion prepared by using undecane (see Figure 6.19) as there is some partial coalescence between the water drops. Therefore, we concluded that the type of the oil has an important effect on the stability of the emulsions.

For solid particles as stabilisers, the interactions between the solid surface and the two liquid phases, determines the three-phase contact angle  $\theta_{ow}$ . The energy of attachment of particles wetted at the interface depends on both  $\theta_{ow}$  and the o/w interfacial tension  $\gamma_{ow}$ . These two parameters are related by the Young equation:

$$\gamma_{so} - \gamma_{sw} = \gamma_{ow} \cos \theta_{ow} \quad (6.1)$$

Where the indexes, (s: solid particle, o: oil phase, w: water phase).  $\gamma_{sw}$  and  $\gamma_{so}$  are the solid-water and solid-oil surface energies.

As the type of the oil changes both  $\gamma_{ow}$  and  $\theta_{ow}$  will change; the surface tension of undecane and octanol in respect of water are 52 and 8.2 mN/m respectively.<sup>101</sup> When octanol was used instead of undecane the interfacial tension is dramatically reduced and the energy of attachment changes. It seems that the attachment of the solid particles is weaker in case of octanol and this is why the particle monolayer on the emulsion drops is incomplete and coalescence increased.

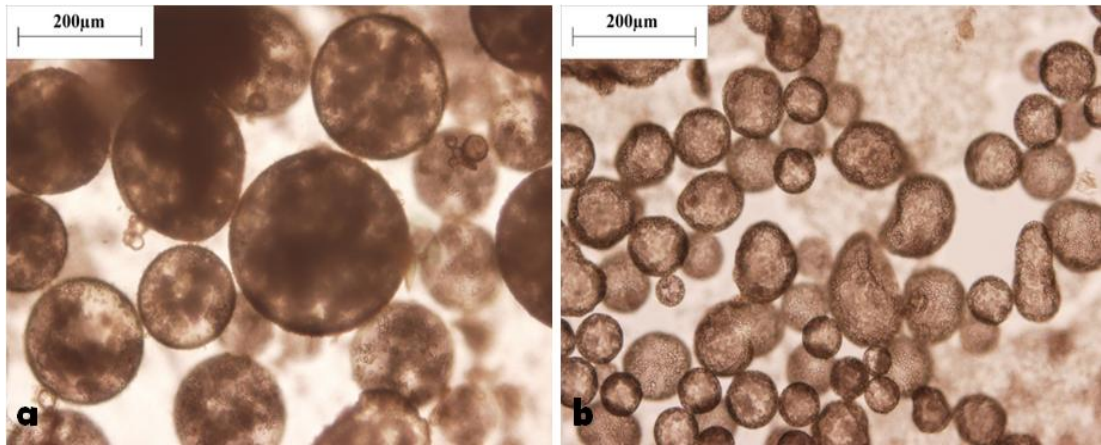


Figure 6.18: Water droplets in octanol prepared from aqueous suspension of 10 % wt. (a) PAH/PSS pre-coated yeast cells and (b) PAH pre-coated yeast cells stabilised with 300 nm amidine latex particles in pre-equilibrated octanol.

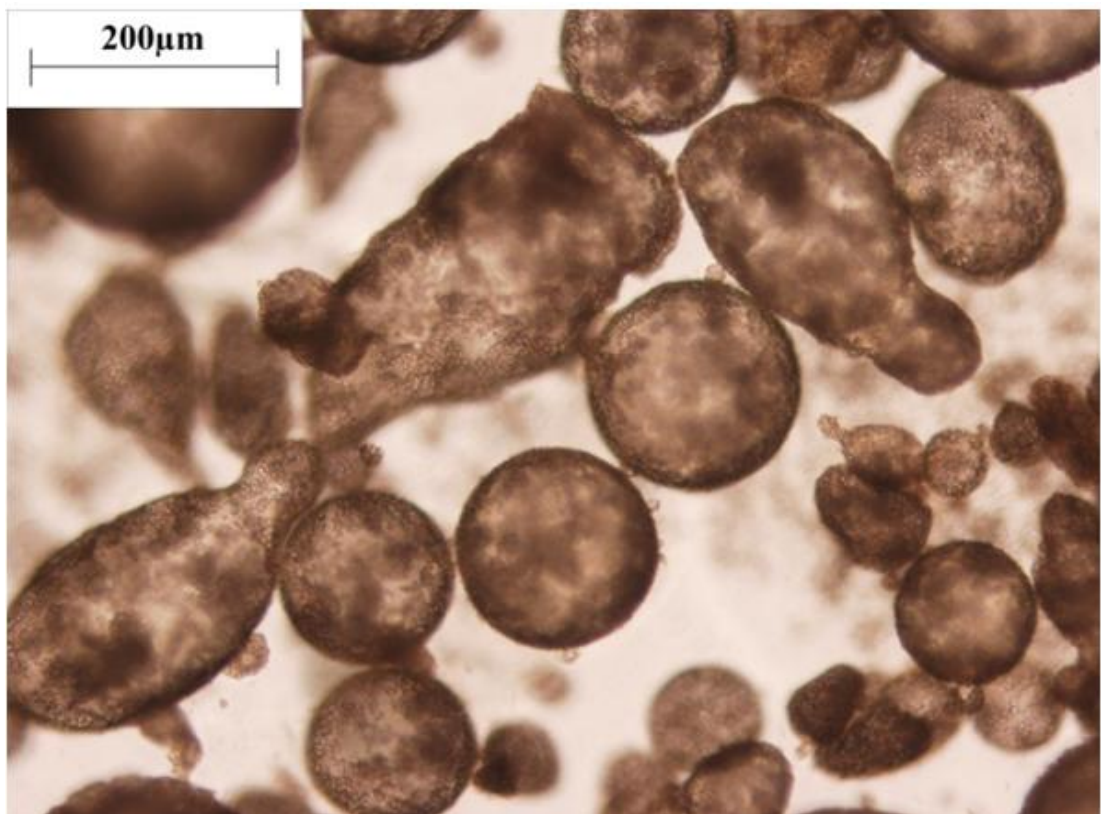


Figure 6.19: Water droplets in octanol after mixing and re-emulsifying two Pickering emulsions containing oppositely charged pre-coated yeast cells stabilised by 300 nm amidine latex particles. The volume fraction of the water phase was 10 % vol. the two Pickering emulsions were mixed in 50:50 ratios.

### 6.1.3 Conclusions

Novel classes of bio-colloidal multicellular structures of living yeast cells have been fabricated by using w/o emulsion templating technique where the water droplets contained the yeast cells and were stabilised by either surfactant or solid particles. In first part we have pre-coated yeast cells with cationic polyelectrolyte and used oleic acid to stabilise w/o emulsions in which the water phase contained polyelectrolyte pre-coated yeast cells. The cells were assembled in cellosomes by shrinking the water droplets using dry octanol; the polyelectrolyte pre-coated yeast cells containing water droplets were frozen followed by centrifugation of the frozen emulsion on top of milli-Q water to transfer the cellosomes from the oil phase into water phase.

We have also fabricated similar cellosomes structures by templating water-in-octanol emulsion, in which both phases were pre-equilibrated with each other and the water phase contains cationic yeast cells pre-coated with PAH and cross linked with the anionic polyelectrolyte PSS. The process was done by preparing two w/o emulsions; one contained PAH pre-coated yeast cells and the other contained concentrated aqueous solution of PSS, the two emulsions were stabilised with Span60 and were mixed and re-emulsified together at the later stage to produce spherical water droplets in octanol which contains PAH coated yeast cells fused together by the anionic PSS. The water droplets were successfully transferred into water to produce the multicellular cellosomes structures by adding calcium carbonate microparticle spacers into the shrunken droplets followed by filtration. The produced cellosomes could find important applications as drug carriers or biological micro-reactors and can be used to preserve the viability of probiotic cells.

## Chapter 7.

### Kinetics of triggered release of cells from composite polymer-cell microcapsules

#### 7.1.1 Introduction

Preservation of cells viability in adverse conditions has many applications, including protection of probiotics<sup>1</sup> and live vaccines. Probiotic bacteria are considered essential for the normal intestinal microflora, enhancement of the immune system and improving the nutritional value of foods.<sup>7,42-43</sup> The beneficial effects of probiotics are dependent on their viability as they go through the gastrointestinal tract at pH as low as 1.5 which has an adverse impact on the probiotics survival.<sup>1</sup> Different strategies for microencapsulation of probiotics have been employed to preserve their viability and deliver sufficient amount of viable probiotics to the lower intestine.<sup>4</sup> The later involve packaging of cells inside microcapsules, gel beads or other media formulated from synthetic materials and biopolymers.<sup>5</sup> Shellac<sup>70</sup> has long been used as coating material in pharmaceutical formulations and food supplement products as it is insoluble in water below pH 7.<sup>7,8</sup>

Campbell *et al.*<sup>9,10</sup> developed a method for fabrication of food-grade shellac micro-rods with yeast cell inclusions which not only encapsulate the cells but also proved to be efficient foaming agents. Stummer *et al.*<sup>11</sup> coated bacteria with shellac formulations and glycerol as plasticiser and studied the cells viability in the low pH of model gastrointestinal fluid. Hamad *et al.*<sup>20</sup> recently reported successful encapsulation of yeast cells into sporopollenin microcapsules from *Lycopodium clavatum*.

Very recently, Hamad *et al.*<sup>12</sup> developed composite shellac-cells microcapsules by using two techniques: (i) Spray co-precipitating dispersion of native cells in ammonium shellac solution /in aqueous solutions of acetic acid or calcium chloride or (ii) spray drying of similar formulation. They demonstrated that those microcapsules can preserve the cells viability through highly acidic conditions (pH 1.5) similar to those in the stomach and to release them by disintegrating at pH around 7 as in the

lower intestine. In this “proof of concept” study,<sup>13</sup> two different triggering mechanisms were programmed for the cell release from these composite polymer-cell microcapsules. The first mechanism involves doping of the shellac matrix of the microcapsules with pH sensitive polyelectrolytes which has the ability to swell upon pH increase. Sodium polyacrylate and carboxymethyl cellulose were used as effective swelling agents which allowed the hydrophobic shellac microcapsules to remain intact and to protect the encapsulated cells at low pH but facilitated the microcapsules rapid swelling and cell release at pH above 7.

The second mechanism, as reported by Hamad *et al.*<sup>13</sup> involves growth-triggered release of cells where the cells on the microcapsule surface exposed to culture media grow and are gradually released from the shellac matrix. The later also leads to complete disintegration of the microcapsules as the release of the surface layer of cells gives access of more encapsulated cells to the culture medium and further promotes their release. This approach is very versatile and could potentially find applications in a range of industrial pharmaceutical and medicinal food formulations for protection and triggered release of other cells, including probiotics, live vaccines, stem cells and cell implants.

In the present study we develop a theoretical model of the kinetics of cells release from composite polymer-cells microcapsules and study the effect of the triggered release mechanisms on the evolution of the cells population in the aqueous media surrounding the microcapsules. We take into account (A) the pH triggered release of cells, (B) the growth of the cells and (C) the simultaneous action of release of cells and their growth in the medium. We also consider the effect of cell death on the evolution of the cells population as they may exhaust the culture medium or produce toxic metabolites. The pH triggered release of cells is schematically represented by Figure 7.1A. There is a distinct difference in the case when aqueous solution is a culture medium in which the cells can grow and multiply. In the case of individual cells (Figure 7.1B) this would result in an exponential growth in the early stage of the cell culture while the culture medium is still not exhausted by the increasing number of cells which growth is still not affected by release of potentially toxic metabolites.

The situation of growth triggered cell release or pH triggered cell release in the presence of culture medium would lead to increasing cell numbers in the aqueous solution as a result of two simultaneously occurring processes:

(i) Release of cells from the surface of the microcapsules and (ii) growth and multiplication of the released cells in the culture medium. This process is schematically represented in Figure 7.1C. In all cases our model assumes that the composite microcapsules are not porous and dissolve continuously in a layer-by-layer manner. More complex mechanisms of cell release are possible in porous microcapsules or ones containing polymers capable of very fast swelling which we have not considered in this analysis.

This chapter is organised as follows. In the theoretical background section we consider a kinetic model of the cells release due to pH and growth trigger from microcapsules and we discuss the analogy with the case of individual cells growth. We derive approximate analytical equations for the release rate constants and the capsules dissolution time as well as the cell concentration profiles in the aqueous medium. Short time kinetics experiments with yeast cell release from shellac-cells microcapsules were designed and experimental data were collected and analysed for the different trigger mechanisms.

#### **7.1.1.1 Theoretical Background**

Let us consider a suspension of composite microcapsules of average initial diameter  $D_0$  containing encapsulated cells of an average diameter  $\delta$  and volume fraction  $\phi$  in the microcapsules. The shellac can be doped with other materials which would provide a trigger for release of the cells upon change in the pH or other external factor. The release of the cells in this case is facilitated by the gradual swelling of the shellac matrix on the surface of the composite microcapsules as its solubility increases at higher pH. In this case the microcapsules will gradually dissolve and release all encapsulated cells into the aqueous media.

**(a) pH triggered release of cells from microcapsules without further growth.** We will consider the process of cell release from the microcapsules without further growth. For an aqueous suspension of volume  $V$  and number of composite

microcapsules  $n_m$  the total number of encapsulated cells will be denoted with  $N_0$ . The number of cells  $N_R(t)$  released into the aqueous media due to the microcapsules disintegration will increase from zero at  $t = 0$  to  $N_0$  at full disintegration.

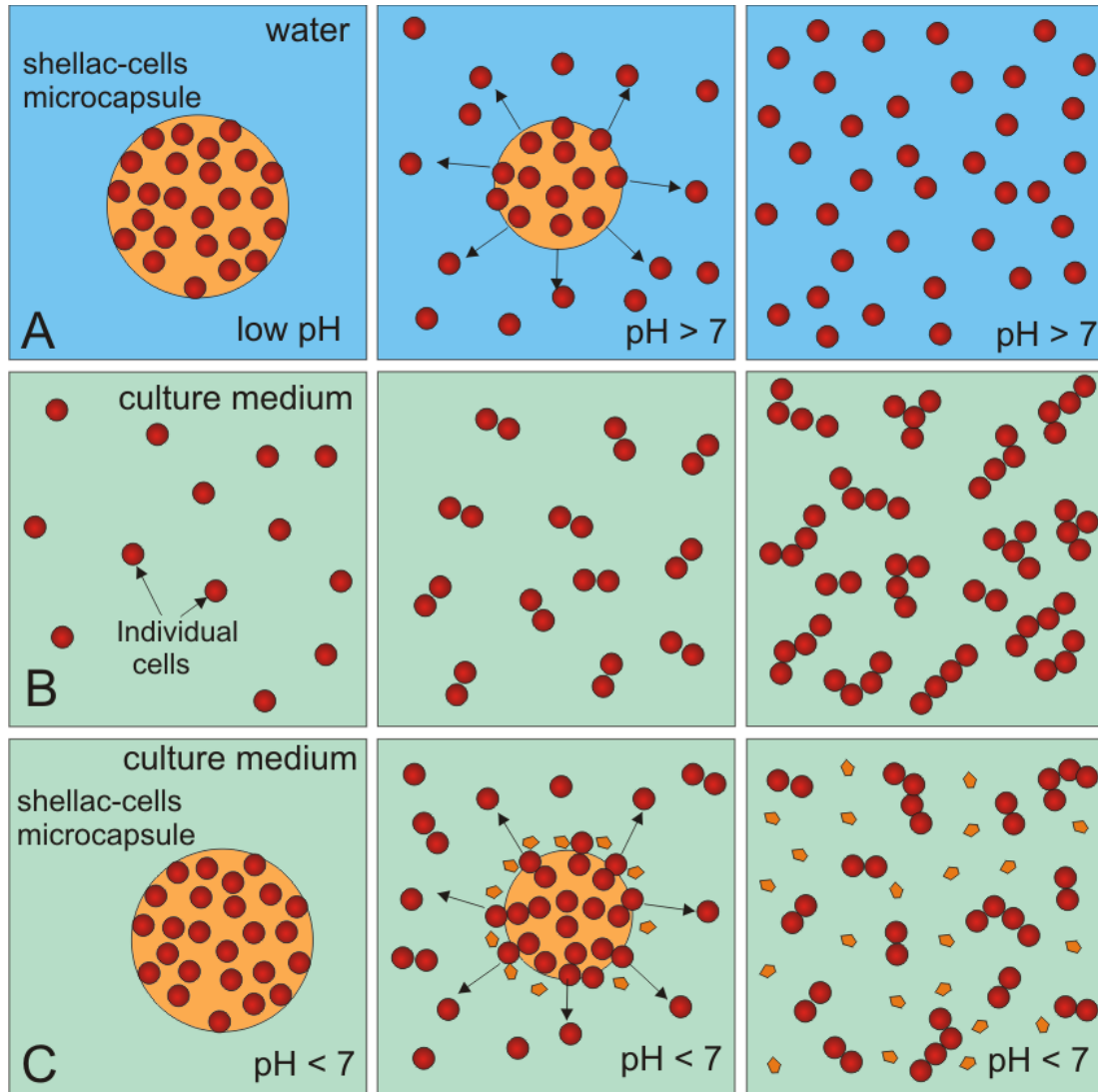


Figure 7.1: Schematic diagram of stimulus triggered release of cells from composite shellac-cells microcapsules. (A) pH triggered release of cells in aqueous solution without cell growth. (B) Cell growth in a culture medium. (C) Growth triggered release of cells from the microcapsules in a culture medium. Note that although (C) illustrates only the effect of the cell growth on the microcapsules surface on the release rate of cells, a combination of (A) pH triggered release and (C) growth triggered release is also possible with bigger release rate constant.



We model the kinetics of this process assuming that the rate of cells release in the aqueous media around the microcapsules,

$$\frac{dN_R}{dt} = k_R N_s \quad (7.1)$$

is proportional to the number of cells  $N_s$  on the microcapsules surface,

$$N_s = n_m \phi v_s / v_c \quad (7.2)$$

$k_R$  is the release constant of the viable cells from the composite microcapsules.

Here  $N_s$  can be estimated from the average volume of the cells  $\phi v_s$  in the surface layer of thickness  $\delta$  and the volume of a single cell  $v_c = \pi \delta^3 / 6$ . The thickness of the surface layer is selected to be approximately equal to the average cell diameter  $\delta$ . On the other hand, the balance of the number of encapsulated cells  $n_m \phi v_m / v_c$  and released cells,  $N_R$  in the system gives

$$n_m \frac{\phi v_m}{v_c} + N_R = N_0 \quad (7.3)$$

Recalling that the volume of a single microcapsule is  $v_m = \pi D^3 / 6$  and the total number of encapsulated cells in the beginning of the process is  $N_0 = n_m \phi (D_0 / \delta)^3$ , and by introducing the following variables

$$\varepsilon = \frac{\delta}{D_0}, \quad y(t) = \frac{D(t)}{D_0}, \quad \tau = k_R t \quad (7.4)$$

Equation (7.3) can be transformed to read

$$N_R(t) = N_0 [1 - y(t)^3] \quad (7.5)$$

Taking into account that the volume of the microcapsule surface layer is

$$v_s = \pi D^3 / 6 - \pi(D - \delta)^3 / 6, \quad (7.6)$$

eq (7.1) and eq (7.2) can be combined to yield

$$\frac{dN_R}{dt} = k_R N_0 \left[ y^3 - (y - \varepsilon)^3 \right] \quad (7.7)$$

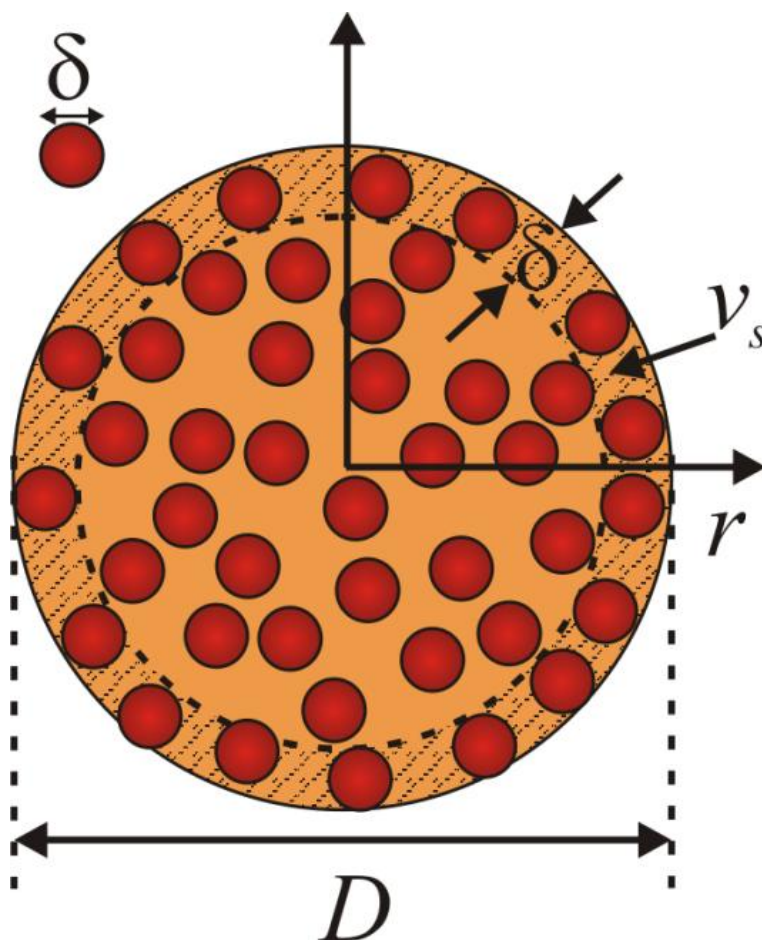


Figure 7.2: Schematic representation of a dissolving composite polymer-cells microcapsule of current diameter  $D$  containing encapsulated cells of diameter  $\delta$  and volume fraction  $\phi$  in the polymer matrix. The microcapsule initial diameter is  $D_0$ . The shaded area represents the surface layer of cells and polymer of volume  $v_s$  in the process of the dissolution. The cells released into the surrounding aqueous media are not shown on this diagram.

Combining eq (7.6) and eq (7.5) we obtain

$$-3\varepsilon y^2 \frac{dy}{d\tau} = y^3 - (y - \varepsilon)^3, \quad \tau = \varepsilon k_R t. \quad (7.8)$$

Equation (7.8) is to be solved with the initial condition,

$$y(\tau = 0) = 1, \quad (7.9)$$

and has an exact analytical solution

$$\tau = 1 - y + \varepsilon \left[ \frac{1}{2} \ln \left( \frac{3 - 3\varepsilon + \varepsilon^2}{3y^2 - 3\varepsilon y + \varepsilon^2} \right) + \frac{1}{\sqrt{3}} \left( \arctan \frac{(2 - \varepsilon)\sqrt{3}}{\varepsilon} - \arctan \frac{(2y - \varepsilon)\sqrt{3}}{\varepsilon} \right) \right]. \quad (7.10)$$

Equation (7.10) is transcendental and gives the dependence  $\tau = \tau(y)$  rather than  $y = y(\tau)$ . Here we focus on the limiting case of practical importance, where the initial microcapsule diameter  $D_0$  is much larger than the average diameter  $\delta$  of the encapsulated cells, i.e.  $\varepsilon \ll 1$ . This corresponds to the experimental parameters of our capsules where the average cell diameter is about 5  $\mu\text{m}$  and the microcapsules diameter ranges from 111  $\mu\text{m}$ , which gives values of  $\varepsilon = 0.045$ . However, for values of  $y$  not extremely close to  $\varepsilon$  (i.e.  $D \sim \delta$ ), the solution of eq (7.11) can be expanded in power series with respect to  $\varepsilon$ :

$$y(\tau) = 1 - \tau + O(\varepsilon^2) = 1 - \varepsilon k_R t + O(\varepsilon^2), \quad \varepsilon \ll 1. \quad (7.11)$$

We checked numerically that at  $\varepsilon = 0.01$ , eq (7.11) is very close to the exact solution, eq (7.10) for all values of  $\tau$  the combination of eq (7.4), eq (7.5) and eq (7.11) yields

$$\frac{N_R(t)}{N_0} \approx 1 - (1 - \varepsilon k_R t)^3. \quad (7.12)$$

Equation (7.12), although approximate and valid only at  $\varepsilon = \delta / D_0 \ll 1$ , allows one to relate the time  $t_d$  of complete disintegration of the microcapsules with the rate

constant of cell release  $k_R$  and the physical size of the cells ( $\delta$ ) and the microcapsules ( $D_0$ ). By using the condition,  $N_R(t = t_d) = N_0$  (or  $y(\tau_d) = \varepsilon$ ), i.e. all cells are released at  $t = t_d$  and equation (7.12) we obtain,

$$\tau_d \approx \varepsilon k_R t_d = 1, \quad t_d \approx \frac{1}{\varepsilon k_R} = \frac{D_0}{k_R \delta}. \quad (7.13)$$

The short time kinetics of cell release as predicted by eq (7.11) is

$$\frac{N_R(t)}{N_0} \approx 3\varepsilon k_R t, \quad t \ll t_d, \quad (7.14)$$

which allows the average disintegration time  $t_d$  of the capsules to be estimated from the initial slope of the relative number of released cells  $N_R/N_0$  vs. time, *initial slope* =  $3\varepsilon k_R = 3k_R \delta / D_0 = 3/t_d$ , or alternatively to determine the rate constant of cells release  $k_R$ . For the shellac-cells composite microcapsules, the release rate constant would depend on the composition of the shellac matrix in the microcapsules and the swelling rate of this composite. Doping the shellac with polyelectrolytes which can swell upon pH change in the medium would effectively increase the value of  $k_R$  compared with the one of unmodified shellac. Alternatively the value of  $k_R$  would increase if the pH of the aqueous medium is increased for unmodified shellac matrix as it has been shown in Figure 7.3.

**(b) Growth of individual cells in a culture medium.** This is a classical problem of exponential growth, where  $N_0$  individual cells are initially dispersed in a culture medium of volume  $V$  and they grow with a rate constant  $k_G$ . The equation describing this process is well known in the literature

$$\frac{dN_G}{dt} = k_G N_G, \quad N_G(t = 0) = N_0. \quad (7.15)$$

$k_G$  is the growth constant of the viable cells in the composite microcapsules.

The solution of equation (7.16) is an exponential function

$$\frac{N_G(t)}{N_0} = \exp(k_G t), \quad (7.16)$$

Whose initial slope (versus time) is the cell growth constant  $k_G$

$$\frac{N_G}{N_0} = 1 + k_G t + O(t^2), \quad \text{initial slope} = k_G. \quad (7.17)$$

Note that in this case  $N_0$  is the total number of free cells in the beginning of the process of their growth.

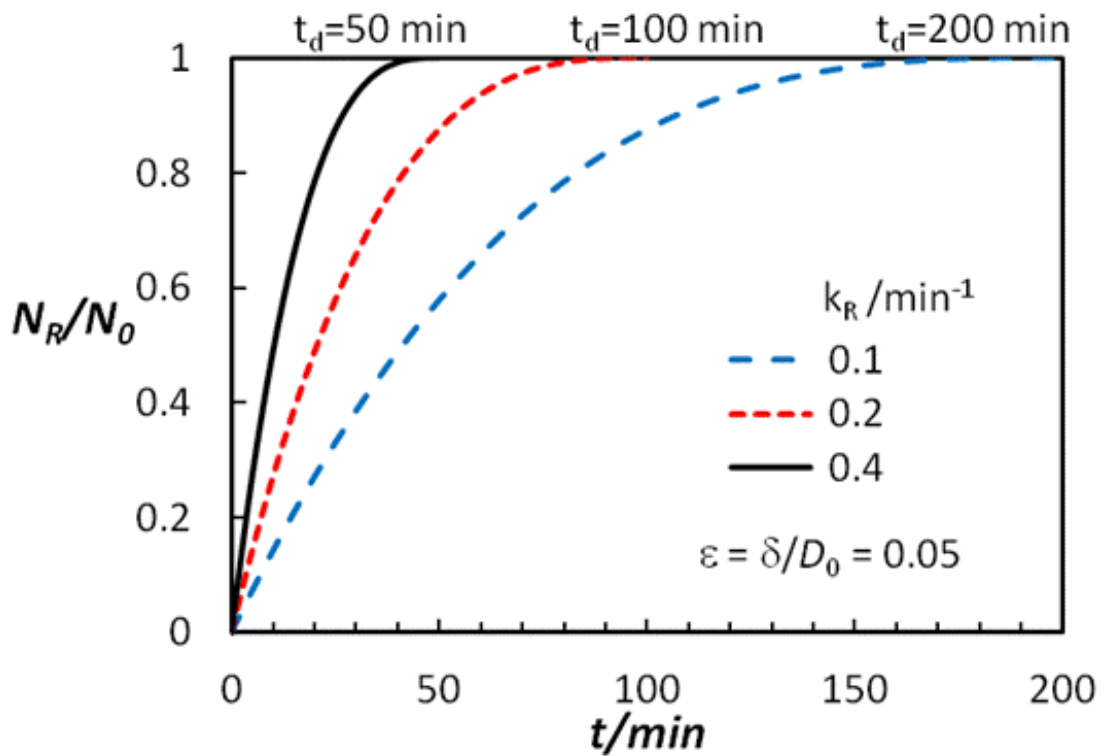


Figure 7.3: Fraction of released cells  $N_R/N_0$  by pH triggered disintegration of the shellac-cells microcapsules. The different values of the release rate constants  $k_R$  depend on the ability of the shellac on the microcapsule surface to dissolve at different pH of the media and correspond to different initial slopes of the three curves and different dissolution times  $t_d$  of the capsules.

**(c) Growth triggered release of individual cells in growth media.** Let us consider a dispersion of composite shellac-cells microcapsules in a culture medium where initially there are no individual cells in the aqueous medium.  $N_0$  is the total number of cells encapsulated in  $n_m$  microcapsules dispersed in a culture medium of volume  $V$ . Here we will assume that there are enough nutrients in the aqueous media to sustain the growth of all cells released from the microcapsules. If the pH of the solution is such that the shellac matrix of the capsule does not swell on its own (e.g. at pH below 5) the only factor releasing the cells is the growth of the cells on the microcapsule surface exposed to the growth media. These “surface exposed “cells expand and gradually chip off the shellac matrix around them which exposed more cells to the culture medium which grow and are released from the microcapsules.

This process we termed “growth triggered release” of cells and at constant agitating of the microcapsule dispersion its kinetics can be described as follows

$$\frac{dN(t)}{dt} = k_G N(t) + \frac{dN_R(t)}{dt} . \quad (7.18)$$

Here  $N(t)$  is the current number of cells in the aqueous media,  $dN_R(t)/dt$  is the rate of release of cells from the microcapsules at time  $t$  since the start of the disintegration process, and  $k_G$  is the cell growth rate constant, identical to those in eq (7.16). In this case, the release of the cells from the microcapsules could be due to (i) growth triggered release only or (ii) a combination of growth triggered release and pH triggered release caused by the swelling of the shellac matrix. Both triggers can contribute to the release rate constant  $k_R$  of cells in this process as it appears in eq (7.12). Note that the growth of cells in the aqueous media does not influence the cell release process, while the accumulation of cells in the aqueous media is a result of the simultaneous action of both processes as implied by eq (7.18). The combination of eq (7.12) and eq (7.18) gives:

$$\frac{dN(t)}{dt} = k_G N(t) + 3\varepsilon k_R N_0 (1 - \varepsilon k_R t)^2 , \quad N(t=0) = 0. \quad (7.19)$$

This equation is an approximation valid only at  $\varepsilon \ll 1$ , which is well satisfied for our experimental parameters. More accurate version can be derived by combination of eq (7.7) and (7.8) with eq (7.19) but this is out of the scope of this analysis.

By introducing the notations:

$$z(\tau) = N(\tau)/N_0, \quad \alpha = k_G/(\varepsilon k_R), \quad \tau = \varepsilon k_R t, \quad (7.20)$$

One can transform eq (7.19) into the following form

$$\frac{dz(\tau)}{d\tau} = \alpha z(\tau) + 3(1-\tau)^2, \quad z(\tau=0) = 0. \quad (7.21)$$

Where the initial condition reads corresponds to absence of cells in the mediums at  $t = 0$ . The analytical solution of equation (7.21) is

$$z(\tau) = \frac{3}{\alpha^3} \left[ (e^{\alpha\tau} - 1)(\alpha^2 - 2\alpha + 2) + \alpha\tau(2\alpha - \alpha\tau - 2) \right]. \quad (7.22)$$

The short time kinetics of this process can be obtained by expanding equation (7.22) in series at small values of  $\tau$

$$z(\tau) = 3\tau + 3\left(\frac{1}{2}\alpha - 1\right)\tau^2 + O(\tau^3). \quad (7.23)$$

Equation (7.23) predicts that the short time kinetics of number of cells in the aqueous media is dominated by the release of cells from the microcapsules

$$\frac{N(t)}{N_0} = 3\varepsilon k_R t + 3\varepsilon^2 k_R^2 \left( \frac{1}{2} \frac{k_G}{\varepsilon k_R} - 1 \right) t^2 + O(t^3), \quad (7.24)$$

The leading (linear) term in equation (7.24), for the short time scale kinetics of the cell population in the solution,  $3\varepsilon k_R t$ , looks practically identical with equation (7.14) for the short term kinetics of  $N_R$ .

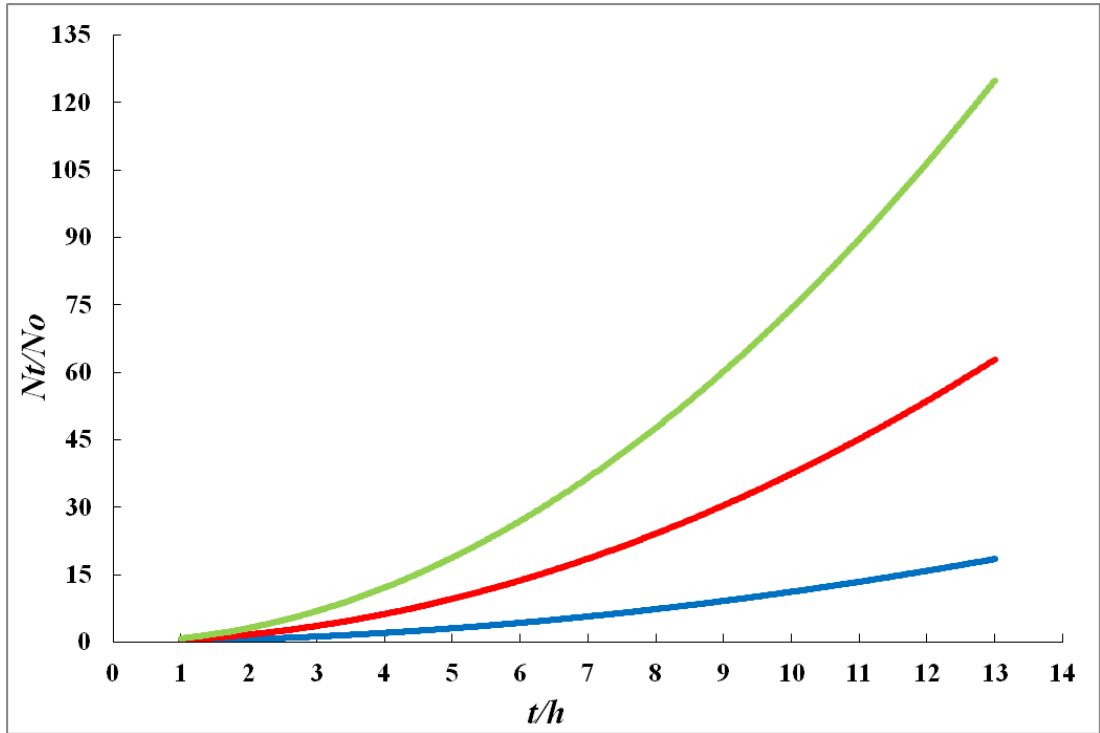


Figure 7.4: Ratio of number of cells released and grown to number of individual cells present in the medium. The plots related to equation 7.24, the value of  $\varepsilon = 0.05$ ,  $k_R = 0.7 h^{-1}$ , but the values of  $k_G$  was changed between 2 (blue), 7 (red), and 14 (green)  $h^{-1}$ .

Equation (7.22) also allows one to predict the cell population in the medium at the moment of complete disintegration of the microcapsules  $t = t_d$  (or  $\tau = 1$ )

$$z(\tau = 1) = \frac{3}{\alpha^3} \left[ e^\alpha (\alpha^2 - 2\alpha + 2) - 2 \right]. \quad (7.25)$$

Note that for small values of  $\alpha \ll 1$ , which typically corresponds to fast cell release (very large  $k_R$ ), the asymptotic expression for equation (7.25) is

$$z(\tau = 1) = 1 + \frac{3}{4} \alpha + O(\alpha^2). \quad (7.26)$$

On the other hand, for large values of  $\alpha \gg 1$ , equation (7.25) predicts exponential growth of the released cell population,



$$z(\tau = 1) \approx \frac{3}{\alpha} \exp(\alpha), \quad \alpha \gg 1. \quad (7.27)$$

One can compare the result from equation (7.27) with the exponential growth kinetics of  $N_0$  free cells in the same culture medium as predicted by equation (7.16) for the same time,  $t = t_d = 1/(\varepsilon k_R)$  it takes  $N_0$  encapsulated cells to be completely released from the microcapsules,

$$\frac{N_G(t = t_d)}{N_0} = \exp(\alpha). \quad (7.28)$$

Hence at conditions of fast cell growth in the aqueous medium,  $\alpha \gg 1$ , the free cells would increase their population approximately  $\alpha/3$  times faster than the equivalent amount of microencapsulated cells at the same conditions.

This is to be expected as the encapsulated cells are released gradually from the microcapsules and start multiplying exponentially only after they are released in the culture medium. In contrast, the sample of free cells would start multiplying immediately after contact with the culture medium. The number of cells in the culture media at the time of complete microcapsule disintegration will be completely dominated by the exponential growth of the released cells. Note the similarity of the exponential terms in equation (7.27) and equation (7.28) which dominate the long-term kinetics of the cells released into the medium. However, the pre-exponential factors in equation (7.27) and (7.28) are completely different as in (7.28) the cells are free to grow from the very start of the process while in (7.27) only the released cells can grow and accumulate in the medium. It is possible to engineer pH triggered release of cells in the medium where the disintegration of the microcapsules is much faster than the growth of the released cells in the medium, i.e.  $k_R \ll k_G$ . This is the case of “explosive release” of cells (very large  $k_R$ ), or very slow growth of the released cells (very small  $k_G$ ) when the aqueous medium is nutritionally poor for them.

In this special case although  $\delta \ll \ll D_0$ , the parameter  $\alpha$  in eq (7.25) may become small enough and give release dominated kinetics even at moderate times.

**(d) Modelling of triggered release of cells with an account for the cell death.** Here we will present more general model for the triggered cell release from the same microcapsules as in section (c) above but with the account for the fact that released cells can multiply or die with growth and death rate constants,  $k_G$  and  $k_D$ , respectively. The modified kinetic scheme for this process is as follows

$$\frac{dN_L}{dt} = k_G N_L - k_D N_L + \frac{dN_R}{dt} , \quad (7.29)$$

$$\frac{dN_D}{dt} = k_D N_L . \quad (7.30)$$

Here  $N_L$  and  $N_D$  are the current number of live and dead cells, respectively, released in the culture medium.

We will assume that all encapsulated cells in the microcapsules are viable prior to their release in the medium. Since the process of cell release starts with fresh medium without any cells, the initial conditions for the system of ordinary differential equations, equation (7.29)-(7.30) is

$$N_D(t=0) = 0, \quad N_L(t=0) = 0 . \quad (7.31)$$

The total number of cells released in the medium is

$$N(t) = N_L(t) + N_D(t) . \quad (7.32)$$

The combination equation (7.13) with equation (7.29)-(7.30) yields

$$\frac{dz_L(\tau)}{d\tau} = \tilde{\alpha} z_L(\tau) + 3(1-\tau)^2, \quad z_L(0) = 0, \quad (7.33)$$

$$\frac{dz_D(\tau)}{d\tau} = \beta z_L(\tau), \quad z_D(0) = 0, \quad (7.34)$$

where

$$z_L(\tau) = \frac{N_L(t)}{N_0}, \quad z_D(\tau) = \frac{N_D(t)}{N_0}, \quad \tilde{\alpha} = \frac{k_G - k_D}{\varepsilon k_R}, \quad \beta = \frac{k_D}{\varepsilon k_R} \quad \tau = \varepsilon k_R t. \quad (7.35)$$

Equation (7.33) is mathematically identical with equation (7.19) for  $\alpha = \tilde{\alpha}$  and both of them are valid for only at  $\varepsilon \ll 1$ . The exact solution of equation (7.33) reads

$$z_L(\tau) = \frac{3}{\tilde{\alpha}^3} \left[ (e^{\tilde{\alpha}\tau} - 1)(\tilde{\alpha}^2 - 2\tilde{\alpha} + 2) + \tilde{\alpha}\tau(2\tilde{\alpha} - \tilde{\alpha}\tau - 2) \right]. \quad (7.36)$$

Which substituted in equation (7.34) with subsequent integration gives

$$z_D(\tau) = \frac{3\beta}{\tilde{\alpha}^4} \left[ (e^{\tilde{\alpha}\tau} - 1)(\tilde{\alpha}^2 - 2\tilde{\alpha} + 2) + \tilde{\alpha}\tau(2\tilde{\alpha} - \tilde{\alpha}\tau - 2 + \tilde{\alpha}^2\tau - \tilde{\alpha}^2 - \tau^2/3) \right]. \quad (7.37)$$

Equation (7.36), similarly to equation (7.26) shows a linear increase of the number of live cells in the medium at short times,

$$z_L(\tau) = 3\tau + O(\tau^2) \approx 3\varepsilon k_R t, \quad (\varepsilon \ll 1, \tilde{\alpha}\tau \ll 1). \quad (7.38)$$

However, equation (7.37) predicts that the short time kinetics of the relative number of dead cells increases quadratically with time

$$z_D(\tau) = \frac{3}{2}\beta\tau^2 + O(\tau^3) \approx \frac{3}{2}\varepsilon k_D k_R t^2, \quad (\varepsilon \ll 1, \tilde{\alpha}\tau \ll 1). \quad (7.39)$$

The long time kinetics of cell release when the growth rate dominates the release and dead rate is

$$z_L(\tau) \approx \frac{3}{\tilde{\alpha}} e^{\tilde{\alpha}\tau}, \quad z_D(\tau) \approx \frac{3\beta}{\tilde{\alpha}^2} e^{\tilde{\alpha}\tau}, \quad \tilde{\alpha} \gg 1. \quad (7.40)$$

Hence the total number of cells  $z = N/N_0$  will be increasing exponentially

$$z(\tau) = z_L(\tau) + z_D(\tau) \approx \frac{3}{\tilde{\alpha}} \left( 1 + \frac{\beta}{\tilde{\alpha}} \right) e^{\tilde{\alpha}\tau} = \frac{3\epsilon k_R k_G e^{(k_G - k_D)t}}{(k_G - k_D)^2}, \quad (\tilde{\alpha} \gg 1) \quad (7.41)$$

Note that in this case at the time of dissolution of the composite microcapsules, ( $t=t_d$ ,  $\tau=1$ ), equation (7.41) predicts that the total number of cells will be an exponential function of  $(k_G - k_D)/(\epsilon k_R)$ ,

$$z(\tau = 1) \approx \frac{3}{\tilde{\alpha}} \left( 1 + \frac{\beta}{\tilde{\alpha}} \right) e^{\tilde{\alpha}}, \quad (\tilde{\alpha} \gg 1). \quad (7.42)$$

This result shows a close similarity with equation (7.27), which is a particular case of equation (7.42) for  $k_D = 0$ . In this analysis, which involves equation (7.40)-(7.42), we have assumed that  $k_G > k_D$ . Equations (7.36) and (7.37) describe the population growth of the individual cells released in the media from the capsules and takes into account both the growth and death events of the released cells.

## 7.1.2 Results and Discussion

We have monitored the release of encapsulated yeast cells in shellac/cells composite microcapsules by incubating the microcapsules in either 0.1 M phosphate buffer solutions of different pH for pH triggered release or using growth triggered process to release and grow encapsulated cells in the microcapsules by incubating the composite microcapsules in a culture media.

### 7.1.2.1 pH-triggered release of cells from shellac/cells microcapsules

We have counted the number of cells released from the microcapsules by using a haemocytometer in different times and the ratio of the released cells to the number of total cells encapsulated ( $N_R/N_0$ ) was plotted against time to produce a graph similar to the one shown in Figure 7.6. We have used two pH values of 7 and 8 to observe the difference in the rate of disintegration of the microcapsules (release of the cells).

Figure 7.4 shows the composite microcapsules during the disintegration and releasing the yeast cells in 0.1 M phosphate buffer solution at pH 8. The yeast cells on the surface of the microcapsules start to free themselves from the microcapsules as the shellac matrix start to dissolve.

We have measured the average diameter of the yeast cells ( $\delta$ ) and the composite microcapsules ( $D_0$ ) by Mastersizer which were found to be 5.3  $\mu\text{m}$  and 111 $\mu\text{m}$  respectively (see Figure 7.5). Hence  $\varepsilon = \delta / D_0 = 5.3\mu\text{m}/111\mu\text{m} = 0.048 \ll 1$ .

At small values of the time, the relationship between ( $N_R/N_0$ ) and time should be linear and the initial slope is given by eq (7.14), i.e.

$$\text{initial slope} = 3\varepsilon k_R = 3/t_d \quad (7.43)$$

Substituting the values of the known parameters in eq (7.43) allowed us to estimate the values of  $k_R$  and  $t_d$  at pH 7 and pH 8 for shellac-cell microcapsules. At pH 7 we obtain  $k_R = 0.031 \text{ min}^{-1}$  and  $t_d = 675 \text{ min}$ , while at pH 8 we estimate that  $k_R = 0.118 \text{ min}^{-1}$  and  $t_d = 180 \text{ min}$ .

As expected, at pH 8 the rate of the cell release and the microcapsules disintegration is faster than the rate at pH 7 since shellac barely dissolves at pH above 7 and the dissolution rate is much faster at pH 8.

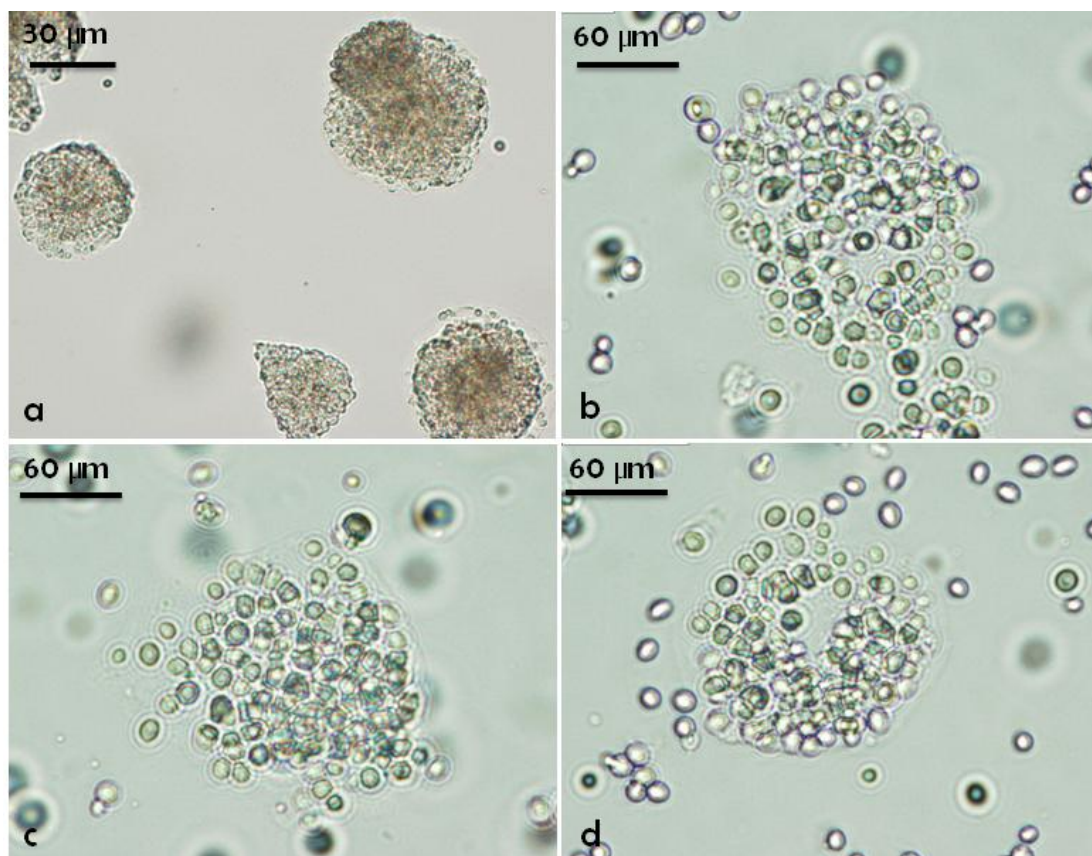


Figure 7.5: (a) Composite shellac/yeast cells microcapsules before being transferred into 0.1 M phosphate buffer at pH 8. (b)-(d) The microcapsules during the disintegration and release of cells while being stirred in the phosphate buffer.

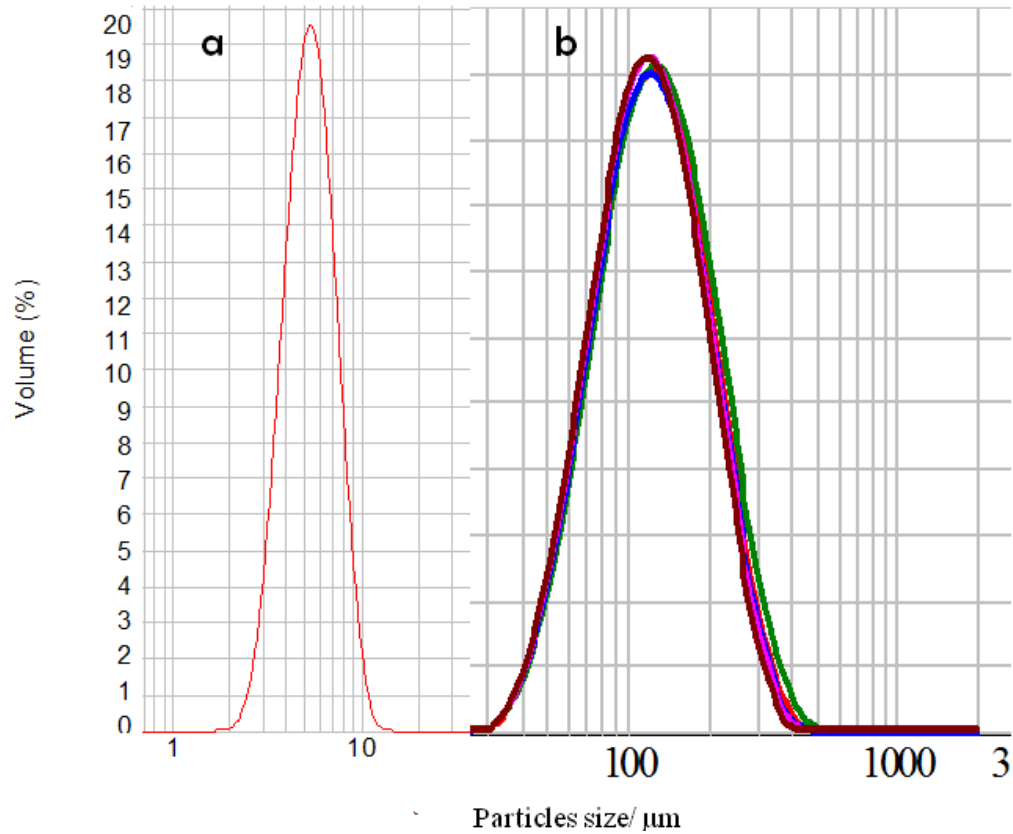


Figure 7.6: Size distribution for native yeast cells (a) (average diameter,  $\delta= 5.3 \mu\text{m}$ ), and (b) for composite shellac/yeast cells microcapsules (average diameter,  $D_0= 111 \mu\text{m}$ ) as obtained from Mastersizer measurements.

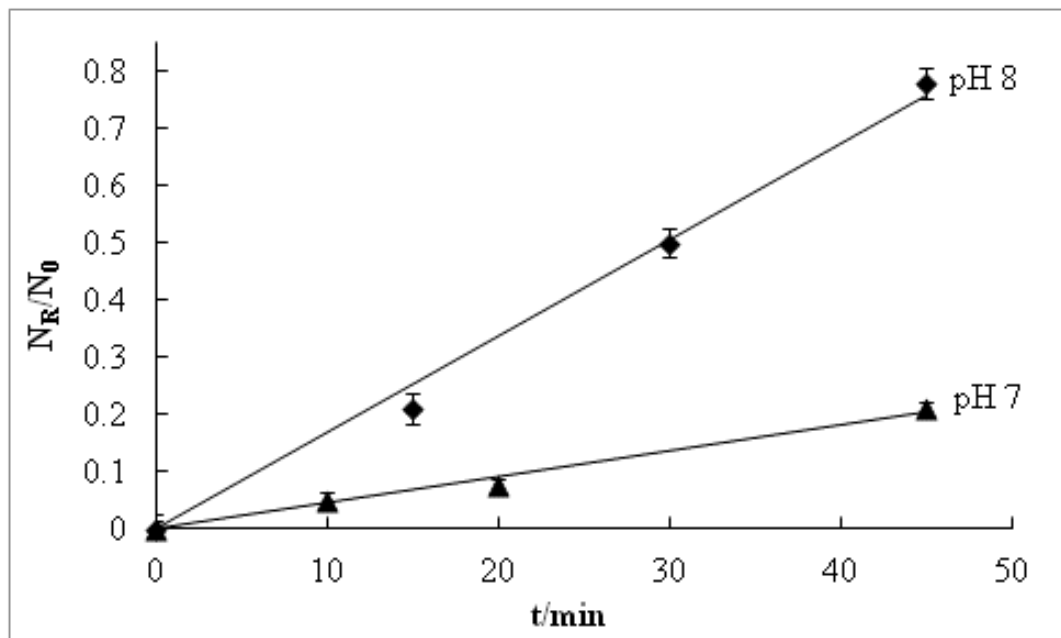


Figure 7.7: Relationship between the relative numbers of released cells from shellac/cells composite microcapsules versus time in phosphate buffer at different pH. The released cells are not growing upon release due to lack of nutrition in aqueous media.

### 7.1.2.2 Growth-triggered release of cells from shellac/cells microcapsules

We have observed the growth of yeast cells both individually and inside composite microcapsules by incubating individual yeast cells and yeast cells containing composite microcapsules in a culture media at 37 °C for a period of 10 hours with constant stirring. The number of grown cells in both cases was counted using a haemocytometer and a graph similar to Figure 7.7 was produced between the ratios of the cells grown: the number of the total cells present in the sample versus time of incubation in the culture media.

$$\frac{N_G}{N_0} = 1 + k_G t + O(t^2), \quad \text{initial slope} = k_G.$$

According to the above equation in small time the initial slope of a straight line between  $N_G/N_0$  in time is equal to the value of  $k_G$  if we set the intercept to 1. The value of  $k_G$  in this case is equal to  $1.69 \text{ h}^{-1}$

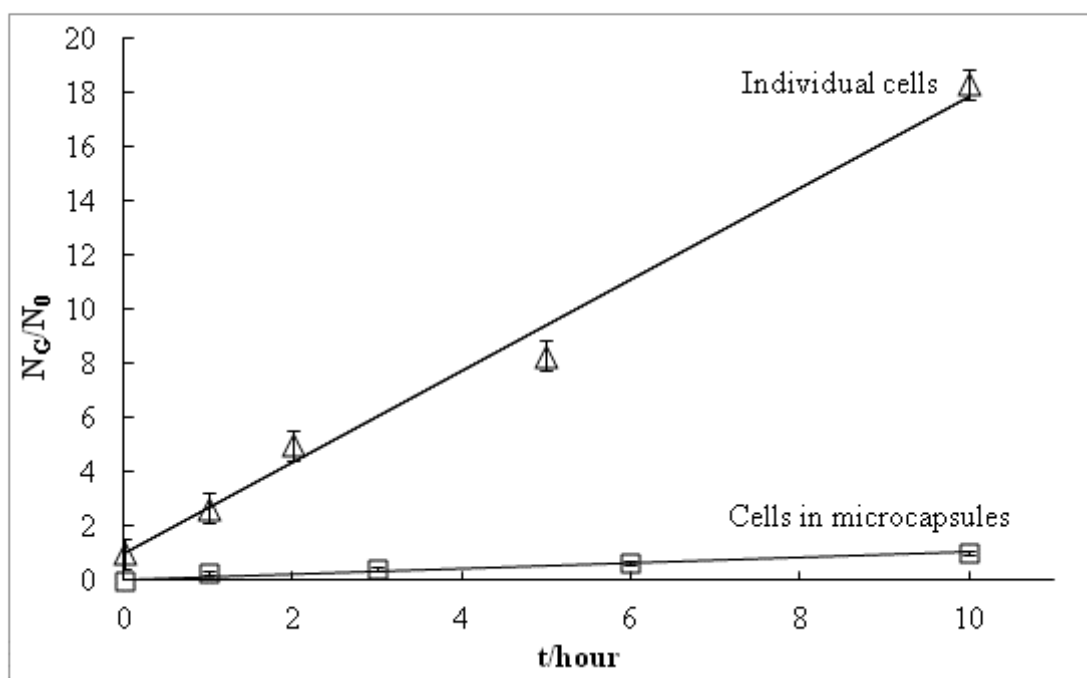


Figure 7.8: Relationship between the numbers of yeast cells grown in culture media versus the incubation time at temperature 37 °C. Triangles represent relative number of growing individual cells, squares represent relative number of yeast cells released and grown from shellac-yeast composite microcapsules. Both samples of individual and microencapsulated cells have been incubated at identical conditions in the same growth media. The growth medium is adjusted to pH 5 to suppress the dissolution of shellac.



In case of the growth-triggered release of the encapsulated cells inside the composite microcapsules, different behaviour can be seen. We calculated the value of release constant ( $k_R$ ) due to growth-triggered release of the encapsulated cells by using the initial slope in equation (7.24) at small times. Therefore the initial slope of a straight line of  $N/N_0$  versus time and should equal to  $3\epsilon k_R$ . Therefore we obtain that  $k_R = 0.74 \text{ h}^{-1}$ . One sees that the value of the rate constant for the growth of individual yeast cells ( $k_G=1.69 \text{ h}^{-1}$ ) is much higher than the rate constant for the growth-triggered release of the encapsulated yeast cells ( $k_R =0.74 \text{ h}^{-1}$ ). The reason for that is that the individual cells are freely dispersed in the culture media and they have full access to the culture media while the encapsulated cells on the surface of the composite microcapsules are partially trapped in the shellac matrix and have limited access to the culture media, hence they are growing much slower compared to the free individual cells (see Figure 7.1b-c for more details).

### 7.1.3 Conclusions

We have done a theoretical analysis of the rate of triggered release of cells from composite polymer-cells microcapsules. Two different triggering mechanisms have been considered, including: (i) pH triggered release of the cells which involves gradual dissolution of the polymer matrix of the polymer in the composite microcapsules which leads to build up of cells in the surrounding aqueous media; (ii) growth triggered release of cells which is a result of the local growth of the cell exposed on the surface of the microcapsules whose release allows more cells to be exposed to the culture media.

In a more complex theoretical analysis we also take into account the cell death rate. The equations predict linear increase of the cells population at short times which is dominated by the rate of cell release from the capsules. We determine the release rate constants of the cells for both the case of (i) pH triggered release and (ii) growth triggered release. Our theory predicts that the long time kinetics of the released cell population follows approximately a power law for pH triggered cell release without further growth. In the contrary, growth triggered cell release from the microcapsules into a culture media leads to an exponential growth of the cell population but the pre-exponential factor is limited by the ratio of the growth and release constant and the cell-to-microcapsule size ratio.

In a 'proof of principle' experiment we determine the cell growth constant at fixed pH in culture media and compare its value with the rate constant of growth triggered release for cells. We also demonstrate that in the absence of growth media the experimental value of the cell release constant is increasing with the increase of pH. This model can help to predict and adjust microcapsule dissolution times and fine-tune the rate of cell release in a variety of cell products, including cell implants, probiotics, live vaccines, etc.

## Chapter 8.

### Summary of main conclusions

- Microencapsulation method of living yeast cells into the exine of pollens from *Lycopodium clavatum* plant has been developed. The method is based on exposing a compressed sporopollenin pellet to a concentrated aqueous dispersion of cells in the presence of a biocompatible surface active agent. The process of efficient cell encapsulation is facilitated by the capillary suction of cells suspension inside the compressed sporopollenin microcapsules, inducing their “re-inflating” with the cells dispersion and closing the opened trilite scars. The viability of the cells was demonstrated after the encapsulation procedure and it was shown that the sporopollenin microcapsules contain a significant amount of entrapped viable cells. The method has applications for protection of probiotic cells and other cells from aggressive environments.
- We have successfully grown encapsulated cells inside the sporopollenin microcapsules by using “in-gel” fermentation process which involves incubation of the loaded sporopollenin microcapsules into a starch gel in culture medium. The encapsulated cells inside the pollens can have a limited growth due to confined space restrictions.
- We also developed sporopollenin microcapsules loaded with magnetic yeast cells, which allows remote manipulation, like fixation, removal or targeted delivery.
- Composite microcapsules of shellac/yeast cells were fabricated by both spray co-precipitating and spray-drying dispersions of yeast cells in aqueous ammonium shellac solution. Two alternative preparation techniques were used: (i) spray co-precipitating a dispersion of yeast cells in aqueous solution of ammonium shellac at  $\text{pH} > 7$ , into either acetic acid or calcium chloride aqueous solution; or (ii) spray-drying the shellac-yeast dispersion. The pH trigger for cell release from these microcapsules and the time of their disintegration were controlled by (a) the shellac concentration and (b) by doping of the solution with pH sensitive polymers.

- We have demonstrated as a proof of concept how carboxymethylcellulose and sodium polyacrylate can be used to trigger the cell release from the microcapsules at neutral and higher pH and to speed up the “shellac-cell” microcapsule disintegration process. The inclusion of sodium polyacrylate in the shellac matrix resulted in much faster disintegration of the microcapsules upon increase of the pH above 7 and in some cases instant cell release. We show that the released yeast cells have preserved their viability during the microencapsulation and the release process from the microcapsules. The produced composite microcapsules were capable of protecting the cells at extremely low pH (pH 1) and still produce viable cells upon disintegration at neutral and higher pH. We discovered that shellac-cell microcapsules can produce triggered release of cells upon exposure to growth media, i.e. growth induced release. We believe that this is a novel mechanism of cell release from microcapsules, which is described for the first time in this thesis.
- We also produced magnetically functionalised shellac-cell microcapsules which can be used for delivery of encapsulated cells directed by an external magnetic field. We demonstrate the robustness and the versatility of shellac as microencapsulating material for protection of cells in acidic environments.
- We have done a theoretical analysis of the rate of triggered release of cells from composite polymer-cells microcapsules. Two different triggering mechanism have been considered, including: (i) pH triggered release of the cells which involves gradual dissolution of the polymer matrix of the polymer in the composite microcapsules which leads to build up of cells in the surrounding aqueous media; (ii) growth triggered release of cells which is a result of the local growth of the cell exposed on the surface of the microcapsules whose release allows more cells to be exposed to the culture media.
- We succeeded in encapsulating living yeast cells in novel colloidosomes prepared from Pickering emulsion templates which were stabilised by cationic amidine latex nanoparticles. Two strategies were used to fabricate and interlock the structure of the Pickering water droplets in oil. (i) The first was to integrate magnetic nanoparticles with yeast cells in a gelled water phase with an agarose gel for their successful transfer from the oil into the water phase. (ii) The second

approach was to increase the droplet stability by interlocking the adsorbed amidine latex nanoparticles monolayer at the water/oil interface with either (a) polystyrene sulfonate from the inside of the droplets or (b) by utilising anionic polyelectrolyte pre-coated yeast cells to electrostatically bind to the cationic amidine latex nanoparticles from the inside of the droplets.

- Water droplets produced from stabilised Pickering emulsions were successfully transferred into water to produce colloidosomes with encapsulated living yeast cells. We developed two main strategies for such a transfer: (i) by using an external magnetic field to collect the magnetic colloidosomes and (ii) by freezing the emulsion after addition of calcium carbonate microparticles as micro-spacers followed by filtration and redispersing in diluted acetic acid to dissolve the the spacer calcium carbonate microparticles.
- Viability tests for the encapsulated cells were performed using both FDA and live/dead cells kit, which indicated viable cells inside the colloidosomes. We developed a special methodology which allows living cells like probiotics or cell implants to be successfully encapsulated and protected from the environment by microencapsulating in colloidosomes without impairing the cells viability.
- In addition, we fabricated novel classes of bio-colloidal multicellular structures of living yeast cells by using water-in-oil emulsion templating technique where the water droplets contained the yeast cells and were stabilised by either surfactant or solid particles. The cells were assembled in cellosomes by shrinking the water droplets in dry octanol; the polyelectrolyte pre-coated yeast cells packed in water droplets were frozen followed by transfer of the frozen cellosomes from the oil phase into a water phase. Such 3D cellosomes structures are reported for a first time in this thesis.

## **Future work**

- For future work, living cells including probiotic bacteria can be protected by means of microencapsulation using polymerisation techniques such as emulsion polymerisation. A thin layer of copolymers can be deposited on top of individual living cells in an aqueous dispersion using polymerisation methods to produce a shell of plastic around the cells, which can be defined as plastic cells.
- In addition by using emulsion polymerisation a layer of copolymer shell can be produced in water/oil interface and hence, produce copolymer microcapsules which will be harvested out of the oil by washing off with ethanol and re-dispersing them in water. The water phase of the original emulsion can contain up to 30 % wt. living cells such as yeast cells or probiotic bacteria. The water phase can be emulsified into the oil phase stabilised by either solid particles or a suitable surfactant.
- The kinetics of disintegration of colloidosomes loaded with yeast cells can be observed using various triggered release of the cells including pH-triggered and growth triggered. The latter can be done by incubating the colloidosomes loaded with yeast cells in an appropriate culture media.

## Glossary

<b>μL</b>	Microliter
<b>μm</b>	Micrometer
<b>mM</b>	Millimolar
<b>°C</b>	Centigrade degree
<b>m</b>	Meter
<b>cm</b>	Centimetre
<b>% vol.</b>	Percentage volume
<b>% wt.</b>	Percentage weight
<b>HLB</b>	Hydrophilic-lipophilic balance
<b>rpm</b>	Rounds per minute
<b>PAH</b>	Poly allylamine hydrochloride
<b>PSS</b>	Polystyrene sulfonate sodium salt
<b>w/o</b>	Water in Oil
<b>o/w</b>	Oil in Water
<b>Span60</b>	Octadecanoic acid [2-[(2R, 3S, 4R)-3, 4-dihydroxy-2-tetrahydrofuran-2-yl]ethyl] ester
<b>FDA</b>	Fluorescein Diacetate
<b>Tween20</b>	Polyoxyethylene (20) sorbitan monolaurate
<b>SEM</b>	Scanning Electron Microscopy
<b>FITC</b>	Fluorescein IsoThioCyanate
<b>nm</b>	Nanometre
<b>TRITC</b>	Tetramethylrhodamine IsoThioCyanate
<b>DNA</b>	Deoxyribonucleic acid

<b>PAA</b>	Polyacrylic acid
<b>Calcein-AM</b>	Acetomethyl derivative of Calcein
<b>3 D</b>	Three-dimensional
<b>2 D</b>	Two-dimensional
<b>CMC</b>	Critical micelle concentration or carboxymehtylcellulose
<b>PBS</b>	Phosphate Buffer Saline
$\lambda_{\text{abs}}$	Absorption wavelength
$\lambda_{\text{em}}$	Emission wavelength
<b>PI</b>	Propidium iodide
<b>w/v</b>	Weight/volume percentage
<b>v/v</b>	Volume/volume percentage
<b>T<sub>g</sub></b>	Glassifying temperature
<b>mN</b>	Milli-Newton
<b>GI</b>	Gastrointestinal tract
<b>ALG</b>	Alginates
<b>POPL</b>	Palm oil and poly-L-lysine
<b>EPS</b>	Exopolysaccharides
<b>PLGA</b>	Poly lactic-co-glycolic acid
<b>GLC</b>	Gas-liquid chromatography
<b>AR</b>	Analytical reagent
<b>GPC</b>	Gel permeation chromatography
<b>PEG</b>	Polyethylene glycol
<b>HPLC</b>	High-performance liquid chromatography
<b>SDS</b>	Sodium dodecyl sulfata



## References

- (1) Czerucka, D.; Piche, T.; Rampal, P. *Alimentary Pharmacology & Therapeutics* **2007**, *26*, 767.
- (2) Havenaar, R.; Huis In't Veld, J. H. J. *Probiotics: A general view*; Elsevier Science Publishers Ltd., Crown House, Linton Road, Oxford IG11 8JU, England; Elsevier Science Publishing Co., Inc., P.O. Box 882, Madison Square Station, New York, New York 10159-2101, USA, 1992.
- (3) Gibbs, B. F.; Kermasha, S.; Alli, I.; Mulligan, C. N. *International Journal of Food Sciences and Nutrition* **1999**, *50*, 213.
- (4) Vilstrup, P. *Microencapsulation of food ingredients*; Leatherhead Publishing: England, 2001.
- (5) Champagne, C. P.; Fustier, P. *Current Opinion in Biotechnology* **2007**, *18*, 184.
- (6) Lee, B. H. *Fundamentals of food biotechnology*; VCH publishers: New York, 1996.
- (7) Benita, S. *Microencapsulation, Methods and Industrial Applications.*; Marcel Dekker, Inc. New York.: New York, Basel, Hong Kong., 1996.
- (8) Wilson, N. a. S., N.P. *ASEAN Food Journal* **2007**, *14*, 1.
- (9) (a) Barrier, S.; Rigby, A. S.; Diego-Taboada, A.; Thomasson, M. J.; Mackenzie, G.; Atkin, S. L. *Lwt-Food Science and Technology* **2010**, *43*, 73(b) Blackwell, L., University of Hull, 2008(c) Mackenzie, G., Atkin, S. L., Digeo-Taboada, A., Barrier, S., Thomasson, M. *Innovations in Pharmaceutical Technology* **2007**, 63(d) Hamad, S. A.; Dyab, A. F. K.; Stoyanov, S. D.; Paunov, V. N. *Journal of Materials Chemistry* **2011**, *21*, 18018.
- (10) Dziezak, J. D. *Food Technology* **1988**, *4*, 136.

- (11) Dinsmore, A. D., Hsu, M. F., Nikolaides, M. G., Marquez, M., Bausch, A. R., Weitz, D. A. *Science* **2002**, 298, 1006.
- (12) Zuidam N.J; Nedovic V *Encapsulation Technologies for Active Food Ingredients and Food Processing.*; 1st Edition. ed.; © Springer Science+Business Media, LLC 2010., 2010.
- (13) Green, B. K. L., Schleicher USA Patent., 1957; Vol. 2800457.
- (14) Anderson, J. L.; Gardner, G. L.; Yoshida, N. H. USA Patent, 1967; Vol. 3341416.
- (15) Lchman L., L., H. A., Kanig, J. L. *The Theory and Practice of Industrial Pharmacy*; 2nd ed.; Marcel Dekker.: New York., 1986.
- (16) (a) Kearney, P. C., Miyamoto, J.; Pergamon Press: Oxford, Uk., 1983; Vol. 4(b) Vidhyalakshmi, R., Bhakyaraj, R., Subhasree, R. S. *Advances in Biological Research* **2009**, 3, 96(c) Jackson, L. S., Lee, K., *Microencapsulation and the food industry*; Lebensmittel-Wissenschaft Technologie, 1991(d) Burgain, J. B. J.; Gaiani, C.; Linder, M.; Scher, J. *Journal of Food Engineering* **2011**, 104, 467.
- (17) Cakshae, M., Pethrick, A., Rashid, H., and Sherrington, D. C. *Polymer Communications*. **1985**, 26, 185.
- (18) Shahidi, F., Han, X. Q. *Critical Reviews in Food Science and Nutrition* **1993**, 33, 501.
- (19) Anal, A. K.; Singh, H. *Trends in Food Science & Technology* **2007**, 18, 240.
- (20) Hamad, S. A., Paunov, V. N., Stoyanov, S. D. *Soft Matter* **2012**, 8, 5069.
- (21) King, A. H. In *Encapsulation and Controlled Release of Food Ingredients*; Risch, S. J., Reineccius, G. A., Ed.; American Chemical Society: Washington DC., 1995; Vol. 590.

- (22) Krasaekoopt, W.; Bhandari, B.; Deeth, H. *International Dairy Journal* **2003**, *13*, 3.
- (23) Kailasapathy, K. *CAB Reviews: Perspectives in Agriculture, Veterinary Science, Nutrition and Natural Resources*. **2009**, *4*.
- (24) (a) Lacroix, C., Paquin, C., and Arnaud, J. P. *Applied Microbiology and Biotechnology* **1990**, *32*, 403(b) Audet, P., Lacroix, C., and Paquin, C. *International Dairy Journal* **1992**, *2*, 1.
- (25) Sultana, K., Godward, G., Reynolds, N., Arumugaswamy, R., Peiris, P., Kailasapathy, K. *International Journal of Food Microbiology*. **2000**, *62*, 47.
- (26) Rowley, J. A., Madlambayan, G., Mooney, D. J. *Biomaterials* **1999**, *20*, 45.
- (27) Liu, H. X.; Wang, C. Y.; Gao, Q. X.; Liu, X. X.; Tong, Z. *International Journal of Pharmaceutics* **2008**, *351*, 104.
- (28) Cook, M. T.; Tzortzis, G.; Charalampopoulos, D.; Khutoryanskiy, V. V. *Biomacromolecules* **2011**, *12*, 2834.
- (29) Klein, J., Vorlop, D. K. In *Foundations of Biochemicals Engineering Kinetics and Thermodynamics in Biological Systems.*; ACS Symposium ed.; Blanch, H., Papoutsakis, E. T., Stephanopoulos, G., Ed.; American Chemical Society: Washington DC, 1983.
- (30) Talwalkar, A., Kailasapathy, K. *Australian Journal of Dairy Technology*. **2003**, *58*, 36.
- (31) Klein, J., Vorlop, D. K. In *Comprehensive Biotechnology.*; Cooney, C. L., Humphery, A. E., Ed.; Pergamon Press.: Oxford, Uk, 1985.
- (32) Murua, A.; Portero, A.; Orive, G.; Hernandez, R. M.; de Castro, M.; Pedraz, J. L. *Journal of Controlled Release* **2008**, *132*, 76.

- (33) Diaspro, A.; Silvano, D.; Krol, S.; Cavalleri, O.; Gliozzi, A. *Langmuir* **2002**, *18*, 5047.
- (34) Dusseault, J.; Leblond, F. A.; Robitaille, R.; Jourdan, G.; Tessier, J.; Menard, M.; Henley, N.; Halle, J. P. *Biomaterials* **2005**, *26*, 1515.
- (35) Orive, G.; Hernandez, R. M.; Gascon, A. R.; Calafiore, R.; Chang, T. M. S.; De Vos, P.; Hortelano, G.; Hunkeler, D.; Lacik, I.; Shapiro, A. M. J.; Pedraz, J. L. *Natural Medicine* **2003**, *9*, 104.
- (36) Yeong, F. M. *Molecular Microbiology* **2005**, *55*, 1325.
- (37) Huis In'T Veld, J. H. J.; Havenaar, R. *Journal of Chemical Technology and Biotechnology* **1991**, *51*, 562.
- (38) Del Piano, M.; Morelli, L.; Strozzi, G. P.; Allesina, S.; Barba, M.; Deidda, F.; Lorenzini, P.; Ballare, M.; Montino, F.; Orsello, M.; Sartori, M.; Garello, E.; Carmagnola, S.; Pagliarulo, M.; Capurso, L. *Digestive and liver disease* **2006**, *38 Suppl 2*, S248.
- (39) Finegold, S. M.; Sutter, V. L.; Sugihara, P. T.; Elder, H. A.; Lehmann, S. M.; Phillips, R. L. *American Journal of Clinical Nutrition* **1977**, *30*, 1781.
- (40) Barza, M.; Giuliano, M.; Jacobus, N. V.; Gorbach, S. L. *Antimicrobial Agents and Chemotherapy* **1987**, *31*, 723.
- (41) Marteau, R. M., de Vrese, M., Cellier, C. J., Schrezenmeir, J. *The American Journal of Clinical Nutrition* **2001**, *73*, 430S.
- (42) Kopp-Hoolihan, L. *Journal of the American Dietetic Association* **2001**, *101*, 229.
- (43) Doleyres, Y.; Lacroix, C. *International Dairy Journal* **2005**, *15*, 973.
- (44) Graff, S.; Chaumeil, J. C.; Boy, P.; Lai-Kuen, R.; Charrueau, C. *Journal of General and Applied Microbiology* **2008**, *54*, 221.

- (45) Ding, W. K.; Shah, N. P. *Journal of Food Science* **2009**, *74*, M53.
- (46) Chang, T. M. S.; Plenum Press. : New York., 1978.
- (47) Kailasapathy, K. *Lwt-Food Science and Technology* **2006**, *39*, 1221.
- (48) (a) Lourens-Hattingh, A.; Viljoen, B. C. *International Dairy Journal* **2001**, *11*,  
1(b) Mattila-Sandholm, T.; Myllarinen, P.; Crittenden, R.; Mogensen, G.;  
Fonden, R.; Saarela, M. *International Dairy Journal* **2002**, *12*, 173.
- (49) (a) Li, M.; Rouaud, O.; Poncelet, D. *International Journal of Pharmaceutics*  
**2008**, *363*, 26(b) Freitas, S.; Merkle, H. P.; Gander, B. *Journal of Controlled*  
*Release* **2005**, *102*, 313.
- (50) Bangham, A. D. *Chemistry and Physics of Lipids* **1993**, *64*, 275.
- (51) Risch, S. J., Reineccius, G. A. *Encapsulation and controlled release of food*  
*ingredients*; American Chemical Society.: USA, 1995.
- (52) Kirby, C. J., Whitte, C. J., Rigby, N., Coxon, D. T., and Law, B. A.  
*International Journal of Food Sciences and Technology* **1991**, *25*, 437.
- (53) Gregoriadis, G. *Liposome Technology*; CRC Press: Boca Raton, FL, 1984.
- (54) Otto, J. T.; Trumbo, D. L. *Journal of Coatings Technology and Research* **2010**,  
*7*, 525.
- (55) Garcia-Alonso, J.; Fakhrullin, R. F.; Paunov, V. N. *Biosensors & Bioelectronics*  
**2010**, *25*, 1816.
- (56) Sigma-Aldrich, 2012.
- (57) Fakhrullin, R. F., Paunov, V. N. *Chemical Communications* **2009**, 2511.
- (58) Sangster, S. *Octanol-Water Partition Coefficient: Fundamentals and Physical*  
*Chemistry.* ; Wiley, 1997.
- (59) Zetsche, F., Kälin, O. *Helvetica Chimica Acta* **1931**, *14*, 517.
- (60) Faegri, I.; Iverson, J. *Textbook of Pollen Analysis*: Oxford, 1984.

- (61) (a) Brooks, J., Shaw, G. *Origin and Development of Living Systems* Academic Press: London and New York, 1973(b) Brooks, J., Shaw, G. *Nature* **1968**, 219, 532(c) Shaw, G. *Phytochemical Phylogeny* Academic Press: London and New York, 1970(d) Brooks, J. G., P.R.; Muir, M.D.; van Gijzel, P.; Shaw, G. *Sporopollenin*: London and New York, 1971
- (e) Brooks, J., Muir, M.D., Shaw, G. *Nature* **1973**, 244, 215(f) Shaw, G. *Pollen: Development and Physiology*; Butherworths: London, 1971.
- (62) Wittborn, J.; Rao, K. V.; El-Ghazaly, G.; Rowley, J. R. *Annals of Botany* **1998**, 82, 141.
- (63) Bohne, G.; Richter, E.; Woehlecke, H.; Ehwaldi, R. *Annals of Botany* **2003**, 92, 289.
- (64) (a) Straka, H. *Pollen und Sporenkunde*; Gustav Fischer Verlag: Stuttgart, 1975(b) Rowley, J. R., Skvarla, J.J., and Walles, B. **2000b**, 225, 201.
- (65) Lorch, M.; Thomasson, M. J.; Diego-Taboada, A.; Barrier, S.; Atkin, S. L.; Mackenzie, G.; Archibald, S. J. *Chemical Communications* **2009**, 6442.
- (66) (a) Barrier, S.; Diego-Taboada, A.; Thomasson, M. J.; Madden, L.; Pointon, J. C.; Wadhawan, J. D.; Beckett, S. T.; Atkin, S. L.; Mackenzie, G. *Journal of Materials Chemistry* **2011**, 21, 975(b) Beckett, S. T., Mackenzie, G. *Chemistry Review* **2010**, 20, 10(c) Wakil, A.; Mackenzie, G.; Diego-Taboada, A.; Bell, J. G.; Atkin, S. L. *Lipids* **2010**, 45, 645.
- (67) Paunov, V. N.; Mackenzie, G.; Stoyanov, S. D. *Journal of Materials Chemistry* **2007**, 17, 609.
- (68) Chrzanowski, T. H.; Crotty, R. D.; Hubbard, J. G.; Welch, R. P. *Microbial Ecology* **1984**, 10, 179.
- (69) Fakhrullin, R. F., Garcia-Alonso, J., Paunov, V. N. *Soft Matter* **2010**, 6, 391.

- (70) Law, D.; Zhang, Z. *Minerva Biotechnologica* **2007**, *19*, 17.
- (71) Barnes, C. E. *Industrial and Engineering Chemistry* **1938**, *30*, 449.
- (72) (a) Cockeram HS, L. S. *Journal of Cosmetic Science* **1961**, *12*, 316(b) Fleix, S., Marianne, S. , Tor, W., Bernd, W. M. *Pharmaceutical Technology* **1999**, *23*, 146(c) Ernest, J. P. *SHELLAC, Its production, manufacture, chemistry, analysis, commerce and uses*; Sir Isaac Pitman & Sons, Ltd.: London, 1935.
- (73) (a) Stummer, S.; Salar-Behzadi, S.; Unger, F. M.; Oelzant, S.; Penning, M.; Viernstein, H. *Food Research International* **2010**, *43*, 1312(b) Limmatvapirat, S.; Limmatvapirat, C.; Luangtana-Anan, M.; Nunthanid, J.; Oguchi, T.; Tozuka, Y.; Yamamoto, K.; Puttipipatkachorn, S. *International Journal of Pharmaceutics* **2004**, *278*, 41.
- (74) (a) Campbell, A. L.; Holt, B. L.; Stoyanov, S. D.; Paunov, V. N. *Journal of Materials Chemistry* **2008**, *18*, 4074(b) Campbell, A. L.; Stoyanov, S. D.; Paunov, V. N. *Soft Matter* **2009**, *5*, 1019.
- (75) Leick, S.; Kott, M.; Degen, P.; Henning, S.; Pasler, T.; Suter, D.; Rehage, H. *Physical Chemistry Chemical Physics* **2011**, *13*, 2765.
- (76) (a) Xue, J.; Zhang, Z. B. *Journal of Microencapsulation* **2008**, *25*, 523(b) Xue, J.; Zhang, Z. B. *Journal of Applied Polymer Science* **2009**, *113*, 1619.
- (77) (a) Pooley, S. A.; Rivas, B. L.; Lillo, F. E.; Pizarro, G. D. *Journal of the Chilean Chemical Society* **2010**, *55*, 19(b) Fang, X. H.; Somasundaran, P. *Journal of Chemical and Engineering Data* **2010**, *55*, 3555.
- (78) (a) Velev, O. D.; Furusawa, K.; Nagayama, K. *Langmuir* **1996**, *12*, 2374(b) Velev, O. D.; Furusawa, K.; Nagayama, K. *Langmuir* **1996**, *12*, 2385(c) Velev, O. D.; Nagayama, K. *Langmuir* **1997**, *13*, 1856.
- (79) Pickering, S. U. *Journal of Chemical Society* **1907**, *91*, 2001.

- (80) Binks, B. P.; Lumsdon, S. O. *Langmuir* **2001**, *17*, 4540.
- (81) Horozov, T. S.; Binks, B. P. *Angewandte Chemie-International Edition* **2006**, *45*, 773.
- (82) Binks, B. P. *Current Opinion in Colloid & Interface Science* **2002**, *7*, 21.
- (83) Aveyard, R., Binks, B. P., Clint, J. H. *Advances in Colloid and Interface Science* **2003**, *100*, 503.
- (84) Aveyard, R.; Clint, J. H.; Nees, D.; Paunov, V. N. *Langmuir* **2000**, *16*, 1969.
- (85) (a) Noble, P. F.; Cayre, O. J.; Alargova, R. G.; Velev, O. D.; Paunov, V. N. *Journal of the American Chemical Society* **2004**, *126*, 8092(b) Cayre, O. J.; Noble, P. F.; Paunov, V. N. *Journal of Materials Chemistry* **2004**, *14*, 3351.
- (86) Paunov, V. N. *Langmuir* **2003**, *19*, 7970.
- (87) Ashby, N. P., Binks, B. P., Paunov, V. N. *Physical Chemistry Chemical Physics* **2004**, *6*, 4223.
- (88) Duan, H. W.; Wang, D. Y.; Sobal, N. S.; Giersig, M.; Kurth, D. G.; Mohwald, H. *Nano Letters* **2005**, *5*, 949.
- (89) Kim, J. W.; Fernandez-Nieves, A.; Dan, N.; Utada, A. S.; Marquez, M.; Weitz, D. A. *Nano Letters* **2007**, *7*, 2876.
- (90) Laib, S.; Routh, A. F. *Journal of Colloid and Interface Science* **2008**, *317*, 121.
- (91) Simovic, S.; Prestidge, C. A. *Langmuir* **2008**, *24*, 7132.
- (92) Shah, R. K.; Kim, J. W.; Weitz, D. A. *Langmuir* **2010**, *26*, 1561.
- (93) Thompson, K. L.; Armes, S. P. *Chemical Communications* **2010**, *46*, 5274.
- (94) Walsh, A.; Thompson, K. L.; Armes, S. P.; York, D. W. *Langmuir* **2010**, *26*, 18039.
- (95) Yuan, Q. C.; Cayre, O. J.; Fujii, S.; Armes, S. P.; Williams, R. A.; Biggs, S. *Langmuir* **2010**, *26*, 18408.



- (96) Nomura, T.; Routh, A. F. *Langmuir* **2010**, *26*, 18676.
- (97) Keen, P. H. R.; Slater, N. K. H.; Routh, A. F. *Langmuir : the ACS journal of surfaces and colloids* **2012**, *28*, 1169.
- (98) Brandy, M. L., Cayre, O. J., Fakhrullin, R. F., Velev, O. D., Paunov, V. N. *Soft Matter* **2010**, *6*, 3494.
- (99) Fakhrullin, R. F., Brandy, M. L., Cayre, O. J., Velev, O. D., Paunov, V. N. *Physical Chemistry Chemical Physics* **2010**, *12*, 11912.
- (100) Strother, P. K., Battison, L., Brasier, M. D., Wellman, C. H. *Nature* **2011**, *473*, 505.
- (101) (a) Zeppieri, S., Rodríguez, J., López de Ramos, A. L. *Journal of Chemical and Engineering Data*. **2001**, *46*, 1086(b) Gunde, R., Kumar, A., Lehnert-Batar, S., Mader, R., Windhab, E. J. *Journal of Colloid and Interface Science* **2001**, *244*, 113.